



**UCAM**  
UNIVERSIDAD CATÓLICA  
DE MURCIA

EIDUCAM International Doctoral School

PhD. in Health Sciences

**Degradación de hidrocarburos aromáticos  
policíclicos de las aguas: Alternativas de  
tratamiento a los procesos convencionales**

*Degradation of polycyclic aromatic hydrocarbons in  
water: Alternative treatments to conventional processes*

Autor

**Ainhoa Rubio Clemente**

Directors

**PhD. MSc. Gustavo Antonio Peñuela Mesa**

**PhD. MSc. Edwin Lenin Chica Arrieta**

Murcia, September 23<sup>rd</sup>, 2018





# UCAM

UNIVERSIDAD CATÓLICA  
DE MURCIA

## AUTHORIZATION OF THE SUPERVISORS OF THE THESIS FOR SUBMISSION

Prof. Dr. Gustavo Antonio Peñuela and Prof. Dr. Edwin Lenin Chica Arrieta, as Supervisors of the Doctoral Thesis “Degradation of polycyclic aromatic hydrocarbons in waters: Alternative treatments to conventional processes” (Degradación de hidrocarburos aromáticos policíclicos de las aguas: Alternativas de tratamiento a los procesos convencionales) in the Programa de Doctorado en Ciencias en la Salud, authorize the Thesis submission since it meet the necessary conditions for its defense.

In order to comply with the Royal Decrees 99/2011, 1393/2007, 56/2005 and 778/98, we sign it in Medellín-Colombia, 19<sup>th</sup> September, 2018.

**PhD. Gustavo Antonio. Peñuela Mesa**  
Profesor titular Facultad de Ingeniería.  
Departamento de Ingeniería Ambiental  
Coordinador Grupo de Investigación en  
Diagnostico y control de la contaminación-  
GBCON  
Sede de Investigación Universitaria  
Universidad de Antioquia  
Cra 53 N° 61-30 Laboratorio 232  
Teléfono 57 (4) 219 65 70  
e-mail: gustavo.penuela@udea.edu.co  
Medellín, Colombia

**PhD. Edwin Lenin Chica**  
Profesor asociado Facultad de Ingeniería,  
Departamento de Ingeniería Mecánica.  
Coordinador del Grupo de Energía  
Alternativa  
Ciudad Universitaria.  
Universidad de Antioquia  
Calle 67 #53-108Bloque 20:444  
Teléfono: (+ 57 4) 219 8553  
e-mail: edwin.chica@udea.edu.co  
Medellín, Colombia

UCAM



**EIDUCAM**  
Escuela Internacional  
de Doctorado



*"We forget that the water cycle and the life cycle are one."*

Jacques Cousteau



## ACKNOWLEDGMENTS

I would like to express my deep gratitude to Professor Gustavo A. Peñuela and Professor Edwin L. Chica, my research supervisors, for their patient guidance, enthusiastic encouragement, useful critiques and constructive recommendations during the planning and development of this research project. Their willingness to give their time so generously is very much appreciated.

I would also like to thank to everyone I shared the laboratory with during last years, for its constant collaboration and valuable technical support.

And finally, last but by no means least, I wish to thank to my parents and sister, as well as my husband, for their support and encouragement throughout the whole research period.

To all of you, thanks for all your encouragement!

*Ainhoa Rubio Clemente*





## RESEARCH RESULTS

### Papers and book chapters:

- Rubio-Clemente A, Chica E, & Peñuela, G. (2018). Photovoltaic array for powering advanced oxidation processes: Sizing, application and investment costs for the degradation of a mixture of anthracene and benzo[a]pyrene in natural water by the UV/H<sub>2</sub>O<sub>2</sub> system. *Journal of Environmental Chemical Engineering*, 6(2), pp. 2751-2761. ISSN: 2213-3437. <https://doi.org/10.1016/j.jece.2018.03.046>.
- Rubio-Clemente A., Chica E., & Peñuela G. High-Performance Liquid Chromatography and Chemometric techniques for Analytical Method Development. Chapter of book in *High-Performance Liquid Chromatography. Types, Parameters and Applications*, 2018, Prof. (Ed.), Ivan Lucero. NOVA. Science Publishers, Inc, pp. 121-144. ISBN 978-1-53613-544-2.
- Rubio-Clemente A, Chica E, & Peñuela, G. (2018). Direct large-volume injection analysis of polycyclic aromatic hydrocarbons in water. *Universitas Scientiarum*, 23(2), pp. 171-189. ISSN: 0122-7483. <https://10.11144/Javeriana.SC23-2.dlvi>.
- Rubio-Clemente A, Chica E, & Peñuela, G. (2018). Evaluation of the UV/H<sub>2</sub>O<sub>2</sub> system for treating natural water with a mixture of anthracene and benzo[a]pyrene at ultra-trace level. *Environmental Science and Pollution Research*, In press. ISSN: 1614-7499. <https://doi.org/10.1007/s11356-018-2411-6>.
- Rubio-Clemente A, Chica E, & Peñuela, G. (2018). Total coliforms inactivation in natural water by UV/H<sub>2</sub>O<sub>2</sub>, UV/US and UV/US/H<sub>2</sub>O<sub>2</sub> systems. *Environmental Science and Pollution Research*, 2018, In press. ISSN: 1614-7499.
- Rubio-Clemente A., Chica E., & Peñuela G. (2017). Kinetic modeling of the UV/H<sub>2</sub>O<sub>2</sub> process: Determining the effective hydroxyl radical

concentration. In *Physico-Chemical Wastewater Treatment and Resource Recovery*, pp. 19-41. Farooq R. & Ahmad Z. (Eds.). InTech.

- Rubio-Clemente A., Chica E., & Peñuela G. (2017). Rapid determination of anthracene and benzo(a)pyrene by high-performance liquid chromatography with fluorescence detection. *Analytical Letters*, 50 (8), 1229-1247.
- Rubio-Clemente A, Chica E, & Peñuela G. (2017). Kinetic model describing the UV/H<sub>2</sub>O<sub>2</sub> photodegradation of phenol from water". *Chemical Industry and Chemical Engineering Quarterly*, 23 (4) 547-562. <https://doi.org/10.2298/CICEQ161119008R>. ISSN: 1451-9372.
- Rubio-Clemente A, Chica E, Cardona A, & Peñuela, G. (2017). Sensitive spectrophotometric determination of hydrogen peroxide in aqueous samples from advanced oxidation processes: Evaluation of possible interferences. *Afinidad*. 75, 579, 159-166. ISSN: 2339-9686.
- Rubio-Clemente A., Chica E., & Peñuela G. (2015). Petrochemical wastewater treatment by photo-Fenton process. *Water, Air, & Soil Pollution*, 226 (62), 61-78. ISSN: 1573-2932.
- Rubio-Clemente A., Torres-Palma R.A., & Peñuela G. (2014). Removal of polycyclic aromatic hydrocarbons in aqueous environment by chemical treatments: A review. *Science of the Total Environment*, 478, 201-225. ISSN: 0048-9697.
- Rubio-Clemente A., Chica E., & Peñuela G. (2014). Aplicación del proceso Fenton en el tratamiento de aguas residuales de origen petroquímico. *Ingeniería y Competitividad*, 16 (2), 211-223. ISSN: 0123-2033.
- Rubio-Clemente A., Chica E., & Peñuela G. (2013). Procesos de tratamiento de aguas residuales para la eliminación de contaminantes orgánicos emergentes. *Ambiente & Agua-An Interdisciplinary Journal of Applied Science*, 8 (3), 93-103. ISSN 1980-993X.

#### **Congresses:**

- Rubio-Clemente A., Chica E., & Peñuela G. Photovoltaic system for the treatment of surface water polluted with polycyclic aromatic hydrocarbons in Colombia. International conference on Renewable

Energies and power Quality (ICREPQ '2018). Salamanca (Spain) 21 – 23 of march, 2018.

- Rubio-Clemente A., Chica E., & Peñuela G. Chemometric tools applied to the sensitive analysis of anthracene and benzo[a]pyrene in water. IV Jornadas de Investigación y Doctorado: Women in Science. UCAM Universidad Católica de Murcia. Mayo 18 de 2018.
- Rubio-Clemente A., Chica E., & Peñuela G. Renewable electrical power generation for the UV/H<sub>2</sub>O<sub>2</sub> system implementation. IV Jornadas de Investigación y Doctorado: Women in Science. UCAM Universidad Católica de Murcia. Mayo 18 de 2018.
- Rubio-Clemente A., Chica E., & Peñuela G. Optimization and validation of an analytical method for the determination of H<sub>2</sub>O<sub>2</sub> at trace levels in aqueous samples. III Jornadas de Investigación y Doctorado EIDUCAM: Reconocimiento de los Doctores en el Mercado. 16 junio 2017. Universidad Católica San Antonio de Murcia (UCAM). Murcia. España.
- Rubio-Clemente A., Chica E., & Peñuela G. Application of the UV/H<sub>2</sub>O<sub>2</sub> system for the treatment of natural water contaminated with anthracene and benzo[a]pyrene. III Jornadas de Investigación y Doctorado EIDUCAM: Reconocimiento de los Doctores en el Mercado. 16 junio 2017. Universidad Católica San Antonio de Murcia (UCAM). Murcia. España.
- Rubio-Clemente A., Chica E., & Peñuela G. H<sub>2</sub>O<sub>2</sub>-based advanced oxidation processes for water pollutant decontamination. H<sub>2</sub>O<sub>2</sub> as indicator of the effectiveness of the UV/H<sub>2</sub>O<sub>2</sub> system. 26<sup>th</sup> International Conference 23–27 June 2017. Elenite Holiday Village, Bulgaria. Artículo publicado en la revista *Ecology & Safety*, Volume 11, 2017. pp. 282-289. ISSN 1314-7234.
- Rubio-Clemente A., Chica E., & Peñuela G. Degradation of a mixture of PAHs in aqueous solution using the UV-A/H<sub>2</sub>O<sub>2</sub>/Fe<sup>2+</sup> process directly powered by photovoltaic energy. 26<sup>th</sup> International Conference 23–27 June 2017. Elenite Holiday Village, Bulgaria. Artículo publicado en la revista *Ecology & Safety*, Volume 11, 2017. pp. 290-298. ISSN 1314-7234.
- Rubio-Clemente A., Chica E., & Peñuela G. Aplicación de MATLAB en la industria: Modelación cinética del proceso de oxidación avanzada UV/H<sub>2</sub>O<sub>2</sub>. XI Congreso Colombiano de Métodos Numéricos. Simulación

en ciencias y aplicaciones industriales. 16-18 agosto 2017. Universidad Industrial de Santander. Bucaramanga. Colombia.

- Rubio-Clemente A., Chica E., & Peñuela G. Direct large volume injection HPLC determination of polycyclic aromatic hydrocarbons (PAHs) in water: An easy and fast analytical method. Italo Latin American Congress of Etnomedicina XXI SILAE, IX Colombia Congress of Chromatography. Cartagena de Indias 25-29 de september 2017.
- Rubio-Clemente A., Chica E., & Peñuela G. Evaluation Of The UV/H<sub>2</sub>O<sub>2</sub> System For Treating Natural Water With A Mixture Of Anthracene And Benzo[a]pyrene at Ultra-trace levels. 3rd Iberoamerican Conference on Advanced Oxidation Technologies. (III CIPOA) and 2nd Colombian Conference on Advanced Oxidation Processes (II CCPAOX). Medellín (Guatapé), Colombia, on November 14 – 17, 2017.
- Rubio-Clemente A., Chica E., & Peñuela G. Bacterial Inactivation in Natural Water by UV/H<sub>2</sub>O<sub>2</sub>, UV/H<sub>2</sub>O<sub>2</sub>/Fe<sup>2+</sup> and US/UV/H<sub>2</sub>O<sub>2</sub> Systems. 3rd Iberoamerican Conference on Advanced Oxidation Technologies. (III CIPOA) and 2nd Colombian Conference on Advanced Oxidation Processes (II CCPAOX). Medellín (Guatapé), Colombia, on November 14 – 17, 2017.
- Rubio-Clemente A., Rodríguez Restrepo A., Chica E., & Peñuela G. Rapid and sensitive determination of polycyclic aromatic hydrocarbons at trace levels in aqueous samples using RP-HPLC with a fluorescence detector. 1<sup>st</sup> International Caparica Conference on Pollutant Toxic Ions and Molecules. PTIM 2015. 2-4 Noviembre 2015. Caparica - Portugal.
- Rubio-Clemente A., Chica E., & Peñuela G. Degradación de contaminantes emergentes de las aguas: alternativas de tratamiento a los procesos convencionales. 2<sup>a</sup> Feria Internacional y III Exposalud. 16 y 17 de octubre de 2015. Universidad de Córdoba. Montería.

## TABLE OF CONTENTS

ACKNOWLEDGMENTS

RESEARCH RESULTS

TABLE OF CONTENTS

ABSTRACT .....	15
1. INTRODUCTION.....	24
2. LITERATURE REVIEW .....	37
3. ANALYTICAL METHODS.....	67
4. WATER TREATMENT.....	127
5. CONCLUDING REMARKS .....	203
REFERENCES .....	219
APPENDIX .....	231



## ABSTRACT

Nowadays, polycyclic aromatic hydrocarbons (PAHs) are a group of chemical substances that deserves a great attention. PAHs consist of two or more condensed benzene rings, bonded in linear, cluster or angular arrangements that are ubiquitous in the environment. Due to their low solubility and high affinity for particulate matter, PAHs are found in water in extreme low concentrations, in the range of  $\text{ng L}^{-1}$  or  $\mu\text{g L}^{-1}$ . However, even at these ultra-trace or trace levels, they exhibit harmful effects on living beings and humans, especially when present as mixtures. That is the case of anthracene (AN), which has been reported as an acute phototoxic compound, and benzo[a]pyrene (BaP), which is a carcinogenic and mutagenic pollutant. Therefore, their presence in the environment and, specifically in aquatic resources must be monitored. For this purpose, the chromatographic behavior of AN and BaP was studied, and three models were found describing the identification of AN and BaP, the quantification of AN and that of BaP. The factors influencing each of the models or indexes were also optimized and a new and fast analytical method allowing the determination of the analytes of interest at ultra-trace concentrations in surface water samples was developed.

In addition to monitor the target pollutants, they must be also eliminated from water because of the adverse health effects associated. However, conventional processes water treatment facilities are operating with are not efficient in tackling the problem of AN and BaP pollution in water. In this regard, the implementation of alternative treatments, including advanced oxidation processes (AOPs), provides a very attractive option. AOPs have demonstrated to be highly interesting technologies for water remediation, particularly the combination of ultraviolet radiation in the UV-C range (UV-C) and hydrogen peroxide ( $\text{H}_2\text{O}_2$ ).

This Thesis addresses the evaluation of the efficiency of the UV-C/ $\text{H}_2\text{O}_2$  oxidation system to treat water sampled from a natural reservoir polluted with AN and BaP. For this purpose, initially, the removal profiles of AN and BaP were

investigated, as well as the organic matter mineralization capacity of the oxidation system and the production of innocuous degradation by-products. The system allowed obtaining very positive results in terms of the degradation of the pollutants of interest and the organic matter mineralization, avoiding the production of dangerous reactive intermediates. Furthermore, after the application of this treatment process, a residual  $\text{H}_2\text{O}_2$  was observed in the reaction solution, which can be used for additional microbial load removal. The residual  $\text{H}_2\text{O}_2$  found within the bulk after the application of the oxidation treatment was analyzed using an analytical method proposed here. Moreover, the oxidation potential of the UV-C/ $\text{H}_2\text{O}_2$  process was assessed for the inactivation of wild total coliforms naturally contained in the water of study and the results were compared with the findings obtained from other photochemical technologies based on sonochemical reactions. It was found that the technology achieving the highest microorganism elimination in the shortest time and with the lowest electrical costs results was the UV-C/ $\text{H}_2\text{O}_2$  process. Nevertheless, in spite of that, it is worth noting that the implementation of the UV-C/ $\text{H}_2\text{O}_2$  oxidation process still requires high electrical needs, which increases the operating costs of the process. Therefore, in order to reduce such as costs, a photovoltaic (PV) array was sized and installed for supplying the energy requirements of the selected water treatment system. The installed PV system allows for the use of renewable energy both in developing and non-developing countries. In this regard, the treatment of water to be drinkable was observed to be plausible in countries with lack of economical resources and in communities far from the electrical grid, which exist in a high number in countries such as Colombia.

In the second stage of the research, and taking into account the necessity of having kinetic models for finding out the optimal operating conditions without the necessity of conducting extensive experimentation, a kinetic model for the performance of the UV-C/ $\text{H}_2\text{O}_2$  oxidation process was constructed and validated using a model compound. The kinetic model allows calculating the optimal level of  $\text{H}_2\text{O}_2$  for efficiently degrading the pollutant of interest, as well as the effective level of  $\text{HO}^\bullet$  to be maintained throughout the reaction time of the UV-C/ $\text{H}_2\text{O}_2$  system for achieving an efficient pollutant degradation, contributing to save costs and time.



---

**Keywords:** Water treatment; advanced photochemical processes; kinetic modelling; bacterial inactivation; UV-C/H<sub>2</sub>O<sub>2</sub> process; residual H<sub>2</sub>O<sub>2</sub>; reaction intermediates



## RESUMEN

Hoy en día, los hidrocarburos aromáticos policíclicos (HAPs) son un grupo de sustancias químicas que merecen una gran atención. Los HAPs constan de dos o más anillos de benceno condensados, unidos en disposiciones lineales, agrupadas o angulares, los cuales están ampliamente distribuidos en el medio ambiente. Debido a su baja solubilidad y alta afinidad por la materia particulada, los HAPs se encuentran en el agua en concentraciones extremadamente bajas, en el rango de  $\text{ng L}^{-1}$  o  $\mu\text{g L}^{-1}$ . Sin embargo, incluso a estos niveles ultra-trazas o trazas, exhiben efectos dañinos en los seres vivos y en humanos, especialmente cuando están presentes formando mezclas. Tal es el caso del antraceno (AN), caracterizado por su foto-toxicidad aguda, y el benzo[a]pireno (BaP), el cual ha sido informado como un contaminante carcinogénico y mutagénico. Por lo tanto, su presencia en el medio y, específicamente, en los recursos hídricos debe ser monitoreada. Para este propósito, se estudió el comportamiento cromatográfico del AN y BaP, y se encontraron tres modelos que describen la identificación de AN y BaP, la cuantificación de AN y la de BaP. Los factores que influyen en cada uno de los modelos o índices anteriores fueron optimizados, de modo que se desarrolló un nuevo y rápido método analítico que permite la determinación de los analitos de interés en concentraciones ultratrazas en muestras de agua superficial.

Además de monitorear los contaminantes objeto de estudio, también deben eliminarse del agua dados los efectos adversos asociados. Sin embargo, los procesos convencionales de las instalaciones de tratamiento de agua no son efectivos para abordar el problema de la contaminación del agua con AN y BaP. En este sentido, la implementación de tratamientos alternativos, incluyendo los procesos avanzados de oxidación (PAOs), ofrece una opción de gran atractivo. Los PAOs han demostrado ser tecnologías altamente interesantes para la remediación del agua, particularmente la combinación de radiación ultravioleta en el rango UV-C (UV-C) y el peróxido de hidrógeno ( $\text{H}_2\text{O}_2$ ).

Esta Tesis evalúa la eficiencia del sistema de oxidación UV-C/ $\text{H}_2\text{O}_2$  en el tratamiento de agua procedente de un reservorio natural contaminada con AN y

BaP. Para este propósito, inicialmente, se investigaron los perfiles de remoción de AN y BaP, así como la capacidad de mineralización de la materia orgánica por parte del sistema de oxidación y la producción de subproductos de degradación inocuos. El sistema permitió obtener resultados muy positivos en términos de degradación de los contaminantes de interés y mineralización de la materia orgánica, evitando la producción de peligrosos intermediarios de reacción. Además, después de la aplicación de este tratamiento, se observó en la solución de reacción un  $\text{H}_2\text{O}_2$  residual, el cual puede ser usado para la eliminación de la carga microbiana adicional. El  $\text{H}_2\text{O}_2$  residual encontrado en la solución después de la aplicación del tratamiento de oxidación se analizó utilizando un método analítico propuesto. Además, se evaluó el potencial de oxidación del sistema UV-C/ $\text{H}_2\text{O}_2$  para la inactivación de coliformes totales contenidos de manera natural en el agua de estudio y los resultados se compararon con los obtenidos por otras tecnologías fotoquímicas basadas en reacciones sonoquímicas. Se encontró que el sistema que consiguió la mayor eliminación de microorganismos, en el menor tiempo posible y con los menores costes eléctricos resultó ser el proceso UV-C/ $\text{H}_2\text{O}_2$ . Sin embargo, a pesar de ello, cabe destacar que la implementación del proceso de oxidación UV-C/ $\text{H}_2\text{O}_2$  aún requiere altas necesidades eléctricas, lo que aumenta los costos del proceso. Por lo tanto, con el fin de reducir dichos costes, se dimensionó e instaló un arreglo fotovoltaico (FV) para suministrar los requerimientos de energía necesarios para llevar a cabo el sistema de tratamiento de agua seleccionado. Además, el sistema FV instalado permite el uso de energía renovable tanto en países en vías de desarrollo como desarrollados. En este sentido, se observó que la producción de agua potable es posible en países con falta de recursos económicos y en comunidades alejadas de la red eléctrica, las cuales existen en gran cantidad en países como Colombia.

En una segunda etapa de la investigación, y teniendo en cuenta la necesidad de tener modelos cinéticos para conocer las condiciones óptimas de operación sin necesidad de realizar una extensa experimentación, se construyó y validó un modelo cinético para el proceso de oxidación UV-C/ $\text{H}_2\text{O}_2$  utilizando un compuesto modelo. El modelo cinético permite calcular el nivel de  $\text{H}_2\text{O}_2$  óptimo para degradar el contaminante de interés, así como la concentración de  $\text{H}_2\text{O}_2$  efectiva a ser mantenida a lo largo del tiempo de reacción del sistema UV-C/ $\text{H}_2\text{O}_2$

para lograr una degradación de los contaminantes eficiente, contribuyendo a ahorrar costes y tiempo.

**Palabras clave:** Tratamiento de agua; procesos avanzados fotoquímicos; modelado cinético; inactivación bacteriana; proceso UV-C/H<sub>2</sub>O<sub>2</sub>; H<sub>2</sub>O<sub>2</sub> residual; degradación de HAPs; intermediarios de reacción



# **INTRODUCTION**





## 1. INTRODUCTION

The increasing worldwide contamination of the aquatic environment with micropollutants, including emerging contaminants, has aroused considerable international concerns (Ma et al., 2018; Hebert et al., 2018; Tröger et al., 2018) since they can pose a potential threat to ecosystems and/or human health even at trace and ultra-trace concentrations (Ma et al., 2018; Tröger et al., 2018). This is the case of polycyclic aromatic hydrocarbons (PAHs) (Rubio-Clemente et al., 2014).

PAHs are widespread contaminants in the environment (Zeng et al., 2018; Rubio-Clemente et al., 2014). They can be originated from various sources by thermal combustion processes, vehicular emissions and biomass burning (Zeng et al., 2018). PAHs are often accumulated in various environmental systems, including water (Pogorzelec & Piekarska, 2018). They can enter water supply by gaseous exchange in the air-water interface, dry deposition of particulate matter, wet deposition (rainfall) and urban runoff (Pogorzelec & Piekarska, 2018; Abdel-Shafy & Mansour, 2016). PAHs, generally, occur as mixtures and not as single compounds (Abdel-Shafy & Mansour, 2016). Although their concentration in aqueous environmental systems is very low, in the order of  $\mu\text{g L}^{-1}$  and  $\text{ng L}^{-1}$ , due to their low water solubility, they are of great importance since they are listed as priority pollutants (Zeng et al., 2018). PAHs can alter the immune system, making living beings prone to suffer from several illnesses. Additionally, PAHs have been reported as endocrine disrupters, and the reason why PAHs are at the top of the priority substances list is the toxicity associated, and their carcinogenic, mutagenic and teratogenic potential (Pogorzelec & Piekarska, 2018; Wang et al., 2018; Zeng et al., 2018; Abdel-Shafy & Mansour, 2016; Vela et al., 2012). Especially, anthracene (AN) and benzo[a]pyrene (BaP) are characterized by the acute phototoxicity of the former one (Lee, 2003) and the carcinogenicity and mutagenicity of the latter one (Fernández-González et al., 2007; Liu & Koneraga, 2001). Consequently, they are regulated in developed countries, such as the European Union, by the relatively recent and stringent Directive 2013/39/EU of the European Parliament and of the Council of 12 August 2013 amending

Directives 2000/60/EC and 2008/105/EC as regards priority substances in the field of water policy (Directive, 2013). In developing countries; e.g., Colombia, PAHs are regulated in the Resolution 2115 of 2007 of the Ministry of Social Protection, Ministry of Environment, Housing and Territorial Development of 7 June 2007, by means of which the characteristics, basic tools and frequencies of the control and monitoring system related to water quality for human consumption are established (Resolution, 2007). Unfortunately, the cited regulation is not as restrictive as international ones. Therefore, in Colombia, PAHs can be found in drinking water at a concentration higher than in the natural environment in European countries.

Because of the physico-chemical properties of PAHs, and focusing on AN and BaP, due to their harmful effects on living beings and humans, they can be normally found in aqueous environments at ultra-trace level (Santos et al., 2018; Sharma et al., 2018; Zeng et al., 2018; Vela et al., 2012), as described previously. This aspect, along with the use of real water matrices, characterized by the presence of a number of constituents that can interfere the analytical method, limit PAH monitoring and control (Rubio-Clemente et al., 2018a; 2017a).

It is important to note that, in recent times, a number of analytical methods for PAH identification and quantification have been developed (Khodae et al., 2016; Petridis et al., 2014; Chizhova et al., 2013; Oliferova et al., 2005). Nevertheless, separation and pre-concentration phases are required; with the subsequent possible losses of important amount of the target analytes. In addition, the contamination of the samples can occur (Rubio-Clemente et al., 2018a). Furthermore, multistep analytical methods are time consuming and suppose a tedious process (Rubio-Clemente et al., 2017a). In this regard, alternative analysis methods must be developed and validated. Consequently, large-volume injection techniques are proposed (Boix et al., 2015), which can be used with reversed-phase high-performance liquid chromatography (RP-HPLC) and gas chromatography (GC), and be combined with fluorescence detector (FLD) or diode array detector, and even with mass spectrometry, finding out accurate and repeatable results within a short period of analysis, without incurring high costs, neither the contamination of the sample nor the loss of the analytes of interest (Rubio-Clemente et al., 2017a).

From this chromatographic techniques, HPLC offers a vast number of benefits since it can be used for monitoring pollutants contained in environmental matrices. Additionally, HPLC develops an important role in several applications in biological and pharmaceutical analyses, food technology and industrial-related processes, among others (Engelhardt, 2012; García & Pérez, 2012). HPLC consists of the separation of the compounds of interest from other interfering substances also present in the same matrix. This fact allows potentially quantifying substances existing in the target matrix at extremely low concentrations (Hernández & González, 2002; Engelhardt, 2012; García & Pérez, 2012).

In this way, considering the advantages linked to the use of HPLC and taking profit of the fluorescent properties exhibited by the target PAHs, the combination of HPLC with FLD has ascribed several benefits compared to other chromatographic techniques, namely higher selectivity and lower cost. Moreover, HPLC allows good separation of compounds with similar physicochemical properties (Rubio-Clemente et al., 2017a). Nevertheless, it must be noted that, for a sensitive determination of the compounds of interest with a good resolution, the chromatographic conditions are recommended to be optimized using chemometric tools, such as principal component analysis (PCA) and design of experiments (DOE) (Ebrahimi-Najafabadi et al., 2014; Ferreira et al., 2007).

The monitoring of AN and BaP in environmental samples is of special concern nowadays. Nonetheless, considering the risk associated with the presence of such as compounds in the environment, as mentioned above, especially in aqueous resources, they must be also eliminated from water.

Nowadays, water treatment plants operate with conventional physical, chemical and biological processes that can be very efficient for some specific compounds; however, they can be inefficient for other substances, especially those pollutants with a high hydrophobic character, such as PAHs, which would pass from an aqueous phase to a solid or gas phase during water treatment without being degraded (Pogorzelec & Piekarska, 2018). Therefore, the development of alternative treatments is required and advanced oxidation processes (AOPs) are regarded as an attractive option (Lopez-Alvarez et al., 2016; Ribeiro et al., 2015).

AOPs can operate using several external energy sources, such as electromagnetic radiation, comprised between the ultraviolet (UV-C, UV-B and UV-A) and visible range; electric power; and even ultrasound energy (Rubio-Clemente et al., 2014). Additionally, reactants, such as oxidizing agents (e.g., H<sub>2</sub>O<sub>2</sub>, O<sub>3</sub>, etc.) and catalysts, either homogeneous or heterogeneous, are also needed for the performance of some AOPs (Ribeiro et al., 2015). Nevertheless, regardless of the type of energy source and reagents used, AOPs are characterized by the generation of very reactive and non-selective oxygen species, such as hydroxyl radicals (HO•). HO• has associated a high oxidation potential (E<sup>0</sup> = 2.8 V) (Litter & Quici, 2010), making possible its rapid reaction with pollutants in water, including AN and BaP, with their subsequent destruction (Rubio-Clemente et al., 2014). The reaction between HO• and the target compounds produces intermediate compounds, which undergo further oxidation until their complete oxidation or mineralization (i.e., the production of CO<sub>2</sub> and H<sub>2</sub>O) (Miklos et al., 2018; Rozas et al., 2016). For the photochemical AOPs to be performed, several influencing operating factors, such as the type and intensity of the energy source, the reactant concentration, and the reaction time, among other parameters, may be considered while the oxidation technology is implemented (Miklos et al., 2018; Litter & Quici, 2010).

There are several studies reporting AOPs as effective treatments for PAH removal, including AN and BaP. Among the photochemical AOPs, the UV-C/H<sub>2</sub>O<sub>2</sub> system has been used with very positive results (Rubio-Clemente et al., 2014).

The UV-C/H<sub>2</sub>O<sub>2</sub> process consists of the production of HO• when photons, with wavelengths associated lower than 300 nm, impact on H<sub>2</sub>O<sub>2</sub> or its conjugated base (HO<sub>2</sub><sup>-</sup>), causing the photolysis of the oxidizing agent (Rodríguez-Chueca et al., 2018; Gassie & Englehardt, 2017), as represented by Eq. 1.



Additionally, the UV-C/H<sub>2</sub>O<sub>2</sub> system can benefit from the direct photolytical effect of UV-C radiation and the oxidation potential of the H<sub>2</sub>O<sub>2</sub> (Gassie & Englehardt, 2017).

It is important to note that the referred alternative oxidation technology has been widely reported as an efficient water treatment when water is polluted with recalcitrant compounds. Additionally, the mentioned process has been utilized for disinfection purposes, as well as the process where UV-C radiation is combined with ultrasounds (US) and simultaneously with US and H<sub>2</sub>O<sub>2</sub> (Hulsman et al., 2010; Bounty et al., 2012; Penru et al., 2012; Rubio-Clemente et al., 2014; Gassie & Englehardt, 2017; Urbano et al., 2017; Giannakis et al., 2018a; Malvestiti & Dantas, 2018).

When US is applied to the water studied, cavitation bubbles are formed, which implode, leading to the generation of HO• (Miklos et al., 2018), as expressed in Eq. 2. During the sonochemical treatment of water, H<sub>2</sub>O<sub>2</sub> can be also formed (Rubio-Clemente et al., 2014). When US is implemented in combination with the UV-C/H<sub>2</sub>O<sub>2</sub> system or the action of UV-C radiation alone, the H<sub>2</sub>O<sub>2</sub> formed internally in the system can be also photolyzed, and the amount of HO• formed is increased in comparison with the HO• generated when US is used individually. In addition, H<sub>2</sub>O<sub>2</sub> can be added externally, promoting the generation of HO•, among other reactive oxygen species (ROS) (Rubio-Clemente et al., 2018b).



During the application of the mentioned systems, the water matrices utilized are usually synthetic ones, based on distilled or deionized water that is spiked with the compounds of interest or the bacterial load to be studied. In order to have a deeper knowledge about the feasibility of a new process to be implemented at large scale, it is necessary to use real matrices while the laboratory-scale experiments are being conducted since the background constituents in natural water develop a crucial role in the efficiency of the tested treatment, as some components of the water can act as HO• scavengers and radiation screeners; reducing, therefore, the efficiency of the system both in terms of degradation of the target pollutants and microbial load destruction (Souza et al., 2014; Matilainen & Sillanpää, 2010). Furthermore, the organic matter cannot be effectively mineralized, so that the chances of disinfection by-product formation might be increased. Moreover, degradation by-products more toxic

than the initial parent compounds can be found following the lack of efficiency of the oxidation process (Rubio-Clemente et al., 2018b).

In addition, concerning the efficiency of the advanced oxidation processes selected for the bacterial load removal, the use of wild bacterial load is of utmost importance since in laboratory strains, either commercial laboratory strains or natural microorganisms extracted and relocated into the laboratory, microorganisms are grown under optimized ideal conditions as individuals (Palkova, 2004). When microorganisms are grown under natural conditions, they develop strategies and mechanisms to be protected against non-favourable conditions since they are prone to be organized into multicellular communities (Palkova, 2004; De la Fuente-Núñez et al., 2013; Lyons & Kolter, 2015) and even are forming consortia with other organisms in water (Bridier et al., 2011).

Therefore, the results obtained using synthetic water matrixes and microorganisms that are grown in the laboratory would not reflect the real effectiveness of the alternative oxidation processes tested. This fact should be taken into account in order to obtain results under conditions close to reality, which is of great importance when implementing a treatment system at large scale (Rubio-Clemente et al., 2018b).

A parameter to be taken into consideration when studying the efficiency of a system for water treatment is the residual  $H_2O_2$  present in the studied water, since when water is going to be release into the environment, such as residual  $H_2O_2$  can alter aquatic ecosystems due to the biocidal action ascribed (Linley et al., 2012). However, in some occasions, the excess of  $H_2O_2$  that remains in the treated water can develop a main function as disinfectant, guarantying the distribution of water of quality, but it could be also involved in the formation of disinfection by-products.

Several methodologies for  $H_2O_2$  determination in aqueous samples have been reported; nonetheless, the more appropriate one was the analytical method developed by Pupo et al. (2005). This method can be used for analysing  $H_2O_2$  in several water samples, but its limit of quantification is limited to  $\sim 0.85 \text{ mg L}^{-1}$ . Consequently, more sensitive methods for the analysis of  $H_2O_2$  at lower levels are required (Rubio-Clemente et al., 2017b).

AOPs can be very effective for water treatment, as mentioned previously; however, generally, they are costly processes, particularly because of the electricity consumption required (Rubio-Clemente et al., 2018c). Consequently, in order to reduce the costs of operation of the process, distributed electrical power generation systems with renewable energy sources can be used (Rahamanov et al., 2013). Distributed generators can provide high reliability by providing on-site generation. As a result, many hybrid systems come in existence, including PV and fuel cells, wind microturbines and small hydrokinetic systems, among others (Rubio-Clemente et al., 2018c).

When renewable resources are being used for electricity generation, the climatological conditions and geographical location of the country or area where the system is going to be applied must be taken into consideration (Rubio-Clemente et al., 2018c). For the particular case of Colombia, a great potential in terms of renewable energy generation is observed, specifically from biomass, water, wind and sun resources. Nonetheless, the use of the energy contained in the biomass, water and wind share several disadvantages that can be overcome by the use of sun as resource (ESMAP, 2010; ECLAC, 2004). In this way, the use of solar energy could be one of the best sources of energy alternative to the conventional ones. In Colombia, thanks to its location in the equatorial zone, solar irradiation hits almost parallel to the terrestrial surface, with the subsequent high amount of energy per area with regard to other regions where the sun rays stroke more obliquely. In this regard, photovoltaic (PV) cells might be a good option for harvesting sunlight and converting it directly into electricity (Ortiz et al., 2008); aspect that is particularly interesting for non-interconnected zones (NIZs) to the electrical grid, which account for just over half the territory of Colombia. In consequence, the use of PV systems in these areas could allow the production of water of quality and, subsequently, the development of these isolated communities (Rubio-Clemente et al., 2018c).

As indicated previously, when a treatment process is going to be implemented at large scale, a previous phase in the laboratory is required so that to understand the fundamentals of the process and to optimize it (Zuorro et al., 2014), consequently, according to the type and properties of the water to be treated. In order to reduce experimental costs and make the process more feasible

for large-scale implementation, kinetic models can be a very useful tool during the optimization of the operating conditions of the treatment process to be implemented (Rubio-Clemente et al., 2017c; 2017d).

In the literature, a number of mathematical models regarding the kinetic conversion of several pollutants and substances for different AOPs have been reported (Yao et al., 2013; Wols & Hofman-Caris, 2012; Audenaert et al., 2011; Song et al., 2008; Primo et al., 2007; Rosenfeldt & Linden, 2007; Crittenden et al., 1999; Hong et al., 1996; Huang & Shu, 1995; Liao & Gurol, 1995). Depending on the kinetic model to be considered, the set of ordinary differential equations (ODE) defining the studied pollutant degradation rate can be simplified into a pseudo-first-order kinetic expression, whose solution is an exponential one. In such as models, experimental results are fit to that solution (Yao et al., 2013; Primo et al., 2007; Rosenfeldt & Linden, 2007). Subsequently, model predictions agree well with laboratory data. In that kind of models the calculated reaction rate constants for the tested pollutant degradation are apparent reaction rate constants (identified as  $K_{app}$ ), which include pollutant removal reaction rate constants and the values of parameters such as the quantum yield for the oxidant, the conjugate base ( $HO_2^-$ ), and the contaminant photolysis, the initial level of the chemical species involved in pollutant oxidation, the optical path length of the system, the UV-light intensity, and the molar extinction coefficients of  $H_2O_2/HO_2^-$  and pollutant, among others. Therefore, knowing those parameters is not required.

Other kinetic models, in turn, consider that reactive chemical species, like  $HO^\bullet$ , are transient ones, and their level can be presumed to be at a pseudo-steady state (Rosenfeldt & Linden, 2007; Hong et al., 1996; Liao & Gurol, 1995). Therefore, they are based on the pseudo-steady state approximation assumption to calculate the concentration of such as chemical species. The non-pseudo-steady state premise is also applied for calculating the concentration of such as reactive chemical species (Yao et al., 2013; Wols & Hofman-Caris, 2012; Audenaert et al., 2011; Song et al., 2008; Primo et al., 2007; Rosenfeldt & Linden, 2007; Crittenden et al., 1999; Hong et al., 1996; Huang & Shu, 1995; Liao & Gurol, 1995).

On the other hand, it is important to take into account that during the performance of the UV-C/ $H_2O_2$  system, in addition to  $HO^\bullet$ , hydroperoxyl radicals



(HO<sub>2</sub><sup>\*</sup>) are also formed, which can also react with pollutants in water and cause their degradation. Therefore, the production of HO<sub>2</sub><sup>\*</sup> should also be included when developing a kinetic model for the conclusions obtained are more accurate. However, none of the referred kinetic models consider the role developed by the HO<sub>2</sub><sup>\*</sup> in the conversion of the target pollutant, with the exception of Huang and Shu (1995), and Liao and Gurol (1995) models. Additionally, some of these models cannot be reproduced unless a conversion factor is included, as demonstrated by Audenaert et al. (2011).

Under this scenario, in this research, the problem of real surface water pollution with refractory contaminants, exposed previously, is intended to be solved by the application of advanced oxidation processes alternative to conventional systems water treatment facilities are operating with, in order to expand horizons in the field of water treatment.

---

This Thesis is written and structured as a compendium of several short scientific or academic pieces of work that are interrelated with each other and are already published. In the whole set of works, the candidate is the main or first author of the publications. The works have been previously peer reviewed by several referees and editors of various journals and publishing houses. Both the supervisors and the PhD. student chose the format related to a compendium of several academic works because when a compilation thesis is written, the PhD. candidate is contributing towards the publication statistics of the University right from the start of her studies. Additionally, by writing the thesis as a compendium of research works, the PhD. student is involved in the publishing and the peer review management processes.

Below, the integrated nature of the whole research is described to provide a comprehensive overview and coherence of the entire document.

After this first introductory Chapter, a review article is opening the compilation of the presented works. This paper conforms Chapter 2 of the current Thesis. The research is focused on the current state of knowledge concerning PAHs, including their physicochemical properties, input sources, occurrence, adverse effects and conventional and alternative chemical processes applied for their removal from water. The paper intends to bring reader's attention to the implementation of AOPs for tackling the problem of PAHs water pollution, especially by the application of photochemical oxidation systems, such as the combination of UV-C and an oxidizing agent, like H<sub>2</sub>O<sub>2</sub>, because of the positive results ascribed to the use of these processes for the treatment of effluents containing PAHs. This work laid the groundwork for the selection of two PAHs, whose behavior was studied. The referred PAHs were AN, with a high acute photo-toxicity, and BaP, which exhibits a carcinogenic and mutagenic potential. In addition, the referred work allowed for the selection of the operating condition ranges under which the AOP was tested.

Afterwards, and considering the limitations of monitoring the presence of the selected compounds in real aqueous environmental matrices, especially when the analytes are found in the range of ng L<sup>-1</sup> and µg L<sup>-1</sup>, sometimes even below the detection limit of the used analytical methods, a second work was conducted to develop an analytical method able to identify and quantify the substances of interest; i.e., AN and BaP. The chromatographic behavior of the target analytes under the conditions tested was studied, obtaining three indexes representing the identification of the compounds tested, the quantification of AN and that of BaP. The parameters having the main influence in the HPLC system, which was coupled to a fluorescence detector and operated in reversed-phase, were subsequently optimized using chemometric tools. Then, the method was validated for the separation and quantification of AN and BaP at ultra-trace levels in aqueous samples by direct injection. The phases involved in the development of this analytical method are described in Chapter 3. Additionally, in this Chapter a brief review on the use of HPLC and statistical multivariate techniques for analytical method development is exposed; as well as the steps involved in the development of an analytical method able to determine residual concentrations of H<sub>2</sub>O<sub>2</sub>.

Once the analytical method for the determination of AN and BaP in real water matrices was developed, the AOP chosen in a previous phase was applied for investigating the efficiency of such as alternative oxidation treatment in degrading the mixture of AN and BaP, and mineralizing the organic matter in the surface water used during the experimentation, without the production of reactive intermediates more dangerous than the parent compounds. The microbial load destruction capacity of the system was also evaluated and the results were compared to those ones obtained using the UV-C/US/H<sub>2</sub>O<sub>2</sub> and UV-C/US advanced oxidation technologies. This research is included in Chapter 4.

Due to the most promising results were obtained by the UV/H<sub>2</sub>O<sub>2</sub> process, in terms of microorganism destruction from water, and along with the positive findings achieved for the conversion of the target PAHs and the organic matter naturally contained in the natural water of study, without the generation of harmful degradation by-products, the combination of the UV-C and the H<sub>2</sub>O<sub>2</sub> was selected for further studies focused on reducing the electrical costs ascribed to the implementation of such as process. For this purpose, a PV array was sized, installed and applied. The research carried out on this issue is also described in Chapter 4.

Furthermore, in this Chapter, a kinetic model for the treatment of water by using UV photolysis and UV-C/H<sub>2</sub>O<sub>2</sub> AOP under low-pressure UV-C lamps is described by two works. The model includes the background matrix effect, as well as the reaction intermediate action and the pH evolution as the treatment is applied. In the first related work, the type of assumption considered to calculate the concentration of reactive chemical species, such as HO<sup>•</sup>, was investigated; as well as the role developed by HO<sub>2</sub><sup>•</sup>, with the subsequent calculation of the reaction kinetic rate between the radical and the target compound. Moreover, in the first work on the kinetic model describing the UV-C/H<sub>2</sub>O<sub>2</sub> process, the presence of an effective HO<sup>•</sup> level to be maintained during the treatment time for an effective degradation of the pollutants of interest was investigated. In the second related work, in turn, the kinetic model developed was applied and validated.

In Chapter 5, a brief summary of the results obtained and their corresponding discussion is addressed. Additionally, the conclusions and future perspectives derived from this Thesis are covered.

Finally, the researches referenced here are listed.

In each of the works compiled in the Thesis, the reagents and materials, as well as the analytical methods and all the aspects related to the experimental part used throughout this research are described in detail.

# **LITERATURE REVIEW**

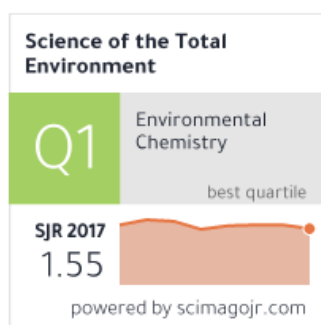


## 2. LITERATURE REVIEW

### Paper

#### Removal of polycyclic aromatic hydrocarbons in aqueous environment by chemical treatments: A review

### Journal



**Scope:** The journal is an international medium for publication of original research on the environment with emphasis on changes caused by human activities. It is concerned with changes in the natural levels and distribution of chemical elements and their compounds that may affect the well-being of the living world, or represent a threat to human health.

### Highlights

- PAHs are present in aquatic ecosystems and affect human health and living beings.
- Conventional water treatments can be unsuccessful in PAH degradation.
- AOPs and their simultaneous combination generally result in high PAH conversions.
- AOPs coupled to biotreatments could be a cost-effective solution for PAH removal.







Contents lists available at ScienceDirect

## Science of the Total Environment

journal homepage: [www.elsevier.com/locate/scitotenv](http://www.elsevier.com/locate/scitotenv)

## Review

## Removal of polycyclic aromatic hydrocarbons in aqueous environment by chemical treatments: A review

Ainhoa Rubio-Clemente<sup>a</sup>, Ricardo A. Torres-Palma<sup>b,\*</sup>, Gustavo A. Peñuela<sup>a</sup><sup>a</sup> Grupo de Diagnóstico y Control de la Contaminación – GDCON, Facultad de Ingeniería, Sede de Investigaciones Universitarias (SIU), Universidad de Antioquia UdeA, Calle 70, No. 52-21, Medellín, Colombia<sup>b</sup> Grupo de Investigación en Remediación Ambiental y Biotatálisis, Instituto de Química, Facultad de Ciencias Exactas y Naturales, Universidad de Antioquia UdeA, Calle 70, No. 52-21, Medellín, Colombia

## HIGHLIGHTS

- PAHs are present in aquatic ecosystems and affect human health and living beings.
- Conventional water treatments can be unsuccessful in the PAH degradation.
- AOPs and their simultaneous combination generally result in high PAH conversions.
- AOPs coupled with biotreatments could be a cost-effective solution for PAH removal.

## ARTICLE INFO

## Article history:

Received 9 October 2013

Received in revised form 30 December 2013

Accepted 30 December 2013

Available online 16 February 2014

## Keywords:

Polycyclic aromatic hydrocarbon

Wastewater treatment

Ozonation

Photolysis

Advanced oxidation process

## ABSTRACT

Due to their carcinogenic, mutagenic and teratogenic potential, the removal of polycyclic aromatic hydrocarbons (PAHs) from aqueous environment using physical, biological and chemical processes has been studied by several researchers. This paper reviews the current state of knowledge concerning PAHs including their physico-chemical properties, input sources, occurrence, adverse effects and conventional and alternative chemical processes applied for their removal from water. The mechanisms and reactions involved in each treatment method are reported, and the effects of various variables on the PAH degradation rate as well as the extent of degradation are also discussed. Extensive literature analysis has shown that an effective way to perform the conversion and mineralization of this type of substances is the application of advanced oxidation processes (AOPs). Furthermore, combined processes, particularly AOPs coupled with biological treatments, seem to be one of the best solutions for the treatment of effluents containing PAHs.

© 2014 Elsevier B.V. All rights reserved.

## Contents

1.	Introduction . . . . .	202
2.	Background . . . . .	202
2.1.	PAHs: definition, classification and physico-chemical properties . . . . .	202
2.2.	Emission sources and occurrence in the environment . . . . .	202
2.3.	Adverse effects of PAHs . . . . .	203
3.	Chemical removal techniques . . . . .	203
3.1.	Conventional processes . . . . .	203
3.1.1.	Ozonation . . . . .	203
3.1.2.	Direct photolysis . . . . .	211
3.2.	Advanced oxidation processes . . . . .	213
3.2.1.	Ozone-based AOPs: UV/O <sub>3</sub> and O <sub>3</sub> /H <sub>2</sub> O <sub>2</sub> . . . . .	214
3.2.2.	Ultraviolet radiation and hydrogen peroxide (UV/H <sub>2</sub> O <sub>2</sub> ) . . . . .	215
3.2.3.	Fenton, photo-Fenton and related processes . . . . .	216
3.2.4.	Heterogeneous photocatalysis with semiconductors . . . . .	217
3.2.5.	Advanced oxidation processes using ultrasound energy . . . . .	219

\* Corresponding author. Tel.: +57 4 219 56 69; fax: +57 4 219 56 66.  
E-mail address: [rtorres@matematicas.udea.edu.co](mailto:rtorres@matematicas.udea.edu.co) (R.A. Torres-Palma).

3.2.6. Electrochemical oxidation	220
3.3. Future perspectives	221
4. Conclusions	222
Nomenclature	222
Acknowledgments	222
References	222

## 1. Introduction

PAHs are a type of organic compounds that consist of two or more condensed benzene rings and/or pentacyclic molecules that are arranged in various chemical configurations. These compounds are formed primarily from the incomplete combustion or pyrolysis of organic material such as oil, petroleum, gas, coal, and wood (González et al., 2012; Manariotis et al., 2011). PAHs have recently attracted a lot of attention in studies on water, soil and air pollution because some of them are highly carcinogenic, mutagenic and teratogenic substances (Busetti et al., 2006; Manoli and Samara, 2008; Menzie et al., 1992; Reynaud and Deschaux, 2006). Additionally, PAHs are persistent organic pollutants due to their chemical stability and biodegradation resistance. For these reasons, they are strictly regulated by law in most industrialized countries. However, many of them are not regulated in developing countries. Several PAHs have been identified by the US-EPA and the European Union (WFD, 2000/60/EC) as priority pollutants in order to reduce the release of these compounds into the environment (Busetti et al., 2006; Manoli and Samara, 2008). In fact, a maximum admissible concentration for the most dangerous PAHs in the environment has been set (WFD, 2008/105/EC).

The removal of such substances from the environment can be performed through physical, biological and chemical processes (Fatone et al., 2011; Manoli and Samara, 2008; Tian et al., 2012; Veignie et al., 2009; Vela et al., 2012; Zeng et al., 2000a). In the case of removing PAHs from aqueous systems, physical processes, such as volatilization and adsorption, have an important role, greatly reducing the amount of PAHs in the water. Nevertheless, physical processes do not solve the problem of PAH pollution because of their inability to degrade these contaminants. For this reason, biological and chemical degradation processes are generally preferred (Veignie et al., 2009; Vela et al., 2012; Zeng et al., 2000a,b). However, due to the biorecalcitrant, toxic character and low aqueous solubility of PAHs, conventional biological systems exhibit limited contribution to PAH removal from water (Manoli and Samara, 2008; Mueller et al., 1989). Therefore, chemical processes may be the most efficient for the conversion of these substances. Among the chemical techniques, direct photolysis is one of the major transformation processes affecting the fate of PAHs in the aquatic environment (Vela et al., 2012). Furthermore, PAHs may undergo oxidation through ozonation (Beltrán et al., 1999; Bernal-Martinez et al., 2007, 2009; Ledakowicz et al., 2001; Zeng et al., 2000b) and chlorination (Manoli and Samara, 2008), among other processes. Advanced oxidation processes (AOPs) have also been broadly investigated. AOPs are techniques that use the highly oxidant and non-selective hydroxyl radical ( $^{\circ}\text{OH}$ ), which is able to react with almost all types of organic compounds, to lead to their total mineralization or the formation of more biodegradable intermediates (Glaze et al., 1987).

In recent years, the research interest in the removal of PAHs from the environment has been increased. However, to the authors' knowledge there is no a review article concerning chemical treatment systems for PAH degradation in aqueous environment. Therefore, the aim of this work is to review, evaluate, discuss and compare different conventional and alternative chemical processes, and their combination with biological ones for the degradation of PAHs and their removal from water.

## 2. Background

### 2.1. PAHs: definition, classification and physico-chemical properties

PAHs, also known as polynuclear aromatic hydrocarbons, or more simply as polyaromatics, are a group of over one hundred organic compounds known for their toxicity and environmental persistence. They are mainly made up of carbon and hydrogen assembled in two or more stable benzene rings. Their physical and chemical properties are determined by their conjugated  $\pi$ -electron systems, which are dependent on the number of aromatic rings and their molecular weight. They are classified as having a low molecular weight if they have two or three condensed aromatic rings, or a high molecular weight if they have four or more condensed benzene rings. PAHs can be also classified as alternant or non-alternant if their structure is composed entirely of benzene rings or if four, five, and six-member non-aromatic rings are included, respectively (Wick et al., 2011).

The solubility of PAHs in water is dependent upon temperature, pH, ionic strength, and water matrix components (i.e. dissolved organic carbon) (Dabestani and Ivanov, 1999; Vela et al., 2012). However, in general PAHs have a relatively low solubility in water (ranging from  $31 \text{ g m}^{-3}$  for NA to  $0.26 \text{ mg m}^{-3}$  for BghiPY) (Dabestani and Ivanov, 1999), but dissolve easily in fats and oils, thus, they have a tendency to accumulate in the fatty tissue of living organisms. PAHs have variable vapor pressures (ranging from 10.4 Pa for NA to 0.37 nPa for DahA) (Dabestani and Ivanov, 1999). Those PAHs with lower vapor pressures are associated with particles, whereas those with higher vapor pressures are found as vapor at ambient temperature in air. Generally, the solubility of PAHs decreases and hydrophobicity increases with an increase in the number of condensed benzene rings. In addition, volatility decreases as the number of condensed aromatic rings increases.

### 2.2. Emission sources and occurrence in the environment

PAHs are widely spread throughout the natural environment and are found in soil, sediments, water, air, plants and animals, as a result of both natural and anthropogenic processes (Chen et al., 2004; Guo et al., 2007). In nature they are generated by natural forest fires, reactions in living beings, volcanic eruptions and natural oil seeps. However, PAHs are more commonly generated by anthropogenic activities, mainly as a result of combustion processes, especially the incomplete burning of organic materials during industrial and other human activities (e.g. industrial discharge, transportation, cooking, biomass burning, tobacco smoking, coal, petrol, gas and wood combustion, and waste incineration) (Ravindra et al., 2008).

PAHs are released into the atmosphere mainly via gaseous emissions, but they can also be discharged from soil and water compartments through evaporation or resuspension of particles. Once in the atmosphere, PAHs are subject to short and long-range transport, and they are removed by wet and dry deposition onto water, soil and vegetation. On the other hand, polyaromatics can reach aquatic systems through natural oil seeps, by atmospheric deposition and/or through accidental or intentional discharges mainly from oil extraction, transportation and refining. PAHs in water can bind to suspended particles or sediments, or bioaccumulate in aquatic organisms through the

food chain. Additionally, a small part of these substances can remain solubilized. Those which are found on the surface are subject to evaporation, and resuspension of the particles they are associated with. In soil, PAHs can be volatilized, solubilized or adsorbed onto organic matter or particulate material, being part of the gaseous, liquid and solid phase, respectively. In the liquid phase, PAHs can enter groundwater and be transported within aquifers (Birgöl et al., 2011; Chizhova et al., 2013; Vela et al., 2012; Zhang et al., 2008), becoming part of aquatic systems. Once PAHs are in water, soil or atmosphere, they are transferred to living beings, bioaccumulating in plants and animals through the food chain. The global movement of PAHs in nature is summarized in Fig. 1.

### 2.3. Adverse effects of PAHs

In recent years, the presence and concentration of PAHs in the environment have been reported in several parts of the world (Huang et al., 2012; Na et al., 2011; Nadal et al., 2004; Sabaté et al., 2001; Wang et al., 2011a,b). The main conclusion of these reports is that the accumulation and persistence of PAHs in the environment can produce harmful effects, in both aquatic and terrestrial ecosystems.

The list of priority PAHs varies in different countries. Sixteen PAHs have been included in the list of priority pollutants by the US-EPA (US-EPA, 2008), as a consequence of their potential carcinogenic, mutagenic and teratogenic effects on organisms, including human beings. It seems that their genotoxic and carcinogenic character is related to the formation of diol epoxides covalently bound to DNA (Meehan and Bond, 1984; Straub et al., 1977).

Throughout history, evidences of PAHs in living organisms have been reported, especially in humans (Chen and Liao, 2006; Chiang et al., 2009; Delgado-Saborit et al., 2011; Guo et al., 2012; Okona-Mensah et al., 2005; Siddens et al., 2012; Straif et al., 2005; Wester et al., 2012; Xu et al., 2013), which come mainly from occupational studies of workers exposed to mixtures containing these pollutants. Polyaromatics have been associated with various types of cancer such as lung, bladder, larynx, scrotum, breast, esophageal, prostate, kidney, skin, and pancreas cancer. They are also able to suppress the immune system and are suspected of being endocrine disrupters (CCME, 2008; US-EPA, 2008; Vela et al., 2012). Therefore, because of their wide

distribution and toxic potential, it is important to monitor these compounds and remove them from the environment.

## 3. Chemical removal techniques

### 3.1. Conventional processes

Conventional chemical oxidation processes can eliminate PAHs from water. Several studies have been carried out on the use of classic oxidants like ozone, chlorine and potassium permanganate (Ali and Tarek, 2009; Beltrán et al., 1995a,b, 1999; Brown et al., 2003; Kornmüller and Wiesmann, 2003; Legube et al., 1983; Miller and Olejnik, 2004, 2001; Rebola et al., 2008; Trapido et al., 1995). However, problems may arise during the decontamination process itself. For instance, chlorine has been shown to react with natural organic matter in water to produce carcinogenic and mutagenic halogenated hydrocarbons like trihalomethanes and haloacetic acids, known as disinfection by-products (Shih and Lederberg, 1976).

Among these chemical processes, those most often used for PAH removal are ozonation and direct photolysis. A summary of the main researches conducted using these treatments for PAH degradation is shown in Table 1.

#### 3.1.1. Ozonation

The removal of some PAHs (e.g. AN, BaP, BghiPY, BkF, BkP, CHR, FA, FLU, PHE and PYR) using ozonation has been investigated by several authors (Beltrán et al., 1995a,b, 1999; Kornmüller and Wiesmann, 2003; Legube et al., 1983; Miller and Olejnik, 2004, 2001; Trapido et al., 1995; Yip et al., 2006). In this process, PAH degradation occurs through two mechanisms: a) direct oxidation of the target compound by  $O_3$  (Eq. (1)); and b) indirect oxidation by  $^{\circ}OH$  from  $O_3$  transformation at a basic pH (Eqs. (2)–(7)) (Andreozzi et al., 1999; Miller and Olejnik, 2004; von Gunten, 2003).

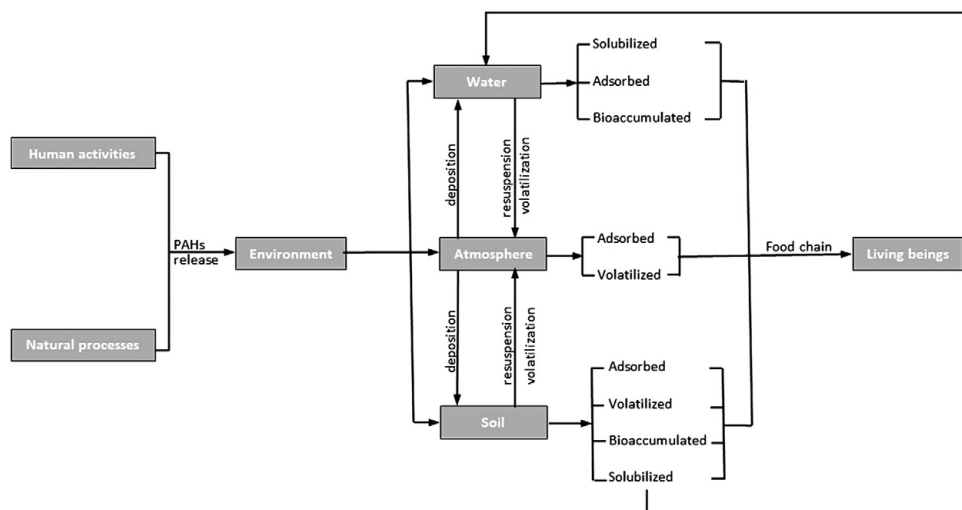


Fig. 1. PAH emission sources and principal pollution pathways.

**Table 1**  
A brief summary of the main applied chemical treatments for the PAHs degradation in aqueous environment.

Treatment	PAHs and type of water	Operating conditions	Concluding remarks	Reference
Ozonation	BaP and BkF in synthetic oil/water emulsion	PAHs = 0.1–1.7 mg L <sup>-1</sup> O <sub>3</sub> = 15.8–46 mg L <sup>-1</sup> ; flow rate <sub>ozone</sub> = 12.5 L h <sup>-1</sup> Dodecane = 75–750 mg L <sup>-1</sup> pH = 6.7; T = 30 °C Lab scale, 3 L glass reactor, batch mode BaP = 2–5 nM; CHR = 2–6 nM; FLU = 0.6–10 μM O <sub>3</sub> = 0.7–9.0 mg dm <sup>-3</sup> ; t-BuOH = 0.02 M pH = 2–12; T = 20 °C; time = 165 s Lab scale, 1 dm <sup>3</sup> axial glass reactor, semibatch mode BaP = 0.15 g Flow rate <sub>ozone</sub> = 44 mL min <sup>-1</sup> Time <sub>ozone</sub> = 50 min; time <sub>biological treatment</sub> = 20 d Lab scale, 7.5 in packed column and 1.7 L batch reactor	– It was found that the ozonation of PAHs in oil/water emulsions was not reduced by mass transfer limitation. – PAHs reaction rate constants in oil/water emulsions were in the upper range of values of those achieved by PAHs ozonation in water without oil. – Direct ozonolysis is the main degradation reaction pathway of all investigated PAHs at low pH. As pH was elevated, the participation of OH in PAHs degradation become of a great importance. – Prevalent intermediates identified at different stages included ring-opened aldehydes, phthalic and aliphatic derivatives. – The degradation of BaP was primarily initiated via O <sub>2</sub> -mediated ring-opening. – Intermediates formed during chemical oxidation were biodegradable.	Kommüller and Wiesmann (2003) Miller and Olejnik (2004) Zeng et al. (2000b)
Ozonation	BaP, CHR and FLU in synthetic water	PAHs = 1.80–600 nM LP UV (254 nm, 16 W, 2.08 × 10 <sup>-6</sup> Eins dm <sup>-3</sup> s <sup>-1</sup> ) pH = 5.6, 7.6	– PYR photodegradation quantum yields decreased about 2 times in micellar media compared to those determined in water. – PYR photolysis in both media results in the generation of 1,6 and 1,8-pyrenequinones, as stable by-products.	Sigman et al. (1998)
Ozonation coupled with a biological treatment	BaP in synthetic water	AN, PYR, BaA and DahA in synthetic water	– AN and BaA degrade faster than PYR and DahA under pH 5.6 in nitrogen purged water. – With the exception of AN, PAHs studied rate constants were higher at pH 5.6 than at pH 7.6. – It was found that PYR was the only one affected by O <sub>2</sub> .	Lehto et al. (2000)
Direct photolysis	PYR in synthetic water	BaP = 2.38 nM, 4.76 nM, 5.65 nM CHR = 2.63 nM, 5.13 nM, 5.26 nM FLU = 5.42 μM LP UV (254 nm, 15 W, 2.49 × 10 <sup>18</sup> quanta dm <sup>-3</sup> s <sup>-1</sup> ) MP UV (256–578 nm, 150 W, 5.99 × 10 <sup>19</sup> quanta dm <sup>-3</sup> s <sup>-1</sup> ) pH = 2.5, 6.8, 11.7 T = 20 °C t-BuOH = 0–0.02 M O <sub>2</sub> = 15–35 dm <sup>3</sup> h <sup>-1</sup> Lab scale, 1 dm <sup>3</sup> glass reactor, semibatch mode	– BaP and CHR degradation rates are dependent of pH values, resulting in the lowest ones at alkaline conditions, and the presence of t-BuOH or the lack of O <sub>2</sub> have an inhibiting effect. – FLU disappearance is accelerated when O <sub>2</sub> is removed from the reaction solution, and it is independent on pH solution. Additionally, t-BuOH does not exert any explicit negative effect. Those results suggest that the degradation mechanism of FLU follows different pathways than that of BaP and CHR. – A synergistic effect was observed between BaP and CHR in the photodegradation process. Meanwhile BaP quantum yield is decreased by FLU, it is increased nearly three times in the presence of CHR.	Miller and Olejnik (2001)
Direct photolysis	NA in synthetic water	Natural sunlight Time = 24 h (3 periods of 8 h) Lab scale, 200 mL glass beaker, batch mode	– The formed by-products by oxidation reactions in aqueous phase were different to those observed in atmospheric oxidation reactions. – Among the reaction intermediates identified were 1-naphthol, coumarin and two hydroxyquinones, which were consistent with initial [2,2] or [2,4] photocycloaddition reactions, with subsequent oxidations and/or rearrangements. – No obvious relationships were evident among the PAHs molecular properties and the quantum yields. – The photodegradation quantum yield is strong dependent of O <sub>2</sub> concentration. – Photodegradation rate constants of many PAHs were unchanged both for solutions of fulvic acids and natural water. DOM effect on reducing PAHs removal is insignificantly in natural waters.	McConkey et al. (2002) Fasnacht and Blough (2002)
Direct photolysis	A mixture of 12 PAHs (AC, AN, BaA, BaP, BbF, FA, BkF, CHR, FLU, PHE, PY and PYR) in synthetic and natural water	PAHs = 0.5–10 μM Xe arc lamp (>290 nm, 300 W) Natural DOM Fulvic acids = 5 mg L <sup>-1</sup> Lab scale, 4 mL batch mode		

Direct photolysis	AN, PHE and NA in synthetic and natural water	PAHs = 2.5–15 $\mu\text{g L}^{-1}$ 5 UV lamp ( $\lambda$ closed to natural sunlight, 1.6 $\text{W m}^{-2}$ (280–320 nm); 13.3 $\text{W m}^{-2}$ (320–400 nm); 12.17 $\mu\text{m}^{-2}$ (400–750 nm)) HS = 0–25 $\text{mg L}^{-1}$ Ionic strength = 6 mM, 600 mM pH = 7, T = 20 °C Time = 1–32 h (>100 h for NA studies) Incubation of aquatic bacteria from lake water Lab scale, sterile quartz glass tubes, batch mode NA = 44 $\mu\text{mol L}^{-1}$ ; PHE = 1.0 $\mu\text{mol L}^{-1}$ ; PYR = 0.15 $\mu\text{mol L}^{-1}$ Xe lamp (500 W) in a solar simulator DOC = 67.5 $\text{mg L}^{-1}$ 9.29 $\text{mg L}^{-1}$ ; $\text{NO}_3^-$ = 0.046 mM, 0.205 mM T = 25 °C; time = 1, 2 h Lab scale, borosilicate culture tubes, batch mode PAHs = 3.9–5.6 $\mu\text{M}$ LP UV (254 nm, 0–1500 $\text{mJ cm}^{-2}$ ) T = 21 °C	<p>Bertilsson and Widénfalk (2002)</p> <p>– Photodegradation of AN and PHE was faster (half-lives of 1 and 20.4 h) than NA (&gt; 100 h). Thus, NA photodegradation is most likely a less important removal mechanism.</p> <p>– AN and PHE have different behavior towards the presence of humic substances in water, because they have differences in the spectral absorbance. At higher HS concentration, PHE photodegradation reduced significantly. However, AN photodegradation was not affected.</p> <p>– Ionic strength did not affect PAHs photodegradation rates.</p> <p>– PAHs and simulated solar UV radiation produced a marked inhibition of bacterial growth, due to the production of quinones.</p>
Direct photolysis	PYR, PHE and NA in synthetic and natural water	NA = 44 $\mu\text{mol L}^{-1}$ ; PHE = 1.0 $\mu\text{mol L}^{-1}$ ; PYR = 0.15 $\mu\text{mol L}^{-1}$ Xe lamp (500 W) in a solar simulator DOC = 67.5 $\text{mg L}^{-1}$ 9.29 $\text{mg L}^{-1}$ ; $\text{NO}_3^-$ = 0.046 mM, 0.205 mM T = 25 °C; time = 1, 2 h Lab scale, borosilicate culture tubes, batch mode PAHs = 3.9–5.6 $\mu\text{M}$ LP UV (254 nm, 0–1500 $\text{mJ cm}^{-2}$ ) T = 21 °C	<p>Jacobs et al. (2008)</p> <p>– Under simulated solar radiation, PYR was found to remove faster than PHE or NA.</p> <p>– Whereas DOC affected PHE degradation negatively, nitrate had a positive effect.</p>
Direct photolysis	AN, BaP and FA in synthetic and natural water	PAHs = 3.9–5.6 $\mu\text{M}$ LP UV (254 nm, 0–1500 $\text{mJ cm}^{-2}$ ) T = 21 °C	<p>Sanches et al. (2011)</p> <p>– BaP and AN disappearance was faster than FLU degradation rate.</p> <p>– Oxygenated by-products were produced, which could be more toxic than the parent compounds.</p> <p>– Water matrix compounds had an inhibitory effect on the removal of the PAHs experienced, due to the presence of organic matter preventing UV-light reaches PAHs.</p>
Direct photolysis coupled with a biotreatment	BaP in synthetic and natural water	BaP = 1 $\mu\text{g L}^{-1}$ (for different types of waters) BaP = 5 $\text{mg L}^{-1}$ diluted (for different organic solvents) Sunlight irradiation Different organic solvents (methanol, acetonitrile, hexane, dichloromethane, cyclohexane) Time = 3 m (photolysis) + 4 m (biotreatment) T = 20 °C	<p>Kor-Wasik et al. (2004)</p> <p>– BaP natural photo-oxidation resulted in oxidized intermediates that are more susceptible to biodegradation than the parent compound.</p> <p>– BaP degradation rates decreased in the following order: dichloromethane &gt; acetonitrile &gt; hexane <math>\geq</math> cyclohexane &gt; methanol. A possible explanation for this effect is the dissolved oxygen in water (higher for dichloromethane).</p> <p>– In the case of natural waters, the order for BaP removal is: pond water &gt; river water &gt; seawater. The explanation of this fact is related to the salt content and flora acclimation of the water.</p>
UV/O <sub>3</sub>	BaP, CHR and FLU in synthetic water	Lab scale, borosilicate glassware, batch mode BaP = 4.76 nM, CHR = 5.12 nM; FLU = 5.42 $\mu\text{M}$ LP UV (254 nm, 15 W, 4.13 $\times 10^{-4}$ $\text{Eins dm}^{-3} \text{s}^{-1}$ ) O <sub>3</sub> = 0.4–30.2 $\text{mg dm}^{-3}$ Flow rate <sub>ozone</sub> = 8–25 $\text{dm}^3 \text{h}^{-1}$ t-BuOH = 0.02 M pH = 2–12, T = 20 °C Time = 75 s (BaP, CHR), 600 s (FLU) Lab scale, 1 $\text{dm}^3$ glass reactor, semibatch mode	<p>Ledakowicz et al. (2001)</p> <p>– The main pathway for PAHs disappearance depended on their chemical structure. For example, at neutral pH, BaP undergoes direct photolysis; CHR is attacked mainly by <math>\text{OH}^-</math> and FLU is degraded by direct ozonolysis.</p> <p>– The addition of t-BuOH had an inhibitory effect on the reaction rate of the whole PAHs investigated. In the case of FLU, the negative contribution of t-BuOH is less appreciable than for BaP and CHR.</p>
O <sub>3</sub> /H <sub>2</sub> O <sub>2</sub>	FLU, PHE and AC in synthetic water	FLU = 4.7–5.9 $\mu\text{M}$ ; PHE = 1.7–5.6 $\mu\text{M}$ ; AC = 17–25 $\mu\text{M}$ H <sub>2</sub> O <sub>2</sub> = 0–0.17 M Flow rate <sub>ozone</sub> = 2 $\times 10^{-2}$ $\text{m}^3 \text{h}^{-1}$ ; pressure <sub>ozone</sub> = 500 Pa	<p>Beltrán et al. (1996b)</p> <p>– H<sub>2</sub>O<sub>2</sub> had a negligible effect in the O<sub>3</sub>/H<sub>2</sub>O<sub>2</sub> system oxidation rate in comparison to that from ozonation alone.</p> <p>– The oxidation process was more effective under neutral conditions. At lower pH, the degradation rate decreased.</p> <p>– Although some hazardous substances could be formed under O<sub>3</sub> oxidation, they are destroyed</p>

(continued on next page)

Table 1 (continued)

Treatment	PAHs and type of water	Operating conditions	Concluding remarks	Reference
UV/H <sub>2</sub> O <sub>2</sub>	FLU, PHE and AC in synthetic water	HCO <sub>3</sub> <sup>-</sup> = 0–10 <sup>-2</sup> M pH = 2–12, T = 20 °C Lab scale, 5000 cm <sup>3</sup> tank, semibatch mode FLU = 4.7–5.9 μM PHE = 1.7–5.6 μM AC = 17–25 μM LP UV (254 nm, 3.8 × 10 <sup>-6</sup> Eins dm <sup>-3</sup> s <sup>-1</sup> ) H <sub>2</sub> O <sub>2</sub> = 0–0.4 M pH = 2–12; T = 20 °C Lab scale, 1 L glass annular reactor, semibatch mode	if the reaction time is extended. – HCO <sub>3</sub> <sup>-</sup> did not affect significantly the studied PAHs degradation. – The presence of H <sub>2</sub> O <sub>2</sub> increases significantly the degradation rate of the PAHs selected compared to UV alone. – There is an optimum H <sub>2</sub> O <sub>2</sub> concentration, below or above which PAHs degradation is reduced. – Higher levels of H <sub>2</sub> O <sub>2</sub> , up to 0.4 M and pH 12 lead to an expected decrease of <sup>•</sup> OH concentration. – Neutral pH seems to be the most appropriate to carry out the UV/H <sub>2</sub> O <sub>2</sub> oxidation. – The intermediate compounds formed could be more toxic and hazardous than the target pollutant. However, an extension in the reaction time converted them into harmless products.	Beltrán et al. (1996a)
UV/H <sub>2</sub> O <sub>2</sub>	BaP, CHR and FLU in synthetic water	BaP = 4.76 nM; CHR = 5.12 nM; FLU = 5.42 μM LP UV (254 nm, 2.49 × 10 <sup>18</sup> quanta dm <sup>-3</sup> s <sup>-1</sup> ) H <sub>2</sub> O <sub>2</sub> = 0–10 <sup>-1</sup> M pH = 2.5, 7, 11.7 t-BuOH = 0–0.02 M T = 20 °C, Time = 240–600 s Lab scale, 1 dm <sup>3</sup> axial glass reactor, batch mode	– BaP <sup>•</sup> and CHR follow radical reaction. FLU pathway is not clear, since whereas the two first ones oxidation was inhibited by the presence of t-BuOH, FLU degradation was not influenced by this <sup>•</sup> OH scavenger.	Ledakowicz et al. (1999)
UV/H <sub>2</sub> O <sub>2</sub> and direct photolysis	PHE and PYR in synthetic water	PHE = 5.6 μM PYR = 0.49 μM LP UV (254 nm, 5.0 × 10 <sup>-8</sup> Eins dm <sup>-3</sup> s <sup>-1</sup> ) H <sub>2</sub> O <sub>2</sub> = 10 mM APPO <sup>•</sup> = 0–100 mM Lab scale, turntable reactor with cylindrical quartz tubes (13 mm O.D. × 10 mm L <sup>3</sup> ) PAHs = 2 μM LP UV (254 nm) MP UV (200–300 nm) Fluence = 0–1000 mJ cm <sup>-2</sup> H <sub>2</sub> O <sub>2</sub> = 10–25 mg L <sup>-1</sup> pH = 7 Toxicity analyses ( <i>Vibrio fischeri</i> test) Lab scale, Petri dish with 100 mL, quasi-collimated beam apparatus	– Micellar APPO <sup>•</sup> solutions enhanced PYR photolysis and reduced PHE photodegradation. – Addition of H <sub>2</sub> O <sub>2</sub> dramatically increased PAHs degradation in comparison with direct photolysis. Nevertheless, it was noticed that micelles provided PAHs some degree of protection from <sup>•</sup> OH attack.	An and Carraway (2002)
UV/H <sub>2</sub> O <sub>2</sub> and direct photolysis	FLU, DBF and DBT in synthetic water	FLU = 2.0–4.1 μM; AN = 0.15–0.34 μM; PYR = 1.3–5.5 μM L; PHE = 0.16–1.1 μM L; FA = 0.13–0.3 μM; BaP = (0.05–1.0) × 10 <sup>-2</sup> μM; BghiPY = (4.0–8.5) × 10 <sup>-4</sup> μM LP UV (254 nm, 2.41 × 10 <sup>16</sup> photons s <sup>-1</sup> ) H <sub>2</sub> O <sub>2</sub> = 20–1 μM O <sub>3</sub> = 0.02–0.15 mg L <sup>-1</sup> ; flow rate <sub>ozonation</sub> = 1 L min <sup>-1</sup> H <sub>2</sub> O <sub>2</sub> :O <sub>3</sub> = 0.5–2 pH = 3, 7, 9; time = 0–300 s Lab scale, 1.5 × 10 <sup>-3</sup> m <sup>3</sup> axial semicontinuous bubble column with a central lamp	– The disappearance rate of each PAH was found to be different, due to the differences in the structure. – Low rates and efficiencies were obtained through direct photolysis, while high reactivity towards <sup>•</sup> OH was found. Therefore, the addition of H <sub>2</sub> O <sub>2</sub> to the system resulted in a dramatically increase in PAHs removal rates, especially when MP UV lamps were used. – As the target pollutant was degraded, a toxicity increase was observed due to the by-products generation during direct photolysis. However, an increase on the light intensity leads to a decrease of the toxicity of the solution to <i>V. fischeri</i> .	Shemer and Linden (2007)
Ozonation, O <sub>3</sub> /H <sub>2</sub> O <sub>2</sub> , direct photolysis, UV/H <sub>2</sub> O <sub>2</sub> , UV/O <sub>3</sub> , UV/O <sub>3</sub> /H <sub>2</sub> O <sub>2</sub>	FLU, AN, PHE, PYR, FA, BaP and BghiPY in synthetic water	ACN = 17.3 μM LP UV (254 nm, 3.48 × 10 <sup>-6</sup> Eins dm <sup>-3</sup> s <sup>-1</sup> ) H <sub>2</sub> O <sub>2</sub> = 10 <sup>-3</sup> –0.4 M Flow rate <sub>ozonation</sub> = 2 × 10 <sup>-2</sup> m <sup>3</sup> h <sup>-1</sup>	– Ozonation was shown to be quite effective for PAHs degradation, particularly in neutral environment. PAHs disappearance rate was lower when PAHs were attacked by <sup>•</sup> OH than when they were directly oxidized through O <sub>3</sub> . Therefore, PAHs disappearance is mainly conducted by means of O <sub>3</sub> direct oxidation if maximum O <sub>3</sub> levels are guaranteed. – The reaction rates of PAHs treated by ozonation were higher in acidic and neutral media than in a basic one. – There is no an acceleration destruction when the combined oxidation methods are applied.	Trapido et al. (1995)
Ozonation, O <sub>3</sub> /H <sub>2</sub> O <sub>2</sub> , direct photolysis, UV/H <sub>2</sub> O <sub>2</sub> , UV/O <sub>3</sub>	ACN in synthetic water		– ACN was removed by different AOPs based on O <sub>3</sub> , as well as UV/H <sub>2</sub> O <sub>2</sub> system. Among them, O <sub>3</sub> was the most efficient. In fact, pollutants conversion values were 16%, 50%, 85% and 98% for UV, UV/H <sub>2</sub> O <sub>2</sub> , UV/O <sub>3</sub> , O <sub>3</sub> /H <sub>2</sub> O <sub>2</sub> and O <sub>3</sub> , respectively. – In the presence of O <sub>3</sub> , the addition of H <sub>2</sub> O <sub>2</sub> (initiator) or t-BuOH (inhibitor) had no effect in ACN conversion.	Rivas et al. (2000)

Fenton	Pressure <sub>atmosphere</sub> = 500 Pa t-BuOH = 10 <sup>-2</sup> M pH = 7, T = 20 °C, time = 0–20 min Lab scale, 1 L glass annular reactor, semibatch mode H <sub>2</sub> O <sub>2</sub> = 0.01 mM–0.1 M; Fe <sup>2+</sup> = 0–0.2 mM HCO <sub>3</sub> <sup>-</sup> = 0–1 mM Commercial HS = 0–25 mg L <sup>-1</sup> pH = 2–12; T = 20 °C; time = 0–25 min Lab scale, 5000 cm <sup>3</sup> reactor, semibatch mode PAH = 5 mM H <sub>2</sub> O <sub>2</sub> = 0.01–1 mM; Fe <sup>2+</sup> = 0.2–2 mM Cyclodextrines β-CD <sup>+</sup> ; HPBCD <sup>+</sup> ; RAMEB <sup>+</sup> Mannitol = 1 M; pH = 5.5; T = 22 °C, time = 12 h Lab scale, 50 mL beaker, batch mode BAP = 10–100 μg L <sup>-1</sup> Fe <sub>2</sub> SO <sub>4</sub> ·7H <sub>2</sub> O = 2.75–5.50 mg L <sup>-1</sup> H <sub>2</sub> O <sub>2</sub> = 20–150 mg L <sup>-1</sup> pH = 3.5–6 T = 30–70 °C, time = 90 min Lab scale, 250 mL (7.5 cm OD) × 11.5 cm L <sup>h</sup> , covered with an aluminum foil, batch mode Fenton: AN = 10 ppm Fe <sub>2</sub> SO <sub>4</sub> ·7H <sub>2</sub> O = 0–20 mM; H <sub>2</sub> O <sub>2</sub> = 0–2.5% pH = 3–7; T = 22–25 °C, time = 90 min Fenton ± non-ionic surfactants: PAHs = 50 ppm; surfactants = 0.1%; time = 48 h Biotreatment: PAHs = 50 ppm Microorganisms ( <i>Erwinia herbicola</i> , <i>Pseudomonas fluorescens</i> , <i>Pseudomonas syringae</i> and <i>Pseudomonas testosteroni</i> ) pH = 7; time = 0–12 d Lab scale, 50 mL serum bottles, batch mode PAH = 45.5 mg L <sup>-1</sup> Fenton: H <sub>2</sub> O <sub>2</sub> = 1.5 mM; Fe <sub>2</sub> SO <sub>4</sub> ·7H <sub>2</sub> O = 0.5 mM Biotreatment: <i>Fusarium solani</i> pH = 7.0; T = 18 °C, time = 12 d Cyclodextrines: HPBCD <sup>+</sup> ; RAMEB <sup>+</sup> Lab scale, 22 mL penicillin flasks, batch mode PAHs = 16.7 mg L <sup>-1</sup> (NA)–0.019 mg L <sup>-1</sup> (BAP) Black lamp (16, 14 W, λ = 300–400 nm, 1.4 × 10 <sup>-3</sup> M photons min <sup>-1</sup> ) H <sub>2</sub> O <sub>2</sub> = 10 mM; Fe <sup>2+</sup> = 1 mM pH = 2.75; T = 25 °C; time = 180 min Toxicity analyses ( <i>Pimephales promelas</i> ; <i>Daphnia pulex</i> ) Lab scale, 400 mL cylindrical borosilicate vessel, batch mode	FLU, PHE and AC in synthetic water	Beltrán et al. (1998)
Fenton	BAP in synthetic water		Veigne et al. (2009)
Fenton	BAP in synthetic water		Homem et al. (2009)
Fenton and Fenton coupled with biological process	AN and BAP in synthetic water		Nadarajah et al. (2002)
Fenton coupled with a biological treatment	BAP in synthetic water		Rafin et al. (2009)
Photo-Fenton	Creosote solution (85% PAHs; 10% phenolic compounds; 5% heterocyclic compounds)/ pentachlorophenol contaminated in synthetic water		Engvall et al. (1999)

(continued on next page)

- In the O<sub>2</sub>/H<sub>2</sub>O<sub>2</sub> process, an addition of H<sub>2</sub>O<sub>2</sub> resulted in a slight worsening at the initial reaction stages.

- Total PAHs decomposition was achieved with 1 mM for H<sub>2</sub>O<sub>2</sub> and 0.07 mM for Fe<sup>2+</sup> at pH 7. PAHs reactivity followed the order: PHE > FLU > AC.

- PAHs oxidation was a OH mediated process, because of the retardant effect of HCO<sub>3</sub><sup>-</sup>, CO<sub>3</sub><sup>2-</sup> and HS in PAHs degradation rates.

- It was observed that BAP apparent solubility was dramatically improved by cyclodextrines in the following order: β-CD<sup>+</sup> < RAMEB<sup>+</sup> < HPBCD<sup>+</sup>.

- RAMEB affected negatively BAP removal in the presence of mannitol (a radical scavenger).

- Cyclodextrines, such as HPBCD<sup>+</sup>, could be useful for BAP Fenton degradation.

- Fenton's reagent was a feasible treatment for BAP degradation.

- It was achieved an increase in the degradation efficiency with an increase of H<sub>2</sub>O<sub>2</sub> from 20 to 50 mg L<sup>-1</sup>, but H<sub>2</sub>O<sub>2</sub> levels above 50 mg L<sup>-1</sup> resulted in a BAP lower removal.

- Regarding Fe<sup>2+</sup>, an increase of Fe<sup>2+</sup> concentration leads to an improvement of the BAP degradation.

- An increase in the removal efficiency from 90 to 100% was observed increasing temperature from 30 to 70 °C.

- The most effective conditions for AN by Fenton's reagent was found to be 0.5% of H<sub>2</sub>O<sub>2</sub> and 10 mM of Fe<sup>2+</sup>, with a molar ratio H<sub>2</sub>O<sub>2</sub>:Fe<sup>2+</sup> of 15:1 at pH 4.

- The use of non-ionic surfactants improved PAHs degradation by Fenton or biological treatment alone.

- The extent of PAHs removal coupling Fenton's biotreatment was 2–4 times higher than with Fenton process or biotreatment alone.

- 80–85% of PAHs removal was achieved in 48 h of Fenton's pre-treatment in the presence of non-ionic surfactant followed by 7 d of biological treatment.

- When Fenton's treatment was combined with biodegradation, a beneficial effect on BAP degradation (25%) was obtained compared with PAH biodegradation (8%), or with chemical oxidation alone (16%).

- The best conversion performance was achieved with HPBCD<sup>+</sup> in comparison with RAMEB<sup>+</sup>.

- 2 and 3-ring PAHs are effectively degraded by the photo-Fenton system. However, 4 and 5-ring PAHs conversion was less complete.

- Toxicity test revealed that the formed by-products were not toxic.

Table 1 (continued)

Treatment	PAHs and type of water	Operating conditions	Concluding remarks	Reference
Photo-Fenton	A mixture of 16 PAHs (NA, AC, ACN, FLU, PHE, AN, FA, PYR, BaA, CHR, BbF, BkF, BaP, IP, DabA and BghiPy) in petrochemical water	PAHs = 1.6 mg L <sup>-1</sup> Solar radiation: 17 mJ m <sup>-2</sup> s <sup>-1</sup> H <sub>2</sub> O <sub>2</sub> = 88–132 mM; Fe <sup>2+</sup> = 0.93 mg L <sup>-1</sup> pH = 3; time = 1–7 h Toxicity analyses ( <i>Lactuca sativa</i> ) Lab scale, Petri dish with 30 mL, batch mode PHE surface coverage = 56–72 μmol g <sup>-1</sup> UV lamp (320–400 nm, 100 W, 30 W m <sup>-2</sup> ) Different photocatalysts (TiO <sub>2</sub> , SiO <sub>2</sub> , Al <sub>2</sub> O <sub>3</sub> ) TiO <sub>2</sub> (Degussa P25, anatase:rutile = 80:20, S <sub>B</sub> <sup>h</sup> = 50 m <sup>2</sup> g <sup>-1</sup> ) = 6.95–55.85 mg pH = 2–10; T = 20 °C, time = 0–120 min Lab scale, 70 mL Pyrex glass vessel, batch mode	– About 92% and 96% of PAHs and aromatic content were removed. Therefore, solar photo-Fenton showed to be an efficient AOP for petrochemical wastewater treatment. – This AOP is able of reducing 53% of COD and 50% of solution toxicity.  – PHE oxidation and mineralization can be carried out by photocatalysis with TiO <sub>2</sub> . – TiO <sub>2</sub> surface coverage by PHE, amount of TiO <sub>2</sub> used and pH solution appeared to have little effect on the removal PHE rate. – PHE UV/TiO <sub>2</sub> process formed by-products through ketolysis and hydroxylation.	da Rocha et al. (2013)  Wen et al. (2002)
UV/TiO <sub>2</sub>	PHE in synthetic water	NA = 0–40 μmol L <sup>-1</sup> UV lamp (λ <sub>max</sub> = 365 nm, 125 W, 0–3.5 × 10 <sup>16</sup> photons s <sup>-1</sup> ) TiO <sub>2</sub> (Degussa P25, S <sub>B</sub> <sup>h</sup> = 50 m <sup>2</sup> g <sup>-1</sup> , size = 30 nm) = 0–4 g L <sup>-1</sup> CO <sub>3</sub> <sup>2-</sup> = 0–0.09 mol L <sup>-1</sup> HCO <sub>3</sub> <sup>-</sup> = 0–0.36 mol L <sup>-1</sup> Cl <sup>-</sup> = 0–2.4 mol L <sup>-1</sup> pH = 3–11; T = 10–40 °C, time = 0 to ~350 min	– The optimum TiO <sub>2</sub> was found to be 2.5 g L <sup>-1</sup> . The pH had insignificant effect at the levels studied, a photon flux in the range of 10 <sup>16</sup> photon s <sup>-1</sup> produced a linear increase in the degradation rate and temperature slightly accelerated NA kinetic. – CO <sub>3</sub> <sup>2-</sup> strongly inhibits NA adsorption and removal. The HCO <sub>3</sub> <sup>-</sup> concentrations analyzed were not involved in the inhibition of NA degradation. Nevertheless, working at pH < pH <sub>max</sub> , NaCl appeared to improve NA adsorption, but this conclusion must be taken carefully. – NA degraded by oxygenated radicals and by direct oxidation in the holes formed.	Lair et al. (2008)
UV/TiO <sub>2</sub>	NA, ACN, PHE, AN and BaA in synthetic water	Lab scale, 50 mL glass flask, batch mode PAHs = 10 mg L <sup>-1</sup> 4 UV lamps (λ <sub>max</sub> = 365 nm, 15 W, 3.9 mW cm <sup>-2</sup> (UVA); 1.1 mW cm <sup>-2</sup> (UVB); 0.3 mW cm <sup>-2</sup> (UVC)) TiO <sub>2</sub> (Degussa P25, anatase:rutile = 70:30, S <sub>B</sub> <sup>h</sup> = 50 m <sup>2</sup> g <sup>-1</sup> , size = 30 nm) = 100 mg L <sup>-1</sup> Acetone = 1–16% (–0.136 M to –2.176 M) Air = 200 cm <sup>3</sup> min <sup>-1</sup> Toxicity analyses (Microtox® test) Time = 0–350 min Lab scale, 100 mL stainless steel cylindrical reactor, batch mode PYR surface coverage = 10–200 μmol g <sup>-1</sup> UV lamp (320–400 nm, 100 W, 25 W m <sup>-2</sup> ) Different photocatalysts (TiO <sub>2</sub> , SiO <sub>2</sub> , Al <sub>2</sub> O <sub>3</sub> ) TiO <sub>2</sub> (Degussa P25, anatase:rutile = 80:20, S <sub>B</sub> <sup>h</sup> = 50 m <sup>2</sup> g <sup>-1</sup> ) = 0.5–3 g L <sup>-1</sup> pH = 1–9, time = 0 to ~120 min Photo-Fenton: Fe <sup>3+</sup> /TiO <sub>2</sub> = 0–5%; pH = 5–9 T = 20 °C Lab scale, 70 mL Pyrex glass vessel, batch mode	– PAHs photolysis generated toxic intermediate products, especially in the case of ACN and PHE. However, all PAHs, particularly AN, completely detoxification was achieved in a 24 h of UV/TiO <sub>2</sub> system by 100 mg L <sup>-1</sup> of catalyst. – Acetone enhanced PAHs degradation, but 16% acetone addition significantly altered the degradation pathway of NA and AC. – PAHs hydroxylation is correlated to the localization energies of different positions of the substances.	Woo et al. (2009)
UV/TiO <sub>2</sub> coupled with Fenton	PYR in synthetic water	UV lamp (320–400 nm, 100 W, 25 W m <sup>-2</sup> ) Different photocatalysts (TiO <sub>2</sub> , SiO <sub>2</sub> , Al <sub>2</sub> O <sub>3</sub> ) TiO <sub>2</sub> (Degussa P25, anatase:rutile = 80:20, S <sub>B</sub> <sup>h</sup> = 50 m <sup>2</sup> g <sup>-1</sup> ) = 0.5–3 g L <sup>-1</sup> pH = 1–9, time = 0 to ~120 min Photo-Fenton: Fe <sup>3+</sup> /TiO <sub>2</sub> = 0–5%; pH = 5–9 T = 20 °C Lab scale, 70 mL Pyrex glass vessel, batch mode	– PYR oxidation and mineralization can be carried out by photocatalysis with Fe <sup>3+</sup> /TiO <sub>2</sub> . – PYR/TiO <sub>2</sub> :water ratio and pH solution appeared to have little effect on the removal PYR rate. However, TiO <sub>2</sub> surface coverage by PYR and Fe <sup>3+</sup> content affected greatly the degradation of PYR. – PYR intermediate products formed by UV/Fe <sup>3+</sup> /TiO <sub>2</sub> system was mainly by ketolysis and hydroxylation.	Wen et al. (2003)
US	AN, PHE and PYR in synthetic and natural water	PAHs = 0.1–0.5 μM Power = 600 W Frequency = 20 kHz Fulvic acid = 1–26 μM; benzoic	– PAHs removal by US was more likely due to pyrolysis mechanism. *OH oxidation was insignificant for PAHs removal. – PAHs sonodegradation was affected negatively by the presence of other dissolved compounds in water, such as fulvic acids.	Taylor et al. (1999)



US	Methylnaphthalene, AC, PHE, PYR, 1,12-benzoperylene and coronene in synthetic water	<p>acid = 172 µM Time = 0–5 min Lab scale, 50–100 mL volume sonication, batch mode</p> <p>PAHs = 0, 10, 20, 40 ng L<sup>-1</sup> at different organic solvent:water ratios Power = 50, 60 W Frequency = 20 kHz T = 25 °C; pH = 2, 6.8, 12; time = 1, 2 h H<sub>2</sub>O<sub>2</sub> = 1.0%; argon = 5 psi Lab scale, 30 mL volume sonication, batch mode</p> <p>PAHs = 0.1–0.5 µM Power = 600 W Frequency = 20 kHz Benzoic acid &lt; 30 mg L<sup>-1</sup>, Pentane &lt; 30 mg L<sup>-1</sup>, pentanol &lt; 30 mg L<sup>-1</sup>, SDS<sup>1</sup> &lt; 2.5 g L<sup>-1</sup>, HS = 0–15 mg L<sup>-1</sup> T = 20 °C; time = 30 min Lab scale, 50–70 mL sonication volume, batch mode</p> <p>PHE = 0.06 mg Power = 32.5 W; frequency = 30 kHz T = 20, 30, 40 °C; time = 300 min Lab scale, 100 mL three necks spherical flasks, batch mode</p> <p>NA = 227 µg L<sup>-1</sup>; PHE = 97 µg L<sup>-1</sup>; AN = 110 µg L<sup>-1</sup>; PYR = 118 µg L<sup>-1</sup>; BkF = 12 µg L<sup>-1</sup> Power = 200 W L<sup>-1</sup>, frequency = 20, 506 kHz T = 20 °C; time = 2 h Lab scale, cylindrical reactor with 150 mL of sonication, batch mode</p> <p>PAHs = 1380 ng mL<sup>-1</sup> Power = 16, 23.02, 37, 51.75 W m<sup>-2</sup>; frequency = 35 kHz DO = 2, 4, 6, 10 mg L<sup>-1</sup> H<sub>2</sub>O<sub>2</sub> = 100, 500, 2000 mg L<sup>-1</sup> Toxicity analyses (<i>Daphnia magna</i> test) T = 30–60 °C; time = 0–150 min Lab scale, serum bottles filled with 10 mL, batch mode</p> <p>NA = 3000 µg L<sup>-1</sup>; PHE = 100 µg L<sup>-1</sup>; PYR = 10 µg L<sup>-1</sup> Power = 67, 100, 133, 167 W Frequency = 582, 862, 1142 kHz pH = 6.5; T = 25 °C; time = 0–120 min Lab scale, 2 L glass reactor, batch mode</p> <p>PAHs = 0.39 mg Power = 47 W cm<sup>-2</sup> Flow<sub>air</sub> = 100 mL min<sup>-1</sup> T = 21–27 °C; time = 20–120 min FeCl<sub>3</sub>·6H<sub>2</sub>O Lab scale, 300 mL vessel, batch mode</p>	<p>– US ability to degrade PAHs was dramatically inhibited by water matrix compounds in natural waters, especially because matrix constituents may inhibit PAHs access to cavitation sites.</p> <p>– PAHs studied degradation followed a <sup>•</sup>OH oxidation pathway, and it was improved in the presence of H<sub>2</sub>O<sub>2</sub> and argon gas.</p> <p>– PAHs sonodegradation rates were increased with a decreased in pH values and an increase in ultrasonic irradiation time. Nevertheless, an increase in the number of PAHs benzene rings resulted in a more difficult conversion by US.</p> <p>– PAHs degradation by sonochemical treatment was affected by water matrix constituents, increasing or decreasing depending on the substance; e.g. humic acids act as <sup>•</sup>OH scavengers, as well as benzoic acid and SDS<sup>1</sup>.</p> <p>– The main PAHs sonodegradation pathways involved oxygen derived radicals. However, PAHs removal by pyrolysis can be improved by addition of volatile species.</p> <p>– It was observed a PHE degradation of 88% under 40 °C at ambient light conditions during 240 min.</p> <p>– The main mechanism of PAHs removal was pyrolysis, achieving highest activity at 506 kHz.</p> <p>– The <sup>•</sup>OH number was insufficient for PAHs oxidation by US. Therefore, the negative effect of t-BuOH was insignificant.</p> <p>– The PAHs rate constants increased as vapor pressure, Henry's constant and water solubility increased.</p> <p>– The optimum operational conditions for achieving a maximum PAHs degradation was found to be 6 mg L<sup>-1</sup> of DO and 2000 mg L<sup>-1</sup> of H<sub>2</sub>O<sub>2</sub>, after 150 min of treatment at 60 °C, resulting in a removal ranging from 87% to 99%.</p> <p>– It has been observed that PAHs sonodegradation pathway was pyrolysis.</p> <p>– The intermediate products toxicity decreased as temperature, dissolved oxygen and H<sub>2</sub>O<sub>2</sub> increased.</p> <p>– PAHs sonodegradation resulted in final PAHs concentrations lower than 10% for PYR and PHE in about 100 min.</p> <p>– NA and PHE had similar rates per unit mass at the three frequencies studied, which were lower for PYR.</p> <p>– The energy required by the three PAHs under the same conditions followed the order: NA &lt; PHE &lt; PYR.</p> <p>– Hexane-extractable metabolites were not identified.</p> <p>– Sonodegradation of PAHs can be induced through intense ultrasonic treatment. The extent and outcome of reaction was a function of irradiation time and aqueous variables.</p> <p>– The principal by-product formed by PHE ultrasonic treatment was found to be phenanthrene-diol.</p> <p>– The use of US with Fe<sup>3+</sup> appeared to be a promising alternative for PAHs degradation.</p>	<p>Park et al. (2000)</p> <p>Laughey et al. (2001)</p> <p>Little et al. (2002)</p> <p>David (2009)</p> <p>Sponza and Oztekin (2010)</p> <p>Maniatis et al. (2011)</p> <p>Wheat and Tumeo (1997)</p>
US	PHE, AN and PHE in synthetic water			
US	PHE in synthetic water			
US	NA, PHE, AN, PYR and BkF in synthetic water			
US	A mixture of 17 PAHs (NA, AC, ACN, FLU, PHE, AN, carbazole, FA, PYR, BaA, CHR, BbF, BkF, BaP, IP, BaA and BghiPy) in petrochemical wastewater			
US	NA, PHE and PYR in synthetic water			
US and US combined with Fenton	PHE and biphenyl in synthetic water			

(continued on next page)

Table 1 (continued)

Treatment	PAHs and type of water	Operating conditions	Concluding remarks	Reference
US and US coupled with Fenton	NA, ACN and PHE in synthetic water	PAHs = 150, 300, 450 $\mu\text{g L}^{-1}$ Power = 45, 75, 150 W; frequency = 24–80 kHz 1-Butanol = 320 $\mu\text{g L}^{-1}$ ; NaCl = 100 $\text{g L}^{-1}$ ; $\text{FeSO}_4 \cdot 7\text{H}_2\text{O}$ = 100 $\text{g L}^{-1}$ T = 20–40 °C; time = 0–120 min Lab scale, 200 mL cylindrical glass vessel, batch mode	– Complete PAHs conversion was achieved in up to 120 min of treatment. – It was observed that PAHs degradation decreased as temperature increased and power and frequency decreased. Matrix constituents present in excess had a negative effect on PAHs sonodegradation. – Coupling US and Fenton reaction enhanced PAHs conversion.	Psillakis et al. (2004)
Electrochemical oxidation	Cresote solution with 16 PAHs (AC, ACN, AN, BaA, BaP, BbJkF, BghiPy, CHR, DabA, FLU, FA, IP, MAN, NA, PHE and PYR) in synthetic water	PAHs = 270–540 $\text{mg L}^{-1}$ Electrolytic cell: Electrodes (anode: Ti/RuO <sub>2</sub> , area = 65 $\text{cm}^2$ ; cathode: stainless steel) Electrolytes (Na <sub>2</sub> SO <sub>4</sub> ) = 500–4000 $\text{mg L}^{-1}$ Current density = 3.08–12.3 $\text{mA cm}^{-2}$ T = 4–35 °C; time = 20–180 min Toxicity analysis ( <i>Daphnia pulex</i> test) Lab scale, 1.5 L cell (5 anodes, 5 cathodes in parallel)	– PAHs reductions about 80% were achieved in 90 min of treatment. – Electrochemical oxidation is able to reduce toxicity of creosote solutions.	Tran et al. (2009)
Electrochemical oxidation	NA, FA and PYR in synthetic water	Electrodes (anode: Ti/PbO <sub>2</sub> ; <sup>a</sup> ; cathode: stainless steel) Electrolytes (Na <sub>2</sub> SO <sub>4</sub> , NaNO <sub>3</sub> , NaCl) = 0.1–1.4 M Current density = 50–200 $\text{mA cm}^{-2}$ Lab scale, one tubular compartment cell, batch recirculation	– Although all PAHs degraded through electrochemical oxidation, NA exhibited the fastest degradation rates. – In a 0.1 M Na <sub>2</sub> SO <sub>4</sub> electrolyte solution, all PAHs were degraded by direct electron transfer at the anode surface. In 0.1 M NaCl solution, PAHs degradation was enhanced by indirect oxidation, due to the hypochlorite formed. – PAHs studied removal rates were increased as current density decreased, particularly for PYR and FLU.	Muff and Søgaard (2010)
Electrochemical oxidation	A mixture of 16 PAHs (NA, AC, ACN, FLU, PHE, AN, FA, PYR, BaA, CHR, BbF, BkF, BaP, IP, DabA and BghiPy) in synthetic water	Electrodes (anode: Ti/Pt, area = 13.5 $\text{cm}^2$ ; cathode: Ti plate) Current density = 11 $\text{mA cm}^{-2}$ T = 25 °C; time = 0–4 h Lab scale, 450 mL electrolytic cell (1 anode, 1 cathode)	– PAHs chemical structure influenced the performance of the system. It was achieved up to 85% of removal for PAHs with simple chemical structure. – After 1 h of electrochemical oxidation, higher removal efficiencies were obtained.	Souza et al. (2011)
Electrochemical oxidation coupled with UV/TiO <sub>2</sub>	AN, FA, PHE and PYR in synthetic water	UV UV (254 nm, 8 W, 500 $\mu\text{W cm}^{-2}$ ) TiO <sub>2</sub> (Degussa P25, anatase:rutile = 3:1, S <sub>A</sub> <sup>b</sup> = 50 $\text{m}^2 \text{g}^{-1}$ , size = 30 nm) Electrolytic cell: Electrodes (solid gold, area = 0.2 $\text{cm}^2$ ) Electrolyte (KCl) = 0.1 $\text{mol L}^{-1}$ Potential applied (vs Ag/AgCl reference electrode) = +0.0–1.0 V Time = 0–23 h Lab scale	– PAHs pre-adsorbed on TiO <sub>2</sub> catalyst are degraded by <sup>•</sup> OH oxidation. However, in a electrochemical system, they are removed by direct electron transfer to the electrode, yielding PAHs cation radicals that undergo subsequent reactions. – AN treated through UV/TiO <sub>2</sub> system and electrochemical oxidation produced the same intermediate products, compared to PYR.	Cordeiro and Corio (2009)

<sup>a</sup> Dissolved organic carbon.<sup>b</sup> Ammonium perfluorooctanoate.<sup>c</sup> Outer diameter.<sup>d</sup> Length.<sup>e</sup>  $\beta$ -Cyclodextrine.<sup>f</sup> Hydroxypropyl- $\beta$ -cyclodextrine.<sup>g</sup> Methylated- $\beta$ -cyclodextrine.<sup>h</sup> Surface area.<sup>i</sup> Sodium dodecyl sulfate.

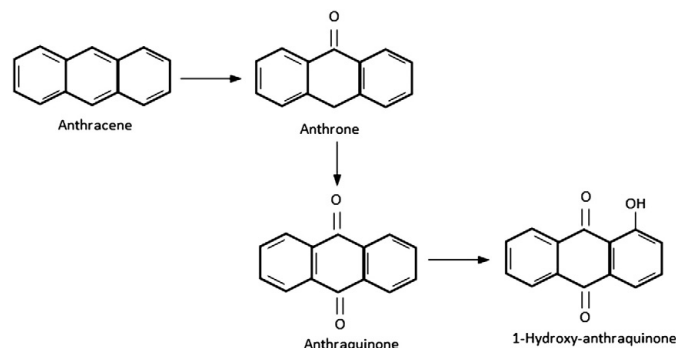


Fig. 2. AN photolysis by-products formation (Sanches et al., 2011).



It is worth noting that apart from  $^\circ\text{OH}$ ,  $\text{HO}_2^\circ$  (Eqs. (3), (8)),  $\text{O}_2^{\circ-}$  (Eq. (4)), and  $\text{O}_3^{\circ-}$  (Eqs. (3), (5)) are yielded, which can also react with PAHs and their intermediates; nevertheless, their oxidation power is lower than that of  $^\circ\text{OH}$  (Litter and Quici, 2010).

The removal pathway of PAHs is enormously influenced by the pH of the solution, since the decomposition of  $\text{O}_3$  is facilitated at high pH values where  $^\circ\text{OH}$  attack takes place. On the contrary, in acidic conditions,  $\text{O}_3$  becomes more stable and direct oxidation by  $\text{O}_3$  can occur (Miller and Olejnik, 2004). Several researches have studied the degradation of PAHs, such as AN, BaP, BghiPY, CHR, FA, FLU, PHE and PYR in aqueous media at concentrations below their solubility limit and at different pH conditions (Miller and Olejnik, 2004; Trapido et al., 1995). They have proven that, even though  $^\circ\text{OH}$  have a high oxidation potential ( $E^\circ = +2.86 \text{ V}$ ),  $\text{O}_3$  is a very powerful oxidizing agent ( $E^\circ = +2.07 \text{ V}$ ) (Kleiser and Frimmel, 2000) as well. Miller and Olejnik (2004) studied the influence of pH on the removal rate of  $5.12 \times 10^{-9} \text{ M}$  CHR with  $15.2 \text{ mg L}^{-1} \text{ O}_3$  fed at a flow rate of  $9 \text{ L h}^{-1}$ , achieving reductions of about 14% and 77% for pH 12 and pH 2, respectively, after 75 s of treatment. When the PAH concentration is below that of  $\text{O}_3$  at an alkaline pH, the role of  $\text{O}_3$  acting as a  $^\circ\text{OH}$  scavenger (Eq. (8)) becomes important, as does the combination reaction between  $^\circ\text{OH}$  and  $\text{HO}_2^\circ$ , resulting in a decrease in the removal of PAHs (Miller and Olejnik, 2004). Even though it is not mentioned by the authors, the lower degradation observed at pH 12 can be also attributed to the inactivation of  $^\circ\text{OH}$  radicals at high pH values ( $\text{p}K_a = 11.9$ ) (Matsugo et al., 1995).

Direct reactions between  $\text{O}_3$  and PAHs lead to ring cleavage by electrophilic mechanisms (Bailey et al., 1968), resulting in the formation of a number of carboxylate and hydroxylated benzenes, quinones and oxygen derivatives of aliphatic compounds (Legube et al., 1983; Miller and Olejnik, 2004). Furthermore, it should be noted that the intermediate compounds formed can also undergo both direct  $\text{O}_3$  and  $^\circ\text{OH}$  oxidation, which can lead to a competition with the target pollutant for the ozone molecules and/or  $^\circ\text{OH}$  (Miller and Olejnik, 2004). Additionally, the presence of  $^\circ\text{OH}$  scavengers, such as  $\text{Cl}^-$ ,  $\text{CO}_3^{2-}$  and other anions present naturally in water, can negatively affect PAH degradation (Miller and Olejnik, 2004; von Gunten, 2003). This assumption was

tested by Miller and Olejnik (2004) for BaP, CHR and FLU, using *t*-BuOH (0.02 M) as a  $^\circ\text{OH}$  scavenger, due to its low and high reaction rate with  $\text{O}_3$  and  $^\circ\text{OH}$  ( $3 \times 10^{-3} \text{ M}^{-1} \text{ s}^{-1}$  and  $5.9 \times 10^8 \text{ M}^{-1} \text{ s}^{-1}$ , respectively) (Elovitz and von Gunten, 1999), achieving an inhibition of about 6%–8% at a pH range of 2–12.

Besides being influenced by the presence of  $^\circ\text{OH}$  scavengers, a major limitation of the ozonation process is the formation of potentially harmful by-products. One of these is bromate, which is formed through waters containing bromide and is considered a possible human carcinogen (Matilainen and Sillanpää, 2010; von Gunten, 2003). In addition, the high costs of equipment and maintenance, as well as the energy required to power the process, are some of the disadvantages of this technique (Kornmüller and Wiesmann, 2003; Kornmüller et al., 1997; Litter and Quici, 2010).

In order to improve the performance of ozonation, some studies have attempted to couple  $\text{O}_3$  with UV radiation and/or  $\text{H}_2\text{O}_2$  (Beltrán et al., 1996b; Ledakowicz et al., 2001; Matilainen and Sillanpää, 2010; Miller and Olejnik, 2004; Rivas et al., 2000). Such processes are described in Section 3.2.1. Ozone combined with conventional biological process could be another way of enhancing  $\text{O}_3$  efficiency (Bernal-Martinez et al., 2007, 2009).

### 3.1.2. Direct photolysis

Direct photolysis is one of the dominant degradation pathway for PAHs in natural aqueous systems (Fasnacht and Blough, 2002, 2003; Jacobs et al., 2008; Kot-Wasik et al., 2004; Wang et al., 1999). Indeed, the photodegradation of AN and CHR at concentration levels of  $44.7 \mu\text{g L}^{-1}$  and  $97 \mu\text{g L}^{-1}$  was found to be 88.3% and 89.6%, respectively, under sunlight irradiation after 40 min for AN and 240 min for CHR (Wang et al., 1999).

The general mechanistic pathway of this technique consists of the absorption of light by PAHs, causing their excitation (Eq. (9)). The excited PAH can: a) return to the ground state, dissipating its energy (Eq. (10)) (Miller and Olejnik, 2001) or b) be transformed into a radical cation ( $\text{PAH}^{\circ+}$ ) and a solvated electron ( $e_{\text{aq}}^\circ$ ) (Eq. (11)). On the other hand,  $\text{O}_2$  from the water could react with the  $e_{\text{aq}}^\circ$  leading to  $\text{O}_2^{\circ-}$  or  $^1\text{O}_2$  formation (Eqs. (12)–(13)) (Fasnacht and Blough, 2002; Miller and Olejnik, 2001). These oxygen species can then react with the organic molecule to form intermediates, which in turn can undergo further oxidation and cause the mineralization of the parent compound (Eqs. (14)–(16)).



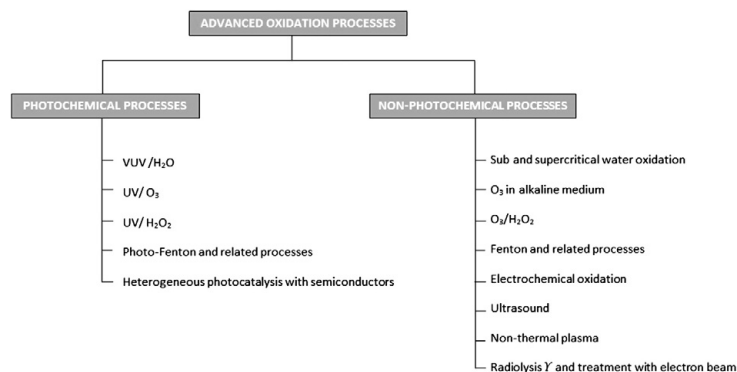
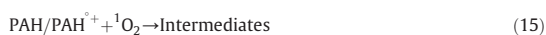
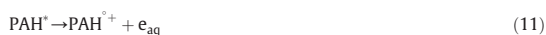


Fig. 3. AOP classification.



There are several reports that have studied the photolysis of PAHs like AN, BaA, BaP, CHR, DBF, DBT, FA, FLU, PHE, PYR and NA, under artificial conditions (Bertilsson and Widenfalk, 2002; Fasnacht and Blough, 2002; Jacobs et al., 2008; Miller and Olejnik, 2001; Sanches et al., 2011; Shemer and Linden, 2007). Under these conditions, the emission spectrum of the light source may overlap the absorption spectrum of the substance of interest thereby causing its degradation (Shemer and Linden, 2007). The wavelengths that can be absorbed by a compound depend on its structure (Sanches et al., 2011). The absorption spectra of PAHs range from 210 nm to 386 nm (Dabestani and Ivanov, 1999). At laboratory scale, Sanches et al. (2011) found AN

and BaP reductions of 83% and 93%, respectively, in a groundwater sample spiked with 3.9–5.6  $\mu\text{M}$  of the PAH of interest, under a LP-UV lamp with a fluence of  $1500 \text{ mJ cm}^{-2}$  after about 3 h and 4 h of irradiation, respectively. Fig. 2 shows the AN degradation pathway.

The most common sources of artificial light used in the reports are LP-UV and MP-UV. The effectiveness of each lamp on the removal of the PAHs depends on the absorption spectrum of the PAH of interest. For example, for BaP, whose absorption spectrum ranges from 235 nm to 410 nm, a MP-UV lamp emitting  $5.99 \times 10^{19} \text{ quanta s}^{-1} \text{ dm}^{-3}$  resulted to be more efficient than a LP-UV lamp ( $2.49 \times 10^{18} \text{ quanta s}^{-1} \text{ dm}^{-3}$ ). However, for CHR (230–330 nm) and FLU (230–310 nm), the LP-UV lamp resulted to be more efficient (Miller and Olejnik, 2001).

Apart from the absorption spectrum of the target compound, photolysis performance depends on the radiation intensity, pH, temperature and water background constituents (Bertilsson and Widenfalk, 2002; Fasnacht and Blough, 2002; Jacobs et al., 2008; Miller and Olejnik, 2001; Shemer and Linden, 2007). Commonly, it is known that an increase in radiation intensity enhances the chances of photon absorption and the subsequent PAH photolysis. Additionally, the effect of pH could be related to the structure of the PAHs and the associated molar extinction coefficient, as pH can alter the ionic form of the compound and make it more susceptible to a photochemical change (Miller and Olejnik, 2001). In turn, the influence of water temperature is indirectly related to the content of DO, since oxygen saturated solutions achieve a

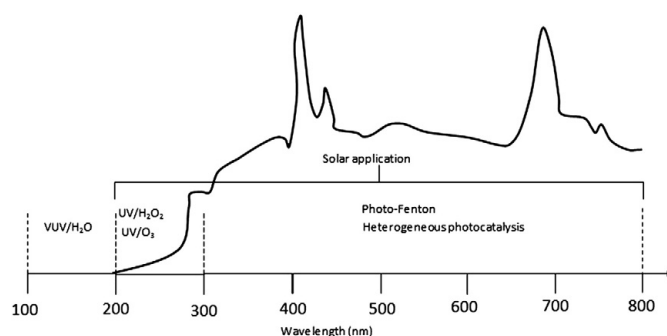


Fig. 4. Solar spectrum and wavelength range of several photochemical degradation processes.

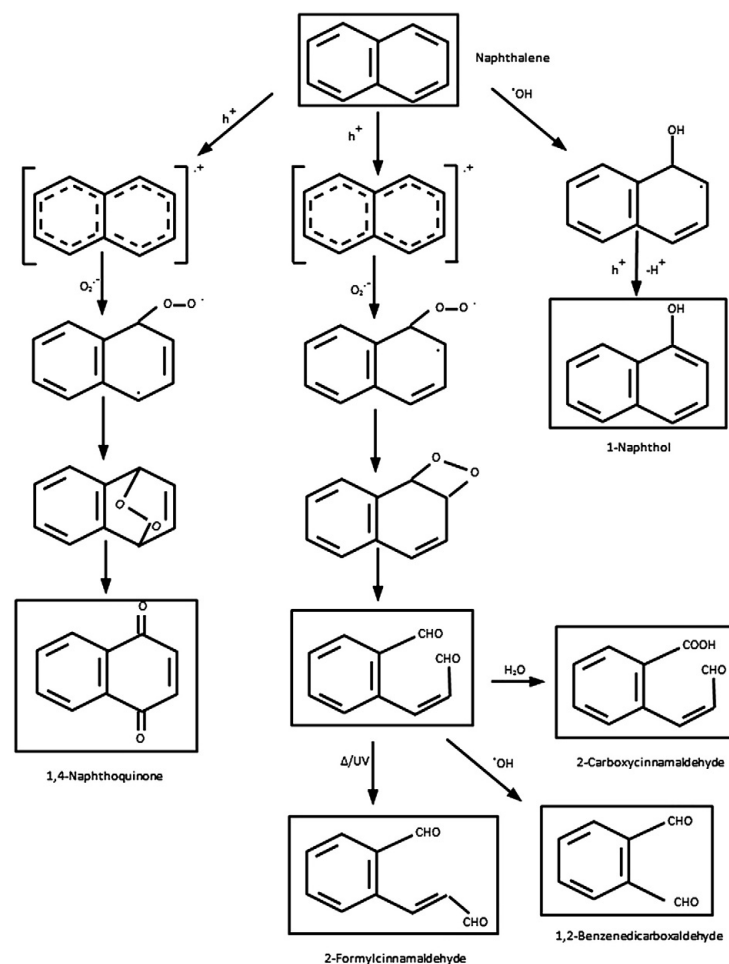


Fig. 5. Possible pathways for the formation of the main intermediates in the degradation of NA through  $\text{TiO}_2$  photocatalysis (Lair et al., 2008).

more efficient PAH photolysis (Miller and Olejnik, 2001; Wang et al., 1999). For instance, it was demonstrated that the removal of  $70 \mu\text{g L}^{-1}$  AN rose from 50% to 93% when the solution was stirred for 60 min, due to the increase in DO (Wang et al., 1999). Regarding the water matrix constituents, natural waters have different substances that may inhibit or improve the process by scavenging or generating oxidant species, respectively. For example, the DOM may be capable of forming reactive species which can oxidize PAHs (Fasnacht and Blough, 2002; Jacobs et al., 2008; Lehto et al., 2000). Furthermore, DOM may inhibit PAH photo-degradation (Sanchez et al., 2011) if the binding PAH-DOM reduces the lifetime of the excited states, decreasing the possibility of generating reactive intermediates (Fasnacht and Blough, 2002). On the contrary,  $\text{NO}_3^-$  may improve PAH degradation because it is able to produce  $^{\circ}\text{OH}$  (Mack and Bolton, 1999). This was corroborated by Jacobs et al. (2008), when they experimented with PHE ( $1.0 \times 10^{-6} \text{ M}$ ) in natural water spiked with 0.2 mM and 0.4 mM  $\text{NO}_3^-$  at pH 6.8, using a solar simulator. The PHE degradation rate increased by  $0.064 \text{ h}^{-1}$  and  $0.09 \text{ h}^{-1}$ , respectively.

Although direct photolysis is a common degradation process that occurs naturally in aqueous environments, it is important to note that some intermediate compounds may be hazardous to aquatic life (El-Alawi et al., 2002; Grote et al., 2005). An example is anthraquinone, which comes from the photolysis of AN (Sanchez et al., 2011). Furthermore, direct photolysis appears to be less effective than other processes where radiation is combined with an oxidant such as  $\text{H}_2\text{O}_2$  or  $\text{O}_3$ , where homogeneous and heterogeneous catalysis are employed (Gogate and Pandit, 2004b) or where UV is even coupled to conventional biological systems (Guieysse and Viklund, 2005; Guieysse et al., 2004).

### 3.2. Advanced oxidation processes

AOPs refer to several chemical oxidation methods whose common characteristic is the production of  $^{\circ}\text{OH}$  (Glaze et al., 1987).  $^{\circ}\text{OH}$  is a highly reactive and non-selective species able to attack and destroy the most persistent and toxic organic molecules (R) (Andreozzi et al., 1999). It

does this mainly by: (a) H-addition to C=C bonds or to aromatic rings (Eq. (17)); (b) H abstraction from C–H, N–H or O–H bonds (Eq. (18)); and (c) electron transfer reactions (Eq. (19)) (Munter, 2001; Von Sonntag, 2006). AOPs can even achieve the total mineralization of organic substances, yielding CO<sub>2</sub>, H<sub>2</sub>O and inorganic ions such as Cl<sup>-</sup>, NH<sub>4</sub><sup>+</sup> and SO<sub>4</sub><sup>2-</sup> (Litter and Quici, 2010).



These alternative chemical oxidation processes use different combinations of oxidants, energy sources and catalysts to generate °OH in water. They can be classified as photochemical and non-photochemical processes (Fig. 3). The former include techniques using UV or visible radiation, from water photolysis in the vacuum ultraviolet (H<sub>2</sub>O/VUV) to homogeneous or heterogeneous photocatalysis with semiconductors or chemical oxidizers, including UV/O<sub>3</sub>, UV/H<sub>2</sub>O<sub>2</sub> and photo-Fenton (UV/H<sub>2</sub>O<sub>2</sub>/Fe<sup>2+</sup>) and related processes. In turn, non-photochemical processes include sub and supercritical water oxidation, ozonation in an alkaline medium, O<sub>3</sub>/H<sub>2</sub>O<sub>2</sub>, Fenton (H<sub>2</sub>O<sub>2</sub>/Fe<sup>2+</sup>) and related processes, techniques involving electrical and ultrasound energy, non-thermal plasma and radiolysis γ, and treatment with an electron beam. In addition, AOPs can be combined with each other, resulting in variant systems, such as electro-Fenton and photo-electro-Fenton, US/UV/TiO<sub>2</sub>, sono-Fenton and UV/O<sub>3</sub>/H<sub>2</sub>O<sub>2</sub> systems, among others (Comminellis et al., 2008; Gogate and Pandit, 2004b).

Fig. 4 represents the wavelengths under which various photodegradation processes take place. As shown in the figure, some of these AOPs involve the interaction of artificial or natural solar light with the target molecule and the induction of photochemical reactions, which can lead to the direct degradation of the molecule and the generation of intermediate products whose further decomposition could yield mineral end-products.

The efficiency of these oxidation techniques depends on various parameters, such as the oxidant dose, UV/visible-light intensity, reaction time, pH, the free radical generation rate, physico-chemical properties and initial concentration of the target pollutant, and the water matrix constituents (suspended materials, presence of anions, HS, etc.). The role of these parameters on AOP performance has been sufficiently described for different types of aqueous matrices (Chong et al., 2010; Pera-Titus et al., 2004), including groundwater (Vela et al., 2012), wastewater (Dopar et al., 2011; Gogate and Pandit, 2004a,b,c), synthetic water (Crittenden et al., 1999; Homem et al., 2009; Lair et al., 2008; Manariotis et al., 2011; Souza et al., 2011) and drinking water (Matilainen and Sillanpää, 2010) with successful results. However, one of the main drawbacks of AOPs is related to the relatively high operational costs associated, due to the use of costly chemicals (e.g. H<sub>2</sub>O<sub>2</sub>) and the increased energy consumption (Comminellis et al., 2008; Oller et al., 2011). Moreover, as mentioned previously, all of these methods are susceptible to °OH scavenging by non-target substances included in the water to be treated.

Nevertheless, it should be noted that the systems that benefit from the solar light source result more economical and, consequently, they are the most promising photochemical AOPs (Comminellis et al., 2008; Malato et al., 2009; Prieto-Rodríguez et al., 2013). For instance, Prieto-Rodríguez et al. (2013) assessed the costs associated to the use of the solar photo-Fenton system and ozonation as tertiary treatments for 98% micropollutant elimination in a concentration range of 40–80 µg L<sup>-1</sup> in a 5000 m<sup>3</sup> d<sup>-1</sup> real MWTP effluent. They showed that solar photo-Fenton total estimated costs were 0.358 € m<sup>-3</sup> (including

reagent, labor, electricity and investment costs), in comparison with 0.560 € m<sup>-3</sup> for ozonation.

On the other hand, the combination of different AOPs could give better results in terms of efficiency in contrast to individual techniques (Comminellis et al., 2008; Gogate and Pandit, 2004b). Regarding US-based AOPs, Torres et al. (2007b) found at lab-scale that the electrical energy consumption for a 300 mL influent mineralization containing 118 µM bisphenol-A in a US/UV/Fe<sup>2+</sup> process (1033 kWh m<sup>-3</sup>) was four or six times lower than the US/UV (3735 kWh m<sup>-3</sup>) and US/Fe<sup>2+</sup> (6010 kWh m<sup>-3</sup>) systems, respectively. Nonetheless, the cost associated to their application is higher in comparison with biological processes (Sánchez et al., 2013). For example, the application of the solar photo-Fenton process to the treatment of 500 mg L<sup>-1</sup> alpha-methyl-phenylglycine costs about seven times more in comparison with the associated costs for nutrient removal through activated sludge treatment (14.1 € m<sup>-3</sup> and 0.25 € m<sup>-3</sup>, respectively) (Hernández-Sancho et al., 2011; Muñoz et al., 2008). However, the use of conventional biological systems for PAH treatment is limited due to the toxic character of these compounds, as mentioned previously.

One way to overcome the cost problems associated with AOPs and to benefit from their oxidation potential is by coupling AOPs with biological treatments, either as pre-treatment or post-treatment (Oller et al., 2011). For instance, the estimated cost for treating 1260 kg COD d<sup>-1</sup> in a combined solar photo-Fenton and biological system at an industrial scale has been found to be about 7 € m<sup>-3</sup>, including plant capital costs (Comminellis et al., 2008). Additionally, it is important to note that in some cases the intermediates formed are more toxic than the parent compounds, therefore, previous toxicity tests are needed when AOPs are proposed as pre-treatments for a biological system (Oller et al., 2011; Vela et al., 2012).

In the following sections, a wide range of advanced oxidation systems that has been explored for the degradation of PAHs is described. The most relevant experimental conditions and the results of these studies are shown in Table 1.

### 3.2.1. Ozone-based AOPs: UV/O<sub>3</sub> and O<sub>3</sub>/H<sub>2</sub>O<sub>2</sub>

According to some research, conventional ozonation process may be ineffective for the oxidation of pollutants that react slowly with ozone (Ledakowicz et al., 2001), such as alachlor, tetrachloroethene and benzene (von Gunten, 2003). The use of UV radiation or another oxidant like H<sub>2</sub>O<sub>2</sub> combined with O<sub>3</sub> could enhance their degradation rates (Litter and Quici, 2010; Matilainen and Sillanpää, 2010; von Gunten, 2003).

For the UV/O<sub>3</sub> combined process, the reaction mechanism initiates with the photolysis of O<sub>3</sub>, which directly produces O<sub>2</sub> and H<sub>2</sub>O<sub>2</sub> (Eq. (20)). H<sub>2</sub>O<sub>2</sub> photolyse to °OH (Eq. (21)) or dissociates to HO<sub>2</sub><sup>-</sup> (Eq. (22)); initiating the further decomposition of residual O<sub>3</sub> into °OH (Eqs. (3)–(7)), which in turn can attack O<sub>3</sub> (Eq. (8)) and H<sub>2</sub>O<sub>2</sub> (Eq. (23)) molecules (Glaze et al., 1987; von Gunten, 2003).



In the case of the O<sub>3</sub>/H<sub>2</sub>O<sub>2</sub> system, O<sub>3</sub> decomposition is initiated by H<sub>2</sub>O<sub>2</sub> by means of electron transfer, yielding °OH and HO<sub>2</sub><sup>°</sup> (Eq. (24)). In both of these techniques, the generated HO<sub>2</sub><sup>°</sup> are involved in °OH production through a chain mechanism described by Eqs. (4)–(7), improving the degradation power of these processes (Domenech et al., 2004; Litter and Quici, 2010).



When PAHs are introduced into the UV/O<sub>3</sub> or O<sub>3</sub>/H<sub>2</sub>O<sub>2</sub> system, they can theoretically undergo °OH, HO<sub>2</sub>° or O<sub>3</sub>° oxidation and direct ozonation, as well as direct photolysis or H<sub>2</sub>O<sub>2</sub> oxidation, in the case of the UV/O<sub>3</sub> and O<sub>3</sub>/H<sub>2</sub>O<sub>2</sub> processes, respectively. This increases the efficiency of these techniques (Ledakowicz et al., 2001; Litter and Quici, 2010). In fact, UV/O<sub>3</sub> experiments carried out by Ledakowicz et al. (2001) showed that BaP, CHR and FLU degradation (4.76 nM, 5.12 nM and 5.42 μM, respectively) was about 85% (BaP) and 90% (CHR and FLU). This was higher in comparison with the removal obtained by O<sub>3</sub> oxidation (~10%, 70% and 50%) or by UV radiation (~80%, 40% and 55%) when acting individually, after a reaction time of 75 s (BaP and CHR), and 600 s (FLU), under a LP-UV lamp (4.13 × 10<sup>-6</sup> Eins dm<sup>-3</sup> s<sup>-1</sup>) and with O<sub>3</sub> levels of 5.2 mg dm<sup>-3</sup> (BaP), 15.2 mg dm<sup>-3</sup> (CHR) and 30.2 mg dm<sup>-3</sup> (FLU). These results, differ from those attained by Trapido et al. (1995) for AN, BaP, FA, FLU, BghiPY, PHE and PYR, and by Rivas et al. (2000) for ACN (see operating conditions in Table 1). The studies of these two authors conclude that there was no acceleration in PAH conversion when UV radiation and/or H<sub>2</sub>O<sub>2</sub> was added to the ozonation system. For example, in the case of PHE, the same removal rates were achieved by ozonation and the O<sub>3</sub>/H<sub>2</sub>O<sub>2</sub> and UV/O<sub>3</sub> systems, while for AN and PYR, UV/O<sub>3</sub> caused detrimental effects (Trapido et al., 1995). This suggests that the O<sub>3</sub>-based AOP effect on PAH degradation depends heavily on the experimental conditions.

The performance of UV/O<sub>3</sub> and O<sub>3</sub>/H<sub>2</sub>O<sub>2</sub> processes is mainly affected by the pH of the medium (von Gunten, 2003). Regarding the UV/O<sub>3</sub> system, after 30 s of treatment 77% of CHR was removed under pH 2, while a 22% removal was achieved at pH 12 (Ledakowicz et al., 2001).

When comparing UV/O<sub>3</sub> and O<sub>3</sub>/H<sub>2</sub>O<sub>2</sub> with the UV/H<sub>2</sub>O<sub>2</sub> process, it is worth noting that the two former systems are less energetically efficient than UV/H<sub>2</sub>O<sub>2</sub> at forming large quantities of °OH due to the low solubility of O<sub>3</sub> in water compared to H<sub>2</sub>O<sub>2</sub> (Litter and Quici, 2010; Pera-Titus et al., 2004). Thus, the operational costs are expected to be higher if large amounts of contaminant are present. Gaseous O<sub>3</sub> must be diffused into the water, resulting in potential mass transfer limitations when compared with H<sub>2</sub>O<sub>2</sub>, which is fed as a liquid solution (Litter and Quici, 2010; Pera-Titus et al., 2004). Consequently, the UV/O<sub>3</sub> and O<sub>3</sub>/H<sub>2</sub>O<sub>2</sub> processes require efficient reactor designs in order to maximize the O<sub>3</sub> mass transfer coefficient (von Gunten, 2003). Additionally, it should be mentioned that, despite the limitations associated with the gas-liquid O<sub>3</sub> mass transfer, AOPs involving O<sub>3</sub> may generate harmful by-products like bromate (Matilainen and Sillanpää, 2010; von Gunten, 2003), as mentioned before.

### 3.2.2. Ultraviolet radiation and hydrogen peroxide (UV/H<sub>2</sub>O<sub>2</sub>)

This AOP entails the formation of °OH generated by the direct photolysis of H<sub>2</sub>O<sub>2</sub> or HO<sub>2</sub><sup>-</sup> and the corresponding propagation reactions. The UV/H<sub>2</sub>O<sub>2</sub> system initiates with the O–O bond cleavage of H<sub>2</sub>O<sub>2</sub> or HO<sub>2</sub><sup>-</sup> by the application of UV radiation, thereby generating °OH (Eq. (25)). The propagation and termination reactions are described by Eqs. (26)–(30) (Kralik et al., 2010; Litter and Quici, 2010). It can be observed that the radical species generated may be combined, reducing the oxidation power of the system.



In the presence of organic compounds in solution (Litter and Quici, 2010; Pera-Titus et al., 2004), such as PAHs, °OH quickly react with the target organic substances, resulting in their oxidation (Eq. (31)). In addition to being oxidized by °OH, PAHs may be subject to direct photolysis under UV radiation as mentioned in Section 3.1.2 (Eq. (32)) and confirmed by Sanches et al. (2011) for AN and BaP, and by Włodarczyk-Makula (2011) for NA. Although H<sub>2</sub>O<sub>2</sub> may attack the PAHs, it has been proven that 0.1 M H<sub>2</sub>O<sub>2</sub> has an insignificant contribution to BaP and CHR (20% of removal) and has no effect on FLU, after 40 min of treatment (Ledakowicz et al., 2001).



During the application of the UV/H<sub>2</sub>O<sub>2</sub> system, the intermediate products formed, such as DBF and 2-methyl-1,1'-biphenyl which come from FLU (Beltrán et al., 1996a), can be potentially hazardous. However, they can be transformed into carboxylic acids, like oxalic acid when the oxidation time is prolonged (Beltrán et al., 1996a).

The combination of UV radiation and H<sub>2</sub>O<sub>2</sub> results in a better degradation of PAHs (Shemer and Linden, 2007). Indeed, it has been demonstrated that the UV/H<sub>2</sub>O<sub>2</sub> combination results in an increase in the removal rates and efficiency of several PAHs in water, including AC, BaP, CHR, DBF, DBT, FLU, PHE and PYR, compared to UV radiation or H<sub>2</sub>O<sub>2</sub> alone (An and Carraway, 2002; Beltrán et al., 1996a; Ledakowicz et al., 1999; Shemer and Linden, 2007). For example, it was observed that only 6% of the initial DBT (2 μM) was eliminated using a 1000 mJ cm<sup>-2</sup> LP-UV lamp. Under the same conditions, the addition of 10 mg L<sup>-1</sup> H<sub>2</sub>O<sub>2</sub> to the system resulted in an efficiency 36 times higher than direct photolysis (Shemer and Linden, 2007).

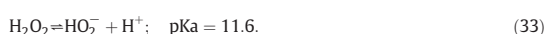
The major factors affecting the UV/H<sub>2</sub>O<sub>2</sub> system are the H<sub>2</sub>O<sub>2</sub> concentration and the initial amount of the target compound, as well as the incident UV light, the water pH, the temperature and the water matrix compounds (Crittenden et al., 1999; Litter and Quici, 2010; Matilainen and Sillanpää, 2010; Pera-Titus et al., 2004).

Theoretically, in this process, the higher the initial H<sub>2</sub>O<sub>2</sub> concentration, the higher the °OH concentration that is produced (Eq. (25)), increasing the conversion of PAHs (Eq. (31)). However, an optimal H<sub>2</sub>O<sub>2</sub> concentration exists because H<sub>2</sub>O<sub>2</sub> overdosing would promote Eqs. (26)–(30) and consume radical species (Kralik et al., 2010; Matilainen and Sillanpää, 2010). This confirms that in the UV/H<sub>2</sub>O<sub>2</sub> system °OH usually plays the main role in the oxidation of organic pollutants (Litter and Quici, 2010). Nevertheless, it is important to note that the reactivity of the PAHs towards °OH depends on their chemical structure (Shemer and Linden, 2007). This was corroborated by Ledakowicz et al. (1999) for FLU, who observed that °OH conversion was not influenced by the well-known °OH scavenger t-BuOH. Therefore, FLU radical pathway through °OH resulted to be less clear than for BaP or CHR. This could be explained by the structural differences between FLU and BaP and CHR, since FLU has a five-member non-aromatic ring on its structure, whereas BaP and CHR are composed entirely of benzene rings.

In order to achieve a highly efficient process, the UV light emission spectrum must overlap the H<sub>2</sub>O<sub>2</sub> absorption spectrum. The best UV-light lamps for the UV/H<sub>2</sub>O<sub>2</sub> process are those emitting under 280 nm (Andreozzi et al., 1999). Among the different lamp possibilities, the LP-UV and DBD lamps represent a good alternative (Hofman-Caris and Beerendonk, 2011; Hofman-Caris et al., 2012).

Additionally, the efficiency of the UV/H<sub>2</sub>O<sub>2</sub> process is pH dependent (Litter and Quici, 2010). The increase of pH leads to an opposite effect. Higher pH values can enhance the production of °OH, since at 253.7 nm the molar extinction coefficient of the HO<sub>2</sub><sup>-</sup> (the main species at a pH above 11.6), is higher than that of H<sub>2</sub>O<sub>2</sub> (240 M<sup>-1</sup> cm<sup>-1</sup> and

19 M<sup>-1</sup> cm<sup>-1</sup>, respectively) (Glaze et al., 1987) (Eq. (33)). In contrast, according to data from the literature, alkaline conditions can also reduce the oxidation rate of PAHs like BaP, CHR and FLU (Beltrán et al., 1996a; Ledakowicz et al., 1999). There are some possible explanations for this: a) the CO<sub>3</sub><sup>2-</sup> and HCO<sub>3</sub><sup>-</sup> levels, generally present in natural waters, increase with increasing pH and they act as effective °OH scavengers, especially CO<sub>3</sub><sup>2-</sup> (Gogate and Pandit, 2004b) and b) when the pH is increased (especially above 11.6), the °OH scavenging effect becomes stronger, as the reaction rate constant of Eq. (26) is about two orders of magnitude lower than Eq. (27) ( $k_{\text{Eq.27}} = 2.7 \times 10^7 \text{ M}^{-1} \text{ s}^{-1}$  and  $k_{\text{Eq.26}} = 7.5 \times 10^9 \text{ M}^{-1} \text{ s}^{-1}$ ). For instance, Ledakowicz et al. (1999) found that CHR conversion at pH = 11.7 and  $1 \times 10^{-3} \text{ M H}_2\text{O}_2$  diminished from about 90% to 70% compared to that obtained at a neutral pH after about 110 s of reaction.



Regarding the matrix constituents, the presence of inorganic anions and HS, generally exert a negative impact on the UV/H<sub>2</sub>O<sub>2</sub> process by scattering or absorbing UV radiation and consuming high amounts of °OH (Baeza and Knappe, 2011; Li et al., 2010; Xu et al., 2005). However, the adverse effect of the water matrix constituents varies according to their concentration levels (Li et al., 2010). For example, Beltrán et al. (1996a) assessed the influence of HCO<sub>3</sub><sup>-</sup> doses from 1 mM to 10<sup>-2</sup> M on the degradation of FLU ( $4.7 \times 10^{-6} \text{ M}$ ), under 1 nM H<sub>2</sub>O<sub>2</sub>, pH 7 and  $3.8 \times 10^{-6} \text{ Ein s}^{-1}$ , showing that the levels of HCO<sub>3</sub><sup>-</sup> tested did not affect the FLU oxidation rate.

In addition to those factors, temperature is another parameter that can impact the UV/H<sub>2</sub>O<sub>2</sub> system (Li et al., 2010; Sanz et al., 2013). However, its role is controversial, since, H<sub>2</sub>O<sub>2</sub> decomposition into H<sub>2</sub>O and O<sub>2</sub> increases as temperature rises (Crittenden et al., 1999). On the other hand, temperature can favor reaction kinetics, as demonstrated by Sanz et al. (2013) for solutions of linear alkylbenzene sulphonates ( $1 \text{ g L}^{-1}$ ) at 60 °C. Moreover, temperature in the range of 9–30 °C can influence water matrix effects, as confirmed by Li et al. (2010) for clofibrac acid, because at higher temperatures, the negative effect of 20 mg L<sup>-1</sup> humic acids became less apparent, enhancing the clofibrac acid removal. In the case of PAHs, the effect of temperature on the UV/H<sub>2</sub>O<sub>2</sub> technique has been scarcely studied; therefore, further investigation is needed.

Furthermore, in order to improve the solubility of PAHs in water and, therefore, their conversion rates, An and Carraway (2002) studied the effect of surfactant solutions in the UV/H<sub>2</sub>O<sub>2</sub> system for PHE and PYR. They found that micelles could provide the tested PAHs with some degree of protection from °OH attack, contrary to what was expected.

Although the UV/H<sub>2</sub>O<sub>2</sub> system has shown to be very effective at the removal of PAHs, including AC, BaP, CHR, DBF, DBT, FLU and PHE, with reduction rates of up to 99% after only a few minutes of treatment (Beltrán et al., 1996a; Ledakowicz et al., 1999; Shemer and Linden, 2007), there are some drawbacks that must be overcome. One of the greatest limitations of this method is related to the °OH scavenging or light scattering effect by water matrix constituents (Litter and Quici, 2010; Pera-Titus et al., 2004). Another disadvantage of this process is that it cannot practically utilize solar light as a light source, due to the fact that the required UV energy for the photolysis of the oxidant is hardly available in the solar spectrum (Litter and Quici, 2010). This results in a rise in the operational costs related to the cleaning and replacement of UV lamps, and the use of the costly reagent H<sub>2</sub>O<sub>2</sub> (Comninellis et al., 2008).

### 3.2.3. Fenton, photo-Fenton and related processes

The Fenton (Fe<sup>2+</sup>/H<sub>2</sub>O<sub>2</sub>) and photo-Fenton processes (Fe<sup>2+</sup>/H<sub>2</sub>O<sub>2</sub>/UV) have been widely used for the abatement of organic pollutants (e.g. pharmaceuticals, pesticides, polyaromatics, dyes, diesel, phenols

and chlorophenols, among others) (Abdessalem et al., 2010; Batista and Nogueira, 2012; Bautitz and Nogueira, 2007; Galvão et al., 2006; Ghaly et al., 2001; Kavitha and Palanivelu, 2004; Lopez-Alvarez et al., 2012; Pérez et al., 2002; Pignatello et al., 2006; da Rocha et al., 2013). These AOPs are based on the use of the Fenton's reagent, which is defined as a mixture of ferrous iron salts (catalyst) and H<sub>2</sub>O<sub>2</sub> (oxidizing agent) (Pignatello et al., 2006). When Fe<sup>2+</sup> react with H<sub>2</sub>O<sub>2</sub>, dissociation of the oxidant is produced and reactive °OH are generated (Eq. (34)). Additionally, the ferric ions formed decompose H<sub>2</sub>O<sub>2</sub> to regenerate Fe<sup>2+</sup> and yield HO<sub>2</sub><sup>°</sup> (Eq. (35)) (Neyens and Baeyens, 2003; Pignatello et al., 2006).



The organic compounds present in water are mainly oxidized by °OH (Eq. (36)), principally by abstracting hydrogen atoms or by adding them to double bonds and aromatic rings (Lundstedt et al., 2006).

In the Fenton process, reaction (35) is the step that limits the process, since the associated rate constant is very low (about 0.02–0.01 M<sup>-1</sup> s<sup>-1</sup>) (Neyens and Baeyens, 2003; Pignatello et al., 2006). Therefore, to increase the efficiency of the Fenton process, elevated concentrations of H<sub>2</sub>O<sub>2</sub> and Fe<sup>2+</sup> are required. However, excessive amounts of H<sub>2</sub>O<sub>2</sub> and Fe<sup>2+</sup> could be detrimental for the system because of their radical scavenging effect (Eqs. (26) and (36)), which inhibits their reaction with the organic pollutants present in water (Galvão et al., 2006). Additionally, an excessive addition of Fe<sup>2+</sup> can reduce the UV radiation penetration in the water solution of the photo-Fenton system, due to its significant opacity (Galvão et al., 2006; Gogate and Pandit, 2004b). Furthermore, if °OH and HO<sub>2</sub><sup>°</sup> are produced in high quantities, recombination reactions can occur (Eqs. (28)–(30)), reducing the effectiveness of the systems (Neyens and Baeyens, 2003).



The effects related to H<sub>2</sub>O<sub>2</sub> and Fe<sup>2+</sup> concentrations have been established in AC, AN, BaP, FLU and PHE removal studies (Beltrán et al., 1998; Homem et al., 2009; Nadarajah et al., 2002). In the case of BaP elimination by the Fenton AOP, it was observed that H<sub>2</sub>O<sub>2</sub> levels higher than 50 mg L<sup>-1</sup> were detrimental for the removal of 10 µg L<sup>-1</sup> at pH 3.5 and 40 °C, reducing BaP conversion from about 85% (50 mg L<sup>-1</sup> H<sub>2</sub>O<sub>2</sub>) to 50% (150 mg L<sup>-1</sup> H<sub>2</sub>O<sub>2</sub>) after 15 min of reaction. Under the same operating conditions, it was noticed that there was a conversion increase (from about 70% to 100%) as Fe<sup>2+</sup> rose (from 3.75 mg L<sup>-1</sup> to 5.5 mg L<sup>-1</sup>, respectively), although no significant differences were found between 2.75 mg L<sup>-1</sup> and 3.75 mg L<sup>-1</sup> (Homem et al., 2009). Apart from the oxidant agent and catalyst levels, the dose of the initial organic contaminant also affects the Fenton and photo-Fenton processes, because it determines the amount of H<sub>2</sub>O<sub>2</sub> and Fe<sup>2+</sup> to be used (Neyens and Baeyens, 2003). For a fixed level of H<sub>2</sub>O<sub>2</sub> and Fe<sup>2+</sup> (50 mg L<sup>-1</sup> and 3.75 mg L<sup>-1</sup>, respectively), Homem et al. (2009) studied the maximum amount of BaP that could be efficiently removed from a Fenton system working at pH 3.5 and 40 °C. They found that BaP doses of 10 µg L<sup>-1</sup> were reduced by 100% after a reaction period of 90 min.

In turn, pH is an extremely important factor affecting the efficiency of both Fenton and photo-Fenton systems. The pH solution for processes involving Fenton's reagent ranges from 2.5 to 4, with an optimum at pH 2.8 (Pignatello et al., 2006). At pH values higher than 4, Fe<sup>3+</sup> form complexes with OH<sup>-</sup>, leading to a precipitate, and inhibiting Fe<sup>2+</sup> regeneration and the production of additional °OH (Neyens and Baeyens, 2003; Pignatello et al., 2006). Furthermore, H<sub>2</sub>O<sub>2</sub> is more stable at pH values below 2.5 because of the generation of oxonium ions (H<sub>3</sub>O<sub>2</sub><sup>+</sup>), and the predominance of iron hexaaqua complexes



( $[\text{Fe}(\text{H}_2\text{O})_6]^{2+}$ ), which at these pH values are less reactive with  $\text{H}_2\text{O}_2$  (Pignatello et al., 2006). In the case of PAHs, when pH values in the range of 3 to 7 were experimented with, it was found that acidic conditions provided the best results for AN, with a maximum at pH 4 (Nadarajah et al., 2002). On the contrary, Beltrán et al. (1998) observed that the pH of water should be near 7 to achieve successful elimination rates of AC, FLU and PHE. In turn, Homem et al. (2009) noted that in the range of 3.5–6, the pH had an insignificant influence on BaP removal. However, in both of the latter two cases, the absorption of pollutants by the iron complexes predominating at the tested pH values was not evaluated by the authors.

Temperature can have a positive effect on these processes, since it could increase the rate of degradation reactions (Pignatello et al., 2006). For instance, experiments conducted by Homem et al. (2009) at different levels of temperature led to BaP ( $10 \mu\text{g L}^{-1}$ ) removal efficiencies of 90% (at 30 °C) and 100% (at 70 °C) after 90 min using  $200 \text{ mg L}^{-1} \text{H}_2\text{O}_2$ ,  $5.5 \text{ mg L}^{-1} \text{Fe}^{2+}$  and pH 3.5. Nevertheless, special attention should be paid to the  $\text{H}_2\text{O}_2$  decomposition with an increase in temperature (Crittenden et al., 1999).

On the other hand, the presence of  $\text{HS}$ ,  $\text{CO}_3^{2-}$  and  $\text{HCO}_3^-$  in the solution can retard the PAH removal rates, as demonstrated by Beltrán et al. (1998) for FLU with Fenton's reagent ( $0.01 \text{ M H}_2\text{O}_2$ ,  $0.1 \text{ mM Fe}^{2+}$ ) at pH 7 and 20 °C. Additionally, Veignie et al. (2009) and Nadarajah et al. (2002) studied the effect of substances that improve PAH water solubility, such as cyclodextrines and surfactants in the Fenton system. For BaP degradation, Veignie et al. (2009) found that when the BaP level was above its solubility limit ( $5 \times 10^{-3} \text{ M}$ ), the presence of cyclodextrines ( $5 \times 10^{-3} \text{ M}$ ) enhanced the efficiency of the system by up to ~12%, since only the solubilized BaP could be oxidized by the  $^\circ\text{OH}$  generated (Flotron et al., 2005).

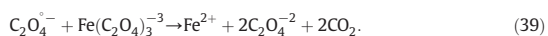
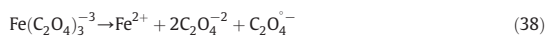
The Fenton and photo-Fenton systems are easy and simple operating processes. Nevertheless, the Fenton technique has the drawback of requiring high amounts of  $\text{Fe}^{2+}$  to achieve a successful efficiency, and subsequently a large amount of sludge is generated (Litter and Quici, 2010). In this sense, the photo-Fenton process seems to be more efficient, since the rate of  $\text{Fe}^{2+}$  regeneration is significantly increased by the interaction of either UV or visible light, with  $\text{Fe}^{3+}$  complexes in solution. This produces additional  $^\circ\text{OH}$ , as represented by Eq. (37) (Kavitha and Palanivelu, 2004; Will et al., 2004), which results in a synergistic effect between the light and the Fenton reagent. Indeed, it has been observed that the photo-Fenton process leads to the mineralization of up to 99% of wastewater containing diesel ( $100 \text{ mL L}^{-1}$ ). This mineralization value is higher than the sum of the individual UV photolysis (28%) and Fenton reagent (26%) efficiencies after 30 min of reaction ( $50 \text{ mM H}_2\text{O}_2$ ,  $0.1 \text{ mM Fe}^{2+}$ ,  $450 \text{ W MP-UV lamp}$ , pH 3 and 33 °C) (Galvão et al., 2006).



On the other hand, apart from being an effective AOP, the photo-Fenton process can be fast. Engwall et al. (1999) studied the efficiency of the photo-Fenton system at the degradation of saturated aqueous solutions of creosote at laboratory scale. They used a PAH content of 85% and the following experimental conditions:  $10 \text{ mM H}_2\text{O}_2$ ,  $1 \text{ mM Fe}^{3+}$ ,  $1.4 \times 10^{-3} \text{ M photons min}^{-1}$  black UV lamp, pH 2.75 and 20 °C. The results showed reductions of about 90% or higher after 5 min of treatment, except for FA (71.8%), BbFLU (66.5%), BbF (57.2%) and BaP (37.6%). However, when extending the reaction time to 180 min, in all cases, further conversion (>90%) was achieved, with the exception of BaP (67.3%).

Additionally, when  $\text{Fe}^{3+}$  oxalate complexes are used as iron sources, additional  $\text{Fe}^{2+}$  are formed (Eqs. (38), (39)), enhancing the speed of pollutant degradation (Gogate and Pandit, 2004b). Furthermore, wavelengths of up to 600 nm can be used, thereby offering the possibility of using solar radiation, which reduces operational costs (Litter and Quici,

2010). Another way of minimizing operational costs is to take advantage of the iron content usually present in natural waters (da Rocha et al., 2013).



Nevertheless, the photoassisted Fenton process has the problem of sludge formation, and it requires an exhaustive pH control to achieve successful results, as well as the Fenton system itself (Homem et al., 2009), which implies greater reactive costs because the pH of water must be decreased and then increased before effluent discharge. In order to overcome these problems and improve the effectiveness of the Fenton and photo-Fenton processes, supported iron catalysts can be used. This prevents the sludge production and its subsequent separation before releasing the effluent into the aqueous environment and allows the system to work at higher pH conditions (Neyens and Baeyens, 2003). The two systems can also be combined with other AOPs, like UV/TiO<sub>2</sub> and electrochemical oxidation (Oonnittan et al., 2008, 2009a,b).

When the TiO<sub>2</sub> heterogeneous photocatalysis is coupled with iron ions, the addition of  $\text{H}_2\text{O}_2$  to the system is required, because the  $\text{H}_2\text{O}_2$  generated via UV/TiO<sub>2</sub> is not sufficient to drive the Fenton reaction (Chong et al., 2010). Nevertheless, the addition of  $\text{H}_2\text{O}_2$  is not needed or can be limited when the Fenton or photo-Fenton process is combined with high frequency ultrasound or electrochemical oxidation (electro-Fenton and photo-electro-Fenton), since  $\text{H}_2\text{O}_2$  can be formed sonochemically (Torres et al., 2007a,b) or electrochemically through O<sub>2</sub> reduction on the cathode (Matilainen and Sillanpää, 2010).

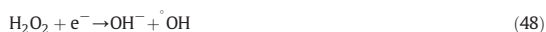
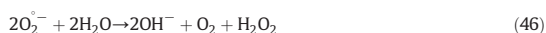
The electro-Fenton and photo-electro-Fenton processes have recently received a lot of attention for their water remediation potential. Compared to the conventional Fenton process, the electro-Fenton method has the following advantages: (a) the one-site production of  $\text{H}_2\text{O}_2$ , that avoids risks related to its transport, storage and handling; (b) the possibility of controlling degradation kinetics to allow mechanistic studies to be performed; (c) the higher degradation rate of organic pollutants because of the continuous regeneration of  $\text{Fe}^{2+}$  at the cathode, which also minimizes sludge production; and (d) the feasibility of overall mineralization at a relatively low cost if the operation parameters are optimized (Brillas et al., 2009; Liu et al., 2007; Nidheesh and Gandhimathi, 2012). These processes have been used for the decontamination of several pollutants in water, such as aniline, phenol, pesticides or dyes (Abdessalem et al., 2010; Anotai et al., 2006; Babuponnusami and Muthukumar, 2012; Panizza and Cerisola, 2009). However, the degradation of PAHs in water using these techniques has not been reported.

### 3.2.4. Heterogeneous photocatalysis with semiconductors

Photocatalysis is widely used to describe the process based on a series of light-induced redox reactions occurring when a semiconductor (e.g. TiO<sub>2</sub>, ZnO, SnO<sub>2</sub>, WO<sub>3</sub> and Al<sub>2</sub>O<sub>3</sub>), interacts with light to produce reactive species. This can lead to the photocatalytic transformation of the target pollutant (Grabowska et al., 2012; Malato et al., 2009; Matilainen and Sillanpää, 2010; Thakur et al., 2010). TiO<sub>2</sub> is one of the most useful semiconductors due to its efficiency, high activity, photochemical inertness and low cost (Litter and Quici, 2010; Lopez-Alvarez et al., 2011; Malato et al., 2009).

The TiO<sub>2</sub> photocatalysis mechanism initiates with the absorption of UV light whose energy is greater than +3.2 eV (corresponding to the TiO<sub>2</sub> band gap energy and to wavelengths between 300 nm and 370 nm) (Pelaez et al., 2012). This results in the generation of conduction band electrons ( $e^-$ ) and valence band holes ( $h^+$ ) (Eq. (40)), which are involved in the production of  $^\circ\text{OH}$ ,  $\text{O}_2^{\cdot-}$  and  $\text{HO}_2^\circ$  (Eqs. (41)–(44)) (Litter and Quici, 2010).  $\text{H}_2\text{O}_2$  can also be formed (Eqs. (28), (45)–(46)), which improves the production of  $^\circ\text{OH}$  (Eqs. (47)–(48)) and slows

down the recombination process of the charges (Eq. (48)) represented by Eq. (49) (Andreozzi et al., 1999; Chong et al., 2010; Pelaez et al., 2012).



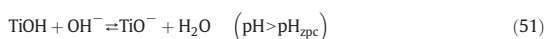
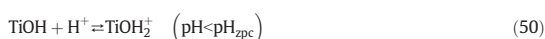
TiO<sub>2</sub> heterogeneous photocatalysis can be an efficient way to eliminate PAHs (e.g. ACN, AN, BaA, BaP, BbF, BghiPY, BkF, FA, IP, NA, PHE and PYR) either from soil or water matrices (McConkey et al., 2002; Pramauro et al., 1998; Sigman et al., 1998; Vela et al., 2012; Wen et al., 2002, 2003; Zhang et al., 2008). In terms of aqueous media, the degradation potential of UV/TiO<sub>2</sub> at lab-scale for PYR and PHE under determined experimental conditions (TiO<sub>2</sub> surface coverage = 2 × 10<sup>-5</sup> mol g<sup>-1</sup> (PYR), 5.6 × 10<sup>-5</sup> mol g<sup>-1</sup> (PHE); fluence = 30 W m<sup>-2</sup> (PYR), 25 W m<sup>-2</sup> (PHE); pH 5 and 20 °C) has been assessed (Wen et al., 2002, 2003). Promising results with reductions of ~90% (PYR) and >90% (PHE) after 60 min of reaction were obtained. The differences in reduction values were attributed to the solubility differences between the two PAHs. Since PYR is more hydrophobic, it has more affinity for TiO<sub>2</sub>; therefore, the TiO<sub>2</sub> surface coverage is higher, as is its subsequent degradation. However, the complete mineralization of PYR and PHE was attained after 120 min of irradiation time.

During PAH photocatalytic degradation with TiO<sub>2</sub>, it was found that °OH and/or O<sub>2</sub><sup>°-</sup>, as well as h<sup>+</sup>, played a major role in the oxidation of NA (Lair et al., 2008), PYR and PHE (Wen et al., 2002, 2003). The route of transformation started with the opening of an aromatic ring (Lair et al., 2008) and with the hydroxylation and ketolysis processes for PYR and PHE (Wen et al., 2002, 2003). As occurred with other AOPs, the intermediates formed are quinones, hydroquinones, formaldehydes and smaller linear organic acids, leading to the production of CO<sub>2</sub>, H<sub>2</sub>O and inorganic ions (Wen et al., 2002, 2003; Woo et al., 2009). Intermediate products are characterized by their high solubility and ease of oxidation (Wen et al., 2002); thus, they can be oxidized by the action of microorganisms in a subsequent biological step. In Fig. 5, possible NA degradation pathways via TiO<sub>2</sub> photocatalysis are described (Lair et al., 2008).

The UV/TiO<sub>2</sub> process performance depends on various parameters, such as the dose of TiO<sub>2</sub> (Malato et al., 2009; Thakur et al., 2010). For example, the removal rate of NA (40 μM) varies with a change in TiO<sub>2</sub> load from 0 to 4 g L<sup>-1</sup> (5.4 × 10<sup>15</sup> photons s<sup>-1</sup>, at pH 4.4 and 20 °C), increasing with a rise in TiO<sub>2</sub> levels and becoming constant above 2.5 g L<sup>-1</sup> (Lair et al., 2008). The reasons for such a constant level are associated to (a) the decrease in the number of surface active sites because of the aggregation of TiO<sub>2</sub> particles, and (b) the increase in turbidity and opacity, leading to UV-light scattering (Lair et al., 2008) and resulting in a reduction of the quantum efficiency of the photocatalyst (Wen et al., 2002, 2003).

Lair et al. (2008) also observed that the initial concentration of NA affected the degradation rate constant. For NA levels up to 40 μM, the rate constant increased linearly to a maximum of ~1.10 μmol min<sup>-1</sup>. Higher NA doses resulted in slower conversion rates.

The pH of the solution is another important parameter in TiO<sub>2</sub> heterogeneous photocatalysis, since it determines the surface charge properties of the catalyst (Chong et al., 2010; Malato et al., 2009; Thakur et al., 2010). When the surface is hydrated (TiOH), Eqs. (50) and (51) acid–base equilibria take place (Malato et al., 2009).



where pH<sub>zpc</sub> is the pH of the point of zero charge. The TiO<sub>2</sub> pH<sub>zpc</sub> value varies with the type of commercial TiO<sub>2</sub>. For instance, for Degussa P-25 titania, the most commonly used commercial TiO<sub>2</sub>, the pH<sub>zpc</sub> is equal to 6.3 (Lair et al., 2008).

If the pollutant contains acid or basic groups, the pH solution influences on the chemical structure of the pollutant, and thus, the adsorption–desorption behavior of the contaminant (Chong et al., 2010). However, Wen et al. (2002, 2003) found that the pH conditions of the solution had little effect on the photo-oxidation rate of PYR and PHE, since the reactants were previously adsorbed onto the surface of the TiO<sub>2</sub> particles.

The TiO<sub>2</sub> photocatalytic degradation can also be favored by increasing the temperature (Chong et al., 2010), with an optimum temperature between 20 °C and 80 °C (Malato et al., 2009). Lair et al. (2008) also studied the temperature effect (10 °C–40 °C) on NA degradation, concluding that the NA degradation rate slightly improved (by about 5.4%) with a temperature increase (Lair et al., 2008). The reason may be related to enhance TiO<sub>2</sub> electron transfers from the valence band to higher energy levels, which facilitate e<sup>-</sup>–h<sup>+</sup> production (Saïen and Shahrezaei, 2012). However, it is important to note that high temperatures can cause NA water vaporization and therefore a change in its concentration (Lair et al., 2008). On the other hand, a decrease in temperature favors adsorption (Malato et al., 2003) and prevents H<sub>2</sub>O<sub>2</sub> inactivation due to decomposition (Crittenden et al., 1999).

Regarding light intensity, it was observed that the degradation rate of NA (40 μM) heightened almost linearly as the photonic flux increased up to 10<sup>16</sup> photons s<sup>-1</sup>, giving a value of 0.06 min<sup>-1</sup> (2.5 g L<sup>-1</sup> of TiO<sub>2</sub> and pH 4.4). Higher light intensity may contribute to e<sup>-</sup>–h<sup>+</sup> recombination (Lair et al., 2008).

The effect of some inorganic ions such as CO<sub>3</sub><sup>2-</sup>, HCO<sub>3</sub><sup>-</sup> and Cl<sup>-</sup> has also been studied (Lair et al., 2008). The presence of CO<sub>3</sub><sup>2-</sup> (0.09 M, pH ~ 11) and HCO<sub>3</sub><sup>-</sup> (0.36 M, pH ~ 8.5) was found to inhibit NA adsorption from ~27.5% to 11% (CO<sub>3</sub><sup>2-</sup>) and from ~22.5% to 11% (HCO<sub>3</sub><sup>-</sup>); whereas NaCl (0–2.4 M) accelerates the reactions by 30% through adsorption enhancement. CO<sub>3</sub><sup>2-</sup> and HCO<sub>3</sub><sup>-</sup> may be adsorbed onto the TiO<sub>2</sub> surface and they can also act as °OH scavengers, resulting in a reduction of the effectiveness of the process. In contrast, Cl<sup>-</sup> enhance NA degradation since an increase in the NaCl content leads to an increase in NA hydrophobicity, resulting in the adsorption of the PAH onto the surface of TiO<sub>2</sub>. Nevertheless, hydrophilic PAH adsorption can be inhibited by NaCl (Lair et al., 2008).

UV/TiO<sub>2</sub> is a low-cost degradation treatment, because TiO<sub>2</sub> is available at reasonable prices (Legrini et al., 1993). However, when using TiO<sub>2</sub> particles in suspension, an additional treatment step is needed before the effluent can be discharged into the environment. To overcome this drawback, semiconductor immobilization on different types of materials has been proposed. However, since this results in a reduction of the specific surface area and leads to mass transfer limitations, the effectiveness of the process is lowered (Matilainen and Sillanpää, 2010; Nakata and Fujishima, 2012; Shan et al., 2010).

Although the UV/TiO<sub>2</sub> system quantum yield is relatively low (φ ≤ 0.05), it has the advantage of being applied under a UV-A domain,

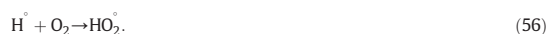
with the potential use of sunlight as an irradiation source (Legrini et al., 1993), which reduces the operational and maintenance costs (Ireland et al., 1995). Nevertheless, sunlight radiation reaching the Earth's surface contains only 3–5% of UV-A (Ljubas, 2005). Therefore, several reports have been focused on extending the absorbance wavelength range of TiO<sub>2</sub> to the visible domain, by doping it with metallic and non-metallic elements (Comninellis et al., 2008; Malato et al., 2009; Matilainen and Sillanpää, 2010; Sirtori et al., 2009). Additionally, dyes could be used as photosensitizers (Domenech et al., 2004; Malato et al., 2009). The use of ZnO as a photocatalyst may also be of a great interest (Hariharan, 2006; Vela et al., 2012; Yassitepe et al., 2008) since it has a larger fraction of solar spectrum absorption than TiO<sub>2</sub> (Chakrabarti and Dutta, 2004). Moreover, the addition of any oxidant, such as H<sub>2</sub>O<sub>2</sub> and O<sub>3</sub>, dramatically improves the efficiency of the process. These oxidants contribute to preventing the recombination of charges (Legrini et al., 1993; Malato et al., 2009) and to the generation of a large number of oxidizing species, enhancing the ability of the process to mineralize organic compounds (Malato et al., 2009; Matilainen and Sillanpää, 2010). In this sense, the coupled AOPs commonly based on UV/TiO<sub>2</sub> are UV/TiO<sub>2</sub>/H<sub>2</sub>O<sub>2</sub> and UV/TiO<sub>2</sub>/O<sub>3</sub>.

Finally, it has been stated that the use of Fe<sup>3+</sup> could positively affect the UV/TiO<sub>2</sub> system. Fe<sup>3+</sup> inhibits the recombination of charges because it acts to trap e<sup>-</sup>, improving the TiO<sub>2</sub> quantum efficiency (Méndez-Arriaga et al., 2009; Wen et al., 2003). Additionally, Fe<sup>3+</sup> can react with the H<sub>2</sub>O<sub>2</sub> generated and absorb UV-light, leading to Fenton and photo-Fenton reactions (referred to in Section 3.2.3).

### 3.2.5. Advanced oxidation processes using ultrasound energy

Over the last few years, ultrasound has been effectively employed as an emerging AOP for the degradation of a wide variety of pollutants present in water, especially for volatile and non-polar compounds (Gogate and Pandit, 2004b), including PAHs (e.g. ACN, NA, PHE, PYR) (Laughrey et al., 2001; Manariotis et al., 2011; Psillakis et al., 2004; Wheat and Tumeo, 1997).

AOPs based on US treatment involve the generation of °OH by acoustic cavitation (Ashokkumar et al., 2007). This phenomenon is produced through compression and expansion cycles of US waves (Ashokkumar et al., 2007; David, 2009; Torres et al., 2009), which result in the growth and collapse of the gas bubbles and the production of local areas of high energy and pressure (ranging from 3000 to 5000 K, and from 506.625 to 10,132.5 × 10<sup>5</sup> Pa, respectively) (Mahamuni and Adewuyi, 2010; Makino et al., 1983). These conditions are so extreme that they are capable of breaking up the entrapped molecules within the bubbles, such as vaporized water or dissolved gases (e.g. O<sub>2</sub>), to produce radicals (Ashokkumar et al., 2007; Park et al., 2000), mainly °OH and HO<sub>2</sub>° (Eqs. (52)–(56)) (Wheat and Tumeo, 1997). These radicals are capable of initiating or promoting many fast oxidation reactions, leading to the degradation of the more hydrophobic compounds at the bubble–bulk solution interface and, to a lesser extent, of the more hydrophilic species via °OH diffused or ejected into the bulk solution. Furthermore, the high temperature and pressure values generated inside the gas bubbles result in the pyrolysis of the more volatile organic compounds (David, 2009; Guzman-Duque et al., 2011; Lesko et al., 2006; Petrier et al., 1998; Psillakis et al., 2004; Taylor et al., 1999; Torres et al., 2008a,b; Wheat and Tumeo, 1997).



PAH water solubility and vapor pressure values are variable and dependent on the chemical structure of the substance (Dabestani and Ivanov, 1999). This is the reason why there is not a unique PAH removal pathway. Sonodegradation of PAHs can occur via: (a) pyrolytic processes within the gas bubbles, for the more volatile PAHs, which can be verified by the production of CO<sub>2</sub> at the early stages of the system; and (b) chemical oxidation via °OH, either in the solution phase or in the interfacial region of the cavitation bubble, for the more hydrophilic or hydrophobic compounds, respectively, which is seen through the formation of hydroxylated by-products (David, 2009; Laughrey et al., 2001; Little et al., 2002; Psillakis et al., 2004; Wheat and Tumeo, 1997).

During the US process, recombination of the radicals that do not react with the target compound occurs to generate H<sub>2</sub>O<sub>2</sub> (Eqs. (28)–(30)).

The extent of the degradation of the organic pollutants in the US treatment depends on several factors (e.g. input power and frequency, temperature, initial pollutant concentration, water matrix and type of gas used, among others) (David, 2009; Manariotis et al., 2011; Psillakis et al., 2004; Sponza and Oztekin, 2010). Regarding PAHs, several authors agree that ACN, NA, PHE and PYR degradation increases with an increase in the applied power (Manariotis et al., 2011; Psillakis et al., 2004; Sponza and Oztekin, 2010; Wheat and Tumeo, 1997). For a solution mixture of NA, ACN and PHE (150 µg L<sup>-1</sup>, with 50 µg L<sup>-1</sup> of each compound), at 80 kHz and 20 °C, an increase in the conversion of 139%, 17.6% and 83.1% for NA, PHE and ACN, respectively, was observed after 30 min of sonication when the power input rose from 45 W to 150 W (Psillakis et al., 2004). This is related to the fact that the number of collapsing cavities rises with an increase in the input power. Since the collapse of the bubbles occurs more rapidly, a greater °OH concentration is yielded, and thus, the PAH degradation rate is improved (Manariotis et al., 2011).

With respect to the operating frequency, it has been found that there is more chance of generating radicals with higher frequencies. This is because of the greater number of cavitation events that occur when the sonication frequency is increased from 24 to 80 kHz (Psillakis et al., 2004), which is in agreement with David (2009), whose tested frequencies were 20 and 506 kHz. In turn, Manariotis et al. (2011), who experimented with frequencies from 582 kHz to 1142 kHz indicated that although an elevation of the frequency resulted in more cavitation bubbles per unit of time, these bubbles were too small and inactive in producing °OH. In summary, the highest amount of °OH is formed in the range of frequencies between 80 and 582 kHz. Considering the physico-chemical variability of PAHs, it would be interesting to assess the effect of PAH chemical structure in further studies, since it has been shown that sonochemical degradation efficiency is strongly influenced by pollutants solubility and vapor pressure.

Another parameter that influences the US process is temperature, which affects the bubble formation energy and the intensity of bubble implosion. Higher temperatures enhance bubble generation but at the same time they promote degassing of the liquid phase, reducing the number of gas nuclei available for yielding bubbles (Psillakis et al., 2004; Sponza and Oztekin, 2010). On the other hand, elevated temperatures cushion bubble implosion, leading to a decrease in the collapse temperature (Psillakis et al., 2004). Moreover, temperature favors the solubility in water of the more hydrophobic PAHs, such as PYR, reducing their adsorption on the interface region (Sponza and Oztekin, 2010) and their interaction with radicals. However, higher temperatures could increase the volatility of PAHs simultaneously and then increase their degradation via pyrolysis. Therefore, the effect of temperature in the system is directly related to the specific PAH (Psillakis et al., 2004).

Regarding the initial PAH concentration, the degradation rates of ACN, NA and PHE appear to be favored by increasing their initial concentration levels. For example, NA removal was 1.7 times higher when the concentration of NA was 100 µg L<sup>-1</sup> in comparison with the oxidation rates achieved at 50 µg L<sup>-1</sup> NA, at 80 kHz, 150 W and 20 °C after 15 min of sonochemical degradation (Psillakis et al., 2004).

PAH removal is also affected by the water matrix constituents present in the sonicated solution, depending on the behavior of the matrix compounds. For example, when PAHs are mainly degraded by  $^{\circ}\text{OH}$ , the presence of  $^{\circ}\text{OH}$  scavengers could be negative (David, 2009; Laughrey et al., 2001; Psillakis et al., 2004; Taylor et al., 1999). This has been demonstrated by Laughrey et al. (2001) by adding humic acid and benzoic acid (a known  $^{\circ}\text{OH}$  scavenger) to a solution with AN, PHE and PYR (0.1–0.5  $\mu\text{M}$ ), resulting in a decrease in their rate constant. Furthermore, apart from acting as a  $^{\circ}\text{OH}$  quencher, HS may form complexes with the PAHs, removing them from the cavitation sites (Laughrey et al., 2001). On the other hand,  $\text{HCO}_3^-$  may act positively or negatively. For instance, it has been demonstrated that  $\text{HCO}_3^-$  enhanced the sonochemical degradation rate of crystal violet (Guzman-Duque et al., 2011) and bisphenol-A (P etrier et al., 2010) when working at highly diluted pollutant concentrations. Nevertheless, the presence of  $\text{HCO}_3^-$  was detrimental to the degradation of DahA (Sponza and Oztekin, 2011), probably because the concentration level of the tested PAH was close to its solubility limit.

With regard to the presence of salts in the water, it is worth noting that they are involved in the well-known salting-out effect, increasing the non-polar character of the PAHs, and enabling  $^{\circ}\text{OH}$  attack at the bubble interface. However, the existence of ions in the water matrix can produce a detrimental effect, because salts are also responsible for reducing vapor pressure and increasing surface tension, resulting in a decrease of the number of bubbles formed (Psillakis et al., 2004).

In turn, the type of gas sparged to the system plays a significant role in PAH sonodegradation. Generally, the addition of  $\text{O}_2$  to the system results in an increase in the degradation rate constants of ACN, AN, BbF, NA, PHE and PYR, among other PAHs (Laughrey et al., 2001; Sponza and Oztekin, 2010). For example, Laughrey et al. (2001) assessed the influence of  $\text{O}_2$  and  $\text{N}_2$  on the degradation rate of PYR, AN and PHE. The first order constants observed in an  $\text{O}_2$  atmosphere increased by about 89%, 67% and 70% for AN, PHE and PYR, respectively, in comparison with those obtained under  $\text{N}_2$  conditions. One possible explanation for this is the production of additional reactions that lead to the formation of a large number of  $^{\circ}\text{OH}$  (Eqs. (53)–(55)) (Guzman-Duque et al., 2011; Torres et al., 2008b).

Generally, the total mineralization of organic pollutants by means of US irradiation alone is energy consuming, since intermediate products (aldehydes, alcohols, carboxylic acids, etc.) are usually more hydrophilic than the parent compound. To overcome this limitation, various combined US treatment systems have been proposed (Adeyuyi, 2001; Sponza and Oztekin, 2010). As mentioned before, during this process,  $\text{H}_2\text{O}_2$  is formed, which may be used as a reagent of another AOP, such as the Fenton, photo-Fenton and related processes (Psillakis et al., 2004; Torres et al., 2008a,b; Wheat and Tumeo, 1997), and the UV/ $\text{H}_2\text{O}_2$  technique or heterogeneous photocatalysis (Torres et al., 2008a, b). This gives simultaneous US/ $\text{Fe}^{2+}/\text{H}_2\text{O}_2$ , US/UV/ $\text{Fe}^{2+}/\text{H}_2\text{O}_2$ , US/UV/ $\text{H}_2\text{O}_2$  or US/UV/ $\text{TiO}_2$  systems. Results have shown that combined US processes have a better performance and are economically more attractive than the US or other advanced oxidation techniques acting alone (Kim et al., 2001; Segura et al., 2009; Torres et al., 2007b).

Additionally, the US technique does not require the use of extra chemicals, such as  $\text{H}_2\text{O}_2$ ,  $\text{O}_3$ , and catalysts, commonly employed in other AOPs. Therefore, the respective costs as well as the need to remove the excess of reagents prior to discharge are avoided (Psillakis et al., 2004), contrary to what occurs in the UV/ $\text{H}_2\text{O}_2$ , Fenton, photo-Fenton and UV/ $\text{TiO}_2$  processes. US could even be used as a pre-treatment for a biological process because the by-products generated are usually biodegradable (Guzman-Duque et al., 2011; Torres et al., 2009, 2007a,b).

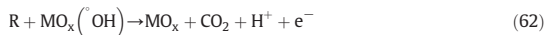
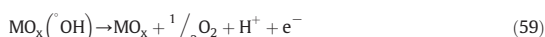
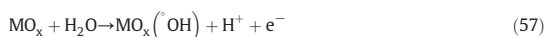
### 3.2.6. Electrochemical oxidation

The most popular electrochemical technique for wastewater remediation is anodic oxidation, since it has shown to be an efficient

and versatile mechanism for the abatement of a wide range of organic substances (Comninellis, 1994; Homem and Santos, 2011; Muff and S oggaard, 2010; Sir es and Brillas, 2012). This technique is a simple method of water decontamination and it consists of passing water through electrodes in the presence of an electrolyte.

There are different kinds of electrodes (Comninellis, 1994). Focusing on anodes, they may be grouped as active anodes (e.g. Pt,  $\text{IrO}_2$  and  $\text{RuO}_2$ ) and non-active ones (e.g.  $\text{PbO}_2$ ,  $\text{SnO}_2$  and BDD). In both kinds of anodes, denoted as  $\text{MO}_x$ , the first reaction is the oxidation of water molecules, which leads to the formation of adsorbed  $^{\circ}\text{OH}$  as described in Eq. (57) (Rivera et al., 2011). The  $^{\circ}\text{OH}$  formed may be strongly or weakly bound to the anode. In the former case, which occurs in active anodes,  $^{\circ}\text{OH}$  interact with the electrode and metal oxides ( $\text{MO}_{x+1}$ ) are formed (Eq. (58)) (Comninellis, 1994; Torres et al., 2003b; Zhang et al., 2013).

In the absence of organic compounds,  $\text{O}_2$  evolution takes place through Eqs. (59)–(60) (Comninellis, 1994; Torres et al., 2003b; Zhang et al., 2013). However, in the presence of oxidizable substances, they can be oxidized directly on the anode surface (Eqs. (61)–(62)) and/or indirectly by the electrochemically generated oxidants, such as  $^{\circ}\text{OH}$  (Eq. (57)),  $\text{H}_2\text{O}_2$  (Eq. (63)) and  $\text{O}_3$  (Eq. (64)) (Sir es and Brillas, 2012; Torres et al., 2003a,b; Tran et al., 2009), resulting in fully oxidized reaction products as  $\text{CO}_2$  (Tran et al., 2009).



Studies investigating the electrochemical oxidation of PAHs, focusing on AN, BaA, BaP, FA, FLU, IP, NA and PYR, among others, from aqueous matrices have been reported (Cordeiro and Corio, 2009; Muff and S oggaard, 2010; Souza et al., 2011; Tran et al., 2009). It has been observed that electrochemical oxidation is initiated by direct electron transfer from the adsorbed PAHs to the electrode, generating PAH cation radicals that undergo subsequent reactions (Cordeiro and Corio, 2009; Muff and S oggaard, 2010). However, indirect oxidation by means of the generation of an oxidizing agent in situ, such as  $^{\circ}\text{OH}$ , can be important as well.

Anode material is one of the most relevant parameters affecting electrochemical oxidation, because the target pollutant follows a different degradation pathway depending on the type of anode (Guzman-Duque et al., 2011). Furthermore, anode material also affects the extent of mineralization, as complete mineralization is usually achieved using anodes with higher oxygen overvoltage, such as BDD,  $\text{PbO}_2$  and  $\text{SnO}_2$  (Torres et al., 2003a,b). However, it must be pointed out that the latter two anodes exhibit low stability and can be corroded, resulting in the release of toxic ions into the solution. On the other hand, Pt,  $\text{RuO}_2$  and  $\text{IrO}_2$  electrodes can generate more oxidized intermediates, which may be of a great interest for coupling to a subsequent biological step (Torres et al., 2003a,b).

The initial concentration of the target pollutant also influences the system, since when low levels of organic contaminant are attained, the role of  $\text{O}_2$  evolution becomes more important (Souza et al., 2011). On the other hand, the efficiency of electrochemical

oxidation is affected by the chemical structure of the target PAH (Muff and Sogaard, 2010; Souza et al., 2011), since an increase in the number of benzene rings negatively affects the process efficiency. This was confirmed by Souza et al. (2011), who used  $124 \mu\text{g L}^{-1}$  NA (2 rings) and  $106 \mu\text{g L}^{-1}$  BghiPY (6 rings) to achieve PAH reductions of 85% and 60%, respectively, after 4 h of treatment with a Ti/Pt anode at  $11 \text{ mA cm}^{-2}$ .

Temperature is another parameter that has been examined. Tran et al. (2009) worked with a  $200 \text{ mg L}^{-1}$  creosote solution at  $9.23 \text{ mA cm}^{-2}$ , pH 6,  $500 \text{ mg L}^{-1}$   $\text{Na}_2\text{SO}_4$  and  $\text{RuO}_2$  as an anode. Under these conditions, the optimum temperature was found to be  $21^\circ\text{C}$ , especially for 2-ring PAHs, such as NA, achieving a removal of 75% after 90 min of treatment. At  $35^\circ\text{C}$ , NA volatilization is assumed.

In addition, the presence of  $\text{Cl}^-$  and  $\text{SO}_4^{2-}$  in water can positively interfere with the removal rate of PAHs, since they are involved in the generation of the oxidant species  $\text{OCl}^-$  and  $\text{S}_2\text{O}_8^{2-}$ , respectively (Muff and Sogaard, 2010; Souza et al., 2011; Torres et al., 2003a,b). Muff and Sogaard (2010) compared the removal rates of a mixture of different PAHs (e.g., AN, BaP, DahA, IP, NA, PHE and PYR, among others) when adding  $0.01 \text{ M NaNO}_3$  and NaCl, and concluded that NaCl had a positive effect, enhancing the PAH degradation by a factor of 2 to 6. However, the negative aspect when using  $\text{Cl}^-$  is the risk of the formation of unwanted chlorinated organic by-products (Torres et al., 2003b). Irrespective of the supporting electrolyte used, it has been observed that the removal rate of NA, FA and PYR increases with a lowering of the current density, proving that current density is another important parameter in the electrochemical oxidation process (Muff and Sogaard, 2010). It is important to note that when the applied current density is greater than the limiting current density, evolution of by-products from parallel reactions is favored (Muff and Sogaard, 2010; Palma-Goyes et al., 2010).

Although electrochemical oxidation seems to be pH independent, this parameter does indirectly affect the performance of this technique because the pH solution conditions can modify the chemical structure of the parent compound (Torres et al., 2003a,b).

The major disadvantages of electrochemical oxidation are the mass transport limitations and the associated energy costs (Souza et al., 2011). Souza et al. (2011) conducted a comparative study of the energy costs involved in the electrochemical oxidation of a diverse range of PAHs (Table 1). The results showed that the  $\text{kWh m}^{-3}$  consumed rose with electrolysis time from 1.37 to  $5.48 \text{ kWh m}^{-3}$ , corresponding to 1 h and 4 h of treatment, respectively. However, this technique is one of the more environmentally friendly AOPs because its main reagent, the electron, is clean (Jüttner et al., 2000). Furthermore, due to the fact that the presence of a supporting electrolyte is required, electrochemical anodic oxidation could be applied for water treatment with a high ionic strength. This would exploit the positive effect provided by ions such as  $\text{SO}_4^{2-}$  or  $\text{Cl}^-$ , unlike other AOPs, whose application may be limited by the scavenging effect associated to them (Palma-Goyes et al., 2010). Moreover, electrochemical oxidation has the possibility of totally mineralizing organic pollutants or converting them into more biodegradable and less toxic intermediates than their parent compounds, allowing electrochemical conversion methods to be coupled with biological ones (Torres et al., 2003a,b).

### 3.3. Future perspectives

When a conventional treatment cannot completely eliminate pollutants from water, alternative removal strategies must be considered to achieve better efficiencies (Gogate and Pandit, 2004b; Homem and Santos, 2011; Oller et al., 2011), especially for potentially toxic contaminants like PAHs (Chen and Liao, 2006; Chiang et al., 2009; Delgado-Saborit et al., 2011; Guo et al., 2012; Okona-Mensah et al., 2005; Siddens et al., 2012; Wester et al., 2012; Xu et al., 2013). In some cases, the combination of different reagents (e.g.  $\text{O}_3$  or  $\text{H}_2\text{O}_2$ , among others), an energy source (UV light, US or electrical energy) and a catalyst (iron,  $\text{TiO}_2$ , ZnO,

Pt, etc.) may be used for the removal of PAHs (Cordeiro and Corio, 2009; Psillakis et al., 2004; Wen et al., 2003; Wheat and Tumeo, 1997). As mentioned above, coupling AOPs results in a higher  $^\circ\text{OH}$  yield, and pollutant oxidation rates are usually improved (Esplugas et al., 2002; Peratitus et al., 2004). Unfortunately, due to the costs associated with the consumption of energy and reagents, in many cases, the combination of different AOPs could not be cost-effective, especially if contaminant mineralization is the final goal of the process (Comminellis et al., 2008; Oller et al., 2011).

Although the application of biological processes for water decontamination is far more economical, they cannot be used alone since many microorganisms are sensitive to toxic pollutants (Gogate and Pandit, 2004b; Homem and Santos, 2011; Oller et al., 2011). In this sense, physical or chemical processes can be applied as a pre-treatment step, in which pollutants are removed or oxidized to by-products that are easily biodegradable and less toxic than their parent compounds. This would also prevent the loss of the microorganisms present in the subsequent biological treatments (Homem and Santos, 2011; Tekin et al., 2006). Different chemical techniques, including AOPs, have been reported to be efficient at treating wastewater when coupled with aerobic or anaerobic biological processes (Oller et al., 2011; Sirtori et al., 2009). Additionally, AOPs may also be placed after a biological system, in particular if the water to be treated is complex and contains non-toxic compounds (Oller et al., 2011). In the case of PAH degradation from wastewater by coupled chemical–biological treatments, several studies have been reported (Bernal-Martinez et al., 2007; Guieysse et al., 2004; Nadarajah et al., 2002; Rafin et al., 2009; Veignie et al., 2009). These studies show that the integrated system seems to be suitable for PAH treatment. Therefore, advanced oxidation technologies combined with conventional biological processes may make the whole system more feasible and cost-effective (Comminellis et al., 2008; Gogate and Pandit, 2004b; Homem and Santos, 2011; Oller et al., 2011; Sánchez et al., 2013).

In addition to conventional biological treatments, alternative biological processes could be used. Of these treatment methods, MBRs are among the most promising (Mutamim et al., 2012; Radjenovic et al., 2009). In a MBR, wastewater is treated by activated sludge in a bioreactor before being filtered by a membrane. The filtering capacity of the membrane depends on the size of the pores, types of materials, type of water to be treated, solubility and retention time. A MBR can provide high performance in treating water. Furthermore, it is more compact compared to conventional activated sludge systems since secondary clarifier processes are eliminated. A MBR also produces high quality effluents, is good at removing organic and inorganic contaminants, capable of resisting high organic loads and generates less sludge. The costs of a MBR, including the initial investment, operation, and maintenance, are higher than those associated to standard biological processes. However, such costs are related to the growth of membrane technology and MBRs are now becoming increasingly acceptable for industrial applications (Mutamim et al., 2012).

MBR technology has already been studied alone for the degradation of PAHs in urban and petrochemical wastewater influents with low PAH concentrations (González et al., 2012; González-Pérez et al., 2012; Verlicchi et al., 2011). For all the studied cases, the MBR systems presented a high efficiency, with performance levels in the range of 90% for PHE, FLU and PYR (González et al., 2012; González-Pérez et al., 2012) or even higher (99%) (Verlicchi et al., 2011). PYR, AC, AN and aniline have also been degraded using membranes improved with cyclodextrines, resulting in an increase in membrane pore density and enhancing the PAH treatment (Huang et al., 2009).

In the future, applications of membrane technology combined with AOPs for water treatment could provide a potential solution for degrading PAHs. However, research is needed to better understand the coupled system behavior, including degradation kinetics,

reactor design, modeling and simulation, and optimization of the operating conditions of these combined processes. Furthermore, the development of strategies for the commercialization of processes which have been so far used at lab scale could also be of great interest to the academic community.

#### 4. Conclusions

Physical, chemical and biological conventional methods wastewater treatment plants are currently operating with may be unsuccessful at the degradation of PAHs. Therefore, the development of more efficient alternative treatments, such as AOPs, is required.

Advanced oxidation technologies are a set of processes involving the production of very reactive oxygen species (e.g.  $^{\circ}\text{OH}$ ) able to destroy a wide range of biorecalcitrant and toxic organic compounds, such as PAHs. The reaction between  $^{\circ}\text{OH}$  and PAHs produces intermediate compounds, which undergo further oxidation until their complete oxidation or mineralization (i.e. production of  $\text{CO}_2$ ,  $\text{H}_2\text{O}$  and inorganic ions). AOPs need external energy sources, such as electric power, ultrasound energy and/or UV/visible radiation, and in some cases, reactants. The efficiency of AOPs in PAH degradation depends not only on the initial pollutant concentration, but also on the operating conditions (e.g. pH and temperature of the solution, reactant and catalyst doses, intensity and type of energy source, and reaction time, among others) and matrix constituents, which determine the quantity of radicals available to oxidize PAHs. Another factor that affects AOP efficiency, which has not been addressed in depth in this review, is the reactor configuration. This is critical in order to provide a better contact of the radicals generated with the pollutant molecules and also to better utilize the oxidants and catalysts.

Several studies report that AOPs used alone are effective at PAH removal. However, the simultaneous application of different AOPs promotes the degradation rates of PAHs, leading to synergistic effects. Typical examples include  $\text{UV}/\text{O}_3/\text{H}_2\text{O}_2$ ,  $\text{UV}/\text{H}_2\text{O}_2/\text{TiO}_2$  and  $\text{UV}/\text{TiO}_2/\text{Fe}^{2+}$ ,  $\text{US}/\text{Fe}^{2+}$  and  $\text{US}/\text{UV}/\text{TiO}_2$ , among others.

The main problem related to AOP application lies in the relatively high operational costs associated to the reagents (e.g.  $\text{H}_2\text{O}_2$ ) and energy consumption, although the use of solar radiation can reduce these costs. Moreover, all of these processes can form by-products that are more toxic than the target compounds, and they may be susceptible to the scavenging effect of  $^{\circ}\text{OH}$  by non-target pollutants, thereby reducing process efficiency.

Even though the use of AOPs coupled with biological processes is not a very common practice yet, it promises to be a cost-effective solution for the treatment of effluents containing PAHs in the future. AOPs can transform PAHs into biodegradable compounds in a relatively short time, therefore, the use of an AOP followed by a biological treatment could be considered an effective option for the degradation of PAHs, especially if a MBR is involved.

The main conclusion that can be derived from the overall assessment of the reported literature is that more studies need to be carried out especially regarding PAH conversion rates using combined AOP-biological processes to evaluate and optimize the operating conditions, study the toxicity of the reaction intermediates, understand the degradation kinetics and develop better reactor geometric configurations and materials, among other critical parameters. Additionally, the development of strategies for the use of combined processes at an industrial scale is also very important.

#### Nomenclature

AC	Acenaphthene
ACN	Acenaphthylene
AN	Anthracene
AOPs	Advanced oxidation processes
BaA	Benz(a)anthracene
BaP	Benzo(a)pyrene

BbF	Benzo(b)fluoranthene
BbFLU	Benzo(b)fluorene
BbjkF	Benzo(b,j,k)fluoranthene
BDD	Boron doped diamond
BghiPY	Benzo(g,h,i)perylene
BkF	Benzo(k)fluoranthene
BkP	Benzo(k)pyrene
CHR	Chrysene
COD	Chemical organic demand
DahA	Dibenzo(a,h)anthracene
DBD	Dielectric barrier discharge
DBF	Dibenzofuran
DBT	Dibenzothiophene
DO	Dissolved oxygen
DOM	Dissolved organic matter
FA	Fluoranthene
FLU	Fluorene
HS	Humic substances
IP	Indeno(1,2,3-cd)pyrene
LP-UV	Continuous low pressure
MAN	2-Methylnaphthalene
MBRs	Membrane bioreactors
MP-UV	Continuous medium pressure
MWTP	Municipal wastewater treatment plant
NA	Naphthalene
PAHs	Polycyclic aromatic hydrocarbons
PHE	Phenanthrene
PY	Perylene
PYR	Pyrene
t-BuOH	Tert-butyl alcohol
US	Ultrasound
US-EPA	The United States Environmental Protection Agency

#### Acknowledgments

The authors would like to thank the Colombian Institute of Educational Credit and Technical Studies (ICETEX), especially the Reciprocity Program for Foreigners in Colombia, for its financial support.

#### References

- Abdessalem AK, Bellakhal N, Oturan N, Dachraoui M, Oturan MA. Treatment of a mixture of three pesticides by photo- and electro-Fenton processes. *Desalination* 2010;250:450–5.
- Adeuyi YG. Sonochemistry: environmental science and engineering applications. *Ind Eng Chem Res* 2001;40:4681–715.
- Ali OA, Tarek SJ. Removal of polycyclic aromatic hydrocarbons from Ismailia Canal water by chlorine, chlorine dioxide and ozone. *Desalin Water Treat* 2009;1:289–98.
- An YJ, Carraway ER. PAH degradation by  $\text{UV}/\text{H}_2\text{O}_2$  in perfluorinated surfactant solutions. *Water Res* 2002;36:309–14.
- Andreozzi R, Caprio V, Insola A, Marotta R. Advanced oxidation processes (AOP) for water purification and recovery. *Catal Today* 1999;53:51–9.
- Anotai J, Lu MC, Chewprecha P. Kinetics of aniline degradation by Fenton and electro-Fenton processes. *Water Res* 2006;40:1841–7.
- Ashokkumar M, Lee J, Kentish S, Grieser F. Bubbles in an acoustic field: an overview. *Ultrason Sonochem* 2007;14:470–5.
- Babuponnusami A, Muthukumar K. Advanced oxidation of phenol: a comparison between Fenton, electro-Fenton, sono-electro-Fenton and photo-electro-Fenton processes. *Chem Eng J* 2012;183:1–9.
- Baeza C, Knappe DRU. Transformation kinetics of biochemically active compounds in low-pressure UV photolysis and  $\text{UV}/\text{H}_2\text{O}_2$  advanced oxidation processes. *Water Res* 2011;45:4531–43.
- Bailey PS, Batterbee JE, Lane AG. Ozonation of benz[a]anthracene. *J Am Chem Soc* 1968;90:1027–33.
- Batista APS, Nogueira RFP. Parameters affecting sulfonamide photo-Fenton degradation—iron complexation and substituent group. *J Photochem Photobiol A* 2012;232:8–13.
- Bautiz IR, Nogueira RFP. Degradation of tetracycline by photo-Fenton process—solar irradiation and matrix effects. *J Photochem Photobiol A* 2007;187:33–9.
- Beltrán FJ, Ovejero G, Encinar JM, Rivas J. Oxidation of polynuclear aromatic hydrocarbons in water. 1. Ozonation. *Ind Eng Chem Res* 1995a;34:1596–606.
- Beltrán FJ, Ovejero G, García-Araya JF, Rivas J. Oxidation of polynuclear aromatic hydrocarbons in water. 2. UV radiation and ozonation in the presence of UV radiation. *Ind Eng Chem Res* 1995b;34:1607–15.

- Beltrán FJ, Ovejero G, Rivas FJ. Oxidation of polynuclear aromatic hydrocarbons in water. 3. UV radiation combined with hydrogen peroxide. *Ind Eng Chem Res* 1996a;35:883–90.
- Beltrán FJ, Ovejero G, Rivas FJ. Oxidation of polynuclear aromatic hydrocarbons in water. 4. Ozone combined with hydrogen peroxide. *Ind Eng Chem Res* 1996b;35:891–8.
- Beltrán FJ, González M, Rivas FJ, Álvarez P. Fenton reagent advanced oxidation of polynuclear aromatic hydrocarbons in water. *Water Air Soil Pollut* 1998;105:685–700.
- Beltrán FJ, Rivas J, Álvarez PM, Alonso MA, Acedo B. A kinetic model for advanced oxidation processes of aromatic hydrocarbons in water: application to phenanthrene and nitrobenzene. *Ind Eng Chem Res* 1999;38:4189–99.
- Bernal-Martinez A, Carrère H, Patureau D, Delgenès JP. Ozone pre-treatment as improver of PAH removal during anaerobic digestion of urban sludge. *Chemosphere* 2007;68:1013–9.
- Bernal-Martinez A, Patureau D, Delgenès JP, Carrère H. Removal of polycyclic aromatic hydrocarbons (PAH) during anaerobic digestion with recirculation of ozonated digested sludge. *J Hazard Mater* 2009;162:1145–50.
- Bertilsson S, Widenfalk A. Photochemical degradation of PAHs in freshwaters and their impact on bacterial growth – influence of water chemistry. *Hydrobiologia* 2002;469:23–32.
- Birgül A, Tasdemir Y, Cindoruk SS. Atmospheric wet and dry deposition of polycyclic aromatic hydrocarbons (PAHs) determined using a modified sampler. *Atmos Res* 2011;101:341–53.
- Brillas E, Sirés I, Oturan MA. Electro-Fenton process and related electrochemical technologies based on Fenton's reaction chemistry. *Chem Rev* 2009;109:6570–631.
- Brown GS, Barton LL, Thomson BM. Permanganate oxidation of sorbed polycyclic aromatic hydrocarbons. *Waste Manag* 2003;23:737–40.
- Buseti F, Heitz A, Cuomo M, Badoer S, Traverso P. Determination of sixteen polycyclic aromatic hydrocarbons in aqueous and solid samples from an Italian wastewater treatment plant. *J Chromatogr A* 2006;1102:104–15.
- CCME (Canadian Council of Ministers of the Environment). Canadian Soil Quality Guidelines for carcinogenic and other polycyclic aromatic hydrocarbons (environmental and human health effects). Scientific Supporting Document; 2008:218.
- Chakrabarti S, Dutta BK. Photocatalytic degradation of model textile dyes in wastewater using ZnO as semiconductor catalyst. *J Hazard Mater* 2004;112:269–78.
- Chen SC, Liao CM. Health risk assessment on human exposed to environmental polycyclic aromatic hydrocarbons pollution sources. *Sci Total Environ* 2006;366:112–23.
- Chen B, Xuan X, Zhu L, Wang J, Gao Y, Yang K, et al. Distributions of polycyclic aromatic hydrocarbons in surface waters, sediments and soils of Hangzhou City, China. *Water Res* 2004;38:3558–68.
- Chiang KC, Chio CP, Chiang YH, Liao CM. Assessing hazardous risks of human exposure to temple airborne polycyclic aromatic hydrocarbons. *J Hazard Mater* 2009;166:676–85.
- Chizhova T, Hayakawa K, Tishchenko P, Nakase H, Koudryashova Y. Distribution of PAHs in the northwestern part of the Japan Sea. *Deep Sea Res II Top Stud Oceanogr* 2013;86–87:19–24.
- Chong MN, Jin B, Chow CWK, Saint C. Recent developments in photocatalytic water treatment technology: a review. *Water Res* 2010;44:2997–3027.
- Comninellis C. Electrochemical conversion/combustion of organic pollutants for waste water treatment. *Electrochim Acta* 1994;39:1857–62.
- Comninellis C, Kapalka A, Malato S, Parsons SA, Poullos I, Mantzavinos D. Advanced oxidation processes for water treatment: advances and trends for R&D. *J Chem Technol Biotechnol* 2008;83:769–76.
- Cordeiro D, Corio P. Electrochemical and photocatalytic reactions of polycyclic aromatic hydrocarbons investigated by raman spectroscopy. *J Braz Chem Soc* 2009;20:80–7.
- Crittenden JC, Hu S, Hand DW, Green SA. A kinetic model for H<sub>2</sub>O<sub>2</sub>/UV process in a completely mixed batch reactor. *Water Res* 1999;33:2315–28.
- Da Rocha ORS, Dantas RF, Bezerra MMM, Lima MM, Lins V. Solar photo-Fenton treatment of petroleum extraction wastewater. *Desalin Water Treat* 2013;51:5785–91.
- Dabestani R, Ivanov IN. A compilation of physical, spectroscopic and photophysical properties of polycyclic aromatic hydrocarbons. *Photochem Photobiol* 1999;70:10–34.
- David B. Sonochemical degradation of PAH in aqueous solution. Part I: monocomponent PAH solution. *Ultrason Sonochem* 2009;16:260–5.
- Delgado-Saborit JM, Stark C, Harrison RM. Carcinogenic potential, levels and sources of polycyclic aromatic hydrocarbon mixtures in indoor and outdoor environments and their implications for air quality standards. *Environ Int* 2011;37:383–92.
- Domenech X, Jardim W, Litter M. Procesos avanzados de oxidación para la eliminación de contaminantes. Eliminación de contaminantes por fotocatalisis heterogénea. Colección DocumentosMadrid: Ciemat; 2004. p. 4–26.
- Dopar M, Kusic H, Koprivanac N. Treatment of simulated industrial wastewater by photo-Fenton process. Part I: the optimization of process parameters using design of experiments (DOE). *Chem Eng J* 2011;173:267–79.
- El-Alawi YS, McConkey BJ, George Dixon D, Greenberg BM. Measurement of short and long-term toxicity of polycyclic aromatic hydrocarbons using luminescent bacteria. *Ecotoxicol Environ Saf* 2002;51:12–21.
- Elovitz MS, von Gunten U. Hydroxyl radical/ozone ratios during ozonation process I: the R<sub>p</sub> concept. *Ozone Sci Eng* 1999;21:239–60.
- Engwall M, Pignatello JJ, Grasso D. Degradation and detoxification of the wood preservatives creosote and pentachlorophenol in water by the photo-fenton reaction. *Water Res* 1999;33:1151–8.
- Esplugas S, Giménez J, Contreras S, Pascual E, Rodríguez M. Comparison of different advanced oxidation processes for phenol degradation. *Water Res* 2002;36:1034–42.
- Fasnacht MP, Blough NV. Aqueous photodegradation of polycyclic aromatic hydrocarbons. *Environ Sci Technol* 2002;36:4364–9.
- Fasnacht M, Blough N. Kinetic analysis of the photodegradation of polycyclic aromatic hydrocarbons in aqueous solution. *Aquat. Sci* 2003;6:352–8.
- Fatone F, Di Fabio S, Bolzonella D, Cecchi F. Fate of aromatic hydrocarbons in Italian municipal wastewater systems: an overview of wastewater treatment using conventional activated-sludge processes (CASP) and membrane bioreactors (MBRs). *Water Res* 2011;45:93–104.
- Flotrun V, Deltell C, Padellec Y, Camel V. Removal of sorbed polycyclic aromatic hydrocarbons from soil, sludge and sediment samples using the Fenton's reagent process. *Chemosphere* 2005;59:1427–37.
- Galvão SA, Mota AL, Silva DN, Moraes JE, Nascimento CA, Chiavone-Filho O. Application of the photo-Fenton process to the treatment of wastewaters contaminated with diesel. *Sci Total Environ* 2006;367:42–9.
- Ghaly MY, Härtel G, Mayer R, Haseneder R. Photochemical oxidation of p-chlorophenol by UV/H<sub>2</sub>O<sub>2</sub> and photo-Fenton process: a comparative study. *Waste Manag* 2001;21:41–7.
- Glaze WH, Kang JW, Chapin DH. The chemistry of water treatment processes involving ozone, hydrogen peroxide and ultraviolet radiation. *Ozone Sci Eng* 1987;9:335–52.
- Gogate PR, Pandit AB. A review of imperative technologies for wastewater treatment I: oxidation technologies at ambient conditions. *Adv Environ Res* 2004a;8:501–51.
- Gogate PR, Pandit AB. A review of imperative technologies for wastewater treatment II: hybrid methods. *Adv Environ Res* 2004b;8:553–97.
- Gogate PR, Pandit AB. Sonophotocatalytic reactors for wastewater treatment: a critical review. *AIChE J* 2004c;50:1051–79.
- González D, Ruiz LM, Garralón G, Plaza F, Arévalo J, Parada J, et al. Wastewater polycyclic aromatic hydrocarbons removal by membrane bioreactor. *Desalin Water Treat* 2012;42:94–9.
- González-Pérez DM, Garralón G, Plaza F, Pérez JJ, Moreno B, Gómez MA. Removal of low concentrations of phenanthrene, fluoranthene and pyrene from urban wastewater by membrane bioreactors technology. *J Environ Sci Health A* 2012;47:2190–7.
- Grabowska E, Rzeszczyńska J, Zaleska A. Mechanism of phenol photodegradation in the presence of pure and modified-TiO<sub>2</sub>: a review. *Water Res* 2012;46:5453–71.
- Grote M, Schüürmann G, Altenburger R. Modeling photoinduced algal toxicity of polycyclic aromatic hydrocarbons. *Environ Sci Technol* 2005;39:4141–9.
- Guieysse B, Viklund G. Sequential UV-biological degradation of polycyclic aromatic hydrocarbons in two-phases partitioning bioreactors. *Chemosphere* 2005;59:369–76.
- Guieysse B, Viklund G, Toes AC, Mattiasson B. Combined UV-biological degradation of PAHs. *Chemosphere* 2004;55:1493–9.
- Guo W, He M, Yang Z, Lin C, Quan X, Wang H. Distribution of polycyclic aromatic hydrocarbons in water, suspended particulate matter and sediment from Daliao River watershed, China. *Chemosphere* 2007;68:93–104.
- Guo Y, Huo X, Wu K, Liu J, Zhang Y, Xu X. Carcinogenic polycyclic aromatic hydrocarbons in umbilical cord blood of human neonates from Guiyu, China. *Sci Total Environ* 2012;427:428:35–40.
- Guzman-Duque F, Pétrier C, Pulgarin C, Peñuela G, Torres-Palma RA. Effects of sonochemical parameters and inorganic ions during the sonochemical degradation of crystal violet in water. *Ultrason Sonochem* 2011;18:440–6.
- Hariharan C. Photocatalytic degradation of organic contaminants in water by ZnO nanoparticles: revisited. *Appl Catal A* 2006;304:55–61.
- Hernández-Sancho F, Moins-Senante M, Sala-Garrido R. Cost modelling for wastewater treatment processes. *Desalination* 2011;268:1–5.
- Hofman-Caris CHM, Beerendonk EFNew concepts of UV/H<sub>2</sub>O<sub>2</sub> oxidation. Nieuwegein, The Netherlands: Watercycle Research Institute; 2011:299.
- Hofman-Caris RCHM, Harmsen DHJ, Beerendonk EF, Knol TH, Houtman CJ, Metz DH, et al. Prediction of advanced oxidation performance in various pilot UV/H<sub>2</sub>O<sub>2</sub> reactor systems with MP- and LP- and DBD-UV lamps. *Chem Eng J* 2012;210:520–8.
- Homem V, Santos L. Degradation and removal methods of antibiotics from aqueous matrices – a review. *J Environ Manage* 2011;92:2304–47.
- Homem V, Dias Z, Santos L, Alves A. Preliminary feasibility study of benzo(a) pyrene oxidative degradation by Fenton treatment. *J Environ Public Health* 2009:1–6.
- Huang J, Luo Y, Xi D, Liu N. Removal of polycyclic aromatic hydrocarbons by the membrane improved with cyclodextrine. 3rd international conference on bioinformatics and biomedical engineering; 2009. p. 1–4.
- Huang W, Wang Z, Yan W. Distribution and sources of polycyclic aromatic hydrocarbons (PAHs) in sediments from Zhanjiang Bay and Leizhou Bay, South China. *Mar Pollut Bull* 2012;64:1962–9.
- Ireland JC, Dávila B, Moreno H, Fink SK, Tasso S. Heterogeneous photocatalytic decomposition of polyaromatic hydrocarbons over titanium dioxide. *Chemosphere* 1995;30:965–84.
- Jacobs LE, Weavers LK, Yu-Ping C. Direct and indirect photolysis of polycyclic aromatic hydrocarbons in nitrate-rich surface waters. *Environ Toxicol Chem* 2008;27:1643–8.
- Jüttner K, Galla U, Schmieder H. Electrochemical approaches to environmental problems in the process industry. *Electrochim Acta* 2000;45:2575–94.
- Kavitha V, Palanivelu K. The role of ferrous ion in Fenton and photo-Fenton processes for the degradation of phenol. *Chemosphere* 2004;55:1235–43.
- Kim IK, Huang CP, Chiu PC. Sonochemical decomposition of dibenzothiophene in aqueous solution. *Water Res* 2001;35:4370–8.

- Kleiser G, Frimmel FH. Removal of precursors for disinfection by-products (DBPs) – differences between ozone and OH-radical-induced oxidation. *Sci Total Environ* 2000;256:1–9.
- Kornmüller A, Wiesmann U. Ozonation of polycyclic aromatic hydrocarbons in oil/water-emulsions: mass transfer and reaction kinetics. *Water Res* 2003;37:1023–32.
- Kornmüller A, Cuno M, Wiesmann U. Selective ozonation of polycyclic aromatic hydrocarbons in oil/water-emulsions. *Water Sci Technol* 1997;35:57–64.
- Kot-Wasik A, Dabrowska D, Namiesnik J. Photodegradation and biodegradation study of benzo(a)pyrene in different liquid media. *J Photochem Photobiol A* 2004;168:109–15.
- Kralik P, Kusic H, Koprivnac N, Bozic AL. Degradation of chlorinated hydrocarbons by UV/H<sub>2</sub>O<sub>2</sub>: the application of experimental design and kinetic modeling approach. *Chem Eng J* 2010;158:154–66.
- Lair A, Ferronato C, Chovelon JM, Herrmann JM. Naphthalene degradation in water by heterogeneous photocatalysis: an investigation of the influence of inorganic anions. *J Photochem Photobiol A* 2008;193:193–203.
- Laughrey Z, Bear E, Jones R, Tarr MA. Aqueous sonolytic decomposition of polycyclic aromatic hydrocarbons in the presence of additional dissolved species. *Ultrason Sonochem* 2001;8:353–7.
- Ledakowicz S, Miller J, Olejnik D. Oxidation of PAHs in water solutions by ultraviolet radiation combined with hydrogen peroxide. *Int J Photoenergy* 1999;1:55–60.
- Ledakowicz S, Miller J, Olejnik D. Oxidation of PAHs in water solution by ozone combined with ultraviolet radiation. *Int J Photoenergy* 2001;3:95–101.
- Legrini O, Oliveros E, Braun AM. Photochemical processes for water treatment. *Chem Rev* 1993;93:671–98.
- Legube B, Guyon S, Sugimitsu H, Dore M. Ozonation of some aromatic compounds in aqueous solution: styrene, benzaldehyde, naphthalene, diethylphthalate, ethyl and chloro benzenes. *Ozone Sci Eng* 1983;5:151–70.
- Lehto KM, Vuorimaa E, Lemmetyinen H. Photolysis of polycyclic aromatic hydrocarbons (PAHs) in dilute aqueous solutions detected by fluorescence. *J Photochem Photobiol A* 2000;136:53–60.
- Lesko T, Colussi AJ, Hoffmann MR. Sonochemical decomposition of phenol: evidence for a synergistic effect of ozone and ultrasound for the elimination of total organic carbon from water. *Environ Sci Technol* 2006;40:6818–23.
- Li W, Lu S, Qiu Z, Lin K. Clofibrate acid degradation in UV<sub>254</sub>/H<sub>2</sub>O<sub>2</sub> process: effect of temperature. *J Hazard Mater* 2010;176:1051–7.
- Litter M, Quici N. Photochemical advanced oxidation processes for water and wastewater treatment. *Recent Patent Eng* 2010;4:217–41.
- Little C, Hefner MJ, El-Sharif M. The sono-degradation of phenanthrene in an aqueous environment. *Ultrasonics* 2002;40:667–74.
- Liu H, Li XZ, Leng YJ, Wang C. Kinetic modeling of electro-Fenton reaction in aqueous solution. *Water Res* 2007;41:1161–7.
- Ljubas D. Solar photocatalysis—a possible step in drinking water treatment. *Energy* 2005;30:1699–710.
- Lopez-Alvarez B, Torres-Palma RA, Peñuela G. Solar photocatalytic treatment of carbofuran at lab and pilot scale: effect of classical parameters, evaluation of the toxicity and analysis of organic by-products. *J Hazard Mater* 2011;191:196–203.
- Lopez-Alvarez B, Torres-Palma RA, Ferraro F, Peñuela G. Solar photo-Fenton treatment of carbofuran: analysis of mineralization, toxicity, and organic by-product. *J Environ Sci Health A Tox Hazard Subst Environ Eng* 2012;47:2141–50.
- Lundstedt S, Persson Y, Öberg L. Transformation of PAHs during ethanol-Fenton treatment of an aged gasworks' soil. *Chemosphere* 2006;65:1288–94.
- Mack J, Bolton JR. Photochemistry of nitrite and nitrate in aqueous solution: a review. *J Photochem Photobiol A* 1999;128:1–13.
- Mahamuni NN, Adeguyi YG. Advanced oxidation processes (AOPs) involving ultrasound for waste water treatment: a review with emphasis on cost estimation. *Ultrason Sonochem* 2010;17:990–1003.
- Makino K, Mossoba MM, Riesz P. Chemical effects of ultrasound on aqueous solutions. Formation of hydroxyl radicals and hydrogen atoms. *J Phys Chem* 1983;87:1369–77.
- Malato S, Blanco J, Vidal A, Alarcón D, Maldonado MI, Cáceres J, et al. Applied studies in solar photocatalytic detoxification: an overview. *Sol. Energy* 2003;75:329–36.
- Malato S, Fernández-Ibáñez P, Maldonado MJ, Blanco J, Gernjak W. Decontamination and disinfection of water by solar photocatalysis: recent overview and trends. *Catal Today* 2009;147:1–59.
- Manariotis ID, Karapanagioti HK, Chrysikopoulos CV. Degradation of PAHs by high frequency ultrasound. *Water Res* 2011;45:2587–94.
- Manoli E, Samara C. The removal of polycyclic aromatic hydrocarbons in the wastewater treatment process: experimental calculations and model predictions. *Environ Pollut* 2008;151:477–85.
- Matilainen A, Sillanpää M. Removal of natural organic matter from drinking water by advanced oxidation processes. *Chemosphere* 2010;80:351–65.
- Matsugo S, Mizuno M, Konishi T. Free radical generating and scavenging compounds as a new type of drug. *Curr Med Chem* 1995;2:763–90.
- McConkey BJ, Hewitt LM, Dixon DG, Greenberg BM. Natural sunlight induced photo-oxidation of naphthalene in aqueous solution. *Water Air Soil Pollut* 2002;136:347–59.
- Meehan T, Bond DM. Hydrolysis of benzo(a)pyrene diol epoxide and its covalent binding to DNA proceed through similar rate-determining steps. *Proc Natl Acad Sci U S A* 1984;81:2635–9.
- Méndez-Arriaga F, Torres-Palma RA, Pétrier C, Esplugas S, Gimenez J, Pulgarin C. Mineralization enhancement of a recalcitrant pharmaceutical pollutant in water by advanced oxidation hybrid processes. *Water Res* 2009;43:3984–91.
- Menzie CA, Potocki BB, Santodonato J. Exposure to carcinogenic PAHs in the environment. *Environ Sci Technol* 1992;26:1278–84.
- Miller JS, Olejnik D. Photolysis of polycyclic aromatic hydrocarbons in water. *Water Res* 2001;35:233–43.
- Miller JS, Olejnik D. Ozonation of polycyclic aromatic hydrocarbons in water solution. *Ozone Sci Eng* 2004;26:453–64.
- Mueller JG, Chapman PJ, Pritchard PH. Creosote-contaminated sites. Their potential for bioremediation. *Environ Sci Technol* 1989;23:1197–201.
- Muff J, Søgaard E. Electrochemical degradation of PAH compounds in process water: a kinetic study on model solutions and a proof of concept study on runoff water from harbour sediment purification. *Water Sci Technol* 2010;61:2043–51.
- Muñoz I, Malato S, Rodríguez A, Doménech X. Integration of environmental and economic performance of processes. Case study on advanced oxidation processes for wastewater treatment. *J Adv Oxid Technol* 2008;11:270–5.
- Munter R. Advanced oxidation processes—current status and prospects. *Proc Est Acad Sci Chem* 2001;50:59–80.
- Mutamim NSA, Noor ZZ, Hassan MAA, Olsson G. Application of membrane bioreactor technology in treating high strength industrial wastewater: a performance review. *Desalination* 2012;305:1–11.
- Na G, Liu C, Wang Z, Ge L, Ma X, Yao Z. Distribution and characteristic of PAHs in snow of Fildes Peninsula. *J Environ Sci* 2011;23:1445–51.
- Nadal M, Schuhmacher M, Domingo JL. Levels of PAHs in soil and vegetation samples from Tarragona County, Spain. *Environ Pollut* 2004;132:1–11.
- Nadarajah N, Van Hamme J, Panju J, Singh A, Ward O. Enhanced transformation of polycyclic aromatic hydrocarbons using a combined Fenton's reagent, microbial treatment and surfactants. *Appl Microbiol Biotechnol* 2002;59:540–4.
- Nakata K, Fujishima A. TiO<sub>2</sub> photocatalysis: design and applications. *J Photochem Photobiol C* 2012;13:169–89.
- Neyens E, Baeyens J. A review of classic Fenton's peroxidation as an advanced oxidation technique. *J Hazard Mater* 2003;98:33–50.
- Nidheesh PV, Gandhimathi R. Trends in electro-Fenton process for water and wastewater treatment: an overview. *Desalination* 2012;299:1–15.
- Okona-Mensah KB, Battershill J, Boobis A, Fielder R. An approach to investigating the importance of high potency polycyclic aromatic hydrocarbons (PAHs) in the induction of lung cancer by air pollution. *Food Chem Toxicol* 2005;43:1103–16.
- Oller I, Malato S, Sánchez-Pérez JA. Combination of advanced oxidation processes and biological treatments for wastewater decontamination—a review. *Sci Total Environ* 2011;409:4141–66.
- Onnintan A, Shrestha RA, Sillanpää M. Remediation of hexachlorobenzene in soil by enhanced electrokinetic Fenton process. *J Environ Sci Health A* 2008;43:894–900.
- Onnintan A, Shrestha RA, Sillanpää M. Effect of cyclodextrin on the remediation of hexachlorobenzene in soil by electrokinetic Fenton process. *Sep Purif Technol* 2009a;4:314–20.
- Onnintan A, Shrestha RA, Sillanpää M. Removal of hexachlorobenzene from soil by electrokinetically enhanced chemical oxidation. *J Hazard Mater* 2009b;162:989–93.
- Palma-Goyes RE, Guzmán-Duque FL, Peñuela G, González I, Nava JL, Torres-Palma RA. Electrochemical degradation of crystal violet with BDD electrodes: effect of electrochemical parameters and identification of organic by-products. *Chemosphere* 2010;81:26–32.
- Panizza M, Cerisola G. Electro-Fenton degradation of synthetic dyes. *Water Res* 2009;43:339–44.
- Park JK, Hong SW, Chang WS. Degradation of polycyclic aromatic hydrocarbons by ultrasonic irradiation. *Environ Technol* 2000;21:1317–23.
- Pelaez M, Nolan NT, Pillai SC, Seery MK, Falaras P, Kontos AG, et al. A review on the visible light active titanium dioxide photocatalysts for environmental applications. *Appl Catal B* 2012;125:331–49.
- Pera-Titus M, García-Molina V, Baños MA, Giménez J, Esplugas S. Degradation of chlorophenols by means of advanced oxidation processes: a general review. *Appl Catal B* 2004;47:219–56.
- Pérez M, Torrades F, Doménech X, Peral J. Fenton and photo-Fenton oxidation of textile effluents. *Water Res* 2002;36:2703–10.
- Pétrier C, Jiang Y, Lamy MF. Ultrasound and environment: sonochemical destruction of chloroaromatic derivatives. *Environ Sci Technol* 1998;32:1316–8.
- Pétrier C, Torres-Palma RA, Combet E, Sarantakos G, Baup S, Pulgarin C. Enhanced sonochemical degradation of bisphenol-A by bicarbonate ions. *Ultrason Sonochem* 2010;17:111–5.
- Pignatello JJ, Oliveros E, MacKay A. Advanced oxidation processes for organic contaminant destruction based on the Fenton reaction and related chemistry. *Crit Rev Environ Sci Technol* 2006;36:1–84.
- Pramauero E, Prevot AB, Vincenti M, Gamberini R. Photocatalytic degradation of naphthalene in aqueous TiO<sub>2</sub> dispersions: effect of nonionic surfactants. *Chemosphere* 1998;36:1523–42.
- Prieto-Rodríguez L, Oller I, Klammerth N, Agüera A, Rodríguez EM, Malato S. Application of solar AOPs and ozonation for elimination of micropollutants in municipal wastewater treatment plant effluents. *Water Res* 2013;47:1521–8.
- Psillakis E, Goula G, Kalogerakis N, Mantzavinos D. Degradation of polycyclic aromatic hydrocarbons in aqueous solutions by ultrasonic irradiation. *J Hazard Mater* 2004;108:95–102.
- Radjenovic J, Petrovic M, Barceló D. Fate and distribution of pharmaceuticals in wastewater and sewage sludge of the conventional activated sludge (CAS) and advanced membrane bioreactor (MBR) treatment. *Water Res* 2009;43:831–41.
- Rafin C, Veignie E, Fayeuille A, Surpateanu G. Benzo(a)pyrene degradation using simultaneously combined chemical oxidation, biotreatment with *Fusarium solani* and cyclodextrins. *Bioresour Technol* 2009;100:3157–60.



- Ravindra K, Sokhi R, van Grieken R. Atmospheric polycyclic aromatic hydrocarbons: source attribution, emission factors and regulation. *Atmos Environ* 2008;42:2895–921.
- Rebola M, Silva MJ, Louro H, Antunes AMM, José S, Rebelo MH, et al. Chlorinated polycyclic aromatic hydrocarbons associated with drinking water chlorination – preparation, quantification and genotoxicity characterization. *Proc ECOPE* 2008;2:373–9.
- Reynaud S, Deschaux P. The effects of polycyclic aromatic hydrocarbons on the immune system of fish: a review. *Aquat Toxicol* 2006;77:229–38.
- Rivas FJ, Beltrán FJ, Acedo B. Chemical and photochemical degradation of acenaphthylene. Intermediate identification. *J Hazard Mater* 2000;75:89–98.
- Rivera M, Pazos M, Sanromán MA. Development of an electrochemical cell for the removal of Reactive Black 5. *Desalination* 2011;274:39–43.
- Sabaté J, Bayona JM, Solanas AM. Photolysis of PAHs in aqueous phase by UV irradiation. *Chemosphere* 2001;44:119–24.
- Saien J, Shahrezaei F. Organic pollutants removal from petroleum refinery wastewater with nanotitania photocatalyst and UV light emission. *Int J Photoenergy* 2012;1–5.
- Sanches S, Leirão C, Penetra A, Cardoso VV, Ferreira E, Benoliel MJ, et al. Direct photolysis of polycyclic aromatic hydrocarbons in drinking water sources. *J Hazard Mater* 2011;192:1458–65.
- Sánchez JA, Román IS, Carra I, Cabrera A, Casas JL, Malato S. Economic evaluation of a combined photo-Fenton/MBR process using pesticides as model pollutant. Factors affecting costs. *J Hazard Mater* 2013;244–245:195–203.
- Sanz J, Lombaño JJ, de Luis A. Temperature-assisted UV/H<sub>2</sub>O<sub>2</sub> oxidation of concentrated linear alkylbenzene sulfonate (LAS) solutions. *Chem Eng J* 2013;215:533–41.
- Segura Y, Molina R, Martínez F, Melero JA. Integrated heterogeneous sono-photo Fenton processes for the degradation of phenolic aqueous solutions. *Ultrason Sonochem* 2009;16:417–24.
- Shan AY, Ghazi TIM, Rashid SA. Immobilisation of titanium dioxide onto supporting materials in heterogeneous photocatalysis: a review. *Appl Catal A* 2010;389:1–8.
- Shemer H, Linden KG. Aqueous photodegradation and toxicity of the polycyclic aromatic hydrocarbons fluorene, dibenzofuran, and dibenzothiophene. *Water Res* 2007;41:853–61.
- Shih KL, Lederberg J. Chloramine mutagenesis in *Bacillus subtilis*. *Science* 1976;192:1141–3.
- Siddens LK, Larkin A, Krueger SK, Bradfield CA, Waters KM, Tilton SC, et al. Polycyclic aromatic hydrocarbons as skin carcinogens: comparison of benzo[a]pyrene, dibenzo [def]chrysene and three environmental mixtures in the FVB/N mouse. *Toxicol Appl Pharmacol* 2012;264:377–86.
- Sigman ME, Schuler PF, Ghosh MM, Dabestani RT. Mechanism of pyrene photochemical oxidation in aqueous and surfactant solutions. *Environ Sci Technol* 1998;32:3980–5.
- Sirés I, Brillas E. Remediation of water pollution caused by pharmaceutical residues based on electrochemical separation and degradation technologies: a review. *Environ Int* 2012;40:212–29.
- Sirtori C, Zapata A, Oller I, Gernjak W, Agüera A, Malato S. Decontamination industrial pharmaceutical wastewater by combining solar photo-Fenton and biological treatment. *Water Res* 2009;43:661–8.
- Souza J, Martínez-Huitle C, Ribeiro da Silva D. Electrochemical treatment for removing petroleum polycyclic aromatic hydrocarbons (PAHs) from synthetic produced water using a DSA-type anode: preliminary. *Sustain Environ Res* 2011;21:329–35.
- Sponza DT, Oztekin R. Removals of PAHs and acute toxicity via sonication in a petrochemical industry wastewater. *Chem Eng J* 2010;162:142–50.
- Sponza DT, Oztekin R. Effect of ultrasonic irradiation on the treatment of poly-aromatic substances (PAHs) from a petrochemical industry wastewater. *Ozone Sci Eng* 2011;33:194–210.
- Straif K, Baan R, Grosse Y, Secretan B, El Ghissassi F, Coglianò V. Carcinogenicity of polycyclic aromatic hydrocarbons. *Lancet Oncol* 2005;6:931–2.
- Straub KM, Meehan T, Burlingame AL, Calvin M. Identification of the major adducts formed by reaction of benzo[a]pyrene diol epoxide with DNA in vitro. *Proc Natl Acad Sci U S A* 1977;74:5285–9.
- Taylor E, Cook BB, Tarr MA. Dissolved organic matter inhibition of sonochemical degradation of aqueous polycyclic aromatic hydrocarbons. *Ultrason Sonochem* 1999;6:175–83.
- Tekin H, Bilkay O, Ataberk SS, Balta TH, Ceribasi IH, Sanin FD, et al. Use of Fenton oxidation to improve the biodegradability of a pharmaceutical wastewater. *J Hazard Mater* 2006;136:258–65.
- Thakur RS, Chaudhary R, Singh C. Fundamentals and applications of the photocatalytic treatment for the removal of industrial organic pollutants and effects of operational parameters: a review. *J Renew Sustain Energy* 2010;2:042701–38.
- Tian W, Bai J, Liu K, Sun H, Zhao Y. Occurrence and removal of polycyclic aromatic hydrocarbons in the wastewater treatment process. *Ecotoxicol Environ Saf* 2012;82:1–7.
- Torres RA, Sarría V, Torres W, Peringer P, Pulgarin C. Electrochemical treatment of industrial wastewater containing 5-amino-6-methyl-2-benzimidazolone: toward an electrochemical–biological coupling. *Water Res* 2003a;37:3118–24.
- Torres RA, Torres W, Peringer P, Pulgarin C. Electrochemical degradation of p-substituted phenols of industrial interest on Pt electrodes: attempt of a structure–reactivity relationship assessment. *Chemosphere* 2003b;50:97–104.
- Torres RA, Abdelmalek F, Combet E, Pétrier C, Pulgarin C. A comparative study of ultrasonic cavitation and Fenton's reagent for bisphenol A degradation in deionised and natural waters. *J Hazard Mater* 2007a;146:546–51.
- Torres RA, Pétrier C, Combet E, Mulet F, Pulgarin C. Bisphenol A mineralization by integrated ultrasound–UV-iron (II) treatment. *Environ Sci Technol* 2007b;41:297–302.
- Torres RA, Nieto JI, Combet E, Pétrier C, Pulgarin C. Influence of TiO<sub>2</sub> concentration on the synergistic effect between photocatalysis and high-frequency ultrasound for organic pollutant mineralization in water. *Appl Catal B* 2008a;80:168–75.
- Torres RA, Sarantakos G, Combet E, Pétrier C, Pulgarin C. Sequential helio-photo-Fenton and sonication processes for the treatment of bisphenol A. *J Photochem Photobiol A* 2008b;199:197–203.
- Torres RA, Mosteo R, Pétrier C, Pulgarin C. Experimental design approach to the optimization of ultrasonic degradation of alachlor and enhancement of treated water biodegradability. *Ultrason Sonochem* 2009;16:425–30.
- Tran LH, Drogui P, Mercier G, Blais JF. Electrochemical degradation of polycyclic aromatic hydrocarbons in creosote solution using ruthenium oxide on titanium expanded mesh anode. *J Hazard Mater* 2009;164:1118–29.
- Trapido M, Veressina Y, Munter R. Ozonation and advanced oxidation processes of polycyclic aromatic hydrocarbons in aqueous solutions – a kinetic study. *Environ Technol* 1995;16:729–40.
- US-EPA Polycyclic aromatic hydrocarbons (PAHs). Washington, DC: Office of Solid Waste; 2008:1–3 (20460, January).
- Veignie E, Rafin C, Landy D, Fourmentin S, Surpateanu G. Fenton degradation assisted by cyclodextrins of a high molecular weight polycyclic aromatic hydrocarbon benzo[a]pyrene. *J Hazard Mater* 2009;168:1296–301.
- Vela N, Martínez-Menchón M, Navarro G, Pérez-Lucas G, Navarro S. Removal of polycyclic aromatic hydrocarbons (PAHs) from groundwater by heterogeneous photocatalysis under natural sunlight. *J Photochem Photobiol A* 2012;232:32–40.
- Verlicchi P, Cattaneo S, Marciano F, Masotti L, Vecchiato G, Zaffaroni C. Efficacy and reliability of upgraded industrial treatment plant at Porto Marghera, near Venice, Italy, in removing nutrients and dangerous micropollutants from petrochemical wastewaters. *Water Environ Res* 2011;83:739–49.
- Von Gunten U. Ozonation of drinking water: part I. Oxidation kinetics and product formation. *Water Res* 2003;37:1443–67.
- Von Sonntag CF. Free-radical-induced DNA damage and its repair. A chemical perspective. Berlin Heidelberg: Springer-Verlag; 2006.
- Wang Y, Fengkal L, Zhulu L, Zheng X, Yubin T. Photolysis of anthracene and chrysene in aquatic systems. *Chemosphere* 1999;38:1273–8.
- Wang W, Huang MJ, Kang Y, Wang HS, Leung AOW, Cheung KC, et al. Polycyclic aromatic hydrocarbons (PAHs) in urban surface dust of Guangzhou, China: status, sources and human health risk assessment. *Sci Total Environ* 2011a;409:4519–27.
- Wang W, Simonich S, Giri B, Chang Y, Zhang Y, Jia Y, et al. Atmospheric concentrations and air–soil gas exchange of polycyclic aromatic hydrocarbons (PAHs) in remote, rural village and urban areas of Beijing–Tianjin region, North China. *Sci Total Environ* 2011b;409:2942–50.
- Wen S, Zhao J, Sheng G, Fu J, Peng P. Photocatalytic reactions of phenanthrene at TiO<sub>2</sub>/water interfaces. *Chemosphere* 2002;46:871–7.
- Wen S, Zhao J, Sheng G, Fu J, Peng P. Photocatalytic reactions of pyrene at TiO<sub>2</sub>/water interfaces. *Chemosphere* 2003;50:111–9.
- Wester PW, Muller JJA, Slob W, Mohn GR, Dortant PM, Kroese ED. Carcinogenic activity of benzo[a]pyrene in a 2 year oral study in Wistar rats. *Food Chem Toxicol* 2012;50:927–35.
- WFD (Water Framework Directive) Directive 2000/60/EC of the European Parliament and of the Council of 23 October 2000 establishing a framework for Community action in the field of water policy; 2000.
- WFD (Water Framework Directive) Directive 2008/105/EC of the European Parliament and of the Council of 16 December 2008 on environmental quality standards in the field of water policy, amending and subsequently repealing Council Directives 82/176/EEC, 83/513/EEC, 84/156/EEC, 86/280/EEC and amending Directive 2000/60/EC of the European Parliament and of the Council; 2008.
- Wheat PE, Tumeo MA. Ultrasound induced aqueous polycyclic aromatic hydrocarbon reactivity. *Ultrason Sonochem* 1997;4:55–9.
- Wick A, Haus N, Sukkariyah B, Haering K, Daniels W. Remediation of PAH-contaminated soils and sediments: a literature review. CSES Department, internal research document; 2011.
- Will IBS, Moraes JEF, Teixeira ACS, Guardani R, Nascimento CAO. Photo-Fenton degradation of wastewater containing organic compounds in solar reactors. *Sep Purif Technol* 2004;34:51–7.
- Włodarczyk-Makula M. Application of UV-rays in removal of polycyclic aromatic hydrocarbons from treated wastewater. *J Environ Sci Health A Tox Hazard Subst Environ Eng* 2011;46:248–57.
- Woo OT, Chung WK, Wong KH, Chow AT, Wong PK. Photocatalytic oxidation of polycyclic aromatic hydrocarbons: intermediates identification and toxicity testing. *J Hazard Mater* 2009;168:1192–9.
- Xu T, Xiao XM, Liu HY. Advanced oxidation degradation of dichlorobenzene in water by the UV/H<sub>2</sub>O<sub>2</sub> process. *J Environ Sci Health A Tox Hazard Subst Environ Eng* 2005;40:751–65.
- Xu X, Hu H, Kearney GD, Kan H, Sheps DS. Studying the effects of polycyclic aromatic hydrocarbons on peripheral arterial disease in the United States. *Sci Total Environ* 2013;461–462:341–7.
- Yassitepe E, Yatmaz HC, Öztürk C, Öztürk K, Duran C. Photocatalytic efficiency of ZnO plates in degradation of azo dye solutions. *J Photochem Photobiol A* 2008;198:1–6.
- Yip HY, Chiu SW, Yu JCM, Wong PK. Comparison of photocatalytic oxidation and ozonation in degrading of polycyclic aromatic hydrocarbons. *Hum Ecol Risk Assess* 2006;12:270–6.
- Zeng Y, Hong PKA, Vavrek DA. Chemical–biological treatment of pyrene. *Water Res* 2000a;34:1157–72.
- Zeng Y, Hong PKA, Vavrek DA. Integrated chemical–biological treatment of benzo[a]pyrene. *Environ Sci Technol* 2000b;34:854–62.
- Zhang S, Zhang W, Shen Y, Wang K, Hu L, Wang X. Dry deposition of atmospheric polycyclic aromatic hydrocarbons (PAHs) in the southeast suburb of Beijing, China. *Atmos Res* 2008;89:138–48.
- Zhang C, Jiang Y, Li Y, Hu Z, Zhou L, Zhou M. Three-dimensional electrochemical process for wastewater treatment: a general review. *Chem Eng J* 2013;228:455–67.



# **ANALYTICAL METHODS**

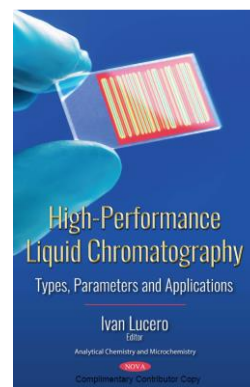


### 3. ANALYTICAL METHODS

#### Book chapter

**High-performance liquid chromatography and chemometric techniques for analytical method development.** In High-performance Liquid Chromatography. Types, Parameters and Applications, 2018, Prof. (Ed.), Ivan Lucero. NOVA. Science Publishers, Inc, pp. 121-144. ISBN 978-1-53613-544-2.

#### Book



**Scope:** In this collection, the authors discuss the way in which it is possible to detect the low concentrations at which toxic compounds and metabolites are present in specimens due to the huge development of chromatographic techniques. The advances in liquid chromatography coupled to different detectors, particularly mass spectrometry, giving examples of its applications in the areas of clinical and forensic toxicology are presented.

#### Highlights

- HPLC is a useful technique for the analysis of specific compounds in environmental samples.
- HPLC allows the identification and quantification of substances at ultra-trace levels.

- During analytical method development, HPLC operating conditions must be optimized.
- PCA and DOE, as multivariate statistical tools, can be used during the optimization phase.

In: High-Performance Liquid Chromatography ISBN: 978-1-53613-543-5  
Editor: Ivan Lucero © 2018 Nova Science Publishers, Inc.

## Chapter 2

# HIGH-PERFORMANCE LIQUID CHROMATOGRAPHY AND CHEMOMETRIC TECHNIQUES FOR ANALYTICAL METHOD DEVELOPMENT

**Ainhoa Rubio-Clemente<sup>1,2,3\*</sup>, Edwin L. Chica<sup>4</sup>  
and Gustavo A. Peñuela<sup>2</sup>**

<sup>1</sup>Facultad de Ciencias de la Salud.

Universidad Católica de Murcia UCAM, Murcia. Spain

<sup>2</sup>Grupo GDCON, Facultad de Ingeniería,

Sede de Investigaciones Universitarias (SIU),

Universidad de Antioquia UdeA, Medellín, Colombia

<sup>3</sup>Facultad de Ingeniería, Tecnológico de Antioquia–Institución  
Universitaria, TdeA, Medellín, Colombia

<sup>4</sup>Departamento de Ingeniería Mecánica, Facultad de Ingeniería,  
Universidad de Antioquia UdeA, Medellín, Colombia

---

\* Corresponding Author Email: [ainhoarubioclem@gmail.com](mailto:ainhoarubioclem@gmail.com).

Complimentary Contributor Copy

## ABSTRACT

As it is worldwide known, high-performance liquid chromatography (HPLC) is a highly useful technique employed for the separation, detection and determination of a number of compounds contained in an analyzed matrix. Undoubtedly, the use of HPLC offers a wide range of advantages in the identification and quantification of samples polluted with substances present at ultra-trace levels, in the range of  $\mu\text{g/L}$  or  $\text{ng/L}$ , such as the monitoring of international regulation accomplishment in terms of water quality. However, in order to take a maximum profit of these advantages, chromatographic operating conditions and sample preparation procedures, if required, must be optimized. For this purpose, chemometric techniques, including design of experiments and principal component analysis, among other multivariate data analysis instruments, offer a powerful tool in contrast to the utilization of one-variable-at-a-time procedures. This work presents the importance of using HPLC in analytical chemistry, as well as the positive aspects related to the use of chemometric approaches for the optimization of processes during the development of analytical methods. Finally, case studies about real applications of chemometric tools focusing on the analysis of water samples polluted with a mixture of polycyclic aromatic hydrocarbons are presented.

**Keywords:** high-performance liquid chromatography, chemometric tool, analytical chemistry, process optimization

## 1. INTRODUCTION

There is no doubt that, currently, one of the main concerns facing humanity is the problem of global pollution, intended as the introduction into the environmental compartments (e.g., surface and sea water, groundwater, atmosphere, soil and biosphere) of compounds causing some kind of detrimental or negative impact on the planet and living beings inhabiting it (Delgado et al., 2004; Alley, 2007). With the industrial development and the exponential growth of the population, a number of foreign substances or products causing these effects have been identified, from energy sources, such as heat or light, to chemicals in the form of

Complimentary Contributor Copy



solids, liquids and gases; including also the environmental pollution in the form of noise (Delgado et al., 2004; Alley, 2007). In fact, as occurred with uranium, even substances naturally present in the environment may cause pollution problems when they are anthropogenically added to the environment in unsafe amounts (Delgado et al., 2004; Alley, 2007).

It is important to note that the number of artificial pollutants entering the different environmental compartments has increased in the last decades. Moreover, they have turned into more and more recalcitrant and persistent compounds, with a tendency to be accumulated into the living beings through the food chain (Rubio-Clemente et al., 2014). In order to control and stop the problem of environmental pollution, several preventive and corrective measures have been carried out, whose efficiency must be monitored to discern the viability of the applied action, and it is here where the analytical chemistry develops a crucial role (Rubio-Clemente et al., 2017).

Throughout the history of humanity, several analytic techniques have been developed, allowing the characterization of the matter. These analytical methods may be classified into chemical methods, which are based on matter-matter interaction, and the instrumental methods, where the occurrence of a chemical reaction for the measurement to be done is not essential (Hernández & González, 2002). Among the latter techniques, the chromatographic ones are of special interest; particularly, high-performance liquid chromatography (HPLC), not only for monitoring environmental pollutants, but also it is important for current applications in biological and pharmaceutical analyses, food technology and industrial-related processes, among others (Engelhardt, 2012; García & Pérez, 2012).

HPLC consists of the separation of the analytes of interest from other possible interference substances, allowing potentially quantifying compounds present in the matrix of interest at trace and ultra-trace concentrations (Hernández & González, 2002; Engelhardt, 2012; García & Pérez, 2012). For a chromatographic method to identify and quantify contaminants at such as low levels, it must be operated under optimal working conditions. In this sense, the optimization of the factors influencing the selectivity and specificity of the analytical method to be

developed must be previously optimized in order to obtain limits of quantification and detection sufficiently low to detect and determine contaminants in the matrix to be analyzed in concentrations in the range of ng/L or  $\mu\text{g/L}$  (Rubio-Clemente et al., 2017).

Currently, one of the most used procedures to optimize the operating conditions of the chromatographic equipment is the study of each individual factor that influences the chromatographic system to be optimized. In other words, each factor or variable is studied at a time within a selected range. This is known as one-variable-at-a-time (OVAT) procedure. However, during this process, valuable information may be lost since OVAT technique mistakenly assumes that factors do not influence each other; statement that is false in many cases (Ferreira et al., 2007; Gonzalez et al., 2007; Dejaegher & Vander, 2011; Ebrahimi-Najafabadi et al., 2014). Additionally, by using OVAT approach, many experiments are required; and finding the optimum of the whole system to be evaluated is not assured (Ebrahimi-Najafabadi et al., 2014). Consequently, the use of chemometric techniques, such as design of experiments (DoE) and principal component analysis (PCA) are recognized as worthy tools to screen and optimize the most influential factors in a process, such as the development of analytical methods using HPLC for the study of environmental, biological, pharmaceutical and industrial matrices (Ebrahimi-Najafabadi et al., 2014; Rubio-Clemente et al., 2017).

Under this scenario, the current work is focused on highlighting the importance of using HPLC for monitoring the substance(s) of interest and chemometric tools to improve the quality of analytical determination through the screening and optimization of the factors most significantly, from a statistical point of view, influencing the chromatographic system. For this purpose, firstly, the HPLC technique was described, including concisely its origins and developments, fundamentals and applications for the separation, detection and determination of the target compounds contained in an analyzed matrix. Secondly, multivariate chemical data analysis tools, such as DoE and PCA, were briefly described. Finally, the application of these powerful chemometric techniques was carried out

focusing on the development of an analytical method based on the separation and quantification of a mixture of polycyclic aromatic hydrocarbons (PAHs), including anthracene (AN) and benzo[a]pyrene (BaP), present in water at ultra-trace levels.

## **2. HIGH-PERFORMANCE LIQUID CHROMATOGRAPHY**

Chromatography encompasses a set of analysis techniques based on the separation of components of a mixture for their subsequent detection (Hernandez & Perez, 2002).

The chromatographic techniques are very varied, but in general terms, two main groups of chromatography can be found: a) gas chromatography and b) liquid chromatography (Hernández & Pérez, 2002; García & Pérez, 2012). These techniques are the most recognized ones in the scientific and industrial field for the separation, identification and quantification of analytes present in a matrix (Hernández & Pérez, 2002). However, the application of liquid chromatography coupled to different detectors has been reported to be wider in comparison with gas chromatography due to the limitations associated with the kind of sample to be analyzed by gas chromatography (García & Pérez, 2012). Among the detectors highly used, the fluorescence (FL) and ultraviolet/visible (UV/vis) detectors are largely used in HPLC (García & Pérez, 2012). Moreover, HPLC allows a good separation of compounds with similar physicochemical properties.

In this section, the origins, development and fundamentals, as well as some possible applications, of HPLC are summarily covered.

### **2.1. Origins and Development of High-Performance Liquid Chromatography**

In 1906, a Russian botanist was able to separate some colored pigments from leaves using an alumina column (Hernández & González,

2002). This first experience was the starting signal for the birth of chromatography and, specifically, liquid chromatography. The development of liquid chromatography was increase up to 1952, where gas chromatography started to be used (Engelhardt, 2012). However, because of the limitation of gas chromatography related to the kind of analyzed samples, the breakthrough in liquid chromatography came in the 60's decade (Engelhardt, 2012). This fact, together with the discovery of more efficient columns, and systems of injection, eluent circulation and detection, boosted the development of HPLC (Engelhardt, 2012).

## **2.2. Fundamentals of High-Performance Liquid Chromatography**

HPLC consists of the separation of the substances of interest, so-called analytes, which circulate into a liquid, known as the mobile phase, which in turn is in contact with the stationary phase, defined as an immiscible liquid or solid packaged inside a chromatographic column. Within the column, each analyte will progress through the system with a different speed depending on its affinity for each of the phases. Therefore, the substances introduced into the system will elute with a different time and, subsequently, they will be separated (Hernández & González, 2002; Engelhardt, 2012). After that, the components of the mixture to be analyzed will pass through a detector that generates a signal, which is characteristic of the analyte to be analyzed and directly proportional to its concentration in the sample. The set of signals are graphically illustrated by a chromatogram (Hernández & González, 2002).

The main elements having an important role in the liquid chromatographic system for the separation of a mixture of substances are the pump, the eluent mixing and sample injection devices, the column, the detector and the recorder (Hernandez & Gonzalez, 2002; Engelhardt, 2012). Briefly, the pump allows supplying the mobile phase with a constant flow free of pulses through the column. The injector, in turn, allows the correct injection of a specific amount of sample in the system. It

**Complimentary Contributor Copy**

should be noted that in liquid chromatography it is possible to work in two modalities: isocratic mode, when the mobile phase maintains the same composition during the elution; and in a gradient mode, when the composition of the mobile phase changes according to a time-dependent function. For each case, a mixing system of the mobile phase used is required. With regard to the column, it is an essential element for the correct separation of the analytes to be placed, since within the column the stationary phase is packaged, as stated above, enabling such as separation depending on the chemical or physical interactions with the stationary phase as they pass through the column. Finally, the detector and recorder enable a physical property of the analytes to be measured, which will depend on their concentration (Hernández & González, 2002; Engelhardt, 2012). In Figure 1, a scheme of the HPLC process is illustrated.

It is highlighted that among the mentioned elements, the conductions and connections are of special interest, mainly those between the injector and the column, and the column and the detector. These connections should avoid dead volumes, as they foster the efficiency reduction of the system. Additionally, filtration and degasification of the sample to be analyzed is recommended to prevent system damages (Hernández & González, 2002; Engelhardt, 2012).

The use of HPLC has proven to be very significant for the study of mixture of components. There are different types of liquid chromatography and they can be classified according to several criteria (Hernández & González, 2002; Engelhardt, 2012). Based on the nature of the stationary phase, four types of liquid chromatography can be named, including the molecular exclusion chromatography, ion exchange chromatography, adsorption chromatography and partition/adsorption chromatography. Among these techniques, the high-performance liquid chromatography operated in reverse phase (RP-HPLC) has been widely used. RP-HPLC consists of the elution of the components of the mixture to be separated so that the most polar compounds elute faster than the most non-polar substances. In other words, the retention times are shorter for polar molecules, whereas molecules of non-polar character elute later (Hernández & González, 2002; Engelhardt, 2012).

### 2.3. Applications of High-Performance Liquid Chromatography

HPLC may be applied for the identification and quantification of a wide variety of organic compounds present in a number of matrices; generally, liquid and solid matrices (García & Pérez, 2012).

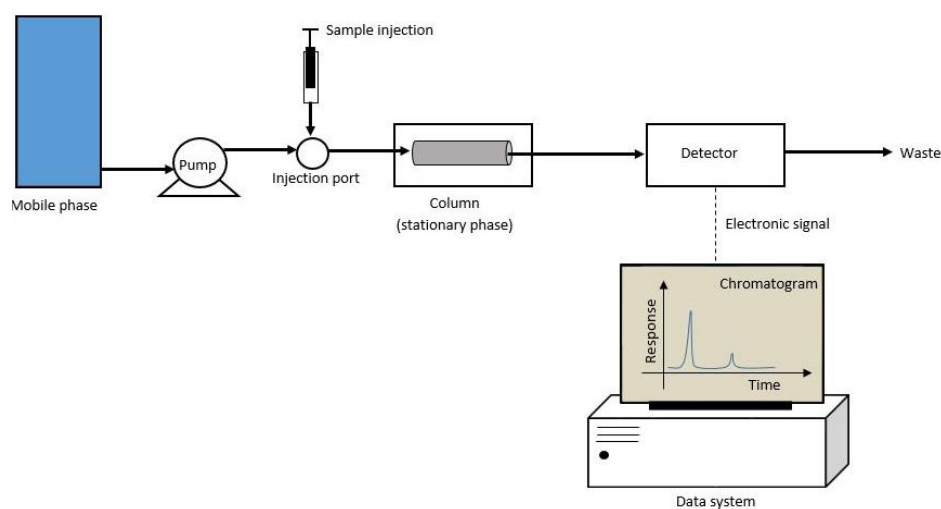


Figure 1. Scheme of high-performance liquid chromatography process.

During the analysis of a mixture of compounds, they are usually firstly separated from the interferences within the sample and, once isolated, they are analyzed. Throughout this process, the sample preparation phase may be very important when the matrix is complex (García & Pérez, 2012; Rubio-Clemente et al., 2017). Traditionally, several techniques for the extraction of the analytes from the sample to be analyzed have been used. Among these procedures, solid and liquid phase extraction techniques can be named (García & Pérez, 2012; Rubio-Clemente et al., 2017). However, in general terms, large amounts of samples are required and high volumes of the reactants involved in the extraction procedure are consumed. Additionally, such as reactants usually exhibit high toxicity. Furthermore, the main limitations of the extraction procedures lie in the high associated costs both for the acquisition of the required supplies and materials used during the separation step, and those ones related to the maintenance of the

system. Moreover, the separation of analytes is usually a laborious procedure that might incur the analyte loss, and it is a time consuming process. Consequently, in those cases where the matrix is relatively simple and there is no a complex mixture of compounds to be analyzed, direct injection may be the selected procedure for the analysis of the target analytes, even if they are present at ultra-trace levels (Rubio-Clemente et al., 2017).

HPLC and derived techniques may be used in pharmacology for the quantification of pharmaceutical active ingredients and the determination of the appropriate dose of drugs according to the response of each patient (Karakuş et al., 2008). In addition, HPLC can be used for the study of drug metabolites in biological samples (Pitt et al., 2009; Nasir et al., 2011). It may also be applied for toxicological analyses, including the identification and quantification of toxics and drugs of abuse, as well as those substances identified during doping controls (Thevis et al., 2005; Gracia-Lor et al., 2011; Boix et al., 2014). In the analysis of environmental samples, HPLC is also widely used (Boix et al., 2015). Likewise, it is employed in the determination of degradation products during the experimentation and performance of decontamination processes of the different environmental matrices (Gracia-Lor et al., 2011; Tran et al., 2013). Besides, the degradation products are studied in the manufacturing processes to determine the durability of mass-produced products, for which HPLC is also used. Likewise, HPLC can be utilized to determine the degree of purity of raw materials (Zhu et al., 2005).

Among the main groups of organic substances, carbonyl compounds, phenols, isocyanates, phthalates, pesticides (organophosphates, carbamates, benzimidazoles, triazines), pharmaceutical compounds (fluoroquinolones, sulfonamides, estrogens, vitamins) and PAHs, have been cited to be analyzed using HPLC. Indeed, in García & Pérez (2012) an extensive and well-documented study about the application of HPLC operating in reverse phase equipped with a FL and a UV/vis detector for the analysis of the substances referred above is reported.

Once the sample to be analyzed has been prepared or directly injected into the chromatograph, the analytes are separated for their correct

identification and quantification. For this purpose, the optimization of the chromatographic operating conditions is of special interest. In section 3 the application of chemometric techniques as alternative to the conventional OVAT techniques, due to the advantages associated with, is proposed and briefly described.

### **3. CHEMOMETRIC TECHNIQUES FOR ANALYTICAL CHEMISTRY**

The use of HPLC for analytical purposes demands investment in equipment, consumer material, facilities and human talent training, when it is intended to comply with the requirements of high quality, accuracy and precision in separation processes for the subsequent identification and quantification of the analytes of interest. In order to save on operating costs and valuable analytical time, the analytical method to be developed should be optimized. Conventionally, OVAT techniques have been used; nevertheless, the utilization of these procedures has associated several drawbacks (Rubio-Clemente et al., 2017). It is highlighted that OVAT approaches may be used for those systems where the influencing factors are independent on each other. However, they are not recommended when the number of factors is very large since this kind of procedures becomes laborious and costly. Additionally, univariate techniques ignore the interactions among factors (Ferreira et al., 2007; Gonzalez et al., 2007; Dejaegher & Vander, 2011), which is very common to happen in most processes.

Therefore, in order to overcome these drawbacks, multivariate techniques, including DoE and PCA, are suggested. The choice of the type of multivariate technique to be employed depends on the study purpose and the number and levels of the factors to be examined.

A concise information about the fundamentals of DoE and PCA are addressed in the following sections.

**Complimentary Contributor Copy**



### 3.1. Design of Experiments

DoE provides a powerful means to achieve breakthrough improvement in chromatographic analyses and, subsequently, in the steps involved (i.e., sample preparation and analyte separation phase, and quantification step) (Ebrahimi-Najafabadi et al., 2014).

Commonly, DoE, which is intended to simultaneously evaluate the influence on the system of the factors taken into consideration, unlike OVAT techniques, may be grouped into two categories, such as screening designs and optimization designs, being response surface methodologies widely employed for the latter purpose. The first kind of DoE is focused on identifying, among the selected factors, those ones statistically significant for the studied system, before their optimization. Within this group, Plackett-Burman and fractional factorial designs are commonly used (Ferreira et al., 2007). After separating the main factors from those statistically non-significant parameters, further investigations are required to find the optimal operating conditions. For this purpose, response surface methodologies, oriented to fit a theoretical response function to the studied experimental domain, are usually used (Hanrahan & Lu, 2006). Several response surface designs may be applied, such as full and fractional factorial designs, as well as the more complex, Doehlert, central composite, mixture and Box-Behnken designs (Ferreira et al., 2007; Ebrahimi-Najafabadi et al., 2014).

The steps to be followed when using DoE for screening and optimizing reasons can be summed up as follows:

1. Selection of the factors and levels to be tested. This obeys to the specifications of the study to be carried out.
2. Evaluation of the influence of each factor on the selected response. It is here where the DoE must be carefully selected for the experimentation to be conducted is successful.
3. Construction of the design matrix and execution of the runs in a random way. Randomization is very important for obtaining an accurate estimation of the experimental error.

Complimentary Contributor Copy

4. Construction of the response surface by performing an analysis of variance (ANOVA) on the results. From the ANOVA, a regression model describing the desired response of the studied system is obtained. This test allows determining the significance and magnitude of each factor involved in the system to be optimized (Dejaheger & Vander, 2011).

It is important to note that when more than one response is to be considered, Derringer's desirability function application is suggested. This algorithm is a multicriteria decision approach that allows finding the best compromise between conflicting goals or desired responses, which are of special interest in chromatography (Ebrahimi-Najafabadi et al., 2014).

Up to date, several studies covering in detail the types of DoE, their characteristics and the cases where each DoE is recommended to be applied have been reported (Hanrahan & Lu 2006; Ferreira et al., 2007; Bezerra et al., 2008; Dejaegher & Vander, 2009, 2011; Ebrahimi-Najafabadi et al., 2014).

In section 4.1, a case study on the application of DoE for the screening and optimization of those factors statistically affecting the identification and quantification of AN and BaP is exposed. As mentioned above, the DoE selected in each case depended on the characteristics of the system, the factors to be analyzed and the chosen experimental domain. As a general consideration, for all the designs used, the data were interpreted graphical and statistically. Among the graphical tests, Pareto charts and main effect plots were performed. Pareto chart indicates the extent of significance and sign of the estimated effects. In turn, the main effect plot informs about when a main effect occurs in the system if the levels of a factor affect the response differently. For the statistical study, ANOVA test was conducted and a regression model was fitted for each considered response.

From the regression model, a response surface function representing each studied response was built. Derringer's desirability function was performed since more than one single response was taken into account and a compromise among the levels of the selected factors must be reached for

achieving the best treatment allowing the identification and quantification of ultra-trace levels of AN and BaP in aqueous samples. During the use of Derringer's desirability function, the same weight to each response was assigned.

Within each DoE, the execution of the runs was done in a randomized order to make sure that the results are accurate and minimize the effect of uncontrolled variables that might introduce a bias on the measurements.

### **3.2. Principal Component Analysis**

As stated above, multivariate statistical approaches by using PCA and DoE may overcome the limitations ascribed to the use of OVAT techniques.

PCA is a statistical tool of synthesis of information that allow reducing a set of original variables and extracting a small number of principal components (PCs), also known as latent factors, used for the evaluation of the relationships among the observed variables (Machala et al., 2001; Golobočanin et al., 2004), losing as little information as possible.

The new PCs are linear combinations of the original variables, that are independent on each other, which will be able to explain the majority of the variability of the obtained data (Golobočanin et al., 2004).

It is important to emphasize that before performing a PCA, the correlation among the analyzed variables must be verified in order to discern whether the matrix of correlation coefficients, which is obtained from the data matrix, is large enough for factoring to be justified. Subsequently, the associated vectors and eigenvalues of the matrix of correlation coefficients are obtained. These eigenvalues and vectors enable us to obtain those linear combinations of the original variables, so that each linear combination is a PC (Abdi et al., 2010).

On the other hand, it should be noted that the determination of the number of PCs to be retained is at the discretion of the researcher (Abdi et al., 2010; Bro et al., 2014); although, those PCs whose eigenvalues are higher than 1 are usually retained. Graphically, this criterion can be observed with the seed plot.

Finally, the interpretation of each PC is a function of the original variables that are most correlated with; i.e., the interpretation of the factors is not given a priori, but it is deduced from the relationship of the factors with the initial variables (Abdi et al., 2010; Bro et al., 2014).

In section 4.2, an example on the application of PCA for the study of the chromatographic behavior of AN and BaP identification and quantification is shown.

#### **4. CASE STUDIES. DEVELOPMENT OF AN ANALYTICAL METHOD FOR THE DETERMINATION OF A MIXTURE OF POLYCYCLIC AROMATIC HYDROCARBONS**

Aqueous resources pollution has brought increasing attention to scientific community and public in general. A number of pollutants can be found in water and among them PAHs can be named (Tian et al., 2012; Rubio et al., 2013; Rubio-Clemente et al., 2014). PAHs are ubiquitous compounds present in the atmosphere, soil, water and living beings due to their bioaccumulative character (Chizhova et al., 2013; Menezes et al., 2013; Alves et al., 2017; Segura et al., 2017; Santos et al., 2017). These pollutants also have hydrophobic properties, being this aspect the reason why PAHs are present in aqueous environments at low concentrations. In spite of the low concentration they are found, PAHs are toxic compounds that may suppress the immune system, are able to be endocrine disruptors and can cause cancer and malformations in living beings (Rubio-Clemente et al., 2014). As a consequence, PAH concentration in water must be monitored in order to determine their presence and the efficiency of the treatment processes used for water decontamination.

For the identification and quantification of PAHs in water and, extensively, in other matrices, RP-HPLC with UV/vis or FL detectors has been used because of the high sensitivity, selectivity and precision associated (Andrade-Eiroa et al., 2010).

In the current case studies, AN and BaP were selected due to the high acute phototoxicity potential of the former one and the carcinogenicity, mutagenicity and teratogenicity of the latter one (Rubio-Clemente et al., 2014). Additionally, RP-HPLC was used. The RP-HPLC was equipped with a FL detector instead of a UV/vis detector, also widely employed in environmental sample analysis, since the FL detector provides an increase in sensitivity from 20 to 30 times in comparison with the UV/vis detector (García & Pérez, 2012). In addition to its high sensitivity with respect to other detectors and even also other chromatographic techniques, the FL detector is highly selective for fluorescent compounds, as it is the case of PAHs. Furthermore, concerning the type of chromatographic column, a Kinetex core shell technology C18 column (150 x 1.6 mm i.d., 5 µm of particle size) was selected. With regard to the mobile phase components, the binary system composed of deionized water and acetonitrile, as organic solvent, resulted to be more adequate for the tested system.

Furthermore, taking into account the provided information on the preparation of the sample and considering that the compounds of interest in the current study are only AN and BaP and a relative clean matrix was used, no extraction technique before sample injection in the RP-HPLC was carried out. Therefore, to increase sensibility of the analytical method and to obtain accurate and repeatable results within a short period of analysis (Boix et al., 2015) without incurring high costs neither the contamination of the sample nor the loss of the target analytes, large-volume injection was conducted.

On the other hand, considering the advantages of chemometric techniques for the development of analytical methods above OVAT techniques, DoE and PCA were executed for a water sample containing 20 and 2 µg/L of AN and BaP, respectively, in order to obtain the optimal level of the factors considered statistically significant for the studied chromatographic system.

It is important to note that along with the need to analyze very low levels of the target pollutants, an effective compound resolution in the shortest analysis time and with the lowest costs is demanded. In this regard, variables such as the flow rate, the mobile phase strength, the

column temperature, the injection volume, and the excitation and emission wavelengths were assessed within a range selected focusing on the literature reports, our own chromatographic experience, previous assays and the technical restrictions of the equipment used. For the statistical treatment of the obtained experimental data, Statgraphics Centurion XVII program package was used at a confidence interval of 95%.

Here, two case studies for the analysis of a mixture of PAHs are briefly exposed so that some notions on the application of chemometric techniques, such as DoE and PCA, can be acquired by the reader.

#### 4.1. Case Study I

In this case, a  $2_{IV}^{6-2}$  fractional factorial design plus 5 central points was considered for the screening purpose. The DoE was performed within two days; therefore, the block effect on the chromatographic system was also evaluated.

The factors to be considered and ranges (between parentheses) were the percentage of acetonitrile of the mobile phase with regard to deionized water (70-90%), the temperature of the column (25-35 °C), the injection volume (50-100  $\mu$ L), the flow rate of the mobile phase (1-1.5 mL/min) and the excitation (230-280 nm) and emission wavelength (408-424 nm).

The experimental data registered were those ones concerning the retention time of BaP, the resolution between AN and BaP, the area of AN and that of BaP. In order to reduce valuable analysis time, as well as the consumption of the organic solvent, the retention time of BaP was intended to be minimized. Additionally, the resolution between the analytes of interest was minimized, although in chromatography this parameter is usually maximized for identification purposes. This was motivated by the high values of resolution previously registered, which were higher than 6 in all cases, allowing thus a sufficient separation between AN and BaP. Furthermore, the area of AN and that of BaP were intended to be maximized in order to quantify ultra-trace levels of these compounds.

After randomly conducting the runs according to the constructed design matrix, the obtained experimental data were analyzed. It was observed that the statistically significant factors (or variables) to be considered in the optimization experiments were the flow rate, the acetonitrile content in the mobile phase, the column temperature, the injection volume and the excitation wavelength. The block was statistically insignificant. Additionally, the emission wavelength resulted to be non-significant under the evaluated conditions. This aspect could be attributed to the narrow range tested for this parameter. Consequently, the emission wavelength was fixed at 416 nm.

Although the injection volume resulted to be a statistically significant factor, very good responses were found when this factor was fixed at 100  $\mu\text{L}$  and no column saturation was observed. Therefore, this parameter was set at 100  $\mu\text{L}$ .

In a second step, the non-fixed factors were evaluated to find the optimal operating conditions of the chromatographic system for the identification and quantification of AN and BaP at ultra-trace levels in aqueous samples. A Box-Benhken DoE plus 3 central points was employed in this occasion. Runs were randomly executed within two days and the block also resulted to be non-significant. Therefore, the environmental conditions seemed to not influence the measurements in the tested chromatographic system under the studied operating conditions.

Once the design matrix was constructed and the samples were run, ANOVA test was carried out and a quadratic model was built for each response. The coefficients of determination adjusted by the degrees of freedom were  $> 97\%$ . This indicates that the second-order models built were reliable for the determination of AN and BaP at ultra-trace levels in aqueous samples.

In order to integrate all the four constructed polynomial models and find the location where the statistically significant factors are optimal, Derringer's desirability function was employed. With a desirability value of 85.80%, the best operating conditions for the flow rate, the acetonitrile concentration and the temperature were 1 mL/min, 90% and 35 °C, respectively. For the excitation wavelength, the optimal resulting value

was located at 260 nm; however, this is a compromise between the optimal excitation wavelength of AN and that of BaP. Since the equipment used allows fixing a particular excitation wavelength as the compounds are eluted, Derringer's desirability function was again run searching for maximizing the area of AN and BaP. 254 and 267 nm were obtained as the optimal excitation wavelengths for AN and BaP, respectively. Therefore, after checking that the area counts of AN and BaP were larger under these new excitation wavelengths, these values were fixed during the corresponding AN and BaP elution time.

Further details on this case study are reported in Rubio-Clemente et al. (2017). In the referred work, the specific reactants, chemicals, working solutions and equipment utilized during the development of the proposed analytical method may be also found, as well as the validation study and the application of the developed analytical method to the analysis of AN and BaP in natural water.

## 4.2. Case Study II

For the identification and quantification of AN and BaP in the range of ultra-trace concentration in aqueous matrices by means of RP-HPLC coupled to a FL detector, understanding the behavior of the target analytes in the chromatographic system is a crucial aspect. For this purpose, PCA was used. Additionally, a fractional factorial DoE was employed to find the optimal operating conditions of the factors having a main impact on the system enabling AN and BaP simultaneous identification and quantification.

In this case, the initial factors to be considered and levels selected were the same than those described in section 4.1. Likewise, the experimental data measured where AN and BaP area of the peak, BaP retention time and the resolution between these two analytes. Moreover, AN and BaP height of the peak were recorded.



**Table 1. Factors statistically significant for the principal components obtained**

Index	PC number	Factors
Identification of AN and BaP	PC 1	Flow rate
		Acetonitrile content
Quantification of AN	PC 2	Excitation wavelength
Quantification of BaP	PC 3	Flow rate
		Injection volume
		Excitation wavelength

All the data obtained for each considered response were checked for normality distribution. It was found that all the responses with the exception of AN area and AN height accomplished for normality assumption. Therefore, AN area and height data were normalized previously to PCA. Three PCs with eigenvalues higher than 1 were found. These PCs explained > 97% of the total variability of the results obtained.

Each PC was interpreted as follows: a) PC 1 represented the identification index of AN and BaP; b) PC 2 described the behavior of AN; and c) PC 3 was indicative of the chromatographic behavior of BaP. In this sense, PC 2 and PC 3 represented the quantification index of AN and BaP, respectively.

In a second step, once the PCs were found, the factors significantly affecting, from a statistical point of view, the PCs were identified and optimized using a fractional factorial design  $2_{IV}^{6-2}$  plus 5 central points.

Following the steps mentioned in section 3.1 when using DoE, ANOVA test was performed for each PC with a confidence interval of 95%. In Table 1, the factors statistically significant influencing each PC are compiled.

By using multicriteria decision approach that allows optimizing the analyzed PCs, the best operating conditions of the original factors affecting the chromatographic system were obtained. 100  $\mu$ L, 90% and 1 mL/min resulted to be the optimal injection volume, acetonitrile content and flow rate of the mobile phase, respectively. With regard to the excitation and emission wavelength, further studies were needed to be performed for

determining the optimal values. 416 nm was selected as the optimal value for the emission wavelength for both analytes and 254 and 267 nm for the excitation wavelength of AN and BaP, respectively. In turn, the column temperature was fixed at 35 °C.

## CONCLUSION

As presented, HPLC operating in reverse phase offers a powerful tool for separating, detecting and quantifying the individual components of a mixture. However, selective equipment and supplies, as well as analytical time to run a sample and analyze the results, are required. In this sense, future prospects in the field of chromatography application are aimed at minimizing these associated costs. In order to save not only on operating costs linked to the materials and supplies used, but also on valuable analytical time, DoE and PCA have been pointed out as chemometric techniques alternative to traditional OVAT procedures. The current work was aimed at highlighting the importance of using HPLC in analytical chemistry, as well as the positive aspects related to the application of chemometric tools for the optimization of processes and their combination with HPLC during the development of analytical methods. Finally, some real applications of chemometric approaches were addressed focusing on the development of an analytical method able to identify and quantify a mixture of AN and BaP present at ultra-trace levels in relatively clean aqueous matrices.

By the use of HPLC along with chemometric techniques, a new window is opened in the field of analytical method evolution.

## REFERENCES

- Abdi, H. & Williams, L. J. (2010). Principal component analysis. Wiley Interdisciplinary Reviews: computational statistics, 2, 433-459.

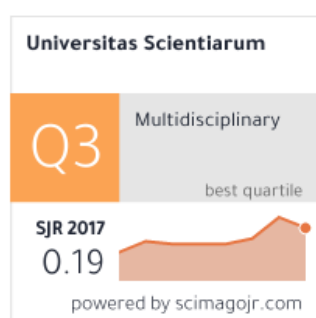
Complimentary Contributor Copy

- Alley, E. R. (2007). *Water quality control handbook*, (Vol. 2). New York: McGraw-Hill.
- Alves, C. A., Vicente, A. M., Custódio, D., Cerqueira, M., Nunes, T., Pio, C., Lucarelli, F., Calzolari, G., Nava, S., Diapouli, E., Eleftheriadis, K., Querol, X. & Musa, B. A. (2017). Polycyclic aromatic hydrocarbons and their derivatives (nitro-PAHs, oxygenated PAHs, and azaarenes) in PM 2.5 from Southern European cities. *Science of the Total Environment*, 595, 494-504.
- Andrade-Eiroa, A., Diévar, P. & Dagaut, P. (2010). Improved optimization of polycyclic aromatic hydrocarbons (PAHs) mixtures resolution in reversed-phase high-performance liquid chromatography by using factorial design and response surface methodology. *Talanta*, 81, 265-74.
- Bezerra, M. A., Santelli, R. E., Oliveira, E. P., Villar, L. S. & Escaleira, L. A. (2008). Response surface methodology (RSM) as a tool for optimization in analytical chemistry. *Talanta*, 76, 965-977.
- Boix, C., Ibáñez, M., Sancho, J. V., León, N., Yusá, V. & Hernández, F. (2014). Qualitative screening of 116 veterinary drugs in feed by liquid chromatography–high resolution mass spectrometry: Potential application to quantitative analysis. *Food Chemistry*, 160, 313-320.
- Boix, C., Ibáñez, M., Sancho, J. V., Rambla, J., Aranda, J. L., Ballester, S. & Hernández, F. (2015). Fast determination of 40 drugs in water using large volume direct injection liquid chromatography tandem mass spectrometry. *Talanta*, 131, 719-27.
- Bro, R. & Smilde, A. K. (2014). Principal component analysis. *Analytical Methods*, 6, 2812-2831.
- Chizhova, T., Hayakawa, K., Tishchenko, P., Nakase, H. & Koudryashova, Y. (2013). Distribution of PAHs in the northwestern part of the Japan Sea. *Deep-Sea Research Part II*, 86, 19-24.
- Delgado, M. N. G., Barrenetxea, C. O., Serrano, A. P., Blanco, J. M. A. & Vidal, F. J. R. (2004). *Contaminación ambiental: una visión desde la química*. Editorial Paraninfo, Madrid. [Environmental pollution: a view from chemistry.]

- Ebrahimi-Najafabadi, H., Leardi, R. & Jalali-Heravi, M. (2014). Experimental design in analytical chemistry-part I: theory. *Journal of AOAC International*, 97, 3-11.
- Engelhardt, H. (2012). *High performance liquid chromatography*. Editorial Springer-Verlag, Berlin Heidelberg New York.
- Ferreira, S. L. C., Bruns, R. E., da Silva, E. G. P., dos Santos, W. N. L., Quintella, C. M., David, J. M., de Andrade, J. B., Breitzkreitz, M. C., Jardim, I. C. S. F. & Neto, B. B. (2007). Statistical designs 575 and response surface techniques for the optimization of chromatographic systems. *Journal of Chromatography A*, 1158, 2-14.
- Dejaegher, B. & Vander, Y. (2009). The use of experimental design in separation science. *Acta Chromatographica*, 21, 161-201.
- Dejaegher, B. & Vander, Y. (2011). Experimental designs and their recent advances in set-up, data interpretation and analytical applications. *Journal of Pharmaceutical and Biomedical Analysis*, 56, 141-58.
- García, S. & Pérez, R. M. (2012). Aplicaciones de la cromatografía líquida con detector de diodos y fluorescencia al análisis de contaminantes medioambientales. *Informes Técnicos Ciemat*. Editorial Ciemat, Madrid. [Applications of liquid chromatography with diode detector and fluorescence to the analysis of environmental contaminants.]
- Gracia-Lor, E., Sancho J. V. & Hernández, F. (2011). Multi-class determination of around 50 pharmaceuticals, including 26 antibiotics, in environmental and wastewater samples by ultra-high performance liquid chromatography–tandem mass spectrometry. *Journal of Chromatography A*, 1218, 2264-2275.
- Golobočanin, D. D., Škrbić, B. D. & Miljević, N. R. (2004). Principal component analysis for soil contamination with PAHs. *Chemometrics and Intelligent Laboratory Systems*, 72, 219-223.
- Gonzalez, A., Foster, K. L. & Hanrahan, G. (2007). Method development and validation for optimized separation of benzo(a)pyrene-quinone isomers using liquid chromatography-mass spectrometry and chemometric response surface methodology. *Journal of Chromatography A*, 1167, 135-42.

- Hanrahan, G. & Lu, K. (2006). Application of factorial and response surface methodology in modern experimental designs and optimization. *Critical Reviews in Analytical Chemistry*, 36, 141-51.
- Hernandez, L. & González, C. (2002). *Introducción al análisis instrumental*. Editorial Ariel, Barcelona. [Introduction to instrumental analysis]
- Karakuş, S., Küçükgüzel, İ. & Küçükgüzel, Ş. G. (2008). Development and validation of a rapid RP-HPLC method for the determination of cetirizine or fexofenadine with pseudoephedrine in binary pharmaceutical dosage forms. *Journal of Pharmaceutical and Biomedical Analysis*, 46, 295-302.
- Machala, M., Dusek, L., Hilscherova, K., Kubinova, R., Jurajda, P., Neca, J., Ulrich, R., Gelnar, M., Studnicková, Z. & Holoubek, I. (2001). Determination and multivariate statistical analysis of biochemical responses to environmental contaminants in feral freshwater fish *Leuciscus cephalus* L. *Environmental Toxicology and Chemistry*, 20, 1141-1148, 2001.
- Menezes, H. C., Paiva, M. J., Santos, R. R., Sousa, L. P., Resende, S. F., Saturnino, J. A., Paulo, B. P. & Cardeal, Z. L. (2013). A sensitive GC/MS method using cold fiber SPME to determine polycyclic aromatic hydrocarbons in spring water. *Microchemical Journal*, 110, 209-14.
- Nasir, F., Iqbal, Z., Khan, A., Ahmad, L., Shah, Y., Khan, A. Z., Khan, J. A. & Khan, S. (2011). Simultaneous determination of timolol maleate, rosuvastatin calcium and diclofenac sodium in pharmaceuticals and physiological fluids using HPLC-UV. *Journal of Chromatography B*, 879, 3434-3443.
- Pitt, J. J. (2009). Principles and applications of liquid chromatography-mass spectrometry in clinical biochemistry. *The Clinical Biochemist Reviews*, 30, 19-34.
- Rubio, A., Chica, E. L. & Peñuela, G. A. (2013). Procesos de tratamiento de aguas residuales para la eliminación de contaminantes orgánicos emergentes. *Revista Ambiente & Água*, 8, 93-103. [Wastewater

- treatment processes for the removal of emerging organic pollutants. *Environmental & Water Magazine*, 8, 93-103].
- Rubio-Clemente, A., Chica, E. & Peñuela, G. A. (2017). Rapid determination of anthracene and benzo(a)pyrene by high-performance liquid chromatography with fluorescence detection. *Analytical Letters*, 50, 1229-1247.
- Rubio-Clemente, A., Torres-Palma, R. A. & Peñuela, G. A. (2014). Removal of polycyclic aromatic hydrocarbons in aqueous environment by chemical treatments: A review. *Science of the Total Environment*, 478, 201-25.
- Santos, L. O., dos Anjos, J. P., Ferreira, S. L. & de Andrade, J. B. (2017). Simultaneous determination of PAHS, nitro-PAHS and quinones in surface and groundwater samples using SDME/GC-MS. *Microchemical Journal*, 133, 431-440.
- Segura, A., Hernández-Sánchez, V., Marqués, S. & Molina, L. (2017). Insights in the regulation of the degradation of PAHs in *Novosphingobium* sp. HR1a and utilization of this regulatory system as a tool for the detection of PAHs. *Science of The Total Environment*, 590, 381-393.
- Thevis, M. & Schänzer, W. (2005). Examples of doping control analysis by liquid chromatography-tandem mass spectrometry: Ephedrines,  $\beta$ -receptor blocking agents, diuretics, sympathomimetics, and cross-linked hemoglobins. *Journal of Chromatographic Science*, 43, 22-31.
- Tian, W., Bai, J., Liu, K., Sun, H. & Zhao, Y. (2012). Occurrence and removal of polycyclic aromatic 660 hydrocarbons in the wastewater treatment process. *Ecotoxicology and Environmental Safety*, 82, 1-7.
- Tran, N. H., Hu, J. & Ong, S. L. (2013). Simultaneous determination of PPCPs, EDCs, and artificial sweeteners in environmental water samples using a single-step SPE coupled with HPLC-MS/MS and isotope dilution. *Talanta*, 113, 82-92.
- Zhu, X., Cai, J., Yang, J. & Su, Q. (2005). Determination of glucosamine in impure chitin samples by high-performance liquid chromatography. *Carbohydrate Research*, 340, 1732-1738.

**Paper****Direct large-volume injection analysis of polycyclic aromatic hydrocarbons in water****Journal**

**Scope:** The journal is a multidisciplinary, Open-Access, peer-reviewed, first-online journal devoted to the promotion of the recent progresses in all fields of exact and natural sciences.

**Highlights**

- PAH monitoring is required due to their detrimental health risks associated.
- An analytical method for AN and BaP determination is developed using chemometric tools.
- The chromatographic behavior of the target analytes is described by three indexes.
- The method is useful for a sensitive analysis of AN and BaP in clean real water.





# Direct large-volume injection analysis of polycyclic aromatic hydrocarbons in water

Ainhoa Rubio-Clemente,<sup>1,2,3,\*</sup> Edwin L. Chica,<sup>4</sup> Gustavo A. Peñuela,<sup>2</sup>

## Edited by

Juan Carlos Salcedo-Reyes  
(salcedo.juan@javeriana.edu.co)

1. Universidad Católica de Murcia UCAM, Facultad de Ciencias de la Salud, Avenida de los Jerónimos, 135, Guadalupe-Murcia, Spain.

2. Universidad de Antioquia UdeA, Facultad de Ingeniería, Sede de Investigaciones Universitarias (SIU), Grupo de Diagnóstico y Control de la Contaminación (GDCON), Calle 70, No. 52-21, Medellín, Colombia.

3. Tecnológico de Antioquia-Institución Universitaria TdeA, Facultad de Ingeniería, Calle 78b No. 72A-220, Medellín, Colombia.

4. Universidad de Antioquia UdeA, Facultad de Ingeniería, Departamento de Ingeniería Mecánica, Calle 70, No. 52-21, Medellín, Colombia.

\*ainhoarubioclem@gmail.com

Received: 07-10-2017

Accepted: 19-04-2018

Published on line: 05-06-2018

Citation: Rubio-Clemente A, Chica EL, Gustavo, Peñuela A. Direct large-volume injection analysis of polycyclic aromatic hydrocarbons in water, *Universitas Scientiarum*, 23 (2): 171-189, 2018. doi: 10.11144/Javeriana.SC23-2.dlvi

## Funding:

Colombian Institute of Science and Technology (COLCIENCIAS) and the Research Vice-rectory of Universidad de Antioquia.

Electronic supplementary material: N.A.



## Abstract

Due to the health risks for both humans and living beings caused by polycyclic aromatic hydrocarbons (PAHs), the monitoring of these compounds in environmental matrices is mandatory. This work proposes an analytical method for analyzing anthracene (AN) and benzo[a]pyrene (BaP), two of the most representative PAHs, at ultra-trace concentrations in water, employing direct injection of large volumes of samples coupled with reversed-phase high-performance liquid chromatography. For this purpose, principal component analysis was used to examine the behavior of AN and BaP within the chromatographic system. Results showed that AN and BaP chromatographic behavior can be described by three models representing their identification, the quantification of AN and that of BaP, respectively. The factors affecting the obtained models, such as the injection volume, column temperature, flow rate, strength of the mobile phase, and the excitation and emission wavelengths, were examined and optimized by means of design of experiments. Finally, the analytical method was validated, obtaining promising limits of detection and quantification. The developed analytical method was demonstrated to be useful for a sensitive analysis of the target analytes in relatively clean natural water matrices.

**Keywords:** anthracene; benzo[a]pyrene; design of experiments; matrix constituents; principal component analysis; ultra-trace level

## Introduction

Aqueous resources pollution is an issue of current special concern. A number of pollutants can be found in water, including polycyclic aromatic hydrocarbons (PAHs) (Tian *et al.* 2012; Rubio *et al.*, 2013; Rubio-Clemente *et al.* 2014a, 2015). These compounds constitute a group of organic pollutants formed of two or more fused benzene rings containing mainly carbon and hydrogen (Rubio-Clemente *et al.* 2014b; Dos Santos *et al.* 2018). PAHs are ubiquitous compounds in the environment (Alves *et al.* 2017; Segura

*et al.* 2017). They come from anthropogenic sources, such as fossil fuel combustion, metal smelting processes and food smoking, among other human activities; and can be found in the atmosphere, soil, water and even in living beings because of their bioaccumulative properties throughout the food chain (Chizhova *et al.* 2013; Menezes *et al.* 2013; Santos *et al.* 2017).

The main concern related to the presence of PAHs in the environment is ascribed to their toxic potential, such as anthracene (AN), which has exhibited a high acute phototoxicity, and carcinogenic, mutagenic and teratogenic characteristics, like benzo[a]pyrene (BaP) (Rubio-Clemente *et al.* 2014b). In this regard, these compounds are subjected to be monitored by national and international regulations (Directive 2013; Ribeiro *et al.* 2015); therefore, the adoption of an analytical method aiming at their determination is required (Rubio-Clemente *et al.* 2017).

Due to their hydrophobicity, PAHs are poorly soluble in water, being present at ultra-trace levels in the range of ng/L or  $\mu\text{g/L}$ ; fact that limits PAH identification and quantification in aqueous matrices (Rubio-Clemente *et al.* 2017). Recently, several analytical techniques have been reported (Nawaz *et al.* 2014; Petridis *et al.* 2014; Ahmadvand *et al.* 2015; Khodae *et al.* 2016). However, they use previous separation and pre-concentration procedures, being PAH analysis a tedious process. Additionally, separation and pre-concentration techniques might contaminate the sample to be analyzed and produce losses of analytes; especially when multistep procedures are performed (Buczyńska *et al.* 2014; Anumol *et al.* 2015; Boix *et al.* 2015). Consequently, large-volume injection techniques are proposed to be used as alternative procedures (Boix *et al.* 2015). Sample large-volume injection techniques can also be used with reversed-phase high-performance liquid chromatography (RP-HPLC) and gas chromatography (GC), and be combined with fluorescence detector (FLD) or diode array detector, and even with mass spectrometry, finding out accurate and repeatable results within a short period of analysis, without incurring high costs, neither the contamination of the sample nor the loss of the target analytes.

On the other hand, during the development of new analytical methods, one-factor-at-a-time techniques are commonly used. However, the evaluation of several factors influencing the chromatographic system by analyzing the effect of one single parameter at a time can be an expensive task, and valuable information about the analyzed factors can be missed (Trably *et al.* 2004; Hanrahan & Lu 2006, Andrade-Eiroa *et al.* 2010; Rubio-Clemente *et al.* 2017). In this regard, multivariate statistical approaches can overcome these drawbacks by using principal component analysis (PCA) and design of experiments (DOE). PCA is a multivariate analytical tool that can be

used to reduce a set of original variables and to extract a small number of latent factors, also called principal components (PCs), which allow the analysis of the relationships among the observed variables (Machala *et al.* 2001; Golobčanin *et al.* 2004). In turn, DOE can be used to determine the most influential factors within the considered experimental system (Ferreira *et al.* 2007; Dejaegher & Vander 2009, 2011).

Under this scenario, this work is focused on analyzing AN and BaP chromatographic behavior in order to optimize the system for the simultaneous analysis of the analytes of interest at ultra-trace levels in aqueous samples by means of RP-HPLC coupled with FLD and using PCA and DOE under different experimental conditions. In addition, the validation of the optimized experimental chromatographic conditions was carried out using different natural water matrices.

## Materials and methods

### Reagents and solutions

Anthracene (AN, 99 %) and benzo[a]pyrene (BaP, 98 %) analytical certified standards from Dr. Ehrenstorfer (Augsburg, Germany) and gradient-grade acetonitrile purchased from Merck (Darmstadt, Germany) were used without further purification. Deionized water with a resistivity of 18.2 M $\Omega$  and obtained from a Millipore purification system (Bedford, USA) was also employed.

Stock standard solutions of AN and BaP were prepared in acetonitrile at a concentration of 1000 mg/L. The working solutions used during the PCA and DOE were prepared by spiking deionized water with a small aliquot of AN and BaP for obtaining a final concentration of 20  $\mu$ g/L and 2  $\mu$ g/L, respectively.

The calibration curves were built within a range of 75 - 3000 ng/L for AN and of 30 - 3000 ng/L for BaP, using diluted standard solutions and 10 % of acetonitrile (v/v) so that the target PAH adsorption on the walls of the vials is prevented (Martinez *et al.* 2004).

### Analytical methods

AN and BaP were identified and quantified in aqueous samples with an Agilent HPLC system series 1100/1200 (Palo Alto, USA) equipped with a G1322a vacuum degasser unit, a G1311a quaternary pump, a G1321a multiwavelength fluorescence detector, a G1316a column oven, and a G1329a autosampler. The

column was a 5  $\mu\text{m}$  Kinetex core-shell technology C18 (150 x 4.6 mm i.d.) from Phenomenex (Torrance, USA). Unless otherwise mentioned, elution was carried out under isocratic conditions using a mobile phase composed of acetonitrile and deionized water (90:10, v/v), a flow rate of 1 mL/min, a column temperature of 35 °C, a sample injection volume of 100  $\mu\text{L}$ , an emission wavelength of 416 nm and excitation wavelengths of 254 nm from 0 to 3.20 min and 267 nm from 3.21 to 5 min. OpenLab CDS Chemstation software (Agilent, Palo Alto, USA) was used for chromatographic data analysis.

### Statistical analysis

PCA was used to examine the behavior of AN and BaP within the chromatographic system under several experimental conditions. The objective of PCA consists of building  $k$  lineal combinations ( $Y_k$ ) of the considered ( $X_p$ ) variables containing the major variability, being  $a$  the associated coefficients. The lineal combinations can be expressed as Eq. 1-3.

$$Y_1 = a_{11}x_1 + a_{12}X_2 + \dots + a_{1p}X_p \quad (1)$$

$$Y_2 = a_{21}x_1 + a_{22}X_2 + \dots + a_{2p}X_p \quad (2)$$

$$Y_k = a_{k1}x_1 + a_{k2}X_2 + \dots + a_{kp}X_p \quad (3)$$

The first PC ( $Y_1$ ) refers to the lineal combination of the response variables with the maximal variability. The second PC ( $Y_2$ ) is the lineal combination with the second major variability that is not correlated with the first PC. The variability grouped by the following PC ( $Y_k$ ) is decreased up to a non-statistical significant variability.

Additionally, a fractional factorial DOE was employed to find the optimal operating conditions that allow for the simultaneous identification and quantification of the target analytes.

Statgraphics Centurion XVII (Statpoint, Warrenton, USA) was used for the statistical treatment of the experimental data.

## Results and discussion

### Chromatographic behavior using principal component analysis

Taking into account the different factors that influence the separation of compounds in a chromatographic system for an accurate identification and quantification, the strength of the mobile phase, which was evaluated in

terms of acetonitrile percentage, was selected to be analyzed. The injection volume is another parameter to be considered, particularly when determining compounds in the range of ng/L, as it is the case, since the injection of large volumes of samples may derive in the increase of the number of molecules and, therefore, in the increase of the detector analytical response. The excitation and emission wavelengths also play a main role in the quantification of compounds that exhibit an excitation and relaxation behavior under ultraviolet radiation, such as PAHs. Consequently, these two factors were also taken into consideration. Moreover, the flow rate of the mobile phase and the temperature of the column were demonstrated to influence the chromatographic system; that is, the determination of analytes due to the correlation between their elution and the pressure of the system. Thus, six factors affecting the chromatographic system were initially considered, and varied within different operational ranges. In **Table 1** the factors and ranges used are listed. These ranges were selected according to different investigations (Bourdat-Deschamps *et al.* 2007; Lucio-Gutierrez *et al.* 2008; Andrade-Eiroa *et al.* 2010), the chromatographic expertise of the authors and previous experimental runs.

Among the different responses to be measured related to the identification and quantification of organic compounds, the retention time of AN and BaP, as well as the resolution between these two compounds, were selected for identification purposes. Since identification is not enough, in terms of regulation accomplishment, the counts of area and height of AN and BaP were also considered for quantification purposes. In order to find out the optimal experimental conditions for AN and BaP analysis in water at ultra-trace concentrations, PCA was firstly conducted to correlate the different responses selected and, therefore, to obtain those models describing the chromatographic behavior of AN and BaP. However, it is highlighted that prior to any further statistical analysis, normality of the response variables was checked. All the measured variables were verified to follow a normal distribution by using Kolmogorov-Smirnov test, with the exception of AN area and AN height. Consequently, these variables were treated and log transformations of AN area and AN height were obtained for assuring normality assumption.

Subsequently, the response variables were subjected to PCA. It was found that the first three PCs explained more than 97% of the total variability among the seven considered response variables. These results were confirmed by the scree plot represented in **Fig. 1**. The scree plot displays the number of principal components versus their corresponding eigenvalues. This kind of plot indicates in a graphical way the number of PCs to be retained based on the size of their eigenvalues. The ideal pattern is a steep curve that is gradually smoothed up to a straight line, as represented by the blue line in the figure.

**Table 1.** Factors and levels tested for the considered responses.

FACTOR (UNIT)	LEVEL
Injection volume ( $\mu\text{L}$ )	50 - 100
Strength of the mobile phase (%)	70 - 90
Excitation wavelength (nm)	230 - 280
Emission wavelength (nm)	408 - 424
Flow rate (mL/min)	1 - 1.5
Column temperature ( $^{\circ}\text{C}$ )	25 - 35

The number of principal components suggested to be selected corresponds to those components with eigenvalues higher than 1; that is, the components that remain above the horizontal red line. In **Table 2**, the estimated values of the coefficients for each extracted principal component are shown.

From **Table 2**, it can be observed that the coefficients having the main weights (weight  $> 0.5$ ) in PC 1 are the retention times of AN and BaP, and the resolution between AN and BaP; that is, all the response variables related to the elution of the target analytes. In this regard, PC 1 can be representative of the identification index of AN and BaP. Concerning PC 2, the main coefficients are the log area of AN and the log height of AN. In turn, for PC 3, the coefficients representing the area and height of BaP are the highest ones. Therefore, PC 2 and PC 3 might be indicative of the behavior of AN and BaP, respectively, in terms of the peak area and height; that is, PC 2 and PC 3 represent the quantification index of AN and BaP, respectively. PCA tool has also been used for developing retention models in liquid chromatography and standard fingerprints, among other uses (Nikitas *et al.* 2012; Qi *et al.* 2017).

### Optimization using design of experiments

Once the identification and quantification of AN and BaP were described by these indices, corresponding to PC 1, PC 2 and PC 3, the factors statistically significant for each component were examined and the experimental conditions were optimized by using DOE; particularly, a fractional factorial

**Table 2.** Coefficient estimated values contained in the considered principal components.

COEFFICIENT	PC 1	PC 2	PC 3
Retention time of AN	0.5453	0.0422	0.1432
Retention time of BaP	0.5573	0.0511	0.0965
Area of BaP	0.0405	-0.3385	0.6593
Height of BaP	-0.2635	-0.2974	0.5825
Resolution between AN and BaP	0.5323	0.1019	0.1420
Log Area of AN	-0.12	0.6288	0.3016
Log Height of AN	-0.1526	0.6219	0.2916

design due to the high number of factors considered initially. A total of 16 runs plus 5 central points were executed within the selected operating ranges, and analysis of variance (ANOVA) test was performed for each chromatographic index. For a confidence interval of 95 %, it was observed that the block effect was not significant for the chromatographic system under the tested experimental conditions. Concerning PC 1, representing the identification index of AN and BaP, it was evidenced to be influenced negatively by the flow rate and the strength, in terms of acetonitrile content of the mobile phase. This means that as the flow rate is increased, the analytes elute faster and the resolution is, subsequently, decreased. This inversely proportional linear relationship between resolution and flow rate was also observed by Andrade-Eiroa *et al.* (2010) while optimizing the separation of the pairs dibenzo[a,h]anthracene-benzo[g, h, i]perylene and benzo[g, h, i]perylene-indeno[1, 2, 3-cd]pyrene. Similar reasoning can be withdrawn when considering the percentage of organic solvent in the mobile phase. An increase of the mobile phase strength leads to AN and BaP are eluted more rapidly, decreasing their retention times by the stationary phase of the chromatographic column, which results in a decrease of resolution between these two organic compounds. From these two factors, the flow rate was found to exert a higher influence in the identification index of both pollutants, since it has a coefficient associated of  $-2.1767$  in comparison with the coefficient linked to the acetonitrile percentage ( $-0.1774$ ) of the mobile phase.

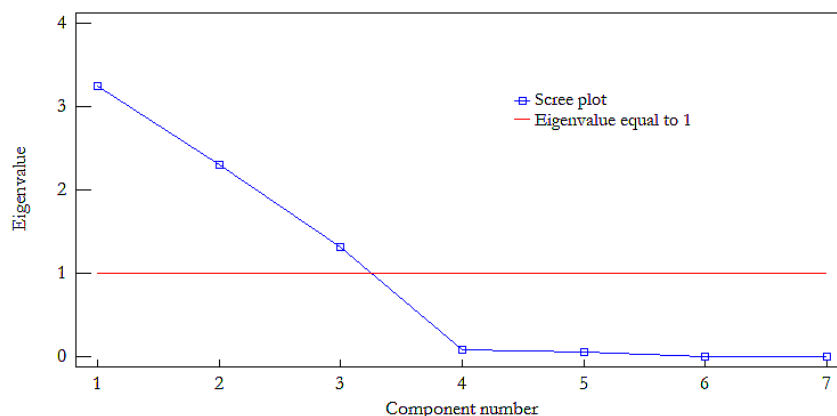


**Figure 1.** Scree plot of the considered responses. Operating conditions: [anthracene]  $0 = 20 \mu\text{g/L}$ ; [benzo[a]pyrene]  $0 = 2 \mu\text{g/L}$ ; injection volume =  $50\text{-}100 \mu\text{L}$ ; strength of the mobile phase =  $70\text{-}90 \%$ ; excitation wavelength =  $230\text{-}280 \text{ nm}$ ; emission wavelength =  $408\text{-}424 \text{ nm}$ ; flow rate =  $1\text{-}1.5 \text{ mL/min}$ ; column temperature =  $25\text{-}35 \text{ }^\circ\text{C}$ .

With respect to PC 2, representing AN quantification index, the excitation wavelength was observed to develop a major role in AN area and height with a weight of  $-0.0542$ . This fact indicates that a decrease of the excitation wavelength results in an increase of the index describing AN quantification and, therefore, an increase of the log area and of the log height of AN. Thus, AN area is increased as well as AN height, improving AN signal detected by the FLD.

Finally, concerning PC 3, it was found that it is statistically affected by the injection volume by a weight of  $0.0286$ . Thus, when the injection volume is increased, the amount of BaP molecules eluting is correspondingly increased with the subsequent augmentation of the area and height of BaP chromatographic peak. Additionally, for a significant level equal to  $0.05$ , the flow rate and the excitation wavelength exerted a negative ( $-2.1898$ ) and positive ( $0.0190$ ) influence, respectively. On the one hand, an increase of the flow rate of the mobile phase leads to a decrease of the area of BaP peak. This can be explained from the fastest elution of the analyte molecules, reducing BaP band and, therefore, decreasing the dimensions of BaP peak. On the other hand, an increase of the excitation wavelength results in an increase of the area and height of BaP. It must be noted that, despite the



non-statistically significance of the excitation wavelength for  $\alpha = 0.05$ , it was considered in the BaP quantification index because its p-value was close to 0.05 (*p-value* = 0.0772).

In **Fig. 2**, the described magnitudes and signs of the selected factors, both the statistically and non-statistically significant ones, for the three PCs are represented through the main effect plots.

The models built describing the three chromatographic indeces representing the chromatographic behavior of AN and BaP under the experimental conditions tested with p-values lower than 0.05, corresponding to 0.0000, 0.0000 and 0.0085, respectively, are described by Eq. 4-6.

$$I_i = 16.9144 - 2.1767 * FR - 0.1774 * S \quad (4)$$

$$I_{ii} = 13.8225 - 0.0542 * EW \quad (5)$$

$$I_{iii} = -4.2625 - 2.1898 * FR + 0.0286 * IV + 0.0190 * EW \quad (6)$$

where  $I_i$  is the AN and BaP identification index,  $I_{ii}$  is the AN quantification index and  $I_{iii}$  is the BaP quantification index. In turn,  $FR$ ,  $S$ ,  $EW$  and  $IV$  represent the flow rate, strength of the mobile phase, excitation wavelength and the injection volume of the sample, respectively.

By optimizing all the principal components obtained simultaneously using multicriteria decision approach, the optimal chromatographic conditions with a desirability of 83.52 % were 1.0 ml/min, 90 %, 100  $\mu$ L, 230 nm, 409 nm and 25  $^{\circ}$ C for the flow rate, acetonitrile content of the mobile phase, injection volume, excitation and emission wavelengths and the column temperature, respectively. However, it is worldwide known that the absorption and fluorescence emission capacities of a substance depend on the substance itself. Additionally, absorption and fluorescence properties of the particularly tested compounds do not follow a linear relationship with the wavelengths used, since their absorption molar coefficients and absorption spectra vary with the single excitation wavelength (Rubio-Clemente *et al.* 2017). For example, in the case of AN, the absorption coefficient at 254 nm is  $\log \epsilon_{254} = 4.9$  in ethanol. For BaP, it has a value of  $\log \epsilon_{254} = 4.6$  in ethanol (Zsila *et al.* 2006; Jones, 1947). BaP absorption spectrum is characterized by several bands of varied intensity; a first one in the range between 245 and 305 nm, higher than 254 nm; and a second one from 320 to 410 nm (Thomas & Burgess, 2007). Moreover, AN absorption spectrum has a distinguished band around 254 nm (Thomas & Burgess, 2007). In this regard, the optimization procedure used in this work is limited when the studied system is influenced by the quadratic effects of the considered factors, as it is the case for these parameters.

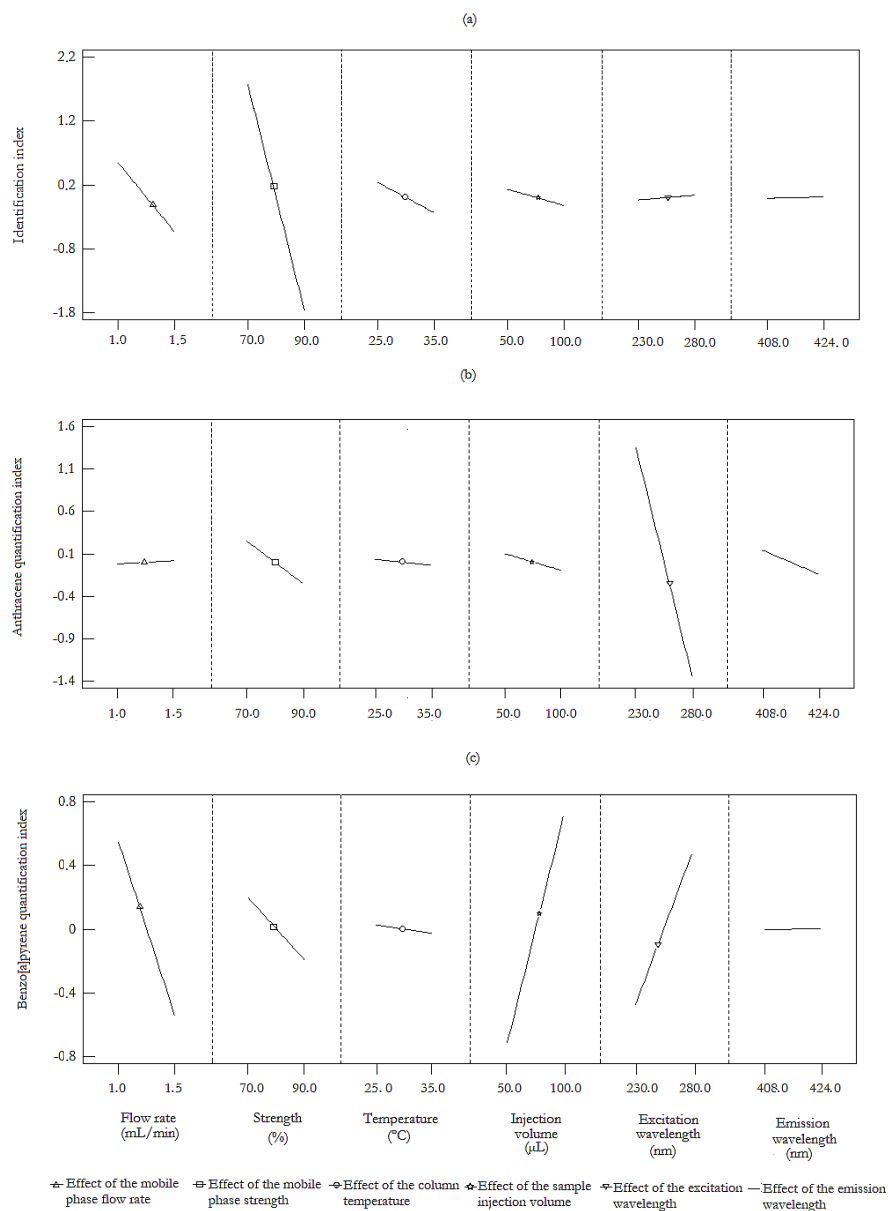


**Figure 2.** Main effect plots for the identification index (a), anthracene quantification index (b) and benzo[a]pyrene quantification index (c). Operating conditions: [anthracene]<sub>0</sub> = 20 μg/L; [benzo[a]pyrene]<sub>0</sub> = 2 μg/L; injection volume = 50-100 μL; strength of the mobile phase = 70-90 %; excitation wavelength = 230-280 nm; emission wavelength = 408-424 nm; flow rate = 1-1.5 mL/min; column temperature = 25-35 °C.

Therefore, a minacious study was subsequently performed to find out the excitation and emission optimal wavelengths of AN and BaP. It was found that 416 nm was the optimal emission wavelength within the selected initial range for both of the examined analytes. The excitation wavelength was fixed at 254 nm and 267 nm during AN and BaP elution time, respectively.

On the other hand, taking into account that the column temperature was not statistically significant for the models built and considering that the analysis time can be reduced by augmenting the temperature of the column oven, reducing also the pressures in the system and improving the column efficiency, as reported by [Andrade-Eiroa et al. \(2010\)](#), the optimal column temperature was kept at 35 °C.

### Validation

Under the optimized conditions, the proposed analytical method was validated. Good linearity values and low limits of quantification and detection of 75 and 5.54 ng/L for AN, and 30 and 4.26 ng/L for BaP were obtained. Additionally, intraday and interday precisions lower than 2 and 11 %, respectively, were found for the high, medium and low levels tested. Accuracy was also verified and relative standard deviations (RSD) lower than 10 % were evidenced. Furthermore, the analysis of AN and BaP in different matrices of real natural water gave satisfactory recoveries (RSD < 13 %).

### Conclusions

The results of the present study indicated that the chromatographic behavior of the selected PAHs under the experimental conditions tested may be explained by PCA using three indices describing the elution of AN and BaP, the peak shape of AN and that of BaP, representing the former one and the latter ones the identification and the quantification of the target compounds, respectively. It was demonstrated that the identification index of the target compounds under the experimental domain studied here was defined by the flow rate and the strength of the mobile phase. Concerning the AN quantification index, the excitation wavelength was found to develop a main role. Finally, the BaP quantification index, as expected, was also influenced by the excitation wavelength; however, the injection volume and the flow rate were observed to exert also a main function.

The optimal operating conditions found using DOE that maximizing the indices referred above were 1 mL/min, 90 %, 35 °C, 100  $\mu$ L, and 416 nm for the flow rate, acetonitrile content of the mobile phase, column temperature, injection volume and the emission wavelength, respectively. The optimal excitation wavelengths were 254 nm and 267 nm for AN and BaP. The developed and validated method showed to be suitable for the identification

and quantification of AN and BaP at ultra-trace levels in relatively clean natural water by direct injection in only 5 min of analysis.

### Acknowledgements

This work was supported by the Colombian Institute of Science and Technology (COLCIENCIAS) and the Research Vice-rectory of Universidad de Antioquia.

### Conflicts of interest

The authors state that their sole interest in the results of this research is scientific.

### References

Ahmadvand M, Sereshti H, Parastar H. Chemometric-based determination of polycyclic aromatic hydrocarbons in aqueous samples using ultrasound-assisted emulsification microextraction combined to gas chromatography-mass spectrometry, *Journal of Chromatography A*, 1413: 117–126, 2015.

doi: [10.1016/j.chroma.2015.08.026](https://doi.org/10.1016/j.chroma.2015.08.026)

Alves CA, Vicente AM, Custódio D, Cerqueira M, Nunes T, Pio C, Lucarelli F, Calzolari G, Nava S, Diapouli E, Eleftheriadis K, Querol X, Musa BA. Polycyclic aromatic hydrocarbons and their derivatives (nitro-PAHs, oxygenated PAHs, and azaarenes) in PM 2.5 from Southern European cities, *Science of the Total Environment*, 595: 494-504, 2017.

doi: [10.1016/j.scitotenv.2017.03.256](https://doi.org/10.1016/j.scitotenv.2017.03.256)

Andrade-Eiroa A, Dievert P, Dagaut P. Improved optimization of polycyclic aromatic hydrocarbons (PAHs) mixtures resolution in reversed-phase high-performance liquid chromatography by using factorial design and response surface methodology, *Talanta*, 81(1-2): 265-274, 2010.

doi: [10.1016/j.talanta.2009.11.068](https://doi.org/10.1016/j.talanta.2009.11.068)

Anumol T, Wu S, Marques M, Daniels KD, Snyder SA. Rapid direct injection LC-MS/MS method for analysis of prioritized indicator compounds in wastewater effluent, *Environmental Science: Water Research & Technology*, 2015(1): 632-643, 2015.

doi: [10.1039/c5ew00080g](https://doi.org/10.1039/c5ew00080g)

Boix C, Ibáñez M, Sancho JV, Rambla J, Aranda JL, Ballester S, Hernández F. Fast determination of 40 drugs in water using large volume direct injection liquid chromatography-tandem mass spectrometry, *Talanta*, 131: 719-727, 2015.

doi: [10.1016/j.talanta.2014.08.005](https://doi.org/10.1016/j.talanta.2014.08.005)

Bourdat-Deschamps M, Daudin JJ, Barriuso E. An experimental design approach to optimise the determination of polycyclic aromatic hydrocarbons from rainfall water using stir bar sorptive extraction and high performance liquid chromatography-fluorescence detection, *Journal of Chromatography A*, 1167(2): 143-153, 2007.

doi: [10.1016/j.chroma.2007.08.025](https://doi.org/10.1016/j.chroma.2007.08.025)

Buczyńska AJ, Geypens B, van Grieken R, de Wael K. Large-volume injection combined with gas chromatography/isotope ratio mass spectrometry for the analysis of polycyclic aromatic hydrocarbons, *Rapid Communications in Mass Spectrometry*, 28: 200-208, 2014.

doi: [10.1002/rcm.6769](https://doi.org/10.1002/rcm.6769)

Chizhova T, Hayakawa K, Tishchenko P, Nakase H, Koudryashova Y. Distribution of PAHs in the northwestern part of the Japan Sea, *Deep-Sea Research Part II: Tropical Studies in Oceanography*, 86-87: 19-24, 2013.

doi: [10.1016/j.dsr2.2012.07.042](https://doi.org/10.1016/j.dsr2.2012.07.042)

Dejaegher B, Vander Y. The use of experimental design in separation science, *Acta Chromatographica*, 21: 161-201, 2009.

doi: [10.1556/achrom.21.2009.2.1](https://doi.org/10.1556/achrom.21.2009.2.1)

Dejaegher B, Vander Y. Experimental designs and their recent advances in set-up, data interpretation and analytical applications, *Journal of Pharmaceutical and Biomedical Analysis*, 56(2): 141-158, 2011.

doi: [10.1016/j.jpba.2011.04.023](https://doi.org/10.1016/j.jpba.2011.04.023)

Directive 2013. Directive 2013/39/EU of the European parliament and of the council of 12 August 2013 amending directives 2000/60/EC and 2008/105/EC as regards priority substances in the field of water policy, *Official Journal of the European Union L*, 226: 1-17.

Retrieved from: <https://eur-lex.europa.eu/legal-content/EN/ALL/?uri=CELEX%3A32013L0039>

Dos Santos IF, Ferreira SLC, Domínguez C, Bayona JM. Analytical strategies for determining the sources and ecotoxicological risk of PAHs in river sediment, *Microchemical Journal*, 137: 90-97, 2018.

doi: [10.1016/j.microc.2017.09.025](https://doi.org/10.1016/j.microc.2017.09.025)

Ferreira SLC, Bruns RE, da Silva EGP, dos Santos WLN, Quintella CM, David JM, de Andrade JB, Breikreitz MC, Jardim ICSF, Neto BB. Statistical designs and response surface techniques for the optimization of chromatographic systems, *Journal of Chromatography A*, 1158: 2-14, 2007.

doi: [10.1016/j.chroma.2007.03.051](https://doi.org/10.1016/j.chroma.2007.03.051)

Golobočanin DD, Škrbić BD, Miljević NR. Principal component analysis for soil contamination with PAHs, *Chemometrics and Intelligent Laboratory Systems*, 72(2): 219-223, 2004.

doi: [10.1016/j.chemolab.2004.01.017](https://doi.org/10.1016/j.chemolab.2004.01.017)

Hanrahan G, Lu K. Application of factorial and response surface methodology in modern experimental design and optimization, *Critical Reviews in Analytical Chemistry*, 36(3-4): 141-151, 2006.

doi: [10.1080/10408340600969478](https://doi.org/10.1080/10408340600969478)

Jones RN. The ultraviolet absorption spectra of anthracene derivatives, *Chemical Reviews*, 41(2): 353-371, 1947.

doi: [10.1021/cr60129a013](https://doi.org/10.1021/cr60129a013)

Khodae N, Mehdinia A, Esfandiarnjad R, Jabbari A. Ultra trace analysis of PAHs by designing simple injection of large amounts of analytes through the sample reconcentration on SPME fiber after magnetic solid phase extraction, *Talanta*, 147: 59-62, 2016.

doi: [10.1016/j.talanta.2015.09.025](https://doi.org/10.1016/j.talanta.2015.09.025)

Lucio-Gutiérrez JR, Salazar-Cavazos ML, Waksman NH, Castro-Ríos R. Solid-phase microextraction followed by high-performance liquid chromatography with fluorimetric and UV detection for the determination of polycyclic aromatic hydrocarbons in water, *Analytical Letters*, 41(1):119-136, 2008.

doi: [10.1080/00032710701746758](https://doi.org/10.1080/00032710701746758)

Machala M, Dusek L, Hilscherova K, Kubinova R, Jurajda P, Neca J, Ulrich R, Gelnar M, Studnicková Z, Holoubek, I. Determination and multivariate statistical analysis of biochemical responses to environmental contaminants in feral freshwater fish *Leuciscus cephalus* L, *Environmental Toxicology and Chemistry*, 20(5): 1141-1148, 2001.

doi: [10.1002/etc.5620200528](https://doi.org/10.1002/etc.5620200528)

Martinez E, Gros M, Lacorte S, Barceló D. Simplified procedures for the analysis of polycyclic aromatic hydrocarbons in water, sediments and mussels, *Journal of Chromatography A*, 1047(2): 181-188, 2004.

doi: [10.1016/s0021-9673\(04\)01100-8](https://doi.org/10.1016/s0021-9673(04)01100-8)

Menezes HC, Paiva MJ, Santos RR, Sousa LP, Resende SF, Saturnino JA, Paulo BP, Cardeal ZL. A sensitive GC/MS method using cold fiber SPME to determine polycyclic aromatic hydrocarbons in spring water, *Microchemical Journal*, 110: 209-214, 2013.

doi: [10.1016/j.microc.2013.03.010](https://doi.org/10.1016/j.microc.2013.03.010)

Nawaz MS, Ferdousi FK, Rahman MA, Alam AM. Reversed phase SPE and GC-MS study of polycyclic aromatic hydrocarbons in water samples from the river Buriganga, Bangladesh, *International Scholarly Research Notices*, 2014: 1-9, 2014.

doi: [10.1155/2014/234092](https://doi.org/10.1155/2014/234092)

Nikitas P, Pappa-Louisi A, Tsoumachides S, Jouyban A. A principal component analysis approach for developing retention models in liquid chromatography, *Journal of Chromatography A*, 1251: 134-140, 2012.

doi: [10.1016/j.chroma.2012.06.049](https://doi.org/10.1016/j.chroma.2012.06.049)

Petridis NP, Sakkas VA, Albanis TA. Chemometric optimization of dispersive suspended microextraction followed by gas chromatography-mass spectrometry for the determination of polycyclic aromatic hydrocarbons in natural water, *Journal of Chromatography A*, 1355: 46-52, 2014.

doi: [10.1016/j.chroma.2014.06.019](https://doi.org/10.1016/j.chroma.2014.06.019)

Qi X, Zhu L, Wang C, Zhang H, Wang L, Qian H. Development of standard fingerprints of naked oats using chromatography combined with principal component analysis and cluster analysis, *Journal of Cereal Science*, 74: 224-230, 2017.

doi: [10.1016/j.jcs.2017.02.009](https://doi.org/10.1016/j.jcs.2017.02.009)

Ribeiro AR, Nunes OC, Pereira MFR, Silva AMT. An overview on the advanced oxidation processes applied for the treatment of water pollutants defined in the recently launched Directive 2013/39/EU, *Environment International*, 75: 35-51, 2015.

doi: [10.1016/j.envint.2014.10.027](https://doi.org/10.1016/j.envint.2014.10.027)

Rubio A, Chica EL, Peñuela GA. Wastewater treatment processes for the removal of emerging organic pollutants, *Ambiente & Agua-An Interdisciplinary Journal of Applied Science*, 8(3): 93-103, 2013.

doi: [10.4136/ambi-agua.1176](https://doi.org/10.4136/ambi-agua.1176) 645

Rubio-Clemente A, Chica E, Peñuela GA. Application of Fenton process for treating petrochemical wastewater, *Ingeniería y Competitividad*, 16(2): 211-223, 2014a.

Rubio-Clemente A, Chica E, Peñuela GA. Petrochemical wastewater treatment by photo-Fenton process, *Water, Air, & Soil Pollution*, 226: 1-18, 2015.

doi: [10.1007/s11270-015-2321-x](https://doi.org/10.1007/s11270-015-2321-x)

Rubio-Clemente A, Chica E, Peñuela G. Rapid determination of anthracene and benzo(a)pyrene by high-performance liquid chromatography with fluorescence detection, *Analytical Letters*, 50(8): 1229-1247, 2017.

doi: [10.1080/00032719.2016.1225304](https://doi.org/10.1080/00032719.2016.1225304)

Rubio-Clemente A, Torres-Palma RA, Peñuela GA. Removal of polycyclic aromatic hydrocarbons in aqueous environment by chemical treatments: A review, *Science of the Total Environment*, 478: 201-225, 2014b.

doi: [10.1016/j.scitotenv.2013.12.126](https://doi.org/10.1016/j.scitotenv.2013.12.126)

Santos LO, dos Anjos JP, Ferreira SL, de Andrade JB. Simultaneous determination of PAHS, nitro-PAHS and quinones in surface and groundwater samples using SDME/GC-MS, *Microchemical Journal*, 133: 431-440, 2017.

doi: [10.1016/j.microc.2017.04.012](https://doi.org/10.1016/j.microc.2017.04.012)

Segura A, Hernández-Sánchez V, Marqués S, Molina L. Insights in the regulation of the degradation of PAHs in *Novosphingobium* sp. HR1a and utilization of this regulatory system as a tool for the detection of PAHs, *Science of the Total Environment*, 590-591: 381-393, 2017.

doi: [10.1016/j.scitotenv.2017.02.180](https://doi.org/10.1016/j.scitotenv.2017.02.180)

Thomas O, Burgess C. UV-visible spectrophotometry of water and wastewater (Vol. 27). Elsevier Science, The Netherlands, 2007.

Tian W, Bai J, Liu K, Sun H, Zhao Y. Occurrence and removal of polycyclic aromatic hydrocarbons in the wastewater treatment process, *Ecotoxicology and Environmental Safety*, 82: 1-7, 2012.

doi: [10.1016/j.ecoenv.2012.04.020](https://doi.org/10.1016/j.ecoenv.2012.04.020)

Trably E, Delgènes N, Patureau D, Delgènes JP. Statistical tools for the optimization of a highly reproducible method for the analysis of polycyclic aromatic hydrocarbons in sludge samples, *International Journal of Environmental Analytical Chemistry*, 84(13): 995-1008, 2004.

doi: [10.1080/03067310412331298412](https://doi.org/10.1080/03067310412331298412)

Zsila F, Matsunaga H, Bikádi Z, Haginaka J. Multiple ligand-binding properties of the lipocalin member chicken  $\alpha$  1-acid glycoprotein studied by circular dichroism and electronic absorption spectroscopy: The essential role of the conserved tryptophan residue, *Biochimica et Biophysica Acta (BBA)-General Subjects*, 1760(8): 1248-1273, 2006.

doi: [10.1016/j.bbagen.2006.04.006](https://doi.org/10.1016/j.bbagen.2006.04.006)



### **Análisis de inyección directa en gran volumen de hidrocarburos aromáticos policíclicos en agua**

**Resumen.** Los hidrocarburos aromáticos policíclicos (HAPs) causan problemas en la salud de los seres humanos y seres vivos, por lo que se requiere un monitoreo de estos compuestos en matrices ambientales. Este trabajo propone un método analítico para analizar el antraceno (AN) y el benzopireno (BAP), los hidrocarburos más representativos en concentraciones de ultra trazas en el agua, empleando inyección directa en grandes volúmenes en muestras acopladas a la fase inversa con cromatografía líquida de alto rendimiento. Por tal razón, se utilizó el análisis de componentes principales para examinar el comportamiento de AN y BAP en el sistema cromatográfico. Los resultados mostraron que el comportamiento cromatográfico de AN y BAP podría describirse por medio de tres modelos que representan su identificación, la cuantificación de AN y de BAP, respectivamente. Se examinaron los factores que afectan a los modelos obtenidos, como el volumen de inyección, la temperatura de la columna, la tasa de flujo, la fuerza de la fase móvil, y las longitudes de las ondas de excitación y emisión, y se optimizaron mediante el diseño de experimentos. Finalmente, se validó el método analítico, obteniendo límites de detección y cuantificación. Se demostró que el método analítico desarrollado fue útil para el análisis sensible de los analitos en matrices de agua natural relativamente limpia.

**Palabras clave:** antraceno; benzopireno; diseño de experimentos; componentes matriciales; análisis de componentes principales; ultra trazas.

### **Análise de injeção direta de grande volume de hidrocarbonos aromáticos policíclicos em água**

**Resumo.** Devido aos riscos para a saúde tanto para humanos como para os seres vivos em geral causados pelos hidrocarbonos aromáticos policíclicos (HAPs), o monitoramento de estes compostos em matrizes ambientais é prioritário. Este trabalho propõe um método analítico para analisar antraceno (AN) e benzo[*a*]pireno (BaP), dois dos hidrocarbonos mais representativos, em concentrações de ultra traços em água, empregando injeções diretas de grandes volumes de amostra acoplada a cromatografia líquida de alta eficiência em fase reversa. Usando Análises por Componentes Principais e desenho experimental, foram avaliados os efeitos de diversos fatores que afetam o sistema cromatográfico, tais como o volume de injeção, a temperatura da coluna, fluxo, força da fase móvel e comprimentos de onda de excitação e emissão. Os resultados demonstraram que o comportamento cromatográfico de AN e BaP pode ser descrito por meio de três que representam sua identificação, quantificação de AN e de BaP, respectivamente. Os resultados mostraram que o comportamento cromatográfico de NA e BAP poderia ser descrito por meio de três modelos que representam sua identificação, a quantificação de NA e de BAP, respectivamente. Examinaram-se os fatores que afetam aos modelos obtidos, como o volume de injeção, a temperatura da coluna, a taxa de fluxo, a força da fase móvel, e as longitudes das ondas de excitação e emissão, e se otimizaram mediante o desenho experimental. Finalmente, se validou o método analítico, obtendo os limites de detecção e quantificação. O método analítico desenvolvido demonstrou ser útil para uma análise sensível para os compostos de interesse em matrizes de água natural relativamente limpas.

**Palavras-chave:** antraceno; benzopireno; desenho experimental; componentes de matriz; análise de componentes principais; ultra traços.

**Ainhoa Rubio-Clemente**

She is an Environmental Engineer by University of Salamanca. She has a MSc. and she is a junior researcher. She has research experiences in the field of water pollution decontamination and drinking water production using conventional and advanced treatment processes. Additionally, she has been involved in developing several analytical methods.

**Edwin L. Chica**

He is a Mechanical Engineer by University of Antioquia. Currently he is a MSc. PhD. associate professor and researcher at University of Antioquia, heading the Research Group 'Energía Alternativa'. He has research experiences in the field of renewable energy production and water decontamination and purification using conventional and advanced treatment processes, regarding design, scaling and performance purposes.

**Gustavo A. Peñuela**

He is a Chemist by the National University. He is the director of the Research Group 'Diagnóstico y Control de la Contaminación' (GDCON) at University of Antioquia. He has large experience in the field of water, soil and air pollution. Additionally, he has conducted a number of researches in developing analytical methods for several purposes.



**Paper****Sensitive spectrophotometric determination of hydrogen peroxide in aqueous samples from advanced oxidation processes: Evaluation of possible interferences****Journal**

Scope: AFINIDAD accepts review articles, original papers (experimental reports as well as theoretical studies) and short communications on all aspects of chemical engineering, process engineering, chemistry and biotechnology.

**Highlights**

- A simple and sensitive analytical method for residual H<sub>2</sub>O<sub>2</sub> determination in water samples is developed.
- The achieved limit of quantification is 2.94x10<sup>-3</sup> mM H<sub>2</sub>O<sub>2</sub>.
- The method is validated using real natural water.
- A study on the interfering substances present in the water matrix is conducted.
- The method is applied for AN and BaP degradation by the UV-C/H<sub>2</sub>O<sub>2</sub> system.



# Sensitive spectrophotometric determination of hydrogen peroxide in aqueous samples from advanced oxidation processes: Evaluation of possible interferences

A. Rubio-Clemente<sup>a, b\*</sup>, A. Cardona<sup>b</sup>, E. Chica<sup>c</sup> and G.A. Peñuela<sup>b</sup>

<sup>a</sup>Facultad de Ciencias de la Salud, Universidad Católica San Antonio UCAM, Avenida de los Jerónimos, 135, C.P. 30107, Guadalupe-Murcia, España. <sup>b</sup>Grupo GDCON, Facultad de Ingeniería, Sede de Investigaciones Universitarias (SIU), Universidad de Antioquia UdeA, A.A. 1226, Calle 70, No. 52-21, Medellín, Colombia. <sup>c</sup>Departamento de Ingeniería Mecánica, Facultad de Ingeniería, Universidad de Antioquia UdeA, A.A. 1226, Calle 70, No. 52-21, Medellín, Colombia.

*Determinación espectrofotométrica sensible del peróxido de hidrógeno en muestras de agua procedentes de procesos de oxidación avanzada: Evaluación de posibles interferencias*

*Determinació espectrofotomètrica sensible del peròxid d'hidrogen en mostres d'aigua procedents de processos d'oxidació avançada: Avaluació de possibles interferències*

RECEIVED: 11 NOVEMBER 2016; REVISED: 6 DECEMBER 2016; ACCEPTED: 9 JANUARY 2017

## SUMMARY

Hydrogen peroxide ( $H_2O_2$ ) determination in real water samples was carried out in a simple and sensitive way. The resulting optimal operating conditions from a  $2^3$  full factorial experimental design were 450 nm, 50 mm and  $6 \times 10^{-3}$  M for the absorption wavelength, the quartz cell path length and the final concentration of the ammonium monovanadate solution, respectively; allowing the quantification of  $H_2O_2$  up to  $2.94 \times 10^{-3}$  mM. The proposed analytical method was validated and the effect of the background matrix was investigated, obtaining a selective method. Additionally, the developed analytical method was applied for studying the evolution of  $H_2O_2$  in the decontamination of water containing  $6.73 \times 10^{-5}$  mM of anthracene and  $1.19 \times 10^{-5}$  mM of benzo[a]pyrene using the UV/ $H_2O_2$  system. It was found that the optimal  $H_2O_2$  level enabling about 45% of mineralisation and a removal of the target polycyclic aromatic hydrocarbons higher than 99% was  $2.94 \times 10^{-1}$  mM, remaining approximately  $1.47 \times 10^{-1}$  mM of  $H_2O_2$  after 90 min of treatment.

**Keywords:** Advanced oxidation process; ammonium monovanadate; matrix background; residual hydrogen peroxide; spectrophotometry

## RESUMEN

La determinación de peróxido de hidrógeno ( $H_2O_2$ ) en muestras de agua real se llevó a cabo de una manera sencilla y sensible. Las condiciones óptimas de funcionamiento resultantes de un diseño experimental factorial completo fueron 450 nm, 50 mm y  $6 \times 10^{-3}$  M de longitud de onda de absorción, longitud de trayectoria de la celda de cuarzo y concentración final de la solución de monovanadato de amonio, respectivamente; permitiendo la cuantificación de  $2.94 \times 10^{-3}$  mM de  $H_2O_2$ . Se validó el método analítico propuesto y se investigó el efecto de la matriz obteniendo un método selectivo. Además, se aplicó el método analítico desarrollado para estudiar la evolución de  $H_2O_2$  en la descontaminación de agua que contenía  $6,73 \times 10^{-5}$  mM de antraceno y  $1,19 \times 10^{-5}$  mM de benzo[a]pireno utilizando el sistema UV/ $H_2O_2$ . Se encontró que el nivel óptimo de  $H_2O_2$  que permitía cerca del 45% de mineralización y una eliminación de los hidrocarburos aromáticos policíclicos objeto de estudio superior al 99% fue de  $2,94 \times 10^{-1}$  mM, perma-

\*Corresponding author: [ainhoa.rubioc@udea.edu.co](mailto:ainhoa.rubioc@udea.edu.co)

neciendo aproximadamente  $1,47 \times 10^{-1}$  mM de  $H_2O_2$  después de 90 min de tratamiento.

**Palabras clave:** Proceso de oxidación avanzada; monovanadato de amonio; constituyentes de la matriz; peróxido de hidrógeno residual; espectrofotometría.

## RESUM

La determinació de peròxid de hidrogen ( $H_2O_2$ ) en mostres autèntiques d'aigua va ser realitzada de forma simple i senzilla. Les condicions de treball òptimes resultants d'un disseny experimental factorial complet  $2^3$  van ser de 450 nm, 50 mm i  $6 \times 10^{-3}$  M per la longitud de onda d'absorció, la longitud de la trajectòria de les cubetes de quars i la concentració final de la solució de monovanadato de amoni, respectivament; això va permetre una quantificació de  $2,94 \times 10^{-3}$  mM de  $H_2O_2$ . Es va avaluar el mètode d'anàlisi proposat i es va investigar l'efecte de la matriu de fons, obtenint un mètode selectiu. Addicionalment, el mètode analític desenvolupat es va aplicar per estudiar la evolució del  $H_2O_2$  en la descontaminació del aigua que contenia  $6,73 \times 10^{-5}$  mM de antracens i  $1,19 \times 10^{-5}$  mM de benzo(a)pireno, fent servir el sistema UV/ $H_2O_2$ . Es va descobrir que el nivell òptim de  $H_2O_2$  capaç de una mineralització del 45% i de una eliminació dels hidrocarburs aromàtics policíclics major del 99% era de  $2,94 \times 10^{-1}$  mM, quan era aproximadament de  $1,47 \times 10^{-1}$  mM de  $H_2O_2$  després de 90 minuts de tractament.

**Paraules clau:** Procés de oxidació avançat; monovanadato de amoni; matriu de fons; peròxid de hidrogen residual; espectrofotometria

## INTRODUCTION

Hydrogen peroxide ( $H_2O_2$ ) is a manufactured product but it can be naturally found at low concentrations in atmospheric, soil and aqueous ecosystems<sup>1,2</sup>.  $H_2O_2$  is widely used for water treatment purposes. With an oxidation potential of 1.763 V<sup>3</sup>,  $H_2O_2$  is known to be a powerful oxidant<sup>4</sup>, able to oxidise organic pollutants. However, the greater relevance of using  $H_2O_2$  for water treatment mainly resides in its ability to undergo photolysis in contact with UV radiation, producing hydroxyl radicals ( $HO^\bullet$ )<sup>5</sup>, whose standard electrode potential is higher than that of  $H_2O_2$  ( $E^\circ=2.80$  V)<sup>6</sup> and, subsequently, is able to remove a larger amount of organic pollutants<sup>7</sup>.

The photolytic ability of  $H_2O_2$  is exploited by several advanced oxidation processes (AOPs), such as UV/ $H_2O_2$ , UV/ $O_3/H_2O_2$ , UV/ $US/H_2O_2$  and photo-Fenton (UV/ $Fe^{2+}/H_2O_2$ ) systems, among other processes.

Recently, a great number of works reporting the efficiency of AOPs for degrading persistent and recalcitrant toxics has been published<sup>7-10</sup>. Due to the demonstrated effectiveness of using  $H_2O_2$  in both photolytic and non-photolytic AOPs, its determination is of spe-

cial interest for efficient water decontamination. Additionally, considering that an excess of  $H_2O_2$  is involved in  $HO^\bullet$  scavenging processes, and because of it is a costly reagent<sup>11</sup>, the analysis of  $H_2O_2$  is even more significant when it is added in a continuous way in order to know when a new addition of  $H_2O_2$  is required for the oxidation of pollutants to continue.

On the other hand, there are other AOPs where  $H_2O_2$  is generated. This is the case of heterogeneous photo-catalysis processes using semiconductors such as  $TiO_2$ . When  $TiO_2$  is illuminated and a photon with energy above its bandgap energy is absorbed, a pair hole ( $h^+$ )–electron ( $e^-$ ) is formed. Both the  $h^+$  and  $e^-$  can oxidise and reduce  $H_2O$  and  $O_2$ , respectively, resulting in the production of  $H_2O_2$ . The generated  $H_2O_2$  acts to prevent the recombination of  $h^+$  and  $e^-$ , leading to a higher decontamination. However, although the generation of  $H_2O_2$  has a positive effect, residual  $H_2O_2$  can also pose a risk for the living beings in the receptor systems of the AOP effluent.  $H_2O_2$  is a widely recognised biocide, since it may interact with organism biomolecules, causing their oxidation<sup>12</sup>. Therefore, the quantification of  $H_2O_2$  is essential for both water treatment and ecosystem conservation purposes.

Several techniques for  $H_2O_2$  determination in solid, gas and aqueous samples have been reported<sup>2,13-16</sup>. For  $H_2O_2$  analysis in water, one of the most applied methods is the permanganate titration. However, it is interfered by  $Fe^{2+}$  ions, which are catalysing agents in Fenton and photo-Fenton systems, due to the complexes formed between these ions and permanganate<sup>14</sup>. In turn, the use of enzyme-catalysed reactions can be a quite sensitivity method; nevertheless, the use of enzyme requires strict experimental conditions, limiting the application of this technology. Under this scenario, Pupo Nogueira and co-workers<sup>14</sup> proposed a colorimetric method based on the formation of complexes between  $H_2O_2$  and ammonium monovanadate in acidic medium. Even though this method can be applied for a wide range of water samples, it does not allow analysing  $H_2O_2$  at residual levels, since its limit of quantification is  $2.5 \times 10^{-2}$  mM<sup>14</sup>. In this sense, the current work aims at extending this limit of quantification. Additionally, the interfering substances commonly found in water matrices, such as  $Fe^{3+}$ ,  $Fe^{2+}$ ,  $Cl^-$ ,  $NO_3^-$ ,  $PO_4^{3-}$ ,  $NH_4^+$ ,  $Mg^{2+}$ ,  $Na^+$ ,  $Mn^{2+}$ ,  $F^-$ ,  $K^+$ ,  $CO_3^{2-}$  and  $Ca^{2+}$ , were evaluated. Furthermore, the proposed analytical method was validated and applied to study the  $H_2O_2$  evolution in real natural water treated using the UV/ $H_2O_2$  system.

## MATERIALS AND METHODS

### Reagents and chemicals

All reagents were analytical grade and the solutions were prepared in deionised water. The used reagents were hydrogen peroxide, 30% w/w ( $H_2O_2$ , J.T. Baker); acetonitrile, gradient grade (Merck); orthophosphoric acid, 85% ( $H_3PO_4$ , Carlo Erba); fuming hydrochloric acid, 37% (HCl, Merck); ammonium hydroxide, 28-30% ( $NH_4OH$ , Mallinckrodt); nitric acid, 65% ( $HNO_3$ ,



Merck); ammonium monovanadate, 99.9% ( $\text{NH}_4\text{VO}_3$ , Merck); sulfuric acid, 95-97% ( $\text{H}_2\text{SO}_4$ , Merck); calcium carbonate ( $\text{CaCO}_3$ , Carlo Erba); sodium carbonate ( $\text{Na}_2\text{CO}_3$ , Merck); ammonium sulfate ( $(\text{NH}_4)_2\text{SO}_4$ , Mallinckrodt); iron (II) sulfate heptahydrate ( $\text{Fe}_2\text{SO}_4 \cdot 7\text{H}_2\text{O}$ , Sigma-Aldrich); iron (III) chloride hexahydrate ( $\text{FeCl}_3 \cdot 6\text{H}_2\text{O}$ , Panreac); standard solution of iron (III) nitrate ( $\text{Fe}(\text{NO}_3)_3$ , Merck); manganese (II) sulfate monohydrate ( $\text{MnSO}_4 \cdot \text{H}_2\text{O}$ , Merck); anthracene 99% and benzo[a]pyrene 96% (Alfa Aesar).

### Solutions

Standard stock solutions of  $\text{H}_2\text{O}_2$  were prepared by diluting suitable amounts of  $\text{H}_2\text{O}_2$ .  $\text{H}_2\text{O}_2$  working solutions were prepared by diluting the stock solutions of  $\text{H}_2\text{O}_2$  and a calibration curve was built from  $2.94 \times 10^{-3}$  to  $4.41 \times 10^{-1}$  mM. Additionally, a 0.06 M  $\text{NH}_4\text{VO}_3$  stock solution was prepared by using a 0.36 M  $\text{H}_2\text{SO}_4$  stock solution and completing with deionised water.

### $\text{H}_2\text{O}_2$ analysis procedure and apparatus

The optimal procedure for the determination of  $\text{H}_2\text{O}_2$  in water samples consisted of adding 40 mL of the sample to be analysed and 5 mL of the  $\text{NH}_4\text{VO}_3$  stock solution in a 50 mL flask. Deionised water was added to the mark and the mixture was transferred to the quartz cell. The control standards of this procedure corresponding to the low, medium and high levels of the calibration curve were  $2.94 \times 10^{-3}$ ,  $5.88 \times 10^{-2}$  and  $4.41 \times 10^{-1}$  mM, respectively. In addition, a reagent blank was performed by adding 5 mL of the  $\text{NH}_4\text{VO}_3$  stock solution into a 50 mL volumetric flask and diluting with deionised water to the mark. With this reagent blank, the baseline of the spectrophotometer was built.

Spectrophotometric studies were carried out using a UV-Vis spectrophotometer Evolution 300 (Thermo Scientific) and a quartz cell of 50 mm optical path length (Macherey-Nagel), unless indicated otherwise. Measures of absorbance were taken by triplicate using a Xenon lamp at a wavelength of 450 nm, unless specified otherwise. For the analysis of anthracene and benzo[a]pyrene, an Agilent RP-HPLC system (series 1100/1200) with a fluorescence detector was used under the operating conditions specified elsewhere<sup>17</sup>. Total organic carbon was measured using an Apollo 9000 series total organic carbon analyser (Teledyne Tekmar).

### Experimental design and irradiation tests

In order to determine the most favourable conditions for  $\text{H}_2\text{O}_2$  quantification, a  $2^3$  full factorial experimental design was used. The influence of the final concentration of  $\text{NH}_4\text{VO}_3$  reacting with  $\text{H}_2\text{O}_2$  in the sample, the absorption wavelength and the quartz cell path length were studied at two main levels. This experimental design resulted in 8 runs, executed in a randomised order. The considered responses were the absorbance maximisation of the calibration curve levels at  $2.94 \times 10^{-3}$ ,  $5.88 \times 10^{-2}$  and  $4.41 \times 10^{-1}$  mM; and the maximisation of the correlation coefficient ( $R^2$ ). Statgraphics Centurion XVII program package (Stat-

Point Technologies) was used for the statistical analysis of the data with a confidence interval of 95%.

UV/ $\text{H}_2\text{O}_2$  photo-degradation experiments were carried out in batch mode using a 2 L annular borosilicate glass photo-reactor. One and three 8 W Hg low-pressure lamps emitting at 254 nm and contained in different quartz tubes were used. The irradiation intensity was measured with a UVX radiometer equipped with a UVX-25 sensor (UVP), resulting to be of 170 and 460  $\mu\text{W}/\text{cm}^2$  for 1 and 3 UV-C lamps, respectively. The photo-reactor was equipped with a cooling jacket, allowing maintaining constant the bulk temperature. The irradiated solution was natural water from "El Peñol" dam, located in Guatapé (Antioquia, Colombia), which was spiked with  $6.73 \times 10^{-5}$  and  $1.19 \times 10^{-5}$  mM of anthracene and benzo[a]pyrene, respectively.

## RESULTS AND DISCUSSION

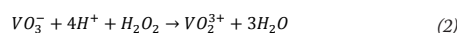
### Preliminary assumptions

As it is widely known, the absorbance of a substance can be expressed as Equation (1).

$$A = \epsilon bc \quad (1)$$

where A is the absorbance of the chemical species;  $\epsilon$ , the molar absorptivity coefficient or molar attenuation coefficient, related to the absorption wavelength; b, the optical path length of the cell containing the sample; and c, the concentration of the target substance.

According to Pupo Nogueira and co-workers<sup>14</sup>,  $\text{H}_2\text{O}_2$  reacts with ammonium monovanadate in acidic medium, yielding a peroxovanadium cation, characterised by its orangey-red colour, as indicated in Equation (2).



Since the generated compound is able to absorb light, in order to determine the optimal wavelength at which the maximum absorption is obtained, a wavelength scan was performed in the range from 370 to 770 nm (Figure 1). As shown in the figure, a maximal absorption is located around 450 nm. Although this value was already reported<sup>14</sup>, high absorptions were also evidenced at 454 nm. Therefore, for discerning which wavelength is the optimal one, both of the wavelength values were considered in the  $2^3$  experimental design.

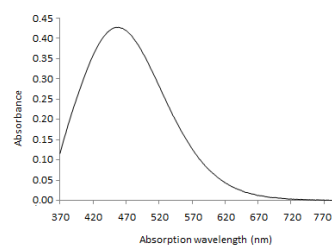


Figure 1. UV-visible absorption spectrum of the peroxovanadium cation.  $\text{H}_2\text{O}_2$  and  $\text{NH}_4\text{VO}_3$  concentrations were  $2.94 \times 10^{-1}$  mM and  $6 \times 10^{-3}$  M, respectively.

As indicated, the path length of the cell is a crucial factor in the spectrophotometric response regarding the amount of absorbed radiation, since a higher cell path length results in a higher amount of energy absorbed by the molecules in the sample. Therefore, lower quantification limits can be obtained with higher cell path lengths, allowing the determination of residual levels of  $H_2O_2$ . In this sense, two quartz cells of 10 and 50 mm path lengths were studied.

In addition to the absorption wavelength and the cell path length, previous experiments evidenced that the concentration of  $NH_4VO_3$  in acidic medium influenced also the system<sup>14</sup>. The effect of the  $NH_4VO_3$  level was ascribed to the number of the formed coloured peroxovanadium cation, which were dependent on the amount of  $H_2O_2$  and the final reacting level of  $NH_4VO_3$ . In order to determine the optimal concentration of  $NH_4VO_3$  for forming coloured peroxovanadium cations,  $6 \times 10^{-3}$  and  $1.2 \times 10^{-2}$  M final solution levels in the 50 mL flask were tested. In turn, unlike  $NH_4VO_3$ ,  $H_2SO_4$  was not observed to influence the system<sup>14</sup>. Therefore, its effect was not studied and a final solution of 0.036 M  $H_2SO_4$  was used during the optimization step and analysis of  $H_2O_2$ . This concentration of  $H_2SO_4$  provided the reaction medium with the required acidic conditions ( $pH < 2$ ) for the generation of peroxovanadium cations, avoiding using high concentrations of acid.

### Optimal condition experiments

The absorption wavelength, the cell path length and the final concentration of  $NH_4VO_3$  were considered as factors affecting the spectrophotometric system. In

order to find the optimal set of values for those factors, a full factorial experimental design was used in water samples spiked with a concentration of  $2.94 \times 10^{-1}$  mM  $H_2O_2$ . The studied levels of  $NH_4VO_3$  final concentration, absorption wavelength and quartz cell path length were  $6 \times 10^{-3}$ – $1.2 \times 10^{-2}$  M, 450–454 nm and 10–50 mm, respectively. The optimisation goal was to maximise the absorption for the low, medium and high level, corresponding to  $2.94 \times 10^{-3}$ ,  $5.88 \times 10^{-2}$  and  $4.41 \times 10^{-1}$  mM  $H_2O_2$ , as well as to obtain an excellent  $R^2$ .

Analysis-of-variance tests were used to find the statistically significant factors for the considered domain. Graphically, the significance of the examined parameters can be observed from the Pareto plots of the considered responses (Figure 2). This graphical tool informs about the estimated effect of each factor through bars, where the bar at the top corresponds to the most statistically significant factor. In turn, the vertical line refers to the value beyond which all the bars exceeding it are considered statistically significant under a significance level of 5%. Thus, as shown in Figure 2a, 2b and 2c, the quartz cell path length is the sole main factor significantly influencing the system for the responses related to the absorption at a low, medium and high level, with a confidence interval of 95%. It was found that the influence of the cell path length was positive. As expected, an increase in the irradiated path length resulted in a higher absorption at the three considered levels. For  $R^2$  (Figure 2d), none of the examined parameters resulted to be statistically significant. A possible explanation can be found in the fact that the obtained responses were quite similar for all of the executed runs.

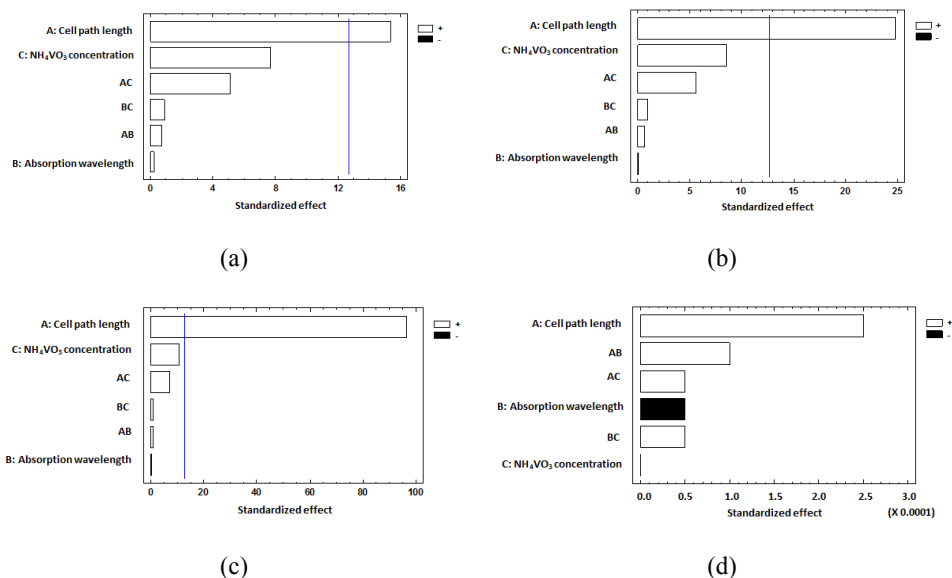


**Figure 2.** Pareto charts for the absorbance at a low (a), medium (b) and high (c) level, and for the  $R^2$  (d). The black and white colours indicate the positive and negative effects, respectively, of the considered factors and interactions. Working ranges:  $6 \times 10^{-3}$ – $1.2 \times 10^{-2}$  M ( $NH_4VO_3$  final concentration), 450–454 nm (absorption wavelength) and 10–50 mm (cell path length).  $[H_2O_2]_0 = 2.94 \times 10^{-1}$  mM.

Consequently, the quartz cell path length was considered at its high level; i.e., a cell path length of 50 mm was used for subsequent studies. With regard to the final concentration of  $\text{NH}_4\text{VO}_3$  solution, due to it was statistically non-significant for the investigated conditions and in order to save in reagent costs, it was used at its low level (i.e., at  $6 \times 10^{-3} \text{ M}$ ).

As far as the absorption wavelength is concerned, even though it is a parameter of great importance in spectrometry, for this study it was statistically non-significant under a confidence interval of 95% because of the low range studied, from 450 to 454 nm. Nevertheless, from the  $R^2$  results, higher values were achieved at 450 nm. Therefore, this absorption wavelength was selected as the optimal one.

The constructed models for the absorbance at the low (Abs LL), medium (Abs ML), and high (Abs HL) level, as well as for the  $R^2$ , with adjusted R-squared statistics higher than 97.5%, are expressed by Equations (3)-(6).

$$\begin{aligned} \text{Abs LL} = & 3.23513 - 0.0324875\text{PL} - 0.00715625\text{AW} - 0.163862\text{AmV} \\ & + 0.000071875\text{PL} * \text{AW} + 0.00021125\text{PL} * \text{AmV} + 0.003625\text{AW} \\ & * \text{AmV} \end{aligned} \quad (3)$$

$$\begin{aligned} \text{Abs ML} = & 3.24775 - 0.023925\text{PL} - 0.0071875\text{AW} - 0.1694\text{AmV} \\ & + 0.00005625\text{PL} * \text{AW} + 0.00021\text{PL} * \text{AmV} + 0.000375\text{AW} * \text{AmV} \end{aligned} \quad (4)$$

$$\begin{aligned} \text{Abs HL} = & 2.542 - 0.0169\text{PL} - 0.005625\text{AW} - 0.12425\text{AmV} + 0.0000625\text{PL} \\ & * \text{AW} + 0.00021\text{PL} * \text{AmV} + 0.000275\text{AW} * \text{AmV} \end{aligned} \quad (5)$$

$$\begin{aligned} R^2 = & 1.03887 - 0.0005625\text{PL} - 0.0000875\text{AW} - 0.0011375\text{AmV} + 0.00000125\text{PL} \\ & * \text{AW} + 2.5\text{E} - 7\text{PL} * \text{AmV} + 0.0000025\text{AW} * \text{AmV} \end{aligned} \quad (6)$$

where PL, AW and AmV correspond to the cell path length, the absorption wavelength and the final concentration of  $\text{NH}_4\text{VO}_3$ , respectively.

It is important to note that the main effect plot in Figure 3 shows that there were no curvature effects in the considered domain for the studied parameters. That was the reason why the quadratic terms were not included in the constructed models.

Hence, from the statistical analysis, the optimal operating conditions were 50 mm,  $6 \times 10^{-3} \text{ M}$  and 450 nm for the quartz cell path length, the final concentration of  $\text{NH}_4\text{VO}_3$  solution and the absorption wavelength, respectively.

### Validation of the developed analytical method

In order to evaluate the practical application of the proposed analytical method, performance parameters such as linearity, limit of quantification, precision and accuracy were measured under the optimal analysis conditions. Results of the validation parameters are given in Table 1.

**Table 1.** Data obtained from the validation of the proposed analytical method

	Working range (mM) (n=3)	Inter-day precision (n=10) (RSD, %)			Accuracy (n=10) (absolute value and RSD, %)			Recovery (n=10) (absolute value and RSD, %)	
		LL	ML	HL	LL	ML	HL	30	70
$\text{H}_2\text{O}_2$	$2.94 \times 10^{-1}$ – $4.41 \times 10^{-1}$	10.14	1.89	0.87	87.87 (10.14)	100.12 (1.90)	99.87 (0.86)	103.47 (13.97)	99.71 (9.79)
LL: Low level ( $2.94 \times 10^{-1}$ mM)		ML: Medium level ( $5.88 \times 10^{-1}$ mM)			HL: High level ( $4.41 \times 10^{-1}$ mM)				

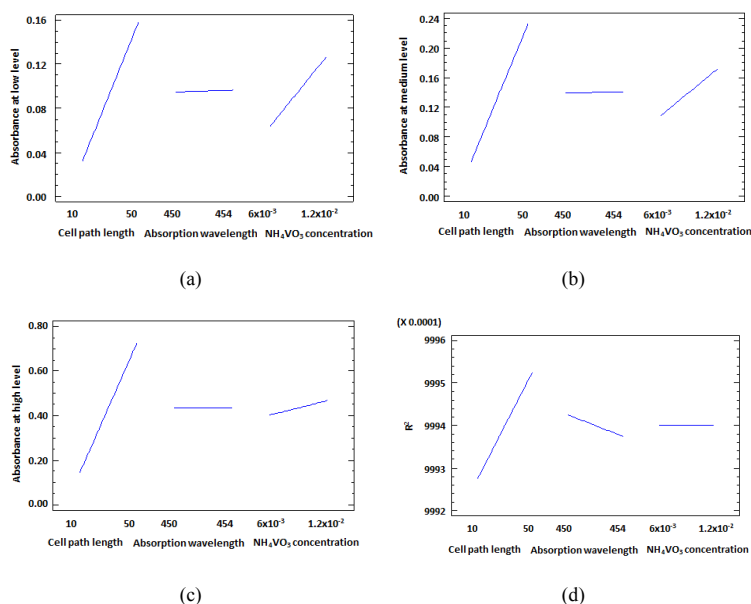


**Figure 3.** Main effect plots for the absorbance at a low (a), medium (b) and high (c) level, and for the  $R^2$  (d). Working ranges:  $6 \times 10^{-3}$ – $1.2 \times 10^{-2} \text{ M}$  ( $\text{NH}_4\text{VO}_3$  final concentration), 450–454 nm (absorption wavelength) and 10–50 mm (cell path length).  $[\text{H}_2\text{O}_2]_0 = 2.94 \times 10^{-1} \text{ mM}$ .

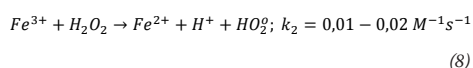
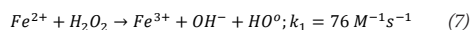
The linearity of the calibration curve was observed over a concentration range of  $2.94 \times 10^{-3}$ – $4.41 \times 10^{-1}$  mM for triplicate measurements and an excellent linearity, with a  $R^2$  equal to 1, was achieved. The limit of quantification was found to be  $2.94 \times 10^{-3}$  mM. It is highlighted that concentration of  $H_2O_2$  in water samples higher than  $4.4 \times 10^{-1}$  mM can be determined by appropriately diluting the sample of interest and introducing the correction factor when calculating the level of this species.

Additionally, the instrumental repeatability was also evaluated at  $2.94 \times 10^{-3}$  mM  $H_2O_2$ , and the relative standard deviation (RSD) resulted to be 0.96%, lower than the reference value of the spectrophotometer used in this study (1%). In turn, the inter-day precision and accuracy RSDs for the low, medium and high level were lower than 11%.

On the other hand, to analyse the applicability of the proposed analytical method, fresh natural water was used ( $n=10$ ). Recoveries of the analyte were measured by speaking this matrix with  $H_2O_2$  at concentrations levels of 30% and 70% (concentration factor) for  $1.47 \times 10^{-1}$  mM. As it can be observed from Table 1, quite acceptable recoveries were obtained.

#### Matrix background. Evaluation of the interfering effect from ions

The effect of common ions present in water was investigated by measuring the absorbance of peroxovanadium complexes in acidic conditions. Several concentrations of foreign ions were studied using a standard solution of  $2.94 \times 10^{-1}$  mM  $H_2O_2$  in deionised water under the determined optimal conditions. In Table 2 the levels of the studied ions and their tolerance limits, i.e., the highest concentration causing a signal variation lower than  $\pm 5\%$  in the absorbance, are listed. It was found that  $Fe^{2+}$  was a major interfering substance, as well as  $CO_3^{2-}$ . The interfering effect of  $Fe^{2+}$  at a concentration higher than 0.005 mM can be attributed to the Fenton reaction expressed by Equation (7). When  $H_2O_2$  is in the bulk, it can react with  $Fe^{2+}$ , giving  $HO^\bullet$  and  $Fe^{3+}$ . Therefore, the catalytic decomposition of  $H_2O_2$  is produced and the higher the level of  $Fe^{2+}$ , the faster the reaction is produced; attaining an absorbance reduction. It is noteworthy that  $Fe^{3+}$  can also react with  $H_2O_2$  to regenerate  $Fe^{2+}$ , as indicated in Equation (8). However, the reaction rate constant ( $k_2$ ) is 7600 times slower than  $k_1$ . Therefore, for practical purposes, it can be affirmed that  $Fe^{3+}$  does not influence the absorbance of the considered system.



With regard to  $CO_3^{2-}$ , changes in colour at the concentration of 25 mM using both  $CaCO_3$  and  $Na_2CO_3$  as  $CO_3^{2-}$  sources were observed, resulting in an absorbance increase. Additionally, when  $CaCO_3$  was used as the reactant for providing  $CO_3^{2-}$ , turbidity was also found at the level of 7.5 mM  $CaCO_3$ , being more noticeable for 50 mM  $CaCO_3$ . Nevertheless, by filtering the samples, suspended solids were removed.

**Table 2.** Influence of coexisting ions for a solution of  $2.94 \times 10^{-1}$  mM of  $H_2O_2$

Interference ion	Concentration range (mM)	Tolerance limit (mM)
$Fe^{3+}$ ( $FeCl_3 \cdot 6H_2O$ ), ( $Fe(NO_3)_3$ )	0.001 - 1	1
$Fe^{2+}$ ( $FeSO_4 \cdot 7H_2O$ )	0.001 - 1	0.005
Cl <sup>-</sup> (HCl)	0.05 - 1000	1000
$NO_3^-$ ( $HNO_3$ )	0.01 - 5	5
$PO_4^{3-}$ ( $H_3PO_4$ )	0.001 - 1	1
$NH_4^+$ ( $NH_4OH$ )	0.01 - 10	10
$Mg^{2+}$ ( $MgSO_4 \cdot 7H_2O$ )	0.001 - 1	1
Na <sup>+</sup> (NaCl)	0.05 - 75	75
$Mn^{2+}$ ( $MnSO_4 \cdot H_2O$ )	0.001 - 1	1
F <sup>-</sup> (NaF)	0.001 - 1	1
K <sup>+</sup> (KCl)	0.05 - 75	75
Ca <sup>2+</sup> (CaCl)	0.05 - 50	50
$CO_3^{2-}$ ( $CaCO_3$ ), ( $Na_2CO_3$ )	0.01 - 50	15

From these results, it can be asserted that the proposed analytical method is quite selective for the determination of low levels of  $H_2O_2$  in different kinds of water.

#### Application to real samples. Photo-degradation experiments

The studied method was applied for the determination of residual  $H_2O_2$  in natural water samples treated with the UV/ $H_2O_2$  advanced oxidation system in the annular photo-reactor described above. Natural water was taken from "El Peñol" dam, located in Guatapé (Colombia), whose characteristics are summarised in Table 3.

**Table 3.** "El Peñol" dam water characteristics

Parameter	Value
Temperature (°C)	23.58
pH	7.35
Dissolved oxygen ( $mg O_2 L^{-1}$ )	8.61
Total organic carbon ( $mg C L^{-1}$ )	2.03
Conductivity ( $mS m^{-1}$ )	39.87
Turbidity (NTU)	1.09
Redox potential (meV)	222.59
Dissolved Fe ( $mg L^{-1}$ )	< 0.05
Total alkalinity ( $mg CaCO_3 L^{-1}$ )	16.33
Total hardness ( $mg CaCO_3 L^{-1}$ )	17.67
$NO_3^-$ ( $mg L^{-1}$ )	2.99
Cl <sup>-</sup> ( $mg L^{-1}$ )	3.393
$SO_4^{2-}$ ( $mg L^{-1}$ )	1.949
$PO_4^{3-}$ ( $mg L^{-1}$ )	0.026
Anthracene	n.d.*
Benzo[a]pyrene	n.d.*

\*Non-detected.

The water was spiked with  $6.73 \times 10^{-5}$  mM anthracene and  $1.19 \times 10^{-5}$  mM benzo[a]pyrene. Different levels of  $H_2O_2$  ( $1.47 \times 10^{-1}$ ;  $2.94 \times 10^{-1}$ ;  $4.41 \times 10^{-1}$  and  $5.88 \times 10^{-1}$  mM) were tested during a reaction time of 90 min. Additionally, the efficiency of 1 and 3 lamps UV-C lamps, corresponding to 8 and 24 W, respectively, was examined for anthracene and benzo[a]pyrene degradation. Measurements of anthracene and benzo[a]pyrene reduction, total organic carbon removal and  $H_2O_2$  evolution were taken in three replicates at different time intervals. The samples were collected in glass containers, stored in the dark at 4 °C and treated as soon as possible.



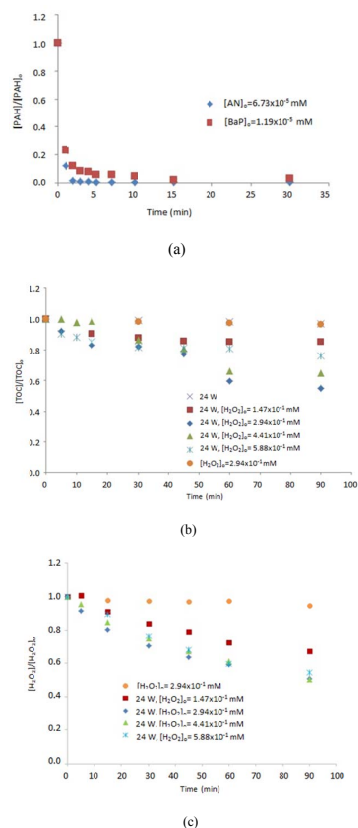


**Figure 4.** (a) Anthracene (AN) and benzo[a]pyrene (BaP) removal using 1 UV-C lamp. (b) Total organic carbon (TOC) reduction. (c) H<sub>2</sub>O<sub>2</sub> evolution.  $[AN]_0 = 6.73 \times 10^{-5}$  mM;  $[BaP]_0 = 1.19 \times 10^{-5}$  mM;  $[TOC]_0 = 2.04$  mgC L<sup>-1</sup>;  $[H_2O_2]_0 = 1.47 \times 10^{-1}$ ,  $2.94 \times 10^{-1}$ ,  $4.41 \times 10^{-1}$  and  $5.88 \times 10^{-1}$  mM; UV-C lamps = 1 and 3 lamps, corresponding to 8 and 24 W, respectively.

When H<sub>2</sub>O<sub>2</sub> is irradiated, it interacts with photons, generating HO<sup>•</sup>, as expressed by Equation (9). The formed HO<sup>•</sup> reacts with the water organic matter, oxidising it and forming reaction intermediate products up to a complete mineralisation to form H<sub>2</sub>O and CO<sub>2</sub>. As illustrated in Figure 4a, a removal of anthracene and benzo[a]pyrene higher than 99% was achieved in 30 min of irradiation with 1 UV-C lamp and without the use of H<sub>2</sub>O<sub>2</sub>. This is due to the absorbance properties of these compounds at 254 nm<sup>19</sup>, especially of anthracene. However, this result did not assure the mineralisation of the target compounds. In fact, in Figure 4b, which represents the evolution of the total organic carbon, it can be observed that the mineralisation attained by using 3 UV-C lamps without H<sub>2</sub>O<sub>2</sub> was < 5%. Although the obtained value of organic matter is within the range allowable in the legislation for drinking water, the mineralisation of the target compounds is not assured, and the presence of degradation by-products with a toxicity even

higher than that of the parent compounds can occur. Hence, the mineralisation evolution must be studied combining the action of 3 UV-C lamps and adding different amounts of H<sub>2</sub>O<sub>2</sub>. As illustrated in the figure, the use of 3 UV-C lamps and  $2.94 \times 10^{-1}$  mM of H<sub>2</sub>O<sub>2</sub> resulted in a sample mineralisation of about 45% after 90 min of reaction time. Additionally, under these working conditions, no toxic reaction intermediate products were evidenced. Therefore, these operating conditions allowed an efficient conversion of anthracene and benzo[a]pyrene to harmless degradation by-products. Moreover, the higher the organic matter removal, the lower the possibility of disinfection by-product formation.

With regard to the evolution of H<sub>2</sub>O<sub>2</sub>, Figure 4c shows that  $2.94 \times 10^{-1}$  mM H<sub>2</sub>O<sub>2</sub> remained almost constant throughout the reaction time when dark conditions were used, which was expected since in Figure 4b the total organic carbon removal by using this level of H<sub>2</sub>O<sub>2</sub> in the dark can be neglected. On the other hand, when H<sub>2</sub>O<sub>2</sub> is irradiated, there is a H<sub>2</sub>O<sub>2</sub> reduction during the reaction time because of the formation of HO<sup>•</sup>, as indicated in Equation (9). High reductions of H<sub>2</sub>O<sub>2</sub> were observed when  $2.94 \times 10^{-1}$ ;  $4.41 \times 10^{-1}$  and  $5.88 \times 10^{-1}$  mM were used. However, higher levels of total organic carbon removal were found when  $2.94 \times 10^{-1}$  mM H<sub>2</sub>O<sub>2</sub> was added to the reaction medium. This result indicated that levels of H<sub>2</sub>O<sub>2</sub> higher than  $2.94 \times 10^{-1}$  mM resulted in an unnecessary reagent cost, since an excess of H<sub>2</sub>O<sub>2</sub> can also act as a quencher of HO<sup>•</sup>, as expressed in Equation (10); subsequently, reducing the efficiency of the oxidation system.

## CONCLUSION

In the current work, an analytical method for the determination of the residual and/or produced H<sub>2</sub>O<sub>2</sub> from AOPs for water decontamination was developed in a simple and rapid way. The effects of the quartz cell path length, the final concentration of the NH<sub>4</sub>VO<sub>3</sub> solution and the absorption wavelength were studied. The optimal conditions allowing the quantification of H<sub>2</sub>O<sub>2</sub> in natural water were 450 nm of absorption wavelength, 50 mm of quartz cell path length and  $6 \times 10^{-3}$  M of NH<sub>4</sub>VO<sub>3</sub> final concentration solution. The developed method was validated and the influence of several ions commonly present in water was examined, resulting to be a selective method. In this sense, due to the achieved low quantification limit and because of the proposed analytical method is relatively free from interferences; it can be used for several types of water. In fact, it was applied for studying the evolution of H<sub>2</sub>O<sub>2</sub> in the decontamination of real natural water spiked with anthracene and benzo[a]pyrene at a level of  $6.73 \times 10^{-5}$  and  $1.19 \times 10^{-5}$  mM, respectively. It was found that after 90 min of treatment and using 3 UV-C lamps, approximately  $1.47 \times 10^{-1}$  mM H<sub>2</sub>O<sub>2</sub> were consumed obtaining a reduction of the total organic carbon around 45% and a removal of anthracene and benzo[a]pyrene higher than 99%.

## ACKNOWLEDGEMENTS

This work was supported by the Spanish Agency for International Development Cooperation (AECID), the Colombian Administrative Department of Science, Technology and Innovation (COLCIENCIAS), and the Sustainability Fund of Universidad de Antioquia.

## REFERENCES

1. Kormann, C.; Bahnemann, D. W.; Hoffmann, M. R. Photocatalytic production of H<sub>2</sub>O<sub>2</sub> and organic peroxides in aqueous suspensions of TiO<sub>2</sub>, ZnO, and desert sand. *Environ. Sci. Technol.* **1988**, *22*, 798-806.
2. Olasehinde, E. F.; Makino, S.; Kondo, H.; Takeda, K.; Sakugawa, H. Application of Fenton reaction for nanomolar determination of hydrogen peroxide in seawater. *Anal. Chim. Acta* **2008**, *627*, 270-276.
3. Bratsch, S. G. Standard electrode potentials and temperature coefficients in water at 298.15 K. *J. Phys. Chem. Ref. Data* **1989**, *18*, 1-21.
4. Chen, H.; Yu, H.; Zhou, Y.; Wang, L. Fluorescent quenching method for determination of trace hydrogen peroxide in rain water. *Spectrochim. Acta Part A* **2007**, *67*, 683-686.
5. Kralik, P.; Kusic, H.; Koprinavac, N.; Bozic, A. L. Degradation of chlorinated hydrocarbons by UV/H<sub>2</sub>O<sub>2</sub>: the application of experimental design and kinetic modeling approach. *Chem. Eng. J.* **2010**, *158*, 154-166.
6. Rubio-Clemente, A.; Chica, E.; Peñuela, G. A. Application of Fenton process for treating petrochemical wastewater. *Ing. Compet.* **2014**, *16*, 211-223.
7. Rubio-Clemente, A.; Torres-Palma, R. A.; Peñuela, G. A. Removal of polycyclic aromatic hydrocarbons in aqueous environment by chemical treatments: a review. *Sci. Total Environ.* **2014**, *478*, 201-225.
8. Karci, A. Degradation of chlorophenols and alkylphenol ethoxylates, two representative textile chemicals, in water by advanced oxidation processes: the state of the art on transformation products and toxicity. *Chemosphere* **2014**, *99*, 1-18.
9. Ribeiro, A. R.; Nunes, O. C.; Pereira, M. F. R.; Silva, A. M. T. An overview on the advanced oxidation processes applied for the treatment of water pollutants defined in the recently launched Directive 2013/39/EU. *Environ. Int.* **2015**, *75*, 33-51.
10. Rubio-Clemente, A.; Chica, E.; Peñuela, G. A. Petrochemical wastewater treatment by photo-Fenton process. *Water Air Soil Pollut.* **2015**, *226*, 61-79.
11. Comninellis, C.; Kapalka, A.; Malato, S.; Parsons, S. A.; Poullos, I.; Mantzavinos, D. Advanced oxidation processes for water treatment: advances and trends for R&D. *J. Chem. Technol. Biotechnol.* **2008**, *83*, 769-776.
12. Linley, E.; Denyer, S. P.; McDonnell, G.; Simons, C.; Maillard, J. Y. Use of hydrogen peroxide as a biocide: new consideration of its mechanisms of biocidal action. *J. Antimicrob. Chemother.* **2012**, *67*, 1589-1596.
13. Sunil, K.; Narayana, B. Spectrophotometric determination of hydrogen peroxide in water and cream samples. *Bull. Environ. Contam. Toxicol.* **2008**, *81*, 422-426.
14. Pupo Nogueira, R. F.; Oliveira, M. C.; Paterlini, W. C. Simple and fast spectrophotometric determination of H<sub>2</sub>O<sub>2</sub> in photo-Fenton reactions using metavanadate. *Talanta* **2005**, *66*, 86-91.
15. Ribeiro, J. P. N.; Segundo, M. A.; Reis, S.; Lima, J. L. F. C. Spectrophotometric FIA methods for determination of hydrogen peroxide: Application to evaluation of scavenging capacity. *Talanta* **2009**, *79*, 1169-1176.
16. Klassen, N. V.; Marchington, D.; McGowan, H. C. E. H<sub>2</sub>O<sub>2</sub> determination by the I<sub>3</sub>-method and by KMnO<sub>4</sub> titration. *Anal. Chem.* **1994**, *66*, 2921-2925.
17. Rubio-Clemente, A.; Chica, E.; Peñuela, G. A. Rapid determination of anthracene and benzo(a)pyrene by high-performance liquid chromatography with fluorescence detection. *Anal. Lett.* **2017**, *50*, 1229-1247.
18. Pignatello, J. J.; Oliveros, E.; MacKay, A. Advanced oxidation processes for organic contaminant destruction based on the Fenton reaction and related chemistry. *Critical Rev. Environ. Sci. Technol.* **2006**, *36*, 1-84.
19. Sanches, S.; Leitão, C.; Penetra, A.; Cardoso, V. V.; Ferreira, E.; Benoliel, M. J.; Crespo, M. T.; Pereira, V. J. Direct photolysis of polycyclic aromatic hydrocarbons in drinking water sources. *J. Hazard. Mater.* **2011**, *192*, 1458-1465.

# **WATER TREATMENT**



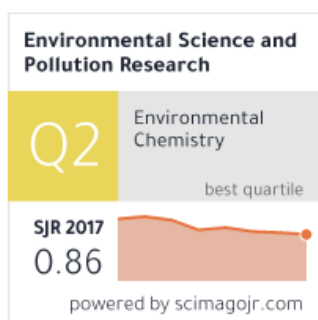


## 4. WATER TREATMENT

### Paper

**Total coliforms inactivation in natural water by UV/H<sub>2</sub>O<sub>2</sub>, UV/US and UV/US/H<sub>2</sub>O<sub>2</sub> systems**

### Journal



Scope: Environmental Science and Pollution Research (ESPR) serves the international community in all areas of Environmental Science and related subjects with emphasis on chemical compounds. It reports from a broad interdisciplinary outlook. Apart from the strictly scientific contributions as research articles (short and full papers) and reviews, ESPR publishes: news & views from research and technology, legislation and regulation, hardware and software, education, literature, institutions, organizations, conferences

### Highlights

- Several photochemical AOPs are studied for wild microorganism destruction in water.
- The application of the AOPs tested resulted in total microbial load inactivation.

- Bacterial regrowth was not evidenced after operating the oxidation treatments.
- The UV/H<sub>2</sub>O<sub>2</sub> system was the most economical process.



## Total coliform inactivation in natural water by UV/H<sub>2</sub>O<sub>2</sub>, UV/US, and UV/US/H<sub>2</sub>O<sub>2</sub> systems

Ainhoa Rubio-Clemente<sup>1,2,3</sup> · Edwin Chica<sup>4</sup> · Gustavo Peñuela<sup>2</sup>

Received: 13 December 2017 / Accepted: 18 September 2018  
© Springer-Verlag GmbH Germany, part of Springer Nature 2018

### Abstract

The presence of pathogens in drinking water can seriously affect human health. Therefore, water disinfection is needed, but conventional processes, such as chlorination, result in the production of dangerous disinfection by-products. In this regard, an alternative solution to tackle the problem of bacterial pollution may be the application of advanced oxidation processes. In this work, the inactivation of total coliforms, naturally present in a Colombian surface water by means of UV/H<sub>2</sub>O<sub>2</sub>, UV/US, and the UV/US/H<sub>2</sub>O<sub>2</sub> advanced oxidation processes, was investigated. Under the investigated conditions, complete bacterial inactivation (detection limit equal to 1 CFU 100 mL<sup>-1</sup>) was found within 5 min of treatment by UV/H<sub>2</sub>O<sub>2</sub> and UV/US/H<sub>2</sub>O<sub>2</sub> systems. UV/US oxidation process also resulted in total bacterial load elimination, but after 15 min of treatment. Bacterial reactivation after 24 h and 48 h in the dark was measured and no subsequent regrowth was observed. This phenomenon could be attributed to the high oxidation capacity of the evaluated oxidation systems. However, the process resulting in the highest oxidation potential at the lowest operating cost, in terms of energy consumption, was UV/H<sub>2</sub>O<sub>2</sub> system. Therefore, UV/H<sub>2</sub>O<sub>2</sub> advanced oxidation system can be used for disinfection purposes, enabling drinking water production meeting the requirements of regulated parameters in terms of water quality, without incurring extremely high energy costs. Nonetheless, further researches are required for minimizing the associated electric costs.

**Keywords** Advanced oxidation process · Disinfection · Total coliform · Water treatment · UV/H<sub>2</sub>O<sub>2</sub> system · UV/US process · UV/US/H<sub>2</sub>O<sub>2</sub> system

### Introduction

Water is an indispensable resource for life (Bagatin et al. 2014; Malato et al. 2009). Therefore, high quality of water for human consumption must be ensured, both in terms of the

removal of toxic contaminants and their by-products, and of the effective treatment of microbial pollution (García-Fernández et al. 2012; Zhou et al. 2018). Water can be contaminated through various sources, including sewage and human and animal wastes, which might contain pathogens, mainly enteric microorganisms (Ortega-Gómez et al. 2014; Alvear-Daza et al. 2018). Therefore, microbial load inactivation must be assessed, as well as pollutant degradation efficiency, when assessing the feasibility of a process for water treatment (Rodríguez-Chueca et al. 2018).

Several techniques are available for tertiary water treatment (e.g., chemical, physical, and biological processes) (Rodríguez-Chueca et al. 2018). Each treatment process has positive aspects and constraints in relation to applicability, efficiency, and cost (Rubio-Clemente et al. 2014, 2015). With regard to the techniques used to eliminate pathogens in water, chlorine is the main disinfectant traditionally used in purification processes, due to their availability, low cost, oxidizing character, and potential to eliminate pathogens (Esteban et al. 2017). Despite the wide application of chlorine as disinfectant agent, it is involved in

Responsible editor: Vitor Pais Vilar

✉ Ainhoa Rubio-Clemente  
ainhoarubioelem@gmail.com

<sup>1</sup> Facultad de Ciencias de la Salud, Universidad Católica de Murcia UCAM, Avenida de los Jerónimos, s/n., Murcia, Spain

<sup>2</sup> Grupo GDCON, Facultad de Ingeniería, Sede de Investigaciones Universitarias (SIU), Universidad de Antioquia UdeA, Calle 70, No. 52-21, Medellín, Colombia

<sup>3</sup> Facultad de Ingeniería, Tecnológico de Antioquia–Institución Universitaria TdeA, Calle 78b No. 72A-220, Medellín, Colombia

<sup>4</sup> Departamento de Ingeniería Mecánica, Facultad de Ingeniería, Universidad de Antioquia UdeA, Calle 70, No. 52-21, Medellín, Colombia

the generation of disinfection by-products (DBPs) (Rodríguez-Chueca et al. 2018). DBPs, including trihalomethanes and haloacetic acids, are formed by the reaction of the disinfectant with the organic matter naturally present in water (Hrudey 2009; Awaleh and Soubaneh 2014; Polo-López et al. 2014; Bach et al. 2015). These compounds have recently become a matter of concern among water utilities and regulators because they are considered as carcinogenic pollutants (Diao et al. 2004; Xie 2016; Szczuka et al. 2017). Ozone can also be used in the disinfection process; however, it can also cause DBPs (Mao et al. 2014). Meanwhile, ultraviolet (UV) radiation in the UV-C range is an efficient sanitation alternative since total microbial load removal can be achieved in a relatively short period of time or UV-C dose (Zhou et al. 2017; Nocker et al. 2018). However, microbial regrowth has been observed after the radiation conditions are ended due to the lack of residual effect and the DNA repair mechanisms (Rodríguez-Chueca et al. 2018).

In this context, the evaluation of alternative disinfection techniques to conventional processes is required. Along these alternatives, advanced oxidation processes (AOPs) employing ultraviolet (UV) radiation are highly efficient systems (Bounty et al. 2012; Penru et al. 2012; Urbano et al. 2017; Aguilar et al. 2018; Serna-Galvis et al. 2018). Photochemical AOPs are based on the formation of non-selective hydroxyl radicals ( $\text{HO}\cdot$ ), a highly reactive oxidant species, able to attack and degrade organic substances. (Mamane et al. 2007; Bounty et al. 2012; Urbano et al. 2017). AOPs have several advantages. These include the chemical transformation of the contaminants, including the organic matter naturally present in water, due to the high oxidizing power of  $\text{HO}\cdot$ ; equivalent to 2.8 V (Litter and Quici 2010; Rubio-Clemente et al. 2014). In addition, AOPs have been demonstrated to be efficient in treating contaminants at low concentration, obtaining highly biodegradable effluents under certain conditions, AOPs can transform the vast majority of organic contaminants into compounds with simpler structures (Ribeiro et al. 2015; Rubio-Clemente et al. 2014, 2017). Moreover, AOPs can be an option for significantly reducing microbial load, since  $\text{HO}\cdot$  can also interact with the chemical structure of the microorganism cell wall and inactivate pathogens (Comminellis et al. 2008; Bounty et al. 2012; Zhou et al. 2017).

Among the photochemical AOPs, UV/ $\text{H}_2\text{O}_2$ , UV/US, and UV/US/ $\text{H}_2\text{O}_2$  systems have been widely used for water treatment purposes (Mahamuni and Adewuyi 2010; Rubio-Clemente et al. 2014; Miklos et al. 2018). UV/ $\text{H}_2\text{O}_2$  process consists of the photolysis of  $\text{H}_2\text{O}_2$  or its conjugate base ( $\text{H}_2\text{O}_2^-$ ) when irradiated by photons of wavelengths lower than 300 nm (Rodríguez-Chueca et al. 2018), as described by Eq. 1, producing  $\text{HO}\cdot$ .



In turn, the combination of ultrasound (US) with UV/ $\text{H}_2\text{O}_2$  system is based on the  $\text{HO}\cdot$  generation by the direct

mechanical action of the cavitation bubble implosion, as represented by Eq. 2 (Rubio-Clemente et al. 2014) and the additional production of  $\text{HO}\cdot$  from the homolysis of  $\text{H}_2\text{O}_2$ , both externally added or internally formed within the oxidation system, by the interaction with UV radiation in the UV-C range (Gassie and Englehardt 2017).



Additionally, these AOPs can benefit from the direct photolytical effect of UV-radiation and/or the oxidation potential of  $\text{H}_2\text{O}_2$  (Rubio-Clemente et al. 2014; Gassie and Englehardt 2017). The AOPs mentioned have been shown to be highly efficient for the mineralization of organic pollutants and the inactivation of microorganisms (Hulsmans et al. 2010; Bounty et al. 2012; Penru et al. 2012; Rubio-Clemente et al. 2014; Gassie and Englehardt 2017; Urbano et al. 2017; Giannakis et al. 2018a; Malvestiti and Dantas 2018). However, to the authors' knowledge, application of AOPs in real water treatment matrices using wild microorganisms is at present scarce. A great number of studies reported in the literature are focused on bacterial load removal using deionized or distilled water and/or commercial laboratory strains (Hulsmans et al. 2010; Zhou et al. 2017; Giannakis et al. 2018a; Rodríguez-Chueca et al. 2018). On the other hand, other reports evaluate the efficiency of a number of AOPs using natural microorganisms that are extracted and relocated into the laboratory (Aguilar et al. 2018). It is important to note that in laboratory strain, microorganisms are grown under optimized conditions as individuals (Palková 2004). In contrast, under natural conditions, microorganisms become organized into multicellular communities and are better protected against harmful environment (De la Fuente-Núñez et al. 2013; Lyons and Kolter 2015). Additionally, natural microorganisms isolated and grown in the laboratory can adapt to the favorable conditions of the laboratory, through complex changes that include the repression of some protective mechanisms that are essential in nature (Palková 2004). Moreover, they can interact with other organisms present in water and form consortiums, becoming even more resistant to the disinfection process (Bridier et al. 2011). Therefore, the results obtained using the microorganism mentioned do not reflect the real effectiveness of alternative oxidation processes since wild microorganisms are more resistant (De la Fuente-Núñez et al. 2013; Lyons and Kolter 2015). This fact should be taken into account in order to obtain results under conditions close to reality, which is of great importance when scaling these water treatment processes up.

Therefore, evaluation of the potential of UV/ $\text{H}_2\text{O}_2$ , UV/US, and UV/US/ $\text{H}_2\text{O}_2$  system oxidation in order to further investigate the feasibility of these UV-C based AOPs to remove microorganism load in real natural water is needed.

A number of microorganisms have been used as indicators of fecal pollution (Lakeh et al. 2013; Moreno-Andrés et al. 2016; Giannakis et al. 2018a; Malvestiti and Dantas 2018; Rodríguez-Chueca et al. 2018). Among the groups of microorganisms evaluated as fecal indicators, total coliforms are useful since they can provide information on the source and type of the pollution present in water (Malvestiti and Dantas 2018). Additionally, they can be used to know the efficiency of the treatment process and the integrity of the storage and distribution systems (WHO 2011).

In this context, and continuing our previous study on anthracene (AN) and benzo[a]pyrene (BaP) polycyclic aromatic hydrocarbons (Rubio-Clemente et al. 2018), this work reports the efficiency of several UV-based AOPs, such as UV/H<sub>2</sub>O<sub>2</sub>, UV/US, and UV/US/H<sub>2</sub>O<sub>2</sub> processes for wild microbial load inactivation, under optimal conditions previously found. As indicators of the presence of pathogens in water, total coliforms naturally contained in the surface water evaluated were used and their inactivation through the application of each advanced oxidation treatment and associated control experiments was studied. Additionally, regrowth experiments were performed simulating the conditions of storage and distribution tanks in order to assess the real inactivation of bacterial load for purification purposes. The operating costs, in terms of energy costs, were estimated for each of the evaluated oxidation systems to know the application feasibility of the assessed AOPs.

## Material and methods

### Reagents

Hydrogen peroxide (H<sub>2</sub>O<sub>2</sub>, 30 wt%, J.T. Baker, USA) was used as the oxidizing agent for UV/H<sub>2</sub>O<sub>2</sub> and UV/US/H<sub>2</sub>O<sub>2</sub> systems. Sodium thiosulfate pentahydrate (Na<sub>2</sub>S<sub>2</sub>O<sub>3</sub>·5H<sub>2</sub>O, 99%, Merck, Germany) was utilized to inhibit the effect of H<sub>2</sub>O<sub>2</sub> on microorganisms. Unless otherwise specified, reagents were analytical grade and used as received without further purification.

### Type of water

Real surface water freshly obtained from the Colombian reservoir “El Peñol” was used. In Fig. 1, the sampling point is illustrated. This reservoir is characterized by its relatively low natural organic matter content (2.03 mg L<sup>-1</sup> of total organic carbon (TOC)) and inorganic anions. Additionally, “El Peñol” dam water has a turbidity of 1.09 NTU, pH of 7.35, temperature of 23.58 °C, and a conductivity of 0.39 mS cm<sup>-1</sup>. The bacterial load used in the current study was the total coliform concentration naturally contained in the water of interest, which was comprised between 10<sup>3</sup> and 10<sup>4</sup> CFU 100 mL<sup>-1</sup>

In Rubio-Clemente et al. (2018), a more complete characterization is reported.

Temperature and pH were measured with a pH 3110 WTW Sentix 41 pH-electrode (New York, USA) portable meter. In turn, dissolved oxygen and electrical conductivity measurements were conducted using a HQ 40D Multi meter equipped, respectively, with an Intellical™ LDO101 Laboratory Luminescent/Optical Dissolved Oxygen sensor and an Intellical™ CDC401 Laboratory 4-Poles Graphite Conductivity Cell (Hach, Loveland, CO, USA). Turbidity was monitored using a WTW 550 IR turbidity meter. Anion content was quantified using a Dionex ICS Ion-1000 Chromatography System (ThermoFisher, CA, USA). For the TKN determination, a Büchi K-355 and K-424 Distillation Unit (México City, Mexico) was used. TOC naturally present in the evaluated water samples was analyzed using an Apollo 9000 TOC analyzer purchased from Teledyne Tekmar Instruments (Mason, OH, USA).

The characterization parameters were measured according to the corresponding analytical procedures and methods set out in the Standard Methods for the Examination of Water and Wastewater (WEF and AWWA 2012). Specifically, pH and temperature were measured using the 2550 B method and the 4500-H+ B electrometric method, respectively. Conductivity measurements were conducted through the 2510 B method. In turn, turbidity was measured by the 2130 B nephelometric method and the dissolved oxygen, by the 4500-O G membrane electrode method. Total alkalinity and hardness were measured using the 2310 B and the 2340 C acidic and EDTA titrimetric methods, respectively. The 4500 ion chromatographic standard method was used to analyze anions and the 4500-N<sub>org</sub> B macro-Kjeldahl method, for the determination of TKN. Finally, TOC was measured by the 5310 B high-temperature combustion method.

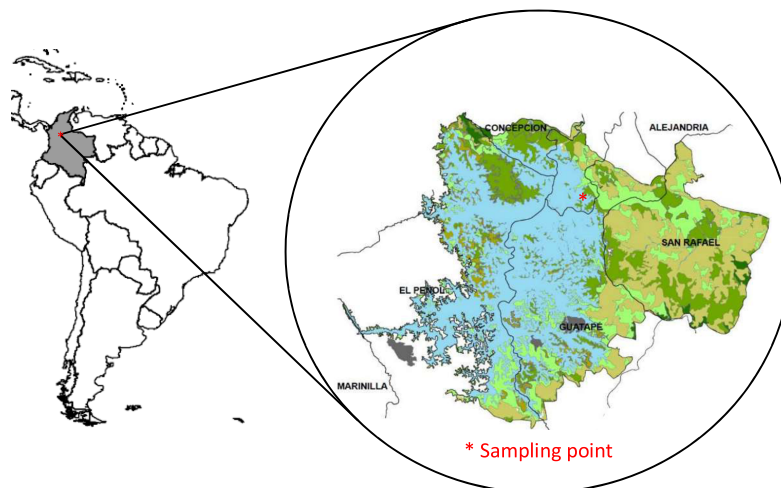
In turn, the bacterial load used in the current study was the total coliform concentration naturally present in the water of interest, which was in the range from 10<sup>3</sup> to 10<sup>4</sup> CFU 100 mL<sup>-1</sup>. Below, the analytical method used for total coliform determination is detailed.

As this kind of water was also used for degradation studies of micropollutants non-specifically found in the matrix, two representative polycyclic aromatic hydrocarbons, anthracene and benzo[a]pyrene, were spiked in the water at 3 µg L<sup>-1</sup> each. However, the presence of these contaminants in the reaction solution resulted in no noticeable effect on the total coliform level. Consequently, toxic effects associated with the presence of these pollutants were discarded.

### Bacterial cell inactivation experiments

For bacterial cell inactivation experiments, two different reactors were used, as represented in Fig. 2, one of them allowing water treatment using ultrasonic assistance. In this

**Fig. 1** Sampling point corresponding to “El Peñol” dam, located in Guatapé, Antioquia, Colombia (N 6° 17' 41.1583" O 75° 9' 31.0821") (SIAC 2018)



regard, photodisinfection batch experiments related to UV/H<sub>2</sub>O<sub>2</sub> were performed using a 2-L cylindrical photochemical reactor made of borosilicate 3.3 glass with a double-walled cooling jacket, enabling the bulk temperature to be maintained at a constant value of 25 ± 1 °C with a type-K thermocouple (Fig. 2a). The combination of ultrasound waves with UV and UV/H<sub>2</sub>O<sub>2</sub> system was, in turn, conducted in a glass sonoreactor of 1-L effective volume, operating in batch mode. In order to control the temperature within the reaction solution of the reactor with ultrasonic assistance, a fan-forced refrigeration system was implemented (Fig. 2b). The radiation source consisted of UV-C Hg low pressure lamps with a main emission wavelength of 254 nm (General Electric International Inc., USA). Four lamps of 8 W for UV/H<sub>2</sub>O<sub>2</sub> process and one lamp of 6 W for the UV/US and UV/US/H<sub>2</sub>O<sub>2</sub> systems were used. The lamps were inserted into quartz glass sleeves and placed axially at the center of the reactor. Irradiance values were measured in triplicate by a UVX radiometer (UVP, Inc., USA) equipped with a UVX-25 sensor placed at the top, middle, and at the bottom of the photo and sonochemical reactors. The radiometer and sensor were calibrated beforehand.

Working conditions used for the operation of UV/H<sub>2</sub>O<sub>2</sub> and the UV/US/H<sub>2</sub>O<sub>2</sub> oxidation systems are listed in Table 1. The operating conditions were previously optimized.

During the inactivation experiments, the natural pH of the surface water used was maintained. Additionally, constant temperature was ensured by the refrigeration systems of the reactors used, and lamps were previously warmed up to ensure stable radiation throughout the treatment time.

The solution analyzed for the determination of the presence of fecal pollution was the effluent from the photoreactor and sonoreactor. Sampling was performed at several time

intervals; specifically, aliquots were withdrawn at 5, 15, 30, 60, and 90 min, equivalent to different UV-C dose depending on the target AOP. The UV dose was calculated by multiplying the irradiance values by the treatment time, as represented in Eq. 3.

$$UV\text{-Dose} = E_0 \times t \quad (3)$$

where  $E_0$  is the irradiance and  $t$  is the treatment time. The UV dose is expressed in  $\text{mJ cm}^{-2}$ .

Sampling was conducted using a sterilized wide mouth glass bottle and containing Na<sub>2</sub>S<sub>2</sub>O<sub>3</sub> 5H<sub>2</sub>O 10%. The amount of Na<sub>2</sub>S<sub>2</sub>O<sub>3</sub> 5 H<sub>2</sub>O used to inhibit H<sub>2</sub>O<sub>2</sub> corresponded to 10 mg L<sup>-1</sup> to quench immediately 1 mg L<sup>-1</sup> of H<sub>2</sub>O<sub>2</sub> (Keen et al. 2012). The samples were analyzed within 24 h of sampling. Additionally, they were kept at 4 ± 0.5 °C, avoiding freezing after the sampling, during the transport and before the analysis.

Reactor washings were performed by multiple washes with ultrapure water and a final wash with acetone, as received, which was evaporated before the following operation of the reactor.

Total coliform inactivation experiments were performed in three replicates.

### Total coliform enumeration

The inactivation of total coliforms was monitored by the 9222 BH membrane filtration method (WEF and AWWA 2012) filtering 100 mL of each sample volume. Prior to analysis, the samples were homogenized to avoid erroneous results. It is important to highlight that an ideal sample volume would yield from 1 to 80 coliform colonies and not more than 200

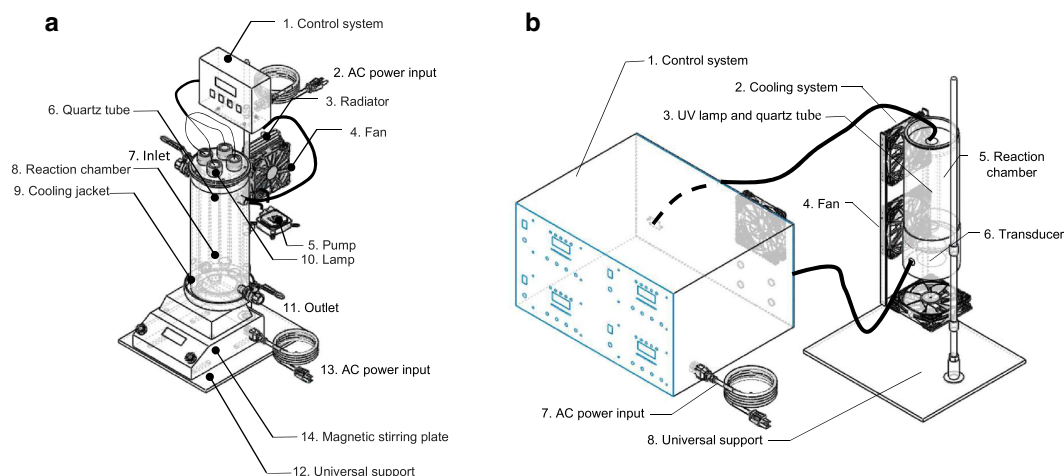


**Fig. 2** Illustration of **a** the annular jacketed multi-lamp photoreactor and **b** the sonochemical reactor

colonies. Consequently, in case the count was very high, appropriate dilutions were prepared according to procedure 9215 B.2 established in WEF and AWWA (2012). Counting was performed in triplicate and the mean values and standard deviation (SD) were represented.

The bacterial suspension was also quantified by the same technique before being added to the reactor. Additionally, control samples were performed in each assay to ensure that bacterial concentration did not change during experimental procedures.

The quantification method detection limit (DL) was 1 CFU 100 mL<sup>-1</sup>.

Results were expressed as colony-forming units per 100 mL of water (CFU 100 mL<sup>-1</sup>).

**Bacterial regrowth experiments**

Total coliform regrowth tests were carried out in the photochemical and sonochemical reactor after 90 min of oxidation treatment, where water was kept in the dark at room

temperature for 24 h and 48 h, simulating the conditions of storage and distribution tanks. In these time periods, planting was performed and enumeration was conducted, as described in section “Total coliform enumeration”. Additionally, residual H<sub>2</sub>O<sub>2</sub>, although it can have a positive effect in reducing the chances of bacteria proliferation, was quenched when present to avoid interferences in the measurements (Malvestiti and Dantas 2018).

The purpose of these measures was to assess the post-irradiation events, after their removal from the experimental set-up.

**Disinfection efficiency determination and data treatment**

Bacterial inactivation was illustrated as direct measurements, represented as CFU 100 mL<sup>-1</sup>. Additionally, removal efficiency, expressed as percentage of total coliform elimination, was calculated as described in Eq. 4, where N and N<sub>0</sub> refer to the number of bacteria after the specific treatment in the photo and

**Table 1** Operating conditions of UV/H<sub>2</sub>O<sub>2</sub>, UV/US, and UV/US/H<sub>2</sub>O<sub>2</sub> oxidation systems

Advanced oxidation process	Operating conditions		
	Irradiation conditions	H <sub>2</sub> O <sub>2</sub> concentration	Other operating conditions
UV/H <sub>2</sub> O <sub>2</sub> system	0.63 mW cm <sup>-2</sup> (4 UV-C lamps of 8 W each)	11 mg L <sup>-1</sup>	–
UV/US system	0.11 mW cm <sup>-2</sup> (1 UV-C lamp of 6 W)	–	60 W input power 80 kHz frequency
UV/US/H <sub>2</sub> O <sub>2</sub> system	0.11 mW cm <sup>-2</sup> (1 UV-C lamp of 6 W)	5 mg L <sup>-1</sup>	60 W input power 80 kHz frequency

sonochemical reactors and the initial concentration of total coliforms in the water of study before disinfection, respectively.

$$\text{Removal efficiency}(\%) = \frac{N - N_0}{N_0} * 100 \quad (4)$$

Three replicates were performed of all treatments and samples, and data were plotted as mean  $\pm$  SD. Additionally, in experiments where radiation is involved, total coliform inactivation was represented versus UV-C dose, while in the experiments where no radiation source was used (see inset of the figures regarding bacterial inactivation), data were represented versus the treatment time.

Statistical analyses were performed with one-way ANOVA  $p < 0.05$ , confidence level  $\geq 95\%$  using the StatGraphics Centurion XVII Software (StatPoint Technologies Inc., Warrenton, VA, USA). It was observed that differences within treatments were considered to be statistically non-significant at  $p < 0.05$ . In contrast, differences among treatments resulted to be statistically significant at  $p < 0.05$ .

## Results and discussion

### Total coliform inactivation by UV/H<sub>2</sub>O<sub>2</sub> system

The disinfection efficiency of UV/H<sub>2</sub>O<sub>2</sub> process was examined under the optimal operating conditions found through the response surface methodology (11 mg L<sup>-1</sup>

H<sub>2</sub>O<sub>2</sub>, 0.63 mW cm<sup>-2</sup> irradiance). In Rubio-Clemente et al. (2018), further information on UV/H<sub>2</sub>O<sub>2</sub> process optimization can be found. Additionally, control experiments were carried out in the dark with and without the addition of H<sub>2</sub>O<sub>2</sub>, and considering the action of UV radiation alone. Results are illustrated in Fig. 3. As can be observed from the figure, the population of total coliforms was practically unaltered in the dark control without H<sub>2</sub>O<sub>2</sub>. By adding 11 mg L<sup>-1</sup> H<sub>2</sub>O<sub>2</sub> to the dark system, the bacteria concentration diminished from  $1.5 \times 10^3 \pm 210$  CFU 100 mL<sup>-1</sup> to  $2.1 \times 10^2 \pm 20$  CFU 100 mL<sup>-1</sup> after 90 min of contact time. This result may be associated with the disinfection capacity of H<sub>2</sub>O<sub>2</sub> through its attack on the lipid membrane of the cells and its combination with the iron inside bacterial cells after H<sub>2</sub>O<sub>2</sub> diffusion into the cell, producing internal Fenton reactions (Eqs. 5 and 6), characterized by the formation of HO $\cdot$ , which in turn attacks the cell (Rubio et al. 2013; Giannakis et al. 2018b). Furthermore, H<sub>2</sub>O<sub>2</sub> can accumulate in the cell and cause a growth defect (Moreno-Andrés et al. 2016). Nonetheless, stabilization in the bacterial inactivation is evidenced, indicating that the inactivation process occurs in two stages: a first stage where bacteria are eliminated from the system, and a second stage where microorganisms exhibit a certain degree of resistance to the bactericidal action of H<sub>2</sub>O<sub>2</sub>.

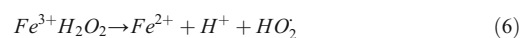
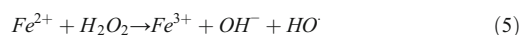
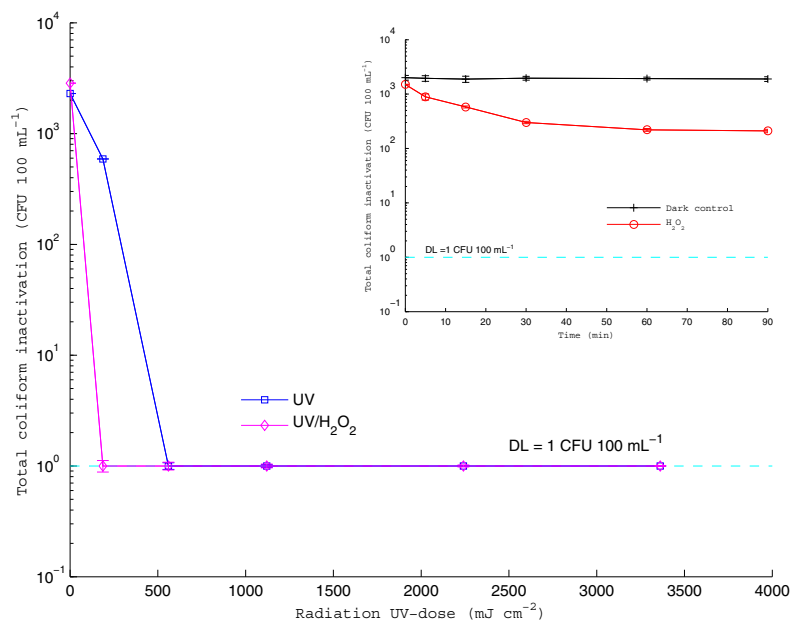


**Fig. 3** Evolution profile of the total coliforms in water subject to UV/H<sub>2</sub>O<sub>2</sub> process under optimal operating conditions. [TOC]<sub>0</sub> = 2.04 mg L<sup>-1</sup>; [H<sub>2</sub>O<sub>2</sub>]<sub>0</sub> = 11 mg L<sup>-1</sup>; UV-C irradiance = 0.63 mW cm<sup>-2</sup>. Data are presented as mean  $\pm$  SD ( $n = 3$ )





The obtained results were similar to those ones achieved in a previous study conducted by Miranda et al. (2016) where surface water disinfection by chlorination and UV/H<sub>2</sub>O<sub>2</sub>, UV/TiO<sub>2</sub>, and UV/N-TiO<sub>2</sub> advanced oxidation processes were evaluated focusing on the inactivation of an antibiotic resistant *E. coli* strain. The referred work revealed that the contact of the addition of H<sub>2</sub>O<sub>2</sub> in the reaction medium did not show any significant inactivation during 75 min of treatment.

Meanwhile, when applying the action of UV radiation alone, a sharp decrease in the bacterial cell content was also observed, reaching total inactivation ( $p < 0.04$ ) after 15 min of irradiation (DL equal to 1 CFU 100 mL<sup>-1</sup>). According to Rubio et al. (2013) and Santos et al. (2013), UV-C radiation causes direct photochemical damage on intracellular DNA, as well as the alteration of essential components in bacteria, such as proteins and lipids, among other biomolecules.

This rapid entrance in tailing is comparable to the results obtained by Aguilar et al. (2018) work, in which pathogen inactivations, including *E. coli* and *Kleibsellla pneumoniae*, were investigated under UV-C radiation. However, in this study, microorganisms were faster removed, since only 16 s and 36 s, respectively, were required. This can be probably ascribed to the use of laboratory strains or wild microorganisms that were isolated in comparison with the use of endogenous microorganisms without previous isolation. Indeed, Aguilar et al. (2018) explained the higher sensitivity of *E. coli* compared to *K. pneumoniae* towards irradiation because of the utilization of commercialized strains used for *E. coli* experiments, while for *K. pneumoniae* assays, microorganisms were isolated. Additionally, although in a minor extent, the higher power density used in the referred study (42.86 W L<sup>-1</sup>) in comparison with the power density of the current work (16 W L<sup>-1</sup>) can also be named.

Despite the positive results obtained under the action of UV-C radiation alone, and considering that microorganism reactivation events have been reported under photolytical treatment (Rubio et al. 2013; Moreno-Andrés et al. 2016), the reaction system was, then, irradiated with four lamps (0.63 mW cm<sup>-2</sup>) together with 11 mg L<sup>-1</sup> H<sub>2</sub>O<sub>2</sub>. Under these new conditions, total removal of bacteria was attained in 5 min of treatment ( $p < 0.05$ ), equivalent to a UV-C dose of 186.75 mJ cm<sup>-2</sup>. This deleterious and rapid decay in the microorganism load can be ascribed to the effects described above plus the production of HO· from H<sub>2</sub>O<sub>2</sub>, or its conjugated base (HO<sub>2</sub><sup>-</sup>), by photolysis (Eq. 1). Additionally, photons reaching coliforms can alter their cell physiological structure and damage their DNA. Moreover, these photons could accelerate the regeneration cycle of the iron ions, increasing the production of HO· from the Fenton reaction, as mentioned above.

Similar findings were reported by Rubio et al. (2013) for *E. coli* inactivation using 1 UV-C lamp emitting mainly at 254 nm and 10 mg L<sup>-1</sup> H<sub>2</sub>O<sub>2</sub>. Aguilar et al. (2018) also studied the oxidation capacity of UV/H<sub>2</sub>O<sub>2</sub> system for bacterial

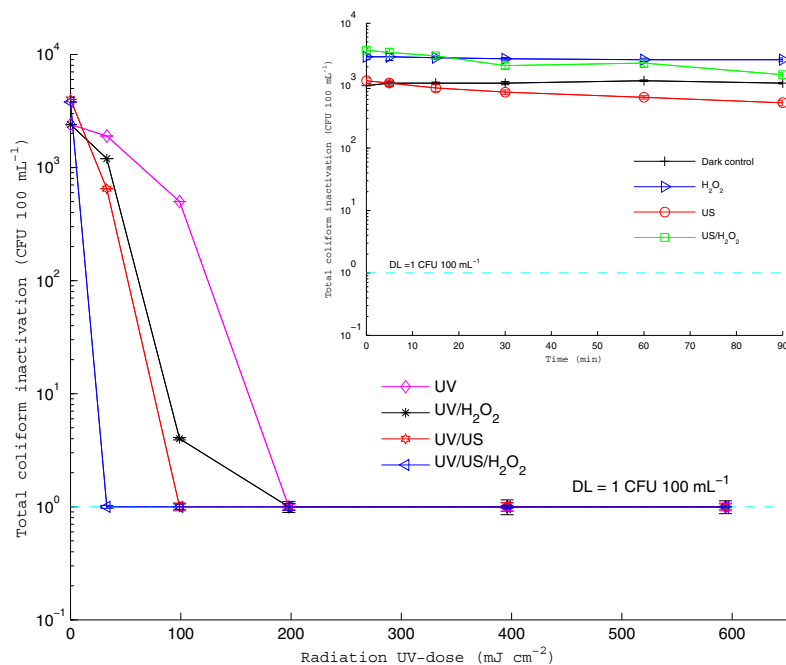
load removal. In this occasion, the authors also found differences between microorganisms, being UV/H<sub>2</sub>O<sub>2</sub> process more efficient for *E. coli* abatement in comparison to *K. pneumoniae* inactivation. The differences can be due to the robust capsule of *K. pneumoniae* compared to *E. coli*, which can protect bacteria cell from direct attacks from oxidizing radicals and reducing the H<sub>2</sub>O<sub>2</sub> diffusion into the cell. The inactivation efficiency of UV/H<sub>2</sub>O<sub>2</sub> oxidation technology on water containing different kinds of microorganisms has been proven to be of great importance (Giannakis et al. 2018a). These authors compared the behavior of *E. coli* in the presence of MS2 bacteriophage and *vice versa* by means of UV/H<sub>2</sub>O<sub>2</sub> system in Milli-Q water, synthetic wastewater, and urine matrices. They found that the presence of MS2 bacteriophage delayed the *E. coli* inactivation kinetics. Indeed, when *E. coli* and MS2 were simultaneously in the water of interest, the latter caused a decrease of 45% in bacterial inactivation in all matrices. These findings allow discerning the relevance of using groups of microorganisms or pathogens when evaluating the efficiency of a system in terms of disinfection capacity.

#### Total coliform inactivation by the UV/US/H<sub>2</sub>O<sub>2</sub> and the UV/US system

In Fig. 4, the microbial load destruction results under the combined UV/US/H<sub>2</sub>O<sub>2</sub> system using 5 mg L<sup>-1</sup> H<sub>2</sub>O<sub>2</sub>, 80 kHz frequency, 60 W rating power, and 0.11 mW cm<sup>-2</sup> UV-C irradiance are illustrated. According to the figure, a slight increase of 10% in the total number of coliforms was observed in dark control experiments; i.e., when neither ultrasonic nor electromagnetic waves were applied and no reactants were added to the reaction system, total coliform number was raised. In this case, this effect could be encouraged by the presence of salts and nutrients that favor bacterial growth. Similar results were observed by Giannakis et al. (2015). When bacteria were in contact with H<sub>2</sub>O<sub>2</sub>, a reduction of about 10.34% in bacterial population was evidenced. This could be ascribed to the disinfectant power of H<sub>2</sub>O<sub>2</sub> (Linley et al. 2012). Nonetheless, a minor effect on bacterial inactivation was observed.

On the other hand, by sonicating the water sample, microbial load removal extent was increased up to 55.83% after 90 min of treatment, since total coliform concentration reduced from 1200 ± 60 CFU 100 mL<sup>-1</sup> to 430 ± 10 CFU 100 mL<sup>-1</sup> ( $p < 0.05$ ). This is likely due to the production of cavitation bubbles, causing mechanical, physical, and chemical effects on bacterial cells (Dadjour et al. 2005; Hulsmans et al. 2010; Naddeo et al. 2014). In this regard, microbial cells can be damaged due to the shear forces induced by micro-streaming within the cell and the mechanical fatigue over a period of time (Naddeo et al. 2014). It has been demonstrated that the efficiency of ultrasound in water disinfection is greater when

**Fig. 4** Evolution of total coliform profile subject to UV/US/H<sub>2</sub>O<sub>2</sub> and UV/US processes under optimal operating conditions. [TOC]<sub>0</sub> = 2.04 mg L<sup>-1</sup>; frequency = 80 kHz; power rating = 60 W; UV-C irradiance = 0.11 mW cm<sup>-2</sup>; [H<sub>2</sub>O<sub>2</sub>]<sub>0</sub> = 5 mg L<sup>-1</sup>. Data are presented as mean ± SD (*n* = 3)



operating at lower frequencies and higher intensities (Joyce et al. 2003; Furuta et al. 2004; Dehghani 2005; Antoniadis et al. 2007). In fact, Paleologou et al. (2007) found higher efficiencies in terms of bacterial disinfection when using lower frequencies. These authors found that ultrasound irradiation for 60 min at constant power resulted in 94.5% and 97.6% of inactivation at 80 kHz and 24 kHz, respectively, at a constant power, while an increase in power when using a frequency of 24 kHz resulted in an inactivation rate of 99.7% after 60 min of ultrasonication. Ultrasounds also intervene in the split of bacterial agglomerates, leading to the dispersion of individual bacterial cells into the bulk, and the inactivation of bacterial cells (Zhou et al. 2017). Additionally, chemical effects, i.e., the oxidation action of the free radicals formed inside the cavitation bubbles and released into the liquid body when these collapse or implode can occur at low frequencies (Zhou et al. 2017), although this effect has been proven to be more significant at high frequencies (Carrère et al. 2010). Bacterial cells can be oxidized by the reactive chemical species formed in consequence of this, particularly HO<sup>•</sup>, leading to the attack of the chemical structure of the bacterial cell walls (Naddeo et al. 2014; Giannakis et al. 2015).

As observed in Fig. 4, the concurrent action of H<sub>2</sub>O<sub>2</sub> (5 mg L<sup>-1</sup>) and US process resulted in higher elimination

extent of total coliforms. This might be due to the individual effects ascribed to ultrasonic waves and H<sub>2</sub>O<sub>2</sub> in attacking cells. In the hybrid US/H<sub>2</sub>O<sub>2</sub> technique, H<sub>2</sub>O<sub>2</sub> can act as a source for reactive oxygen species (Abbasi and Asl 2008; Wei et al. 2015). H<sub>2</sub>O<sub>2</sub> increases the formation rate of HO<sup>•</sup> from self-decomposition as a result of US application (Abbasi and Asl 2008). The enhancement in HO<sup>•</sup> production within the bulk will result in a rise in the oxidation rate of the whole system. In fact, in the current case, the application of US concomitantly with the addition of H<sub>2</sub>O<sub>2</sub> led to a bacterial removal increase of 62.16% after 90 min of treatment time, since total coliform concentration reduced from 3700 ± 440 CFU 100 mL<sup>-1</sup> to 770 ± 60 CFU 100 mL<sup>-1</sup> (*p* < 0.03). This removal percentage is in accordance with Wei et al. (2015) results (a reduction of 64.96%) obtained when ultrasound was introduced into the H<sub>2</sub>O<sub>2</sub> oxidation process (US/H<sub>2</sub>O<sub>2</sub>). This phenomenon was attributed to the formation of reactive radicals, such as ·OH, by means of the thermal decomposition of H<sub>2</sub>O<sub>2</sub> in the cavitation bubbles.

In Fig. 4, it can also be observed that microbial load inactivation was rapidly attained when the aqueous solution was irradiated with a UV-C irradiance of 0.11 mW cm<sup>-2</sup>, with complete total coliform elimination being achieved. Zhou et al. (2017) also found that accumulated UV-C dose could exert lethal effect on bacteria. However, the obtained results for *E. coli* showed a poorer inactivation with regard to the

findings achieved in the current study. The reason might lie on the kind of radiation source used that consisted of UV-C light-emitting diodes, and therefore, the lower UV-C dose used for irradiating the reaction solution.

Additionally, when  $5 \text{ mg L}^{-1} \text{ H}_2\text{O}_2$  was introduced into the system, a relatively rapid microbial decomposition was attained, as after an accumulation UV-C dose of  $198 \text{ mJ cm}^{-2}$  within the reaction medium, equivalent to a treatment time of 30 min, the colony-forming units of total coliforms reached the DL. This might be due to the cell damages caused by the synergetic action of UV and  $\text{H}_2\text{O}_2$  (Rubio et al. 2013) as occurred in UV/ $\text{H}_2\text{O}_2$  system under the working conditions evaluated. The coupled application of UV/US system also resulted in dramatic microbial cell elimination within a short period of time (15 min), allowing for an accumulation of UV-C dose in the system of  $99 \text{ mJ cm}^{-2}$ . Lakeh et al. (2013) also found interesting results when applying UV/US oxidation treatment in recirculation aquaculture systems containing the ciliate *Paramecium* sp., the second larval stage of the nematode *Anguillicola crassus* and the metanauplii *Artemia* sp. They found that the combination of ultrasound waves of low frequency (25 kHz) with UV-C radiation could be regarded as an appropriate water treatment with regards to all the target pathogens in recirculating aquaculture systems.

Nevertheless, the combined system that facilitates the highest level of bacterial cell inactivation with the lowest UV-C dose accumulation, i.e., with the shortest treatment time (5 min), was the combined UV/US/ $\text{H}_2\text{O}_2$  system, achieving total bacterial elimination under  $33 \text{ mJ cm}^{-2}$  ( $p < 0.02$ ), or in only 5 min of treatment, as illustrated in Fig. 4.

### Regrowth studies

Very positive results, in terms of bacterial load inactivation, were achieved by the action of UV-C, both at  $0.63 \text{ mW cm}^{-2}$  or  $0.11 \text{ mW cm}^{-2}$ . Additionally, by combining  $11 \text{ mg L}^{-1} \text{ H}_2\text{O}_2$  and  $0.63 \text{ mW cm}^{-2}$  or  $5 \text{ mg L}^{-1} \text{ H}_2\text{O}_2$  and  $0.11 \text{ mW cm}^{-2}$ , total coliform elimination was achieved. When 80 kHz, 60 W, and  $0.11 \text{ mW cm}^{-2}$  were coupled or used along with  $5 \text{ mg L}^{-1} \text{ H}_2\text{O}_2$ , total removal of the cells was also observed. However, bacterial regrowth can occur, especially, when only slight damage has been caused by the target water treatment to the bacteria structure (Malvestiti and Dantas 2018; Rodríguez-Chueca et al. 2018). Therefore, total coliform regrowth capacity after inactivation is an important factor to be evaluated during water disinfection process. For this purpose, the studied water was stored in the dark at  $25 \pm 1 \text{ }^\circ\text{C}$  for 24 h and 48 h after the 90 min of the oxidation treatment.

In Fig. 5, the results obtained from the regrowth experiments are represented. It can be seen that when the sole action

of the UV-C irradiation was applied both with 4 UV-C lamps of 8 W, microorganism reactivation was observed after the reaction solution was in the dark for 24 h and 48 h, since  $1200 \pm 150 \text{ CFU } 100 \text{ mL}^{-1}$  and  $4500 \pm 200 \text{ CFU } 100 \text{ mL}^{-1}$  were achieved after 24 h and 48 h in the dark and after an UV-C dose accumulation of  $3362 \text{ mJ cm}^{-2}$ . The reactivation of bacterial load, even after complete inactivation, can be ascribed to the slight damage caused by the UV-C irradiation used and the genetic material repair mechanisms (Moreno-Andrés et al. 2016; Malvestiti and Dantas 2018). However, no bacterial reactivation was found once UV/ $\text{H}_2\text{O}_2$  process was applied. This indicates that cellular damage was so high under the experimental conditions tested that the bacterial repair mechanism related to the catalase enzymatic activity, allowing  $\text{H}_2\text{O}_2$  detoxification, as reported by Moreno-Andrés et al. (2016), was not effective.

Microorganism reactivation was also found when the reaction solution was irradiated with 1 UV-C lamp of 6 W during 90 min, equivalent to a UV-C dose accumulated in the system of  $594 \text{ mJ cm}^{-2}$ . In this case, final total coliforms counting after 48 h and 24 h in the dark corresponded to  $5600 \pm 210 \text{ CFU } 100 \text{ mL}^{-1}$  and  $2400 \pm 530 \text{ CFU } 100 \text{ mL}^{-1}$ ; therefore, higher reactivation was observed compared to the use of 4 lamps of 8 W. This fact can be explained from the higher accumulated UV-C dose in the photolytical system where 4 lamps of 8 W were used, since more severe damages were caused. However, when  $5 \text{ mg L}^{-1} \text{ H}_2\text{O}_2$  was introduced into the system conformed of 1 lamp of 6 W, the reactivation of bacterial cells was not observed. This might be due to the irreversible cell destruction caused by the synergetic action of UV and  $\text{H}_2\text{O}_2$ .

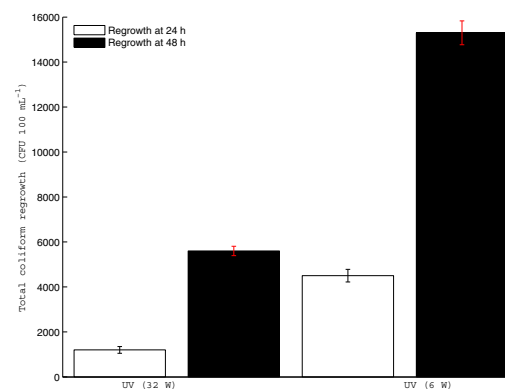


**Fig. 5** Bacterial regrowth after 24 h (□) and 48 h (■) in the dark in relation to the application of UV/ $\text{H}_2\text{O}_2$ , UV/US, and UV/US/ $\text{H}_2\text{O}_2$  oxidation processes and their control experiments.  $[\text{TOC}]_0 = 2.04 \text{ mg L}^{-1}$ ; frequency = 80 kHz; power rating = 60 W; UV-C irradiance =  $0.63 \text{ mW cm}^{-2}$  (UV/ $\text{H}_2\text{O}_2$ ),  $0.11 \text{ mW cm}^{-2}$  (UV/US/ $\text{H}_2\text{O}_2$ );  $[\text{H}_2\text{O}_2]_0 = 11 \text{ mg L}^{-1}$  (UV/ $\text{H}_2\text{O}_2$ ),  $5 \text{ mg L}^{-1}$  (UV/US/ $\text{H}_2\text{O}_2$ ). Data are presented as mean  $\pm$  SD ( $n = 3$ )

Regrowth of bacteria after photolysis was also observed by Moreno-Andrés et al. (2016) when determining the disinfection efficiency of photolysis on *Enterococcus faecalis* in salt-water after keeping samples in the dark to simulate storage in a ballast tank. Pablos et al. (2013) also found this effect after UV-C photolysis of *E. coli*. This phenomenon can be explained by the reparation mechanisms of the physical and chemical damage caused to the DNA by the UV radiation. The presence of inorganic ions in real water matrices is also related to reactivation events, since anions contribute to the absence of osmotic stress, preventing H<sub>2</sub>O<sub>2</sub> diffusion into the bacterial cell. It is emphasized that the presence of inorganic ions can prevent cells from direct attack of H<sub>2</sub>O<sub>2</sub> and HO<sup>-</sup> when formed, since inorganic ions compete with H<sub>2</sub>O<sub>2</sub> for cell membrane contact sites (Grebel et al. 2010; Spuhler et al. 2010; Malvestiti and Dantas 2018) and with HO<sup>-</sup> by the widely known scavenging reactions (Grebel et al. 2010; Rubio-Clemente et al. 2014; Alvear-Daza et al. 2018; Malvestiti and Dantas 2018).

### Estimation of operational costs

To make an economical comparison of the AOPs employed, the electric energy per order of pollutant removal (EE/O) was used (Bolton et al. 2001). EE/O is the electric energy in kilowatt-hours (kWh) required to cause degradation of a contaminant or the inactivation of microorganisms by 1 order of magnitude in 1 m<sup>3</sup> (1000 L) of polluted water (Eq. 7).

$$EE/O = \frac{P \cdot t \cdot 1000}{V \cdot 60 \cdot \log \frac{N_0}{N}} \quad (7)$$

where P is the power rating (kW) of the AOP system, V is the volume (L) during the treatment time, t (min). N<sub>0</sub> and N correspond to the initial and final concentration of total coliforms, respectively.

The operational cost of treating a water volume of 2 L or 1 L, depending if UV/H<sub>2</sub>O<sub>2</sub> process (4 lamps of 8 W), or UV/US and UV/US/H<sub>2</sub>O<sub>2</sub> systems (1 lamp of 6 W) are taken into account, respectively, for disinfecting 10<sup>3</sup>–10<sup>4</sup> CFU 100 mL<sup>-1</sup> of total coliforms and assuring no reactivation, was calculated to be 6.95, 27.48 y 27.66 kWh m<sup>-3</sup>. Assuming energy costs of 0.15 \$ kW<sup>-1</sup>, the estimated cost for each treatment is 1.04, 4.12, and 4.15 \$ h m<sup>-3</sup>, respectively. It is important to note that the investment costs, such as those related to reagents, chemicals, apparatus, and replacement of parts, were not considered. Consequently, the EE/O values refer only to the energy costs.

Comparing these operational costs to those associated with traditional disinfection methods, such as chlorine (Moghadam and Dore 2012), it was found that the operational costs of using UV/H<sub>2</sub>O<sub>2</sub>, UV/US, and UV/US/H<sub>2</sub>O<sub>2</sub>

systems are higher. Similar findings were found by Hulsmans et al. (2010) when evaluating the process parameters of ultrasonic treatment of 10<sup>4</sup> CFU mL<sup>-1</sup> bacterial suspensions, *E. coli* (strain LMG 2092T), *Pseudomonas aeruginosa* (strain LMG 1242), *Flavobacterium breve* (strain LMG 4011), and *Aeromonas hydrophila* (strain LMG 2844T) in a pilot scale water disinfection system.

The EE/O of UV/H<sub>2</sub>O<sub>2</sub> system using 1 lamp of 6 W and 5 mg L<sup>-1</sup> H<sub>2</sub>O<sub>2</sub> was also calculated in the current study due to the positive results obtained with respect to bacterial inactivation and no subsequent reactivation. The associated EEO and corresponding estimated cost were 29.28 kWh m<sup>-3</sup> and 4.40 \$ h m<sup>-3</sup>, respectively, still even larger than by using UV/H<sub>2</sub>O<sub>2</sub> (11 mg L<sup>-1</sup> H<sub>2</sub>O<sub>2</sub> and 0.63 mW cm<sup>-2</sup>), UV/US and UV/US/H<sub>2</sub>O<sub>2</sub> oxidation systems.

Considering the above, the combination of UV-C radiation with H<sub>2</sub>O<sub>2</sub> alone and/or coupled to ultrasound waves allowed obtaining promising results in the field of water disinfection. This indicates the possibility of applying UV/H<sub>2</sub>O<sub>2</sub>, UV/US, and UV/US/H<sub>2</sub>O<sub>2</sub> oxidation systems to reduce bacterial pollution naturally contained in surface water. However, the energy demands of irradiation and ultrasound equipment are somewhat high, particularly when UV/US, UV/US/H<sub>2</sub>O<sub>2</sub> and UV/H<sub>2</sub>O<sub>2</sub> (1 lamp of 6 W and 5 mg L<sup>-1</sup> H<sub>2</sub>O<sub>2</sub>) are used. Therefore, further investigations are recommended to be carried out for evaluating the efficiency of solar light in powering the water treatment systems studied in order to reduce the associated energy operational costs.

Furthermore, even though no regrowth was demonstrated when applying the evaluated AOPs, a very interesting aspect would be the assessment of the reactivation capacity of such as oxidation systems at the UV-C dose accumulation or time interval right where total coliform inactivation (99.99%) is achieved. This would allow a significant saving in the electric costs associated for the oxidation processes to be performed.

### Conclusion

In order to tackle the problem of microbial pollution in natural water, UV/H<sub>2</sub>O<sub>2</sub>, UV/US, and UV/US/H<sub>2</sub>O<sub>2</sub> processes were applied. All the oxidation systems resulted in total coliform inactivation (99.9%) in a short period of time, equivalent to a UV-C dose accumulation of 186.75, 99, and 33 mJ cm<sup>-2</sup>, respectively. Bacterial regrowth was also assessed and no total coliform reactivation was observed after the implementation of the treatments. Additionally, cost analysis in terms of electrical costs was conducted. The results indicated that UV/H<sub>2</sub>O<sub>2</sub> system was the most economical process, with EE/O associated of 6.95 kWh m<sup>-3</sup>. In this way, the disinfection of bacterial load naturally contained in surface water was

demonstrated to be plausible and without incurring in extremely high energy costs by UV/H<sub>2</sub>O<sub>2</sub> advanced oxidation process. However, further researches are required to reduce the costs associated with UV/H<sub>2</sub>O<sub>2</sub> process.

**Acknowledgements** The authors thank the Spanish Agency for International Development Cooperation (AECID), the Colombian Administrative Department of Science Technology and Innovation (COLCIENCIAS), and the Sustainability Fund of the Vice-rectory of Research at the University of Antioquia for supporting this work.

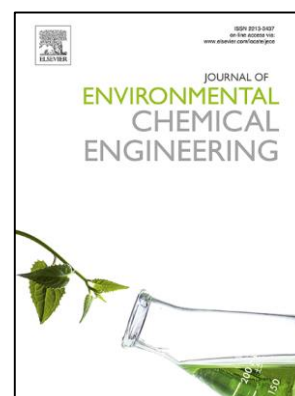
## References

- Abbasi M, Asl NR (2008) Sonochemical degradation of basic blue 41 dye assisted by nanoTiO<sub>2</sub> and H<sub>2</sub>O<sub>2</sub>. *J Hazard Mater* 153(3):942–947
- Aguilar S, Rosado D, Moreno-Andrés J, Cartuche L, Cruz D, Acevedo-Merino A, Nebot E (2018) Inactivation of a wild isolated *Klebsiella pneumoniae* by photo-chemical processes: UV-C, UV-C/H<sub>2</sub>O<sub>2</sub> and UV-C/H<sub>2</sub>O<sub>2</sub>/Fe<sup>3+</sup>. *Catal Today* 313:94–99
- Alvear-Daza JJ, Sanabria J, Herrera JAR, Gutierrez-Zapata HM (2018) Simultaneous abatement of organics (2, 4-dichlorophenoxyacetic acid) and inactivation of resistant wild and laboratory bacteria strains by photo-induced processes in natural groundwater samples. *Sol Energy* 171:761–768
- Antoniadis A, Poullos I, Nikolakaki E, Mantzavinos D (2007) Sonochemical disinfection of municipal wastewater. *J Hazard Mater* 146:492–495
- Awaleh MO, Soubaneh YD (2014) Waste water treatment in chemical industries: the concept and current technologies. *Hydrol: Curr Res* 5(1):1
- Bach L, Garbelini ER, Stets S, Peralta-Zamora P, Emmel A (2015) Experimental design as a tool for studying trihalomethanes formation parameters during water chlorination. *Microchem J* 123:252–258
- Bagatin R, Klemesš JJ, Reverberi AP, Huisinsh D (2014) Conservation and improvements in water resource management: a global challenge. *J Clean Prod* 77:1–9
- Bolton JR, Bircher KG, Tumas W, Tolman CA (2001) Figures-of-merit for the technical development and application of advanced oxidation technologies for both electric- and solar-driven systems. *Pure Appl Chem* 73:627–637
- Bounty S, Rodriguez RA, Linden KG (2012) Inactivation of adenovirus using low-dose UV/H<sub>2</sub>O<sub>2</sub> advanced oxidation. *Water Res* 46(19):6273–6278
- Bridier A, Briandet R, Thomas V, Dubois-Brissonnet F (2011) Resistance of bacterial biofilms to disinfectants: a review. *Biofouling* 27(9):1017–1032
- Carrère H, Dumas C, Battimelli A, Batstone DJ, Delgenès JP, Steyer JP, Ferrer I (2010) Pretreatment methods to improve sludge anaerobic degradability: a review. *J Hazard Mater* 183:1–15
- Comninellis C, Kapalka A, Malato S, Parsons SA, Poullos I, Mantzavinos D (2008) Advanced oxidation processes for water treatment: advances and trends for R&D. *J Chem Technol Biotechnol* 83(6):769–776
- Dadjour MF, Ogino C, Matsumura S, Shimizu N (2005) Kinetics of disinfection of *Escherichia coli* by catalytic ultrasonic irradiation with TiO<sub>2</sub>. *Biochem Eng J* 25(3):243–248
- De la Fuente-Núñez C, Refeuveille F, Fernández L, Hancock RE (2013) Bacterial biofilm development as a multicellular adaptation: antibiotic resistance and new therapeutic strategies. *Curr Opin Microbiol* 16(5):580–589
- Dehghani MH (2005) Effectiveness of ultrasound on the destruction of *E. coli*. *Am J Environ Sci* 1:187–189
- Diao HF, Li XY, Gu JD, Shi HC, Xie ZM (2004) Electron microscopic investigation of the bactericidal action of electrochemical disinfection in comparison with chlorination, ozonation and Fenton reaction. *Process Biochem* 39(11):1421–1426
- Esteban B, Rivas G, Arzate S, Pérez JS (2017) Wild bacteria inactivation in WWTP secondary effluents by solar photo-Fenton at neutral pH in raceway pond reactors. *Catal Today* 313:72–78
- Furuta M, Yamaguchi M, Tsukamoto T, Yim B, Stavarache CE, Hasiba K, Maeda Y (2004) Inactivation of *Escherichia coli* by ultrasonic irradiation. *Ultrason Sonochem* 11:57–60
- García-Fernández I, Polo-López MI, Oller I, Fernández-Ibáñez P (2012) Bacteria and fungi inactivation using Fe<sup>3+</sup>/sunlight, H<sub>2</sub>O<sub>2</sub>/sunlight and near neutral photo-Fenton: a comparative study. *Appl Catal B Environ* 121:20–29
- Gassie LW, Englehardt JD (2017) Advanced oxidation and disinfection processes for onsite net-zero greywater reuse: a review. *Water Res* 125:384–399
- Giannakis S, Androulaki B, Comninellis C, Pulgarin C (2018a) Wastewater and urine treatment by UVC-based advanced oxidation processes: implications from the interactions of bacteria, viruses, and chemical contaminants. *Chem Eng J* 343:270–282
- Giannakis S, Papoutsakis S, Darakas E, Escalas-Cañellas A, Pétrier C, Pulgarin C (2015) Ultrasound enhancement of near-neutral photo-Fenton for effective *E. coli* inactivation in wastewater. *Ultrason Sonochem* 22:515–526
- Giannakis S, Voumard M, Rtimi S, Pulgarin C (2018b) Bacterial disinfection by the photo-Fenton process: extracellular oxidation or intracellular photo-catalysis? *Appl Catal B Environ* 227:285–295
- Grebel JE, Pignatello JJ, Mitch WA (2010) Effect of halide ions and carbonates on organic contaminant degradation by hydroxyl radical-based advanced oxidation processes in saline waters. *Environ Sci Technol* 44(17):6822–6828
- Hrudey SE (2009) Chlorination disinfection by-products, public health risk tradeoffs and me. *Water Res* 43(8):2057–2092
- Hulsmans A, Joris K, Lambert N, Rediers H, Declercq P, Delaet Y, Ollevier F, Liers S (2010) Evaluation of process parameters of ultrasonic treatment of bacterial suspensions in a pilot scale water disinfection system. *Ultrason Sonochem* 17(6):1004–1009
- Joyce E, Phull SS, Lorimer JP, Mason TJ (2003) The development and evaluation of electrolysis in conjunction with power ultrasound for the disinfection of bacterial suspensions. *Ultrason Sonochem* 10:231–234
- Keen OS, Dotson AD, Linden KG (2012) Evaluation of hydrogen peroxide chemical quenching agents following an advanced oxidation process. *J Environ Eng* 139(1):137–140
- Lakeh AAB, Kloas W, Jung R, Ariav RA, Knopf K (2013) Low frequency ultrasound and UV-C for elimination of pathogens in recirculating aquaculture systems. *Ultrason Sonochem* 20(5):1211–1216
- Linley E, Denyer SP, McDonnell G, Simons C, Maillard JY (2012) Use of hydrogen peroxide as a biocide: new consideration of its mechanisms of biocidal action. *J Antimicrob Chemother* 67(7):1589–1596
- Litter M, Quici N (2010) Photochemical advanced oxidation processes for water and wastewater treatment. *Recent Pat Eng* 4(3):217–241
- Lyons NA, Kolter R (2015) On the evolution of bacterial multicellularity. *Curr Opin Microbiol* 24:21–28
- Mahamuni NN, Adewuyi YG (2010) Advanced oxidation processes (AOPs) involving ultrasound for waste water treatment: a review with emphasis on cost estimation. *Ultrason Sonochem* 17(6):990–1003
- Malato S, Fernández-Ibáñez P, Maldonado MI, Blanco J, Gernjak W (2009) Decontamination and disinfection of water by solar photocatalysis: recent overview and trends. *Catal Today* 147(1):1–59

- Malvestiti JA, Dantas RF (2018) Disinfection of secondary effluents by  $O_3$ ,  $O_3/H_2O_2$  and  $UV/H_2O_2$ : influence of carbonate, nitrate, industrial contaminants and regrowth. *J Environ Chem Eng* 6(1):560–567
- Mamane H, Shemer H, Linden KG (2007) Inactivation of *E. coli*, *B. subtilis* spores, and MS2, T4, and T7 phage using  $UV/H_2O_2$  advanced oxidation. *J Hazard Mater* 146(3):479–486
- Mao Y, Wang X, Yang H, Wang H, Xie YF (2014) Effects of ozonation on disinfection byproduct formation and speciation during subsequent chlorination. *Chemosphere* 117:515–520
- Miklos DB, Remy C, Jekel M, Linden KG, Drewes JE, Hübner U (2018) Evaluation of advanced oxidation processes for water and wastewater treatment—a critical review. *Water Res* 139:118–131
- Miranda AC, Lepretti M, Rizzo L, Caputo I, Vaiano V, Sacco O, Silva W, Sannino D (2016) Surface water disinfection by chlorination and advanced oxidation processes: inactivation of an antibiotic resistant *E. coli* strain and cytotoxicity evaluation. *Sci Total Environ* 554:1–6
- Moghadam AK, Dore M (2012) Cost and efficacy of water disinfection practices: evidence from Canada. *Rev Econ Anal* 4(2):209–223
- Moreno-Andrés J, Romero-Martínez L, Acevedo-Merino A, Nebot E (2016) Determining disinfection efficiency on *E. faecalis* in saltwater by photolysis of  $H_2O_2$ : implications for ballast water treatment. *Chem Eng J* 283:1339–1348
- Naddeo V, Cesaro A, Mantzavinos D, Fatta-Kassinos D, Belgiomo V (2014) Water and wastewater disinfection by ultrasound irradiation—a critical review. *Global NEST J* 16(3):561–577
- Nocker A, Shah M, Dannenmann B, Schulze-Osthoff K, Wingender J, Probst AJ (2018) Assessment of UV-C-induced water disinfection by differential PCR-based quantification of bacterial DNA damage. *J Microbiol Methods* 149:89–95
- Ortega-Gómez E, García BE, Martín MB, Ibáñez PF, Pérez JS (2014) Inactivation of natural enteric bacteria in real municipal wastewater by solar photo-Fenton at neutral pH. *Water Res* 63:316–324
- Pablos C, Marugán J, van Grieken R, Serrano E (2013) Emerging micropollutant oxidation during disinfection processes using UV-C,  $UV-C/H_2O_2$ ,  $UV-A/TiO_2$  and  $UV-A/TiO_2/H_2O_2$ . *Water Res* 47(3):1237–1245
- Paleologou A, Marakas H, Xekoukoulotakis NP, Moya A, Vergara Y, Kalogerakis N, Gikas P, Mantzavinos D (2007) Disinfection of water and wastewater by  $TiO_2$  photocatalysis, sonolysis and UV-C irradiation. *Catal Today* 129:136–142
- Palková Z (2004) Multicellular microorganisms: laboratory versus nature. *EMBO Rep* 5(5):470–476
- Penru Y, Guastalli AR, Esplugas S, Baig S (2012) Application of UV and  $UV/H_2O_2$  to seawater: disinfection and natural organic matter removal. *J Photochem Photobiol A* 233:40–45
- Polo-López MI, Castro-Alfárez M, Oller I, Fernández-Ibáñez P (2014) Assessment of solar photo-Fenton, photocatalysis, and  $H_2O_2$  for removal of phytopathogen fungi spores in synthetic and real effluents of urban wastewater. *Chem Eng J* 257:122–130
- Ribeiro AR, Nunes OC, Pereira MF, Silva AM (2015) An overview on the advanced oxidation processes applied for the treatment of water pollutants defined in the recently launched directive 2013/39/EU. *Environ Int* 75:33–51
- Rodríguez-Chueca J, García-Cañibano C, Lepistö RJ, Encinas Á, Pellinen J, Marugán J (2018) Intensification of UV-C tertiary treatment: disinfection and removal of micropollutants by sulfate radical based advanced oxidation processes. *J Hazard Mat*. In press
- Rubio D, Nebot E, Casanueva JF, Pulgarin C (2013) Comparative effect of simulated solar light, UV,  $UV/H_2O_2$  and photo-Fenton treatment ( $UV-vis/H_2O_2/Fe^{2+,3+}$ ) in the *Escherichia coli* inactivation in artificial seawater. *Water Res* 47:6367–6379
- Rubio-Clemente A, Chica E, Peñuela GA (2015) Petrochemical wastewater treatment by photo-Fenton process. *Water Air Soil Pollut* 226(3):62–79
- Rubio-Clemente A, Chica E, Peñuela G (2017) Kinetic model describing the  $UV/H_2O_2$  photodegradation of phenol from water. *Chem Ind Chem Eng Q* 13(4):547–562
- Rubio-Clemente A, Chica E, Peñuela G (2018) Evaluation of the  $UV/H_2O_2$  system for treating natural water with a mixture of anthracene and benzo[a]pyrene at ultra-trace levels. *Environ Sci Pollut Res* 1–12
- Rubio-Clemente A, Torres-Palma RA, Peñuela GA (2014) Removal of polycyclic aromatic hydrocarbons in aqueous environment by chemical treatments: a review. *Sci Total Environ* 458:201–225
- Santos AL, Oliveira V, Baptista I, Henriques I, Gomes NC, Almeida A, Correia A, Cunha Á (2013) Wavelength dependence of biological damage induced by UV radiation on bacteria. *Arch Microbiol* 195(1):63–74
- Serna-Galvis EA, Salazar-Ospina L, Jiménez JN, Pino NJ, Torres-Palma RA (2018) Elimination of carbapenem resistant *Klebsiella pneumoniae* in water by UV-C, UV-C/persulfate and UV-C/ $H_2O_2$ . Evaluation of response to antibiotic, residual effect of the processes and removal of resistance gene. *J Environ Chem Eng*. In press
- SIAC (2018). Catálogo de mapas. Sistema de Información Ambiental de Colombia. Ministerio de Ambiente, Vivienda y Desarrollo Sostenible. Retrieved from: <http://www.siac.gov.co/catalogo-de-mapas> (September 13, 2018)
- Spuhler D, Rengifo-Herrera JA, Pulgarin C (2010) The effect of  $Fe^{2+}$ ,  $Fe^{3+}$ ,  $H_2O_2$  and the photo-Fenton reagent at near neutral pH on the solar disinfection (SODIS) at low temperatures of water containing *Escherichia coli* K12. *Appl Catal B Environ* 96(1):126–141
- Szczuka A, Parker KM, Harvey C, Hayes E, Vengosh A, Mitch WA (2017) Regulated and unregulated halogenated disinfection byproduct formation from chlorination of saline groundwater. *Water Res* 122:633–644
- Urbano VR, Peres MS, Maniero MG, Guimarães JR (2017) Abatement and toxicity reduction of antimicrobials by  $UV/H_2O_2$  process. *J Environ Manag* 193:439–447
- WEF & AWWA (2012) Standard Methods for the Examination of Water and Wastewater, 22nd edn. American Public Health Association, Washington, DC
- Wei H, Hu D, Su J, Li K (2015) Intensification of levofloxacin sonodegradation in a  $US/H_2O_2$  system with  $Fe_3O_4$  magnetic nanoparticles. *Chin J Chem Eng* 23(1):296–302
- WHO (2011) Guidelines for drinking-water quality. *WHO Chron* 38(4): 104–108
- Xie Y (2016) Disinfection byproducts in drinking water: formation, analysis, and control. CRC press
- Zhou S, Huang S, Li X, Angelidaki I, Zhang Y (2018) Microbial electrolytic disinfection process for highly efficient *Escherichia coli* inactivation. *Chem Eng J* 342:220–227
- Zhou X, Li Z, Lan J, Yan Y, Zhu N (2017) Kinetics of inactivation and photoreactivation of *Escherichia coli* using ultrasound-enhanced UV-C light-emitting diodes disinfection. *Ultrason Sonochem* 35: 471–477

**Paper**

**Photovoltaic array for powering advanced oxidation processes: Sizing, application and investment costs for the degradation of a mixture of anthracene and benzo[a]pyrene in natural water by the UV/H<sub>2</sub>O<sub>2</sub> system**

**Journal**

Scope: The Journal of Environmental Chemical Engineering provides a forum for the publication of original research on the development of sustainable technologies focusing on water and wastewater treatment and reuse; pollution prevention; resource recovery of waste; nanomaterials for environmental applications; sustainability and environmental safety; and recent developments on green chemistry.

**Highlights**

- A PV system for using advanced oxidation processes is sized.
- The PV array provides the energy requirements demanded by the UV/H<sub>2</sub>O<sub>2</sub> process.
- The integrated UV/H<sub>2</sub>O<sub>2</sub>/PV system allows achieving high degradation efficiencies.
- The investment costs of the integrated system were estimated and discussed.
- The system fosters the development of NIZs in developed and developing countries.







Contents lists available at ScienceDirect

Journal of Environmental Chemical Engineering

journal homepage: [www.elsevier.com/locate/jece](http://www.elsevier.com/locate/jece)

# Photovoltaic array for powering advanced oxidation processes: Sizing, application and investment costs for the degradation of a mixture of anthracene and benzo[a]pyrene in natural water by the UV/H<sub>2</sub>O<sub>2</sub> system

Ainhoa Rubio-Clemente<sup>a,b,c,\*</sup>, E. Chica<sup>d</sup>, Gustavo A. Peñuela<sup>b</sup><sup>a</sup> Facultad de Ciencias de la Salud, Universidad Católica de Murcia UCAM, Avenida de los Jerónimos, s/n, Murcia, Spain<sup>b</sup> Grupo GDCON, Facultad de Ingeniería, Sede de Investigaciones Universitarias (SIU), Universidad de Antioquia UdeA, Calle 70, No. 52-21, Medellín, Colombia<sup>c</sup> Facultad de Ingeniería, Tecnológico de Antioquia–Institución Universitaria TdeA, Calle 78b No. 72A-220, Medellín, Colombia<sup>d</sup> Departamento de Ingeniería Mecánica, Facultad de Ingeniería, Universidad de Antioquia UdeA, Calle 70, No. 52-21, Medellín, Colombia

## ARTICLE INFO

## Keywords:

Photovoltaic energy  
Renewable energy  
Advanced oxidation process  
Water pollution  
Polycyclic aromatic hydrocarbon  
Investment cost

## ABSTRACT

Advanced oxidation processes (AOPs) are commonly known as efficient water treatment techniques able to oxidize a great variety of pollutants from water that are otherwise difficult to be converted. Nevertheless, AOPs are costly processes, particularly, because of the electrical costs associated. In this regard, photovoltaic (PV) energy can be used to power the AOP in a reliable and autonomous way. In this work, the steps for sizing a solar PV system for water treatment using AOPs are described. Additionally, the feasibility of the use of a PV array without batteries to supply the electrical power needs of a UV/H<sub>2</sub>O<sub>2</sub> advanced oxidation system for degrading natural water containing 12 and 3 μg L<sup>-1</sup> of anthracene and benzo[a]pyrene, respectively, two of the priority polycyclic aromatic hydrocarbons because of their harmful effects on living beings, was studied. It was found that more than 99% of anthracene and benzo[a]pyrene were removed and about 45% of the total organic matter was mineralized after 15 and 90 min of treatment, indicating the high efficiency of the system. Finally, the investment costs of the UV/H<sub>2</sub>O<sub>2</sub>-PV system for a small application were estimated with and without batteries in order to define the optimum PV array configuration. The PV array designed and applied allows for the decontamination of persistent pollutants in natural water in an environmentally-friendly and sustainable way.

## 1. Introduction

With the rapid economic growth experienced in the last decades, aquatic resources are being more and more polluted, mainly from industrial discharges, with recalcitrant and persistent toxic substances. In order to remove these harmful compounds and preserve the aquatic systems, different treatment processes have been conventionally used. Among them, the mechanical, physical, chemical and biological traditional processes, such as filtration, flocculation and chemical coagulation, can be named [1–3]. Nevertheless, although these kind of techniques can remove the toxic substances, they are not able to efficiently degrade them; being required the use of alternative treatments [1–5]. Under this scenario, the application of advanced oxidation processes (AOPs) is regarded as promising alternative treatments able to convert recalcitrant organic substances [3].

AOPs consist of the formation of hydroxyl radicals (HO<sup>•</sup>). With an oxidation potential of 2.8 V [6], these chemical species are highly reactive and transform the more persistent molecules into

environmentally safe degradation by-products, such as H<sub>2</sub>O, CO<sub>2</sub> and inorganic ions [7]. Due to their low selectivity, HO<sup>•</sup> are able to attack a wide range of pollutants, exhibiting rate constants in the range from 10<sup>6</sup> to 10<sup>9</sup> M<sup>-1</sup> s<sup>-1</sup> [8]. Consequently, AOPs are very versatile processes that can be used for the treatment of both wastewater and drinking water [3,4,9,10]. Several AOPs have been developed and the efficiency of these advanced oxidation techniques varies as a function of the operating conditions used and the compound to be treated [11]. However, AOPs using radiation are usually preferred; especially the UV/H<sub>2</sub>O<sub>2</sub> system has been reported as a very effective process, achieving high pollutant reductions in a short period of time [4,10,12,13].

UV/H<sub>2</sub>O<sub>2</sub> system is based on the photolysis of H<sub>2</sub>O<sub>2</sub> or its conjugate base (HO<sub>2</sub><sup>-</sup>) under light with a wavelength below 300 nm [3], being germicide lamps widely used. The homolysis of H<sub>2</sub>O<sub>2</sub> gives HO<sup>•</sup> (Eq. (1)).



\* Corresponding author at: Facultad de Ingeniería, Tecnológico de Antioquia–Institución Universitaria TdeA, Calle 78b No. 72A-220, Medellín, Colombia.  
E-mail address: [ainhoa.rubio@tdea.edu.co](mailto:ainhoa.rubio@tdea.edu.co) (A. Rubio-Clemente).

<https://doi.org/10.1016/j.jece.2018.03.046>

Received 18 September 2017; Received in revised form 4 March 2018; Accepted 24 March 2018

Available online 27 March 2018

2213-3437/ © 2018 Elsevier Ltd. All rights reserved.

In spite of the strong potential of this oxidation process in degrading substances and purifying water, it is well known that their operating costs regarding the input of chemicals and energy [14], as occurred with other AOPs, are relatively high compared to the costs associated with conventional water treatment processes [3] although AOP installing costs are quite low. As a matter of fact, Hofman-Caris and Beerendonk [15] found that a reduction of 90% of MTBE using the UV/H<sub>2</sub>O<sub>2</sub> system operating with UV-C lamps implies an Electrical Energy per Order (EEO) between 11 and 55 kWh m<sup>-3</sup> using 10 mg L<sup>-1</sup> of H<sub>2</sub>O<sub>2</sub> and an energy dose of 450 mJ cm<sup>-2</sup>. Hansen and Andersen [16] studied the required energy per m<sup>3</sup> of water treated for several emerging pollutants, including the families of parabens, industrial phenols, sunscreen chemicals and estrogens. It was found an EEO from 1.8 to 8.7 kWh m<sup>-3</sup> with benzophenone-7 and bisphenol A as the most recalcitrant products requiring higher EEO to be eliminated [16]. Even though the use of H<sub>2</sub>O<sub>2</sub> reduces the electrical costs compared to the energy costs associated with the utilization of UV radiation alone, they are high when compared to those ones generated in a conventional process. For instance, it has been evidenced a cost of 0.25 € m<sup>-3</sup> in removing nutrients using activated sludge treatment [17]. Under this scenario, in order to overcome this drawback, the efficiency of some AOPs, such as photo-Fenton processes and systems using heterogeneous catalysts, like TiO<sub>2</sub>, has been studied under solar light since these processes can be performed directly using this natural and economical source of energy [3,9,18]. However, the UV/H<sub>2</sub>O<sub>2</sub> process can benefit from a reduced amount of solar radiation corresponding to the UV-C spectrum, limiting the efficiency of this oxidation process when driven by direct solar light. Consequently, an alternative source of energy must be used to reduce the UV/H<sub>2</sub>O<sub>2</sub> system electrical operating costs associated with the utilization of conventional forms of energy.

Among the types of renewable electrical energy, the generation of photovoltaic (PV) electricity is one of the most widespread. PV cells directly convert sunlight into electricity [19–22]. Therefore, PV systems can be used as a power supply for AOP application, such as the UV/H<sub>2</sub>O<sub>2</sub> system; i.e., the electricity generated with a solar PV system can be either stored or used directly in the water pump, lamps, magnetic stirrer, etc.; and, generally, in the equipment used in the water treatment systems.

Typically, as illustrated in Fig. 1, a PV system consists of several stacks of PV modules, batteries, a regulator or charge controller, an inverter and loads. These components should be selected according to the system type, site location and application. As it is widely known, PV modules can be connected in series and/or parallel, transforming the solar radiation incident on the surface of the PV array into electrical energy (direct current). Then, the electrical energy is passed to a regulator before being sent to the batteries. The function of the regulator is to prevent the batteries from an overcharging discharge. In turn, the energy stored in the batteries is used as backup electricity during low solar radiation and at night [21,23,24]. On the other hand, the role of the inverter is to convert the direct current (DC) into alternating current (AC) for devices that work in AC mode.

The advantages of using PV energy are that it is a non-polluting source of energy once the solar panels have been produced, and it is a silent, abundant, decentralized, free and long life source of energy. The low operating and maintenance costs of PV systems are also another positive factor [22] compared to the associated costs of other renewable energy systems. In this regard, generation of electricity by means of solar PV systems has gained popularity in recent years because of the capability of these systems to convert sunlight into direct electricity, contributing to the world energy supply in a way that is compatible with the concept of sustainable development [21,25,26]. On the other hand, PV systems can be utilized in remote sites for the self-sufficiency of electrical power in a reliable and autonomous way. However, a disadvantage of solar PV arrays is that, as the majority of renewable energy sources, solar energy is intermittent; i.e., it is not shining at night or during daytime with cloudy or rainy weather. Consequently,

intermittency and unpredictability of solar energy makes solar energy panels a less reliable solution. Additionally, solar energy panels require additional equipment, such as inverters, for the generated electricity to be used on the power network. For a continuous supply of electrical power; especially, for on-grid connections, PV panels also require storage batteries; thus, the investment cost for PV panels are considerably increased. Furthermore, the cycling capability of a battery is an important factor on the PV system lifetime, as well as the operating temperature and resistance to internal corrosion. In general terms, in PV systems, the batteries must be periodically replaced due to their lifetime is about 10 or 15 years [27], which increases the PV array costs and leads to a potential pollution of the environment [28,29,21]. Moreover, solar panel efficiency levels are relatively low (between 14%–25%) compared to the efficiency levels of other renewable energy systems. Finally, in case of land-mounted PV panel installations, relatively large areas for deployment are needed when a high installed capacity is desired; being usually the land space committed for this purpose for a period of 15–20 years, or even longer, when the investment payback is intended to be achieved [21,25,26]. Therefore, in order to reduce the drawbacks associated, an accurate design and sizing of the PV systems is required.

In this context, this work is focused on the description of the steps for properly designing a solar PV system for water treatment using AOPs. The system was sized and applied for supplying the energy required in the implementation of the UV/H<sub>2</sub>O<sub>2</sub> oxidation process for degrading natural water containing 12 and 3 µg L<sup>-1</sup> of anthracene and benzo[a]pyrene, respectively, which are toxic compounds, using an annular photoreactor at laboratory-scale operating in batch conditions. Additionally, the cost of the UV/H<sub>2</sub>O<sub>2</sub>-PV system for small applications was estimated with and without batteries.

## 2. Materials and methods

### 2.1. Chemicals and reagents

The following reagents without further purification were used. For photodegradation studies, anthracene (AN) (C<sub>14</sub>H<sub>10</sub>, 99.5%, HPLC grade) and benzo[a]pyrene (BaP) (C<sub>20</sub>H<sub>12</sub>, 96% HPLC grade) purchased from Alfa Aesar (Ward Hill, MA, USA) were used. As analytical controls, for analytical determinations, AN (98.5%, HPLC grade) and BaP (99.6%, HPLC grade) reference standard provided by Dr. Ehrenstorfer (Augsburg, Germany) were utilized, as well as acetonitrile gradient grade supplied by Merck (Darmstadt, Germany) and deionized water obtained from a Millipore purification system (Bedford, MA, USA), as mobile phase components. Hydrogen peroxide (H<sub>2</sub>O<sub>2</sub>, 30% w/w), used as oxidant, was obtained from J.T. Baker (Ecatepec, Estado de Mexico, Mexico). For AN and BaP reaction intermediate studies, acetone analytical grade (> 99%) (Honeywell International Inc., NJ, USA), isopropanol analytical grade (> 99%), methanol HPLC grade from Merck, and 1-octyl-3-methylimidazolium hexafluorophosphate (> 98%) (Acros Organics, Geel, Belgium) were utilized. Additionally, during H<sub>2</sub>O<sub>2</sub> determination ammonium monovanadate (NH<sub>4</sub>VO<sub>3</sub>, 99.9%) and sulfuric acid (H<sub>2</sub>SO<sub>4</sub>, 95–97%) purchased from Merck were used.

### 2.2. Feed water quality

The photochemical experiments were conducted using natural water from a Colombian surface reservoir located in “El Peñol” (Guatapé, Antioquia, Colombia) (N 6° 17′ 41.1583″ O 75° 9′ 31.0821″). The collected natural water was characterized by its low organic matter concentration, in terms of total organic carbon (2.03 mg L<sup>-1</sup>), and dissolved iron content (0.047 mg L<sup>-1</sup>). Additionally, the tested water had an average temperature, pH, turbidity, conductivity and dissolved oxygen of 23.58 °C, 7.35, 1.09 NTU, 39.87 µS cm<sup>-1</sup>, and 8.61 mg L<sup>-1</sup>, respectively. Since in the tested water, the compounds of interest, AN and BaP, were not detected, they were spiked at a concentration of 12

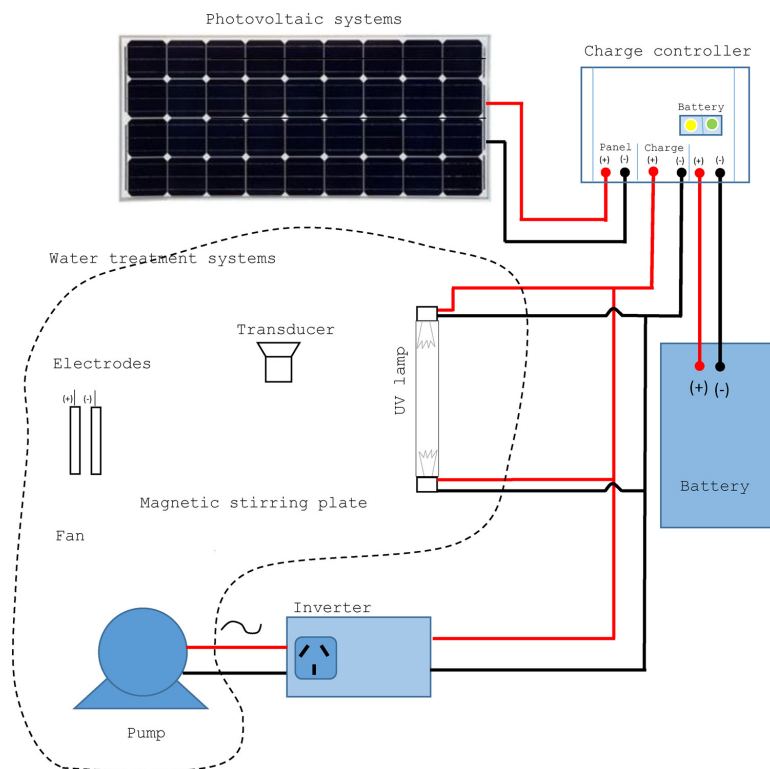


Fig. 1. Diagram of a PV system.

and  $3 \mu\text{g L}^{-1}$ , respectively. On the other hand, deionized water containing  $0.5 \text{ mg L}^{-1}$  of AN and BaP individually added was utilized for the degradation by-product studies.

### 2.3. Photochemical experimental system

A PV system was utilized to supply the electric needs of the photochemical reactor used for the implementation of the UV/H<sub>2</sub>O<sub>2</sub> process (Fig. 2). The PV system was sized without batteries and included 9 PV modules, a charge controller and an inverter. On the other hand, the photoreactor consisted of a 2 L annular basin made of borosilicate glass. The photoreactor was operated in batch mode and was equipped with one and three 8 W Hg vapor UV-C low pressure (LP) lamps from General Electric International Inc. (Fairfield, CT, USA), emitting mainly at 254 nm and contained in quartz tubes. The irradiance was measured in the photoreactor using a UVX radiometer equipped with a UVX-25 sensor (UVP, Upland, CA, USA) once the radiation beam emitted by the lamps went through the quartz tube separating each lamp and the reaction chamber. The sensor was placed at different locations within the reaction chamber; specifically, at the top, in the middle and at the bottom, and the irradiance values were registered in triplicate. The radiation recording values were averaged, resulting to be 170 and  $460 \mu\text{W cm}^{-2}$  for 1 and 3 UV-C LP lamps, respectively. It is important to note that lamps were previously warmed up for at least 30 min prior to sample photolysis to enable them to stabilize and reach their maximum relative spectral output.

On the other hand, in order to simulate the natural temperature water can be found and aiming at avoiding incurring in unnecessary operating costs, the experiments were performed at a constant

temperature of  $25 \pm 1 \text{ }^\circ\text{C}$ . This was possible due to the photochemical reactor was equipped with a cooling jacket. Additionally, 5, 10 and  $15 \text{ mg L}^{-1}$  of H<sub>2</sub>O<sub>2</sub>, which was added in one step before operating the photoreactor, were used. These H<sub>2</sub>O<sub>2</sub> concentrations were selected focusing on the experimental conditions and conclusions withdrawn from a number of studies applying the UV/H<sub>2</sub>O<sub>2</sub> system for the removal of polycyclic aromatic hydrocarbons (PAHs), as reviewed by Rubio-Clemente et al. [3]. Photoreactor effluent sampling procedure was conducted at different time intervals. Samples were stored in the dark at  $4 \pm 0.5 \text{ }^\circ\text{C}$  and analyzed as soon as possible in order to avoid losses of the target analytes. The experiments were performed in triplicate.

The pH of the reaction solution was not altered during the experiments in order to reduce the operating costs linked to the reduction of this parameter and its increase before serving the treated water.

### 2.4. Analysis and instrumentation

For the analysis of AN and BaP, an Agilent Technologies Inc. RP-HPLC system series 1100/1200 (Palo Alto, CA, USA) with a fluorescence detector was used under the operating conditions specified elsewhere [30]. Moreover, total organic carbon (TOC) was determined based on the high temperature combustion analytical method (5310B) described in [31]. For this purpose, an Apollo 9000 series TOC analyzer (Teledyne Tekmar, Mason, OH, USA) was used.

For the identification of the degradation by-products, sample preparation was performed according to the procedure reported elsewhere [32] and 20  $\mu\text{L}$  of the sample were injected into a 7890A gas chromatograph (GC) coupled to a 5975C mass spectrometer (MS) equipped with a programmed temperature vaporizing injector purchased from

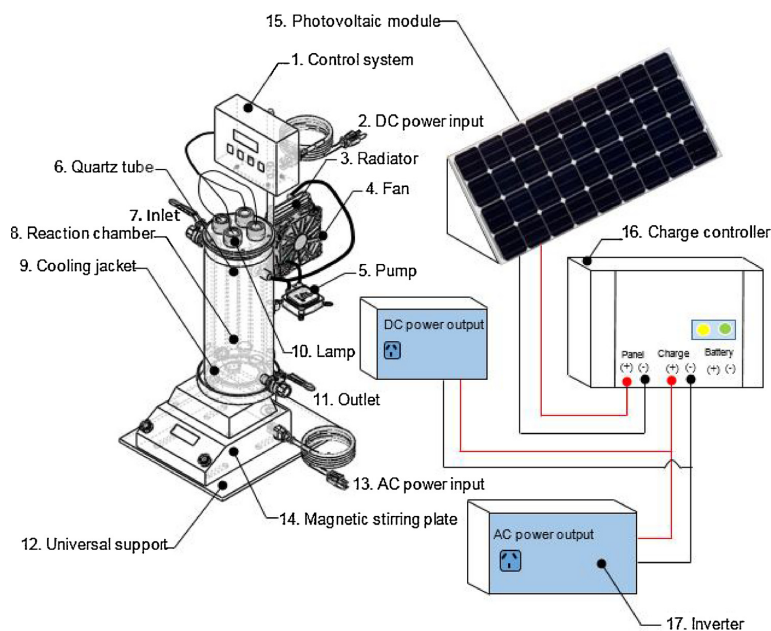


Fig. 2. Annular jacketed multi-lamp photoreactor directly powered by a photovoltaic array.

Agilent Technologies Inc. A HP-5MS UI (60 m  $\times$  250  $\mu\text{m}$  i.d.  $\times$  0.25  $\mu\text{m}$  film thickness) obtained from Agilent Technologies Inc. was used for the separation of the sample constituents. The column was held at 60  $^{\circ}\text{C}$  for 4 min and then increased at 15  $^{\circ}\text{C min}^{-1}$  to 325  $^{\circ}\text{C}$ , where it was held for 7 min. Helium (Linde, Medellín, Colombia) was employed as the carrier gas at a constant flow rate of 1.1  $\text{mL min}^{-1}$  and a linear velocity of 27.14  $\text{cm s}^{-1}$ . The MS was operated in the electron impact ionization mode and the energy of electrons was kept at 70 V. The temperature of the interface, ionization source and the quadrupole were kept at 280, 230 and 150  $^{\circ}\text{C}$ , respectively. Data were acquired in the full-scan detection mode from 40 to 500 u. HP MSD ChemStation software (Hewlett Packard Co., CA, USA) was employed.

$\text{H}_2\text{O}_2$  evolution was also determined using a UV–vis spectrophotometer Evolution 300 from Thermo Scientific (Waltham, MA, USA). Further information on the analytical method and equipment used for  $\text{H}_2\text{O}_2$  analysis can be found in [33].

With regard to solar irradiance measurements, a CM 6B solar radiation meter (Kipp & Zonen B.V., Delft, The Netherlands) placed on a horizontal plane surface located in University of Antioquia, Medellín, Colombia (N 6 $^{\circ}$  11' 55.428" O 75 $^{\circ}$  34' 1.943") was used. The instrument was installed on the roof-top of a block of the University at a relatively free position from external obstructions and accessible for general inspection and maintenance.

### 3. Results and discussion

#### 3.1. Optimal tilt angle for the PV system

Designing an installation to yield a maximum annual energy helps to minimize the necessary installed capacity and reduce the cost of equipment. Therefore, it is important to identify the variables that affect the design [20,22,34–37]. For example, the output voltage of solar panels essentially remains constant even as the solar irradiance is changing; however, the amount of the current produced by the solar panels is directly proportional to the solar irradiance [35,38]. In this

regard, solar irradiation is one of the most important parameters that may be taken into consideration for designing and utilizing a PV system.

The amount of solar irradiation received on a PV panel depends on the latitude ( $\varphi$ ), day of the year, slope or tilt angle ( $\beta$ ), surface azimuth angle ( $\alpha$ ), time of the day, and the angle of incident radiation. The factors that can be controlled to maximize the amount of irradiation received upon the panel are the surface azimuth and the tilt angle. In the current case, due to the geographical situation of Medellín, the PV modules are oriented towards the South; therefore, the azimuth angle is equal to 0 $^{\circ}$ . Concerning the tilt angle, there are some theoretical and empirical models in the literature for calculating the optimal tilt angle and solar irradiation absorbed by a PV panel when mounted at right angles to the sun rays [20,22,35,36]. It is noteworthy that the optimization of the tilt angle is one of the essential processes during PV system sizing in order to achieve the maximum profit from solar radiation for energy generation.

Moreover, as it is widely known, the output power of a PV system is increased with the increase of the solar irradiance in the morning and is decreased with the decrease of the solar irradiance in the afternoon. Additionally, solar irradiance ( $\text{W m}^{-2}$ ) and, relatedly, irradiation or insolation ( $\text{kWh m}^{-2}\text{day}^{-1}$ ) are measurements of how much solar power a location receives. Naturally, solar irradiance varies throughout the day according to the sun position, the presence of clouds and throughout the year depending on the season [34]. In the case of study, Medellín is characterized by a subtropical climate with two rainy and dry seasons throughout the year.

Since the number of operating appliances depends on the output power of the PV system, the equipment used in the AOP should fully operate during the period from 9:30–15:30, where the maximum output power occurs, as the maximum values of solar irradiance are achieved at this time slot, as shown in Fig. 3, in which the variation of the solar irradiance during a typical day from dry and rainy seasons in University of Antioquia is illustrated. From the figure, it can be observed that a peak of solar irradiance at noon is achieved, with a maximal solar

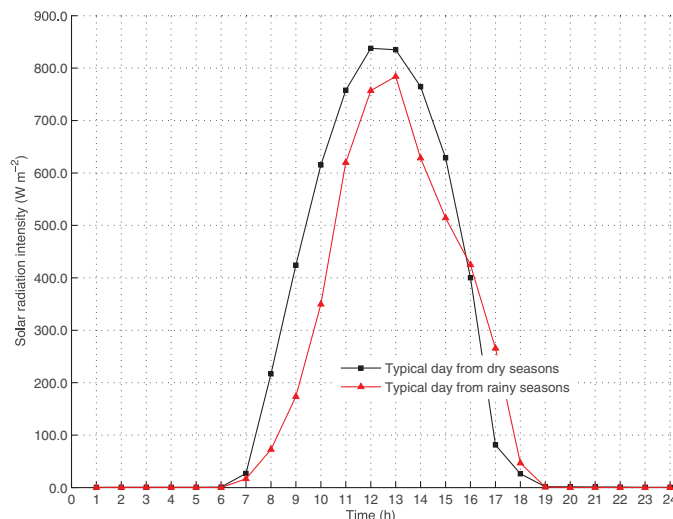


Fig. 3. Solar radiation intensity variation during a typical day from dry and rainy seasons.

irradiance corresponding to a typical day from the dry seasons. At night, the solar irradiance had a value of zero in both of the considered situations. These results indicate that the optimal working hours in a typical sunny and cloudy day for using solar radiation are about 6 h per day distributed around noon, as mentioned above. Based on the observational data of solar radiation intensities during 2015, the average solar irradiance in Medellín was found to be  $273.7 \text{ W m}^{-2}$ .

In Table 1, the average solar irradiation values received per month in University of Antioquia during 2015 on a horizontal plane surface, are compiled, observing maximal and minimal values for the dry and rainy seasons, respectively. From these data, the average value of the solar insolation received was  $4.33 \text{ kWh m}^{-2} \text{ day}^{-1}$  during 2015. Table 1 also details the tilt angle, as well as the solar irradiation on a tilted surface and the equivalent peak solar hour (PSH); values that are required to determine the number of panels used in the PV system. It is highlighted that PSH indicates the number of hours per month the modules receive  $1000 \text{ W m}^{-2}$ . Therefore, from these PSH, the energy generated by the PV module can be calculated using the specification given by the manufacturer, since all the nominal characteristics are provided for an irradiation of  $1000 \text{ W m}^{-2}$ .

In this work, during the sizing phase of the PV system, the design criterion was the worst irradiation month at the installation site of the solar plant. Therefore, an equivalent PSH of 4.10 (corresponding to the month of April or May) was used for sizing the PV system required to supply the energy demand of the selected UV/H<sub>2</sub>O<sub>2</sub> system for degrading natural water containing AN and BaP at a concentration of 12 and  $3 \mu\text{g L}^{-1}$ , respectively. Furthermore, the optimum tilt angle in this study was found to be  $15.64^\circ$ , which corresponds to the average value of the optimal tilt angle for each month, as shown in Table 1.

### 3.2. Steps for sizing a PV system

The selection and design of the required equipment, such as the batteries, inverter, controller, power electronic devices and wiring, are vital for guarantying a high efficiency and operation of the PV systems. Therefore, during the sizing of a PV array, selecting the proper technology to reduce losses and improve the power conversion efficiency of the PV system is needed [39]. In addition, a reliable knowledge of the equipment efficiency used for the PV array operation is essential to accurately predict the electricity production. Consequently, for the

calculation of the current PV system sizing, the efficiency of the equipment used was taken into account (Table 2). On the other hand, several environmental factors contributing to the system output losses, including sub-optimal orientation with respect to the sun, soiling, shading and, in some countries, seasonal snow cover, must be also considered for an efficient PV array design [39].

On the basis that one of the primary concerns in designing any PV system is the determination of the correct size of the PV array [21,37,40,41], the most important design factor is the power consumption by the equipment used during the AOP operation. Thus, the first step in designing a solar PV system is to find out the total power of the energy consumed by the devices involved in the water treatment process. The next step consists of sizing the PV modules, inverter, batteries and the solar charge controller. For this purpose, the electricity demand must be considered in order to avoid over or undersizing the system. PV module sizing procedure must be based on the nominal power of the modules so that the required power rating can be met by the different combinations of the modules in series or parallel [20,22,34–37]. Moreover, an inverter is used in the system where AC power output is needed. The input rating of the inverter should never be lower than the total Watts of appliances. The inverter must have the same nominal voltage as the battery. For stand-alone systems, the inverter must be large enough to handle the total amount of Watts to be used at a time. In this regard, the inverter size should be 25–30% larger than the total Watts of appliances. In case of the appliance is a motor or a compressor, then the inverter size should be minimum 3 times the capacity of those appliances, and must be added to the inverter capacity to handle the surge current during starting. For grid-connected systems, the input rating of the inverter should be the same as the PV array rating to allow for safe and efficient operation. Additionally, in stand-alone PV systems the battery plays an important role in matching the load requirement for the system. The battery type recommended to be used in a solar PV system is deep cycle battery. Deep cycle battery is specifically designed for being discharged to low energy level and rapid recharged or cycle charged and discharged day after day for years. The battery should be large enough to store sufficient energy for the appliances to operate at night and cloudy days. In locations where there is a big fluctuation in irradiation, at least 2–3 days and 3–5 days of reserve for the summer and winter months, respectively, can be required. Finally, in order to match the voltage of the PV array and batteries, the

**Table 1**  
Calculation of the PSH and optimal tilt angle for the operation of a PV array in Medellín, Antioquia, Colombia [22,20,34–37,40].

Parameter	Jan	Feb	Mar	Apr	May	Jun	Jul	Aug	Sep	Oct	Nov	Dec	Formula
Number of days of the month	31	28	31	30	31	30	31	31	30	31	30	31	-
Solar insolation on a plane horizontal surface, $G_{\alpha}$ (kWh m <sup>-2</sup> day <sup>-1</sup> )	4.40	4.42	4.26	4.16	4.00	4.26	4.67	4.58	4.57	4.18	4.10	4.32	-
Day year <sup>-1</sup> ( $\delta_s$ ) <sup>a</sup>	15	45	76	106	137	168	198	229	259	290	321	351	-
Declination angle ( $\delta$ ) <sup>b</sup>	-21.27	-13.62	-2.02	9.78	19.26	23.39	21.18	13.12	1.81	-10.33	-19.60	-23.40	$\delta = 23.458 \sin \left( \frac{360 \cdot 284 + 5n}{365} \right)$
Solar elevation angle ( $\theta$ )	62.50	70.15	81.75	93.55	103.03	107.16	104.95	96.89	85.58	73.44	64.17	60.37	$\theta = (90 - \varphi - \delta)$ at the winter solstice $\theta = (90 - \varphi + \delta)$ at the summer solstice
Tilt angle ( $\beta$ )	27.50	19.85	8.25	3.55	13.03	17.16	14.95	6.89	4.42	16.56	25.83	29.63	$\beta = \varphi - \delta$ at the summer solstice $\beta = \varphi + \delta$ at the winter solstice $\beta = \varphi$ at the equinoxes.
Solar insolation on a tilted surface, $G_{\alpha}(\beta_{opt})$ (kWh m <sup>-2</sup> day <sup>-1</sup> )	4.90	4.68	4.31	4.17	4.11	4.45	4.83	4.62	4.59	4.35	4.51	4.90	$G_{\alpha}(\beta_{opt}) = \frac{G_{\alpha}(\theta)}{1 - 4.46 \times 10^{-4} \beta_{opt} - 1.19 \times 10^{-6} \beta_{opt}^2}$
Insolation factor (IP)	0.98	1.00	0.99	0.98	1.00	1.00	1.00	0.99	0.98	1.00	0.99	0.98	$IP = 1 - [1.2 \times 10^{-4} (\beta - \beta_{opt})^2 + 3.5 \times 10^{-5} \beta^2]$ for $15^\circ < \beta < 90^\circ$ $IP = 1 - [1.2 \times 10^{-4} (\beta - \beta_{opt})^2]$ for $\beta \leq 15^\circ$
PSH day <sup>-1</sup>	4.82	4.67	4.28	4.10	4.10	4.45	4.83	4.58	4.52	4.35	4.45	4.78	$G_{\alpha}(\beta_{opt}) / IP / 1000$

<sup>a</sup> Day of the year (1, ..., 365, taking 1 for January the 1st). One day of each month was selected, which corresponded to one day in the middle of the month.  
<sup>b</sup> Angle between the Equator and a line drawn from the center of the Earth to the center of the sun. This angle varies seasonally due to the tilt of the Earth on its axis of rotation and the rotation of the Earth around the sun.  
<sup>c</sup> Amount of solar radiation incident on a tilted module surface (i.e., the component of the incident solar insolation which is perpendicular to the module surface).

**Table 2**  
Predefined design parameters.

Item	ID <sup>a</sup>	Characteristics (units)	Value	
General data	A1	Equivalent peak solar hour (PSH)	4.10	
	A2	Days of autonomy (days)	2	
	A3	System voltage (V)	12	
Battery data sheet	A4	Nominal battery voltage (V)	12	
	A5	Battery loss (%)	85	
	A6	Battery capacity (Ah)	100	
	A7	Depth of battery discharge (%)	60	
Inverter data	A8	Inverter efficiency (%)	90	
	A9	PV module (Wp)	250	
PV module data sheet	A10	Nominal power of the PV module (V)	12	
	A11	Panel efficiency (%)	15.10	
	A12	Maximum power voltage, Vm (V)	31	
	A13	Maximum power current, Im (A)	8.08	
	A14	Weight (kg)	20	
	A15	Size (mm)	1625 × 1019	
	A16	Open circuit voltage, Voc (V)	21.6	
	A17	Short circuit current, Isc (V)	9.16	
	Solar charge controller data	A18	Solar charge controller loss (%)	30

<sup>a</sup> Identifier.

solar charge controller must be selected. It is important to note that the solar charge controller must have enough capacity to handle the current from the PV array.

Particularly, for the UV/H<sub>2</sub>O<sub>2</sub> treatment, electrical energy is consumed during the effluent mechanical stirring, UV radiation generation, recirculation pumping and the systems of refrigeration and ventilation. Thus, the spreadsheet shown in Tables 2 and 3 was used to obtain the components of the PV system for the UV/H<sub>2</sub>O<sub>2</sub> system at pilot-scale operating in batch conditions. For sizing the PV system with batteries, an operating time of the UV/H<sub>2</sub>O<sub>2</sub> system per day of 6 h was taken into consideration. In addition, the PV system with batteries was sized considering an autonomy of the system of 2 days.

Tables 2 and 3 can be used for sizing any PV system supplying the energy required for the operation of the considered AOP, taking into account that the energy consumption of the selected AOP varies with the particular AOP equipment needed during the operation time. Consequently, the data referred in step 1 of Table 3, regarding the energy consumption, must be modified as a function of the particular AOP carried out. Additionally, the days of autonomy and the total hours demanded per day can be modified according to the requirements of the considered advanced oxidation system.

### 3.3. Operation of the UV/H<sub>2</sub>O<sub>2</sub>-PV system

Based on the experimental conditions mentioned above and reported in detail elsewhere [33], the efficiency of the UV/H<sub>2</sub>O<sub>2</sub> water treatment system directly powered by a PV array for degrading of AN and BaP present in natural water at a concentration of 12 and 3 μg L<sup>-1</sup>, respectively, was evaluated. The operating conditions consisted of the use of 1 and 3 UV-C LP lamps for removing the target PAHs and the organic matter, respectively. In Fig. 4, the evolution of AN and BaP removal percentage with the reaction time using only 1 lamp is showed. It can be observed that the system using solar energy as power is able to remove more than 90% of both of the selected PAHs in a treatment period of 5 min, as occurred with the system connected to the electrical grid [33]. After 15 min of treatment, more than 99% of AN and BaP were converted. As observed, for removing 99% of the selected PAHs at the studied concentrations, only the UV-C light was needed due to the absorbance properties of these pollutants for this wavelength [42,43]. However, organic matter elimination was insignificant under these

**Table 3**  
Computed parameters [20,22,34–37,40].

Solar PV system sizing		Equipment used in the considered AOP							
		Amount	Power consumption DC at 12 V (W)	Power consumption AC (W)	Total power consumption (W)	Daily use (h day <sup>-1</sup> )	Total power DC (Wh day <sup>-1</sup> )	Total power AC (Wh day <sup>-1</sup> )	Total power (Wh day <sup>-1</sup> )
Step 1. Power consumption demand determination	Lamp	3	8	0	24	6	144	0.0	144
	Pumping system	1	1.8	0	1.8	6	10.8	0.0	10.8
	Magnetic stirrer	1	0	500	500	6	0	3000.0	3000
	Fan	1	3.6	0	3.6	6	21.6	0.0	21.6
	Total	6	13.4	0	529.4	6	176.4	3000.0	3176.4
Step 2. PV panel sizing	ID <sup>a</sup>	B1	E2	B3	B4		B5	B6	B7
	Formula	Value	Observations						
	C1	$\frac{(B6)_{/A8} + B5}{(A1)_{/A3}}$							
	C2	$B1_{/A13}$							
	C3	$A3_{/A10}$							
	C4	C2*C3							
Step 3. Inverter sizing	D1	B6							
	D2	B6*0.3							
	D3	D1 + D2							
Step 4. Battery sizing	E1	$B6_{/A8} + B5$							
	E2	$\frac{B1_{/A2}}{(A4)_{/A5} * A7_{/A8}}$							
	E3	$E2_{/A6}$							
	E4	$A3_{/A4}$							
	E5	E3*E4							
Step 5. Charge controller sizing	F1	C2*(1 + A18) <sup>a</sup> A17							

<sup>a</sup> Identifier.

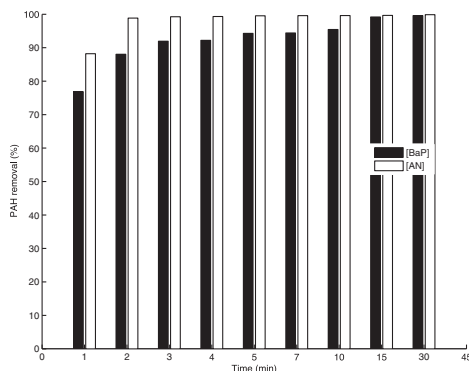


**Fig. 4.** Evolution profiles of anthracene (AN) and benzo[a]pyrene (BaP) removal vs. time through the UV/H<sub>2</sub>O<sub>2</sub> system directly powered by a photovoltaic array. Operating conditions: [AN]<sub>0</sub> = 12 μg L<sup>-1</sup>; [BaP]<sub>0</sub> = 3 μg L<sup>-1</sup>; source power rating = 8 W; irradiance = 170 μW cm<sup>-2</sup>.

operating conditions (data not shown). Consequently, UV radiation was increased from 170 to 460 μW cm<sup>-2</sup> by the use of 3 UV-C LP lamps, and H<sub>2</sub>O<sub>2</sub> was added to the system at 5, 10 and 15 mg L<sup>-1</sup>. Fig. 5 illustrates the percentage of organic matter reduction using 3 UV-C LP lamps alone and in combination with 5, 10 and 15 mg L<sup>-1</sup> H<sub>2</sub>O<sub>2</sub>. As noticed, the highest TOC removal was obtained using 3 UV-C LP lamps and 10 mg L<sup>-1</sup> of H<sub>2</sub>O<sub>2</sub>, corresponding to a TOC percentage removal of about 45% after 90 min of operation. Under these operating conditions, H<sub>2</sub>O<sub>2</sub> evolution profile was also investigated. It was found that when adding 10 mg L<sup>-1</sup> a higher amount of H<sub>2</sub>O<sub>2</sub> remained in the solution to be photolyzed for a subsequent more efficient production of HO<sup>•</sup> (data not shown). 5 mg L<sup>-1</sup> H<sub>2</sub>O<sub>2</sub> was not enough for achieving good reduction results and 15 mg L<sup>-1</sup> H<sub>2</sub>O<sub>2</sub> resulted to promote the side reactions that can occur during the UV/H<sub>2</sub>O<sub>2</sub> system operation [3,6]. A more detailed explanation on this issue is reported in [33]. Moreover, AN and BaP degradation by-products formation was assessed to discern their transformation extent under optimal operating conditions and the

action of HO<sup>•</sup>. Among the reaction intermediates, anthracene-9,10-dione and benzo[a]pyrene-4,5-dione for AN and BaP, respectively, were found. These quinones were subsequently transformed into 1-hydroxyanthracene-9,10-dione and other products during AN oxidation, and 6-(3-hydroxyphenyl)-2-naphthol and 2-methylnaphthalene, among others, during BaP conversion. These degradation by-products were, then, further oxidized to produce simple aromatic acids and alcohols; and, finally, short-chain organic acids, resulting in a decrease in the solution pH. The production of the identified products was already reported when PAHs were subjected to other AOPs [44–46], with the exception of 6-(3-hydroxyphenyl)-2-naphthol, which has not been reported yet. These results indicate that the HO<sup>•</sup> generated attack the organic molecules of the target PAH, pointing out the important role developed by HO<sup>•</sup> in the degradation of AN and BaP. These findings were corroborated by adding 1 mM 2-propanol in the reaction solution, since a poor elimination of the target PAH was achieved (data not shown), due to 2-propanol acts as a HO<sup>•</sup> scavenger.

Therefore, it has been demonstrated that the integrated water treatment system utilizing solar energy as power provided the electrical power needs required to achieve removal efficiencies of AN and BaP higher than 99% and about 45% of organic matter mineralization without the production of toxic by-products. These findings are comparable to the results reported by [33].

Promising results have also been obtained by using hybrid systems combining AOPs and PV systems. Han et al. [36] studied the efficiency of an integrated system utilizing solar energy as power for decentralized wastewater treatment, consisting of a bioreactor with double channels and a PV system without batteries. The experiments were carried out at laboratory-scale and with real wastewater. The results showed a reduction of chemical oxygen demand, ammonia, total nitrogen and total phosphorus of 88%, 98%, 70% and 83%, respectively. Additionally Jin et al. [47], evaluated the performance of a PV cell integrated with solar water disinfection to treat drinking water and generate electricity under different weather conditions with and without heat exchanger. These authors found the system without heat exchanger as a better option for the removal of microbial load, in terms of *Escherichia coli*, obtaining complete disinfection after 1.5 h of solar exposition.

In this regard, the hybrid system PV-water treatment process seems to be an efficient alternative to treat water, both drinking and

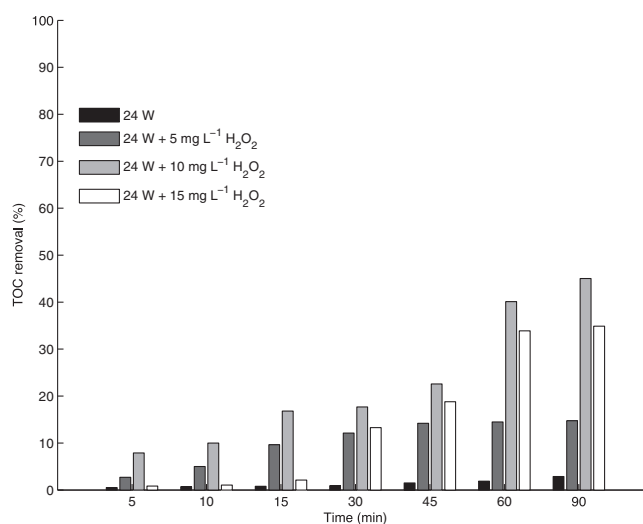


**Fig. 5.** Evolution profiles of total organic carbon (TOC) removal vs. time through the UV/H<sub>2</sub>O<sub>2</sub> system directly powered by a photovoltaic array. Operating conditions: [AN]<sub>0</sub> = 12 μg L<sup>-1</sup>; [BaP]<sub>0</sub> = 3 μg L<sup>-1</sup>; source power rating = 24 W; irradiance = 460 μW cm<sup>-2</sup>.



wastewater, using solar light.

### 3.4. Costs of investment for the UV/H<sub>2</sub>O<sub>2</sub>-PV system operation at small-scale

A number of factors determine the final price of a PV system, including investment costs (i.e., the number of components and configuration of equipments), labor costs and fixed and variable operating and maintenance costs. Additionally, in some countries the local permitting costs, available incentives and tax credits must be taken into account. It is noteworthy that PV arrays incur few operating costs and are easy to install. Furthermore, PV system costs can be reduced when the required storage capacity and PV array size are decreased. In general, PV systems with and without batteries require low maintenance since they do not have moving parts in contrast to other renewable systems. Under this scenario, PV arrays should be inspected a few times per year for removing dirt or some other things that might have piled on the top so that there is nothing blocking them from efficiently absorbing the sun energy. However, for PV systems where batteries are used, besides the above detailed maintenance costs, battery replacement every 10–15 years must be considered, increasing the whole maintenance costs [48]. Among these costs, the investment costs are perhaps the single most important factor in determining whether an alternative energy technology can reach implementation and commercialization. Independently on the characteristics of a particular site, the savings in energy costs must outweigh that initial investment for its economic feasibility through time.

Therefore, the cost analysis of a PV array can be very detailed; however, for comparison purposes, the approach used in the current work is a simplified one. Only the investment costs were taken into account for the cost analysis. This allows for a greater scrutiny of the underlying data and a reduced number of assumptions regarding the operating and maintenance costs of each system with and without batteries. In this sense, the transparency and confidence in the analysis is improved. Additionally, the comparisons of costs among countries or regions for the same technologies are facilitated.

Thus, the economic analysis was done with the purpose of knowing the investment cost of the PV system for the evaluated UV/H<sub>2</sub>O<sub>2</sub> process applied to a small-scale. Moreover, the payback cost, which refers to the cost of installing the PV module at the site paid back by the reduction in electricity bills, was also estimated. This payback can vary based on the location of the PV installation and the cost of electricity produced from conventional sources, such as coal and natural gas, and large hydropower plants. In general, prices of electricity are highly dependent on the particular country. For example, the present unitary electricity cost for industrial use in Colombia is around 0.25 \$ per kWh<sup>-1</sup>.

In Table 4, the investment costs for the PV system with and without batteries are compiled. These costs were calculated considering the PV system with 2 and 1 days of autonomy, and an operation time of the equipment of 6 h per day. Undoubtedly, if the days of autonomy and the hours of operation of the equipment during the day are augmented, the investment costs will increase.

From Table 4, it can be found that 81.05% of the money invested in the PV system for 2 days of autonomy operating 6 h per day corresponds to the cost of the batteries. Similarly, 69.72% of the required money for a PV system with 1 single day of autonomy and 6 h of operation corresponds to the cost of the batteries. Moreover, the investment return of the implementation of a PV system that supplies the energy required for the considered AOP with batteries with 2 or 1 day of autonomy and without batteries would be achieved in 14 or 9 years and 5 years, respectively.

In general, most of the conventional PV applications use PV modules connected to a storage battery system. However, in the literature several works using PV systems without batteries can be found [36,47,49,51]. As a matter of fact [49], in a remote town in South

**Table 4**  
Investment costs for a PV system with and without batteries.

PV system description	Item	Cost/unit (\$)	Amount	Total (\$)
With batteries and 2 days of autonomy	PV module	120	4	480
	Battery	250	13	3250
	Solar charge controller	70	1	70
	Inverter	210	1	210
	Total (\$)			4010
With batteries and 1 day of autonomy	PV module	120	4	480
	Battery	250	7	1750
	Solar charge controller	70	1	70
	Inverter	210	1	210
	Total (\$)			2510
Without batteries	PV module	120	9	1080
	Solar charge controller	70	1	70
	Inverter	210	1	210
	Total (\$)			1360
	Analysis cases (units)			Value
Cost per kWh of electricity of the electrical grid (\$ kWh <sup>-1</sup> )			0.25	
Cost of the energy consumption of the electrical grid per year for the UV/H <sub>2</sub> O <sub>2</sub> system considering an operation time of 6 h per day (\$ year <sup>-1</sup> )			289.8	
Estimated energy payback for rooftop PV system with batteries and 2 days of autonomy (year)			13.83	
Estimated energy payback for rooftop PV system with batteries and 1 day of autonomy (year)			8.66	
Estimated energy payback for rooftop PV system without batteries (year)			4.69	

Australia with abundant solar radiation and scarce and low quality water, where a reverse osmosis plant was operating, evaluated the feasibility of powering the plant with solar or PV panels whilst avoiding energy storage in batteries. A pilot test was performed with a small-scale PV-powered hybrid ultrafiltration-reverse osmosis (UF/RO) membrane filtration system. It was concluded that a RO plant utilizing UF pre-treatment and powered by PV panels without battery storage is a promising alternative to overcome the high energy costs for the existing RO plants. Jin et al. [47] also assessed a hybrid PV – SODIS system without batteries for water disinfection, as previously mentioned, obtaining complete disinfection. In turn, Vivar et al. [51] presented a cost-effective hybrid solar electricity and water purification design to meet the needs for electricity and clean water in a single integrated and affordable system. The process was solar water disinfection using photo-catalysts and UV radiation. Additionally, for the photocatalytic reaction electrodes were included, which provided an opportunity for the enhancement of the photocatalytic process.

The use of the electrical energy directly supplied by the PV modules to the equipment used in the UV/H<sub>2</sub>O<sub>2</sub> process would substantially decrease the costs of investment and maintenance of the system, due to the high prices of the batteries and the difficulty for controlling their state of charge. This fact represents an energy saving because of the elimination of energy losses during the transformation; i.e., the investment costs of the PV system are reduced since the inverter is not needed when the equipment operates in DC mode. Additionally, the environmental problems related to the disposal of batteries are avoided and the sustainability of the process is increased. On the other hand, a small rechargeable battery of very low consumption may be needed in order to power the control/measurement devices to keep the equipment in good working order even in sunlight shortage periods.

Obviously, the absence of batteries implies that water production depends on and varies with the solar irradiation; which, in turn, depends on the meteorological conditions, geographical location, season, daily time and PV array orientation. Since the decontamination of water with the UV/H<sub>2</sub>O<sub>2</sub> process under the studied conditions can be only produced during the sunlight hours, the UV/H<sub>2</sub>O<sub>2</sub> system should have a higher capacity in order to decontaminate more water volume while the sun is shining. Therefore, the equipment and system

maintenance costs will be incremented.

On the other hand, during the day it is possible to produce a surplus of the energy required for the AOP and to store it chemically by a system power to gas; i.e., the electrical power can be converted into a gas fuel. Typically, the electricity can be used to split water into hydrogen and oxygen by means of electrolysis using an electrolyzer. Consequently, the chemical energy from hydrogen can be utilized later. For this purpose, hydrogen is converted into electricity through a fuel cell. The produced electricity might be utilized to provide power to the applied AOP when there are no hours of radiation during the day.

Additionally, it is important to note that the use of a PV system with batteries can be profitable in those areas without electrical grid. In this regard, in remote areas of the national electrical grid, a detailed evaluation must be conducted about if connecting to the national electrical grid is more profitable than utilizing PV systems with an energy storing for providing the required energy to the equipment used during the period of water treatment using AOPs.

Either with or without batteries, in order to reduce the costs associated with wastewater decontamination and drinking water production, water treatment technologies driven by solar light are recently regarded as alternative options towards the use of fossil fuels. In fact, in a recent study conducted by Zhang et al. [50], the application of solar energy for water treatment is reported as a sustainable solution to treat water in an environmental friendly manner. This work reviews in detail the technologies driven by solar energy and used for water treatment, including the use of PV systems for desalination purposes. With respect to this issue, although solar collector material price is the main limitation in terms of costs, the estimated low water costs (0.9–2.2 \$) for large-scale solar plants indicate that water treatment alternatives driven by solar light will become potentially viable in the near future.

In this regard, hybrid systems that allow obtaining electricity and treating water can be used in both rural and urban areas, being the latter ones of particular interest since it is estimated that two-thirds of the world population will live in cities by 2025 [51].

#### 4. Conclusions

During this work, a detailed sizing of PV energy systems used for supplying the required power in the AOP implementation was carried out due to the major operating costs associated with these processes are the energy costs to put into operation the equipment employed in these advanced oxidation technologies. For this purpose, several factors, such as the latitude, the day and the surface orientation where the PV system is mounted were considered in order to properly calculate the optimal tilt angle and orientation of the fixed solar panel for maximizing the energy collection and, subsequently, maximizing the solar radiation availability at the required location. For the PV system installed in Medellín, Colombia, the optimum tilt angle resulted to be 15.64°.

The sized PV system was used to directly power a UV/H<sub>2</sub>O<sub>2</sub> system for degrading natural water containing AN and BaP at a concentration of 12 and 3 µg L<sup>-1</sup>, respectively. It was found that the integrated system was able to achieve a removal efficiency higher than 99% of both PAHs using the single action of 1 UV-C LP lamp in an irradiation period of 15 min. Additionally, about 45% of the organic matter of the water, in terms of total organic carbon, was mineralized using 3 UV-C LP lamps in combination with 10 mg L<sup>-1</sup> of H<sub>2</sub>O<sub>2</sub> after 90 min of treatment and no toxic degradation by-products were produced.

Moreover, the investment costs of the UV/H<sub>2</sub>O<sub>2</sub>-PV system for small applications were estimated. It was concluded that PV energy can be used to power AOPs in a reliable and autonomous way; especially, in isolated locations with lack of electrical grid. It is important to note that the high cost associated with PV modules and equipment, compared to conventional energy sources, is the primary limiting factor for the technology. However, the PV array can be also connected directly to the equipment used in the water treatment systems without batteries, as demonstrated, obtaining good efficiencies in water treatment. Thus, the

environmental threat of improper battery disposal is eliminated and, subsequently, the sustainability of the process is increased. Furthermore, the investment costs decrease compared to the costs associated with a PV system with batteries.

Thus, PV systems can be designed for a variety of applications and operational requirements, and can be used for either centralized or distributed power generation. The obtained results might be of great interest for other studies related to direct connection of PV systems to other AOPs powered by PV energy both in developed and developing countries, allowing an environmentally-friendly and sustainable development.

#### Acknowledgements

This work was supported by the Spanish Agency for International Development Cooperation (AECID), the Colombian Administrative Department of Science, Technology and Innovation (COLCIENCIAS) and the sustainability fund of the University of Antioquia Vice-rectory.

#### References

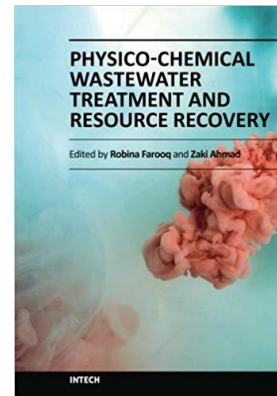
- [1] S. Malato, J. Blanco, A. Vidal, C. Richter, Photocatalysis with solar energy at a pilot-plant scale: an overview, *Appl. Catal. B-Environ.* 37 (2002) 1–15.
- [2] I. Oller, S. Malato, J. Sánchez-Pérez, Combination of advanced oxidation processes and biological treatments for wastewater decontamination—a review, *Sci. Total Environ.* 409 (2011) 4141–4166.
- [3] A. Rubio-Clemente, R.A. Torres-Palma, G.A. Peñuela, Removal of polycyclic aromatic hydrocarbons in aqueous environment by chemical treatments: a review, *Sci. Total Environ.* 478 (2014) 201–225.
- [4] C.F. Bustillo-Lecompte, S. Ghafoori, M. Mehrvar, Photochemical degradation of an actual slaughterhouse wastewater by continuous UV/H<sub>2</sub>O<sub>2</sub> photoreactor with recycle, *J. Environ. Chem. Eng.* 4 (2016) 719–732.
- [5] A.M. Parker, Y. Lester, E.K. Spangler, U. von Gunten, K.G. Linden, UV/H<sub>2</sub>O<sub>2</sub> advanced oxidation for abatement of organophosphorous pesticides and the effects on various toxicity screening assays, *Chemosphere* 182 (2017) 477–482.
- [6] M. Litter, N. Quici, Photochemical advanced oxidation processes for water and wastewater treatment, *Recent Pat. Eng.* 4 (2010) 217–241.
- [7] W.H. Glaze, J.W. Kang, D.H. Chapin, The chemistry of water treatment processes involving ozone, hydrogen peroxide and ultraviolet radiation, *Ozone Sci. Eng.* 9 (1987) 335–352.
- [8] X. Domenech, W. Jardim, M. Litter, Procesos avanzados de oxidación para la eliminación de contaminantes. Eliminación de contaminantes por fotocatalisis heterogénea, Ciemat, 2004, pp. 4–26 Colección Documentos Madrid.
- [9] L. Clarizia, D. Russo, I. Di Somma, R. Marotta, R. Andreozzi, Homogeneous photofenton processes at near neutral pH: a review, *Appl. Catal. B-Environ.* 209 (2017) 358–371.
- [10] G. Liu, J. Ji, H. Huang, R. Xie, Q. Feng, Y. Shu, Y. Zhan, R. Fang, M. He, S. Liu, X. Ye, D.Y.C. Leung, UV/H<sub>2</sub>O<sub>2</sub> An efficient aqueous advanced oxidation process for VOCs removal, *Chem. Eng. J.* 324 (2017) 44–50.
- [11] A. Rubio-Clemente, E. Chica, G.A. Peñuela, Petrochemical wastewater treatment by photo-Fenton process, *Water Air Soil Pollut.* 226 (2015) 61–79.
- [12] M. Edalatmanesh, R. Dhib, M. Mehrvar, Kinetic modeling of aqueous phenol degradation by UV/H<sub>2</sub>O<sub>2</sub> process, *Int. J. Chem. Kinet.* 40 (2008) 34–43.
- [13] R. Zhang, Y. Yang, C.H. Huang, L. Zhao, P. Sun, Kinetics and modeling of sulfonamide antibiotic degradation in wastewater and human urine by UV/H<sub>2</sub>O<sub>2</sub> and UV/PDS, *Water Res.* 103 (2016) 283–292.
- [14] C. Comninellis, A. Kapalka, S. Malato, S.A. Parsons, I. Poullos, D. Mantzavinos, Perspective advanced oxidation processes for water treatment: advanced oxidation processes for water treatment: advances and trends for R&D, *J. Chem. Technol. Biotechnol.* 83 (2008) 769–776.
- [15] C.H.M. Hofman-Caris, E.F. Beerendonk, New Concepts of UV/H<sub>2</sub>O<sub>2</sub> Oxidation, KWR Watercycle Research Institute, Nieuwegein, 2011.
- [16] K. Hansen, H.R. Andersen, Energy effectiveness of direct UV and UV/H<sub>2</sub>O<sub>2</sub> treatment of estrogenic chemicals in biologically treated sewage, *Int. J. Photoenergy* (2012) 1–9 2012.
- [17] F. Hernandez-Sancho, M. Molinos-Senante, R. Sala-Garrido, Cost modelling for wastewater treatment processes, *Desalination* 268 (2011) 1–5.
- [18] X. Hu, Y. Li, J. Tian, H. Yang, H. Cui, Highly efficient full solar spectrum (UV-vis-NIR) photocatalytic performance of Ag<sub>2</sub>S quantum dot/TiO<sub>2</sub> nanobelt heterostructures, *J. Ind. Eng. Chem.* 45 (2017) 189–196.
- [19] N. Drouiche, F. Djouadi-Belkadda, T. Ouslimane, A. Kefaifi, J. Fathi, E. Ahmetovic, Photovoltaic solar cells industry wastewater treatment, *Desalin. Water Treat.* 51 (2013) 5965–5973.
- [20] A. McEvoy, T. Markvart, L. Castañer, T. Markvart, L. Castañer, *Practical Handbook of Photovoltaics: Fundamentals and Applications*, Elsevier Science, Amsterdam, 2003.
- [21] H.S. Rauschenbach, *Solar Cell Array Design Handbook: the Principles and Technology of Photovoltaic Energy Conversion*, Springer Netherlands, The Netherlands, 2012.

- [22] C.S. Solanki, *Solar Photovoltaic Technology and Systems: A Manual for Technicians, Trainers and Engineers*, PHI Learning Private Limited, Delhi, 2013.
- [23] D. Valero, J.M. Ortiz, E. Exposito, V. Montiel, A. Aldaz, Electrocoagulation of a synthetic textile effluent powered by photovoltaic energy without batteries: direct connection behaviour, *Sol. Energy Mater. Sol. Cells* 92 (2008) 291–297.
- [24] D. Valero, J.M. Ortiz, E. Exposito, V. Montiel, A. Aldaz, Electrochemical wastewater treatment directly powered by photovoltaic panels: electrooxidation of a dye-containing wastewater, *Environ. Sci. Technol.* 44 (2010) 5182–5187.
- [25] J.M. Ortiz, E. Exposito, F. Gllud, V. Garcia, V. Montiel, A. Aldaz, Electrolysis of brackish water powered by photovoltaic energy without batteries: direct connection behavior, *Desalination* 208 (2007) 89–100.
- [26] J.M. Ortiz, E. Exposito, F. Gallud, V. García-García, V. Montiel, A. Aldaz, Desalination of underground brackish waters using an electrolysis system powered directly by photovoltaic energy, *Sol. Energy Mater. Sol. Cells* 92 (2008) 1677–1688.
- [27] M.A.M. Ramli, A. Hiendro, Y.A. Al-Turki, Techno-economic energy analysis of wind/solar hybrid system: case study for western coastal area of Saudi Arabia, *Renew. Energy* 91 (2016) 374–385.
- [28] C. Armenta-Deu, Prediction of battery behaviour in SAPV applications, *Renew. Energy* 28 (2003) 1671–1684.
- [29] E. Potteau, D. Desmettre, F. Mattera, O. Bach, J.L. Martin, P. Malbranche, Results and comparison of seven accelerated cycling test procedures for the photovoltaic application, *J. Power Sources* 113 (2003) 408–413.
- [30] A. Rubio-Clemente, E. Chica, G.A. Peñuela, Rapid determination of anthracene and benzo(a)pyrene by high-performance liquid chromatography with fluorescence detection, *Anal. Lett.* 50 (2017) 1229–1247.
- [31] W.E.F. AWWA, *Standard Methods for the Examination of Water and Wastewater*, 22nd ed., American Public Health Association, Washington, DC, 2012 2012.
- [32] M.T. Pena, M.C. Casais, M.C. Mejuto, R. Cela, Development of an ionic liquid based dispersive liquid-liquid microextraction method for the analysis of polycyclic aromatic hydrocarbons in water samples, *J. Chromatogr. A* 1216 (2009) 6356–6364.
- [33] A. Rubio-Clemente, A. Cardona, E. Chica, G.A. Peñuela, Sensitive spectrophotometric determination of hydrogen peroxide in aqueous samples from advanced oxidation processes: evaluation of possible interferences, *Afinidad* (2017) 161–168.
- [34] M. Boxwell, *Solar Electricity Handbook. A Simple Practical Guide to Solar Energy Designing and Installing Photovoltaic Solar Electric Systems*, 15th ed., Code Green Publishing, United Kingdom, 2015.
- [35] R. Foster, M. Ghassemi, A. Cota, *Solar Energy: Renewable Energy and the Environment*, CRC Press, United States, 2010.
- [36] C. Han, J. Liu, H. Liang, X. Guo, L. Li, An innovative integrated system utilizing solar energy as power for the treatment of decentralized wastewater, *J. Environ. Sci.* 25 (2013) 274–279.
- [37] S.I. Sulaiman, T.K.A. Rahman, I. Musirin, Novel intelligent sizing algorithm for grid-connected photovoltaic system design, *Int. Rev. Model. Simul.* 3 (2010) 639–652.
- [38] E.A. Handoyo, D. Ichsani, Prabowo, The optimal tilt angle of a solar collector, *Eng. Procedia* 32 (2013) 166–175.
- [39] M.E. Meral, F. Dincer, A review of the factors affecting operation and efficiency of photovoltaic based electricity generation systems, *Renew. Sustain. Energy Rev.* 15 (2011) 2176–2184.
- [40] A.M. Omar, S. Shaari, Sizing verification of photovoltaic array and grid-connected inverter ratio for the Malaysian building integrated photovoltaic project, *Int. J. Low-Carbon Technol.* 4 (2009) 254–257.
- [41] S.I. Sulaiman, T.K.A. Rahman, I. Musirin, S. Shaari, Sizing grid-connected photovoltaic system using genetic algorithm, *Industrial Electronics and Applications (ISIEA)*, 2011 IEEE Symposium, IEEE, Langkawi, 2011, pp. 505–509.
- [42] O. Thomas, C. Burgess (Eds.), *UV-visible Spectrophotometry of Water and Wastewater*, 27 Elsevier Science, The Netherlands, 2007.
- [43] F. Zsila, H. Matsunaga, Z. Bikádi, J. Haginaka, Multiple ligand-binding properties of the lipocalin member chicken  $\alpha$  1-acid glycoprotein studied by circular dichroism and electronic absorption spectroscopy: the essential role of the conserved tryptophan residue, *Biochimica et Biophysica Acta (BBA)-General Subjects* 1760 (2006) 1248–1273.
- [44] M. Bendouz, L.H. Tran, L. Coudert, G. Mercier, J.F. Blais, Degradation of polycyclic aromatic hydrocarbons in different synthetic solutions by Fenton's oxidation, *Environ. Technol.* 38 (2017) 116–127.
- [45] A. Lair, C. Ferronato, J.M. Chovelon, J.M. Hermann, Naphthalene degradation in water by heterogeneous photocatalysis: an investigation of the influence of inorganic anions, *J. Photochem. Photobiol. A* 193 (2008) 193–203.
- [46] O.T. Woo, W.K. Chung, K.H. Wong, A.T. Chow, P.K. Wong, Photocatalytic oxidation of polycyclic aromatic hydrocarbons: intermediates identification and toxicity testing, *J. Hazard. Mater.* 168 (2009) 1192–1199.
- [47] Y. Jin, Y. Wang, Q. Huan, L. Zhu, Y. Cui, L. Cui, The performance and applicability study of a fixed photovoltaic-solar water disinfection system, *Energy Convers. Manag.* 123 (2016) 549–558.
- [48] S. Watson, D. Bian, N. Sahraei, A.G. Winter, T. Buonassisi, I.M. Peters, Advantages of operation flexibility and load sizing for PV-powered system design, *Sol. Energy* 162 (2018) 132–139.
- [49] A. Munari, D.P.S. Capão, B.S. Richards, A.I. Schäfer, Application of solar powered desalination in a remote town in South Australia, *Desalination* 248 (2009) 72–82.
- [50] Y. Zhang, M. Sivakumar, S. Yang, K. Enever, M. Ramezani-pour, Application of solar energy in water treatment processes: a review, *Desalination* 428 (2018) 116–145.
- [51] M. Vivar, I. Skryabin, V. Everett, A. Blakers, A concept for a hybrid solar water purification and photovoltaic system, *Solar Energy Mater. Solar Cells* 94 (2010) 1772–1782.



**Book chapter**

**Kinetic modeling of the UV/H<sub>2</sub>O<sub>2</sub> process: Determining the effective hydroxyl radical concentration.** In *Physico-Chemical Wastewater Treatment and Resource Recovery*, 2017, Prof. Robina Farooq (Ed.), InTech, pp. 19-41. ISBN 978-953-51-3130-4

**Book**

Scope: The book on Physico-Chemical Treatment of Wastewater and Resource Recovery provides an efficient and low-cost solution for remediation of wastewater. This book focuses on physico-chemical treatment via advanced oxidation process, adsorption, its management and recovery of valuable chemicals. It discusses treatment and recovery process for the range of pollutants including BTX, PCB, PCDDs, proteins, phenols, antibiotics, complex organic compounds and metals. The occurrence of persistent pollutants poses deleterious effects on human and environmental health. Simple solutions for recovery of valuable chemicals and water during physico-chemical treatment of wastewater are discussed extensively. This book provides necessary knowledge and experimental studies on emerging physico-chemical processes for reducing water pollution and resource recover.

**Highlights**

- The model describes the effects of the matrix background and pH changes.

- Different assumptions were used to calculate  $\text{HO}^\circ$  time-evolution.
- The model can predict the effective  $\text{HO}^\circ$  level for the efficient pollutant degradation.
- The reaction rate constant of the  $\text{HO}_2^\circ$  with the probe pollutant is estimated.
- The action of the  $\text{HO}_2^\circ$  in removing pollutants is not significant.

---

## Kinetic Modeling of the UV/H<sub>2</sub>O<sub>2</sub> Process: Determining the Effective Hydroxyl Radical Concentration

---

Ainhoa Rubio-Clemente, E. Chica and  
Gustavo A. Peñuela

Additional information is available at the end of the chapter

<http://dx.doi.org/10.5772/65096>

---

### Abstract

A kinetic model for pollutant degradation by the UV/H<sub>2</sub>O<sub>2</sub> system was developed. The model includes the background matrix effect, the reaction intermediate action, and the pH change during time. It was validated for water containing phenol and three different ways of calculating HO<sup>°</sup> level time-evolution were assumed (non-pseudo-steady, pseudo-steady and simplified pseudo-steady state; denoted as kinetic models A, B and C, respectively). It was found that the kind of assumption considered was not significant for phenol degradation. On the other hand, taking into account the high levels of HO<sub>2</sub><sup>°</sup> formed in the reaction solution compared to HO<sup>°</sup> concentration (~10<sup>-7</sup> M >>> ~10<sup>-14</sup> M), HO<sub>2</sub><sup>°</sup> action in transforming phenol was considered. For this purpose, phenol-HO<sub>2</sub><sup>°</sup> reaction rate constant was calculated and estimated to be 1.6×10<sup>3</sup> M<sup>-1</sup> s<sup>-1</sup>, resulting in the range of data reported from literature. It was observed that, although including HO<sub>2</sub><sup>°</sup> action allowed slightly improving the kinetic model degree of fit, HO<sup>°</sup> developed the major role in phenol conversion, due to their high oxidation potential. In this sense, an effective level of HO<sup>°</sup> can be determined in order to be maintained throughout the UV/H<sub>2</sub>O<sub>2</sub> system reaction time for achieving an efficient pollutant degradation.

**Keywords:** UV/H<sub>2</sub>O<sub>2</sub> process, matrix background, kinetic model, reaction rate constant

---

### 1. Introduction

Nowadays, one of the major problems associated with the presence of toxic and persistent pollutants in the aquatic environment is the unfeasibility of conventional treatments for the effective removal of those substances [1-3]. Hence the application of alternative technologies,

---

such as advanced oxidation processes, is needed [4]. Among these techniques, the UV/H<sub>2</sub>O<sub>2</sub> system is included. It consists of the photolysis of hydrogen peroxide (H<sub>2</sub>O<sub>2</sub>) by applying ultraviolet (UV) radiation resulting in the generation of hydroxyl radicals (HO°) [5, 6]. This process may be performed at room temperature and pressure, it has no mass transfer problems, it is easy to maintain and operate, no sludge requiring a subsequent treatment and disposal is produced, and it may achieve a complete pollutant mineralization [5]. Therefore, the UV/H<sub>2</sub>O<sub>2</sub> system seems to be a promising alternative for the treatment of water containing toxic and recalcitrant substances. However, this kind of technology can be expensive due to the associated electrical and oxidant costs [7].

In order to reduce costs and make the process more feasible for industrial applications, the UV/H<sub>2</sub>O<sub>2</sub> system optimization is required [8] and kinetic models can be considered as functional tools for this purpose. Up to date, several kinetic models have been proposed for describing the UV/H<sub>2</sub>O<sub>2</sub> process and predicting different pollutant removal rates [6–15]. In some of these models [13, 15], the proposed set of ordinary differential equations (ODE) defining the studied pollutant degradation rate can be simplified into a pseudo-first-order kinetic expression, whose solution is an exponential one. In such as models, experimental results are fit to that solution. Subsequently, model predictions agree well with laboratory data. In that kind of models the calculated reaction rate constants for the tested pollutant degradation are apparent reaction rate constants ( $K_{app}$ ), which include pollutant removal reaction rate constants and the values of parameters such as the quantum yield for the oxidant, the conjugate base (HO<sub>2</sub><sup>-</sup>), and the contaminant photolysis, the initial level of the chemical species involved in pollutant oxidation, the optical path length of the system, the UV-light intensity, and the molar extinction coefficients of H<sub>2</sub>O<sub>2</sub>/HO<sub>2</sub><sup>-</sup> and pollutant, among others. Therefore, knowing those parameters is not required.

On the other hand, there are dynamic kinetic models that try to solve the considered ODE set, for which the values of the mentioned variables are required, increasing the complexity of the kinetic model. In order to solve the proposed ODE set, the pseudo-steady state approximation assumption for reactive intermediates, such as HO°, is invoked by arguing that these chemical species are as transient ones as their concentration can be presumed to be at a pseudo-steady state [10, 12, 14]. In other models [6–15], on the contrary, the non-pseudo-steady state premise in free radical rate expressions for predicting the degradation of the probe compound in a more accurate way is applied. However, although hydroperoxyl radicals (HO<sub>2</sub>°) are involved in those models, none of them, excluding Huang and Shu [11] and Liao and Gurol [12] models, includes HO<sub>2</sub>° in the target pollutant oxidation final expression. Additionally, some of these models cannot be reproduced unless a conversion factor is included, as demonstrated by Audenaert et al. [8].

In this sense, the aim of this work was to develop a kinetic model based on the main chemical and photochemical reactions for pollutant degradation in water systems by the UV/H<sub>2</sub>O<sub>2</sub> process taking into account the decomposition of the pollutant through direct photolysis, HO° oxidation, and HO<sub>2</sub>° and superoxide radical (O<sub>2</sub><sup>°-</sup>) transformation. Furthermore, HO° scavenging effects of carbonate (CO<sub>3</sub><sup>2-</sup>), bicarbonate (HCO<sub>3</sub><sup>-</sup>), sulfate (SO<sub>4</sub><sup>2-</sup>), and chloride (Cl<sup>-</sup>) ions were considered. pH changes in the bulk and the detrimen-



tal action of the organic matter (OM) and the reaction intermediates in shielding UV and quenching HO° were studied. The influence of the pseudo-steady and non-pseudo-steady state hypothesis for determining HO° concentration-evolution with time was also examined and the second-order HO<sub>2</sub>° reaction rate constant for the studied pollutant was determined. MATLAB software was used to solve the ODE set that characterizes the current model and the results were validated by using experimental data obtained from the literature for phenol (PHE) degradation by the UV/H<sub>2</sub>O<sub>2</sub> process in a completely mixed batch photoreactor.

## 2. Experimental model approach

A mathematical model for predicting pollutant degradation and the concentrations of the main species involved in a UV/H<sub>2</sub>O<sub>2</sub> system was developed. The developed model describes radical chain reactions occurring during the UV/H<sub>2</sub>O<sub>2</sub> process in the presence of HO° scavengers and UV-radiation absorbers, such as dissolved organic matter (DOM), anions and reaction intermediate products. Pollutant degradation mechanisms, direct UV photolysis and radical attack by HO°, HO<sub>2</sub>°, O<sub>2</sub>° and other anion radicals (CO<sub>3</sub>°-, SO<sub>4</sub>°-, H<sub>2</sub>ClO°, HClO°, Cl°, and Cl<sub>2</sub>°-) were included. Additionally, the model incorporates the competitive UV-radiation absorption by H<sub>2</sub>O<sub>2</sub>, the parent compound and the DOM in terms of dissolved organic carbon (DOC), as well as the formation and disappearance of intermediate products, also considered as DOC. Moreover, it accounts for the solution pH change due to the mineralization of organic compounds and the formation of acids.

### 2.1. UV/H<sub>2</sub>O<sub>2</sub> system fundamentals

The UV/H<sub>2</sub>O<sub>2</sub> system initiates with the primary photolysis of H<sub>2</sub>O<sub>2</sub> or HO<sub>2</sub><sup>-</sup>, producing HO° according to Eqs. (1) and (2) [6, 13]. Based on the Beer-Lambert law and quantum yield definition, the reaction rates for H<sub>2</sub>O<sub>2</sub>/HO<sub>2</sub><sup>-</sup> direct photodegradation and HO° generation are obtained through Eqs. (3)–(5), respectively.



$$\frac{d[\text{H}_2\text{O}_2]}{dt} = -\phi_{\text{H}_2\text{O}_2} I_{a, \text{H}_2\text{O}_2} \quad (3)$$

$$\frac{d[\text{HO}_2^-]}{dt} = -\phi_{\text{HO}_2^-} I_{a, \text{HO}_2^-} \quad (4)$$

$$\frac{d[\text{HO}^\circ]}{dt} = 2\phi_{\text{H}_2\text{O}_2} I_{a, \text{H}_2\text{O}_2} + 2\phi_{\text{HO}_2^-} I_{a, \text{HO}_2^-} \quad (5)$$

where  $\phi_{\text{H}_2\text{O}_2}$  and  $\phi_{\text{HO}_2^-}$  (mol Ein<sup>-1</sup>) are the quantum yields of the photochemical reactions of H<sub>2</sub>O<sub>2</sub> and HO<sub>2</sub><sup>-</sup>.  $I_{a, \text{H}_2\text{O}_2}$  and  $I_{a, \text{HO}_2^-}$  (Ein L<sup>-1</sup> s<sup>-1</sup>) refer to the UV-radiation intensities absorbed by H<sub>2</sub>O<sub>2</sub> and HO<sub>2</sub><sup>-</sup>, respectively, calculated according to Eqs. (6) and (7), where  $f_{\text{H}_2\text{O}_2}$  and  $f_{\text{HO}_2^-}$  are the fractions of the UV-radiation absorbed by H<sub>2</sub>O<sub>2</sub> and HO<sub>2</sub><sup>-</sup>, respectively (Eqs. (8) and (9)) [7, 8].

$$I_{a, \text{H}_2\text{O}_2} = I_0 f_{\text{H}_2\text{O}_2} \{1 - \exp[-2.3l(\varepsilon_{\text{H}_2\text{O}_2}[\text{H}_2\text{O}_2] + \varepsilon_{\text{HO}_2^-}[\text{HO}_2^-] + \varepsilon_{\text{C}}[\text{C}] + \varepsilon_{\text{DOC}}[\text{DOC}])]\} \quad (6)$$

$$I_{a, \text{HO}_2^-} = I_0 f_{\text{HO}_2^-} \left\{1 - \exp\left[-2.3l\left(\varepsilon_{\text{H}_2\text{O}_2}[\text{H}_2\text{O}_2] + \varepsilon_{\text{HO}_2^-}[\text{HO}_2^-] + \varepsilon_{\text{C}}[\text{C}] + \varepsilon_{\text{DOC}}[\text{DOC}]\right)\right]\right\} \quad (7)$$

$$f_{\text{H}_2\text{O}_2} = \frac{\varepsilon_{\text{H}_2\text{O}_2}[\text{H}_2\text{O}_2]}{\varepsilon_{\text{H}_2\text{O}_2}[\text{H}_2\text{O}_2] + \varepsilon_{\text{HO}_2^-}[\text{HO}_2^-] + \varepsilon_{\text{C}}[\text{C}] + \varepsilon_{\text{DOC}}[\text{DOC}]} \quad (8)$$

$$f_{\text{HO}_2^-} = \frac{\varepsilon_{\text{HO}_2^-}[\text{HO}_2^-]}{\varepsilon_{\text{H}_2\text{O}_2}[\text{H}_2\text{O}_2] + \varepsilon_{\text{HO}_2^-}[\text{HO}_2^-] + \varepsilon_{\text{C}}[\text{C}] + \varepsilon_{\text{DOC}}[\text{DOC}]} \quad (9)$$

in which [H<sub>2</sub>O<sub>2</sub>], [HO<sub>2</sub><sup>-</sup>], [C], and [DOC] are H<sub>2</sub>O<sub>2</sub>, HO<sub>2</sub><sup>-</sup>, contaminant and DOM, in terms of DOC, concentrations, respectively.  $\varepsilon_{\text{H}_2\text{O}_2}$ ,  $\varepsilon_{\text{HO}_2^-}$ ,  $\varepsilon_{\text{C}}$  and  $\varepsilon_{\text{DOC}}$  (M<sup>-1</sup> m<sup>-1</sup>) are the molar extinction coefficients of H<sub>2</sub>O<sub>2</sub>, HO<sub>2</sub><sup>-</sup>, the pollutant and the DOC, respectively. In turn,  $l$  (mm) is the photoreactor path length and  $I_0$  (Ein s<sup>-1</sup>), the incident UV-light intensity.

In addition to the oxidant photolysis, the target pollutant (C) may interact with the UV-radiation, undergoing degradation and producing reaction intermediates. A fraction of those by-products can be dissolved in the solution [16]. This fraction is denoted as DOC (Eq. (10)) [6]. The reaction rate for the contaminant direct photolysis is obtained through Eq. (11).



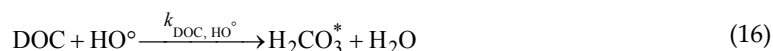
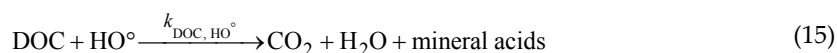
$$\frac{d[C]}{dt} = -\phi_c I_{a,C} \quad (11)$$

where  $\phi_c$  is the quantum yield of pollutant photolysis and  $I_{a,C}$  is the amount of UV-light absorbed by the contaminant, calculated through Eqs. (12) and (13).

$$I_{a,C} = I_0 f_C \left\{ 1 - \exp \left[ -2.3l \left( \varepsilon_{H_2O_2} [H_2O_2] + \varepsilon_{HO_2^-} [HO_2^-] + \varepsilon_C [C] + \varepsilon_{DOC} [DOC] \right) \right] \right\} \quad (12)$$

$$f_C = \frac{\varepsilon_C [C]}{\varepsilon_{H_2O_2} [H_2O_2] + \varepsilon_{HO_2^-} [HO_2^-] + \varepsilon_C [C] + \varepsilon_{DOC} [DOC]} \quad (13)$$

Once HO° are produced, they rapidly react with the pollutant of interest, degrading it to form reaction intermediates (Eq. (14)), which subsequently can be attacked by HO° and undergo further degradation to produce final products, such as CO<sub>2</sub>, H<sub>2</sub>O, and mineral acids (Eq. (15)) [7]. In this model, intermediate substances were considered as HO° scavengers as well as UV-light absorbers. Additionally, it was assumed that the pH of the solution decreased due to the conversion of the target pollutant, and consequently the reaction intermediates, into carbon dioxide (i.e., H<sub>2</sub>CO<sub>3</sub>\* in the aqueous phase); although it must be highlighted that not all the DOC is mineralized, since carboxylic acids are also formed during the oxidation process, making the pH of the bulk decreases as well [8]. Under this presumption, Eq. (15) is simplified as Eq. (16). The mass balances for the evolution of the pollutant, the dissolved organic fraction of the formed by-products, HO° and the H<sub>2</sub>CO<sub>3</sub>\* concentrations with time are shown by Eqs. (17)–(20), respectively.



$$\frac{d[C]}{dt} = -k_{C,HO^\circ} [HO^\circ][C] \quad (17)$$

$$\frac{d[DOC]}{dt} = k_{C,HO^\circ} [HO^\circ][C] - k_{DOC,HO^\circ} [HO^\circ][DOC] \quad (18)$$

$$\frac{d[HO^\circ]}{dt} = -k_{C,HO^\circ} [HO^\circ][C] - k_{DOC,HO^\circ} [HO^\circ][DOC] \quad (19)$$

$$\frac{d[H_2CO_3^*]}{dt} = k_{DOC,HO^\circ} [HO^\circ][DOC] \quad (20)$$

where  $[C]$ ,  $[DOC]$ ,  $[HO^\circ]$ , and  $[H_2CO_3^*]$  correspond to pollutant, dissolved by-products,  $HO^\circ$  and  $H_2CO_3^*$  levels, respectively.  $k_{C,HO^\circ}$  and  $k_{DOC,HO^\circ}$  are the rate constants of Eq. (14) and (15) or (16).

In the UV/ $H_2O_2$  system, recombination of  $HO^\circ$  can occur to produce  $H_2O_2$ . However, these free radicals can also react with  $H_2O_2$  and  $HO_2^-$ , particularly when the oxidant is in excess, to produce  $HO_2^\circ$ . Although  $HO_2^\circ$  are less reactive than  $HO^\circ$  ( $E^\circ = 0.98$  and  $2.8$  V, respectively) [8], they can also be involved in pollutant degradation, especially if these radicals are produced in high amounts in the system. Furthermore,  $HO_2^\circ$  can produce  $O_2^{\circ-}$ , which subsequently can participate in pollutant degradation and mineralization [17]. Therefore, the role of these reactive oxygen species was included in the proposed kinetic model.

It is important to note that as the oxidation process develops, the pH of the solution generally goes down, and consequently, some chemical species appear while other species vanish. In order to consider the change of chemical species inside the bulk according to the pH of the solution in the kinetic model, a correction factor ( $\delta_{R_i}$ ) was introduced for the photolysis of  $H_2O_2$ ,  $HO_2^-$ , and for the reaction between  $H_2O_2$  and  $HO^\circ$ . This correction factor can adopt two values (0 and 1). When  $\delta_{R_i}=1$ , reaction  $R_i$  is promoted (i.e., the time-varying concentrations of the chemical species involved in reaction  $R_i$  are taken into account in the model). When  $\delta_{R_i}=0$ , reaction  $R_i$  is not considered in the model and, subsequently, the chemical species taking part in reaction  $R_i$  are neglected.

On the other hand, species commonly present in water, such as DOM and inorganic anions (e.g.,  $CO_3^{2-}$ ,  $HCO_3^-$ ,  $SO_4^{2-}$ , and  $Cl^-$ , among others) may also have a significant effect because of their ability to absorb UV-light and/or to scavenge  $HO^\circ$ . The  $HO^\circ$  scavenging effect of matrix

constituents drastically limits the oxidation action of HO°, leading to a decrease in the performance of the system [18].

Taking into account all the mentioned processes and in order to give a more realistic view of what happens in the UV/H<sub>2</sub>O<sub>2</sub> process, the kinetic equation describing pollutant degradation can be expressed as Eq. (21).

$$-\frac{dC}{dt} = \phi_c I_{a,C} + k_{14}[C][HO^\circ] + k_{15}[C][HO_2^\circ] + k_{16}[C][O_2^{\circ-}] + \sum_{i=35}^{40} k_i[C][AR_i] \quad (21)$$

where the terms  $\phi_c I_{a,C}$ ,  $k_{14}[C][HO^\circ]$ ,  $k_{15}[C][HO_2^\circ]$ ,  $k_{16}[C][O_2^{\circ-}]$  and  $\sum_{i=35}^{40} k_i[C][AR_i]$  represent the specific contributions of UV-radiation, the oxidation of HO°, HO<sub>2</sub>°, O<sub>2</sub>°- and the formed anion radicals (AR) (including CO<sub>3</sub>°-, SO<sub>4</sub>°-, H<sub>2</sub>ClO°, HClO°, Cl°, and Cl<sub>2</sub>°-) to the overall pollutant degradation, respectively.

In order to quantitatively evaluate the contribution of the cited terms in the contaminant removal, parameters  $d$ ,  $f$ ,  $g$ , and  $h$  were introduced in Eq. (21), as described by Eq. (22).

$$-\frac{dC}{dt} = \phi_c I_{a,C} + k_{14}[C][HO^\circ]d + k_{15}[C][HO_2^\circ]f + k_{16}[C][O_2^{\circ-}]g + \sum_{i=35}^{40} k_i[C][AR_i]h \quad (22)$$

When  $d = f = g = h = 0$  (i.e., when the initial concentrations of oxidant radical species are equal to zero), the kinetic model only describes the degradation of the pollutant by photolysis. If  $d = h = 1$  and  $f = g = 0$ , in addition to the photolysis conversion, in a deionized water, the model can predict pollutant transformation through HO° and CO<sub>3</sub>°- (the latter from the reaction between HO° and HCO<sub>3</sub><sup>-</sup> or CO<sub>3</sub><sup>2-</sup>). When  $d = f = h = 1$  and  $g = 0$ , contaminant removal by photolysis and the action of HO° and HO<sub>2</sub>°, as well as CO<sub>3</sub>°-, is described. When all the parameters are equal to 1 (i.e.,  $d = f = g = h = 1$ ) and there are no inorganic anions different from HCO<sub>3</sub><sup>-</sup> and CO<sub>3</sub><sup>2-</sup> in the studied water, the kinetic model accounts for the degradation of the pollutant by direct photolysis and oxidation through HO°, HO<sub>2</sub>°, O<sub>2</sub>°-, and CO<sub>3</sub>°-. As the model includes the reactions where Cl<sup>-</sup>, SO<sub>4</sub><sup>2-</sup>, CO<sub>3</sub><sup>2-</sup>, and HCO<sub>3</sub><sup>-</sup> are involved, it can be used for the treatment of different types of water.

Based on the reactions illustrated in **Figures 1** and **2**, and the different involved parameters, the mass balances and the corresponding ODE of the species of interest (C, DOC, H<sub>2</sub>O<sub>2</sub>, HO<sub>2</sub>, HO°, HO<sub>2</sub>°, O<sub>2</sub>°-, CO<sub>3</sub>°-, SO<sub>4</sub>°-, HClO°, H<sub>2</sub>ClO°, HClO°, Cl°, Cl<sub>2</sub>°-, OH<sup>-</sup>, H<sup>+</sup>, H<sub>2</sub>CO<sub>3</sub><sup>\*</sup>, CO<sub>3</sub><sup>2-</sup>, HCO<sub>3</sub><sup>-</sup>, HSO<sub>4</sub><sup>-</sup>, SO<sub>4</sub><sup>2-</sup>, and Cl<sup>-</sup>) are summarized in **Table 1**.



No.	Species	Kinetic expressions
ODE <sub>1</sub>	C	$\frac{d[C]}{dt} = -\phi_c I_{a,c} - k_{14}[C][HO^\circ]d - k_{15}[C][HO_2^\circ]f - k_{16}[C][O_2^{\cdot-}]g - (k_{35}[C][CO_3^{\cdot-}] + k_{36}[C][SO_4^{\cdot-}] + k_{37}[C][H_2ClO^\circ] + k_{38}[C][HClO^\circ] + k_{39}[C][Cl^\cdot] + k_{40}[C][Cl_2^{\cdot-}])h$
ODE <sub>2</sub>	H <sub>2</sub> O <sub>2</sub>	$\frac{d[H_2O_2]}{dt} = -\phi_{H_2O_2} I_{a,H_2O_2} \delta_{R_8} - k_1[H_2O_2] + k_2[HO_2^-][H^+] - k_5[H_2O_2][HO^\circ] \delta_{R_7} - k_5[H_2O_2][HO^\circ] \delta_{R_8} + k_7[{}^\circ OH][HO^\circ] + k_{10}[HO_2^\circ][HO_2^\circ] - k_{11}[H_2O_2][HO_2^\circ] - k_{12}[H_2O_2][O_2^{\cdot-}] - k_{20}[H_2O_2][CO_3^{\cdot-}] - k_{24}[SO_4^{\cdot-}][H_2O_2] - k_{31}[Cl_2^{\cdot-}][H_2O_2] - k_{32}[Cl^\cdot][H_2O_2]$
ODE <sub>3</sub>	HO <sub>2</sub> <sup>-</sup>	$\frac{d[HO_2^-]}{dt} = -\phi_{HO_2^-} I_{a,HO_2^-} \delta_{R_4} + k_1[H_2O_2] - k_2[HO_2^-][H^+] - k_6[HO^\circ][HO_2^-] + k_{13}[HO_2^\circ][O_2^{\cdot-}] - k_{21}[HO_2^-][CO_3^{\cdot-}]$
ODE <sub>4</sub>	°OH	$\frac{d[HO^\circ]}{dt} = 2\phi_{H_2O_2} I_{a,H_2O_2} \delta_{R_8} + 2\phi_{HO_2^-} I_{a,HO_2^-} \delta_{R_4} - k_5[H_2O_2][HO^\circ] \delta_{R_7} - k_5[H_2O_2][HO^\circ] \delta_{R_8} - k_6[HO^\circ][HO_2^-] - k_7[HO^\circ][HO^\circ] - k_8[HO^\circ][HO_2^\circ] - k_9[HO^\circ][O_2^{\cdot-}] + k_{11}[H_2O_2][HO_2^\circ] + k_{12}[H_2O_2][O_2^{\cdot-}] - k_{14}[C][HO^\circ]d - k_{17}[DOC][HO^\circ] - k_{18}[CO_3^{\cdot-}][HO^\circ] - k_{19}[HCO_3^-][HO^\circ] - k_{23}[HSO_4^-][HO^\circ] - k_{26}[Cl^\cdot][HO^\circ] - k_{30}[Cl_2^{\cdot-}][HO^\circ]$
ODE <sub>5</sub>	HO <sub>2</sub> <sup>°</sup>	$\frac{d[HO_2^\circ]}{dt} = -k_3[HO_2^\circ] + k_4[O_2^{\cdot-}][H^+] + k_5[H_2O_2][HO^\circ] \delta_{R_8} + k_6[HO^\circ][HO_2^-] - k_8[HO^\circ][HO_2^\circ] - k_{10}[HO_2^\circ][HO_2^\circ] - k_{11}[H_2O_2][HO_2^\circ] - k_{13}[HO_2^\circ][O_2^{\cdot-}] - k_{15}[C][HO_2^\circ]f + k_{20}[H_2O_2][CO_3^{\cdot-}] + k_{21}[HO_2^-][CO_3^{\cdot-}] + k_{24}[SO_4^{\cdot-}][H_2O_2] - k_{25}[SO_4^{\cdot-}][HO_2^\circ] + k_{31}[Cl_2^{\cdot-}][H_2O_2] + k_{32}[Cl^\cdot][H_2O_2] - k_{33}[Cl_2^{\cdot-}][HO_2^\circ]$
ODE <sub>6</sub>	O <sub>2</sub> <sup>·-</sup>	$\frac{d[O_2^{\cdot-}]}{dt} = k_3[HO_2^\circ] - k_4[O_2^{\cdot-}][H^+] + k_5[H_2O_2][HO^\circ] \delta_{R_7} - k_9[HO^\circ][O_2^{\cdot-}] - k_{12}[H_2O_2][O_2^{\cdot-}] - k_{13}[HO_2^\circ][O_2^{\cdot-}] - k_{16}[C][O_2^{\cdot-}]g - k_{22}[O_2^{\cdot-}][CO_3^{\cdot-}] - k_{34}[Cl_2^{\cdot-}][O_2^{\cdot-}]$
ODE <sub>7</sub>	OH <sup>-</sup>	$\frac{d[OH^-]}{dt} = \phi_{HO_2^-} I_{a,HO_2^-} \delta_{R_4} + k_6[HO^\circ][HO_2^-] + k_9[HO^\circ][O_2^{\cdot-}] + k_{12}[H_2O_2][O_2^{\cdot-}] + k_{18}[CO_3^{\cdot-}][HO^\circ]$
ODE <sub>8</sub>	H <sup>+</sup>	$\frac{d[H^+]}{dt} = k_1[H_2O_2] - k_2[HO_2^-][H^+] + k_3[HO_2^\circ] - k_4[O_2^{\cdot-}][H^+] + k_5[H_2O_2][HO^\circ] \delta_{R_7} + k_{24}[SO_4^{\cdot-}][H_2O_2] + k_{25}[SO_4^{\cdot-}][HO_2^\circ] - k_{27}[HClO^\cdot][H^+] + k_{31}[Cl_2^{\cdot-}][H_2O_2] + k_{32}[Cl^\cdot][H_2O_2] + k_{33}[Cl_2^{\cdot-}][HO_2^\circ] + k_{41}[H_2CO_3] - k_{42}[HCO_3^-][H^+] + k_{43}[HCO_3^-] - k_{44}[CO_3^{\cdot-}][H^+] + k_{45}[HSO_4^-] - k_{46}[SO_4^{\cdot-}][H^+]$
ODE <sub>9</sub>	DOC	$\frac{d[DOC]}{dt} = \phi_c I_{a,c} + k_{14}[C][HO^\circ]d + k_{15}[C][HO_2^\circ]f + k_{16}[C][O_2^{\cdot-}]g - k_{17}[DOC][HO^\circ] - \phi_{DOC} I_{a,DOC} + (k_{35}[C][CO_3^{\cdot-}] + k_{36}[C][SO_4^{\cdot-}] + k_{37}[C][H_2ClO^\circ] + k_{38}[C][HClO^\circ] + k_{39}[C][Cl^\cdot] + k_{40}[C][Cl_2^{\cdot-}])h$
ODE <sub>10</sub>	CO <sub>3</sub> <sup>2-</sup>	$\frac{d[CO_3^{2-}]}{dt} = -k_{18}[CO_3^{2-}][HO^\circ] + k_{21}[HO_2^-][CO_3^{2-}] + k_{22}[O_2^{\cdot-}][CO_3^{2-}] + k_{43}[HCO_3^-] - k_{44}[CO_3^{2-}][H^+]$
ODE <sub>11</sub>	CO <sub>3</sub> <sup>·-</sup>	$\frac{d[CO_3^{\cdot-}]}{dt} = k_{18}[CO_3^{2-}][HO^\circ] + k_{19}[HCO_3^-][HO^\circ] - k_{20}[H_2O_2][CO_3^{\cdot-}] - k_{21}[HO_2^-][CO_3^{\cdot-}] - k_{22}[O_2^{\cdot-}][CO_3^{\cdot-}] - k_{35}[C][CO_3^{\cdot-}]h$

$ODE_{12}$	$HCO_3^-$	$\frac{d[HCO_3^-]}{dt} = -k_{19}[HCO_3^-][HO^\circ] + k_{20}[H_2O_2][CO_3^{\cdot-}] + k_{41}[H_2CO_3] - k_{42}[HCO_3^-][H^+] - k_{43}[HCO_3^-] + k_{44}[CO_3^{\cdot-}][H^+]$
$ODE_{13}$	$H_2CO_3^*$	$\frac{d[H_2CO_3^*]}{dt} = k_{17}[DOC][HO^\circ] - k_{41}[H_2CO_3^*] + k_{42}[HCO_3^-][H^+]$
$ODE_{14}$	$HSO_4^-$	$\frac{d[HSO_4^-]}{dt} = -k_{23}[HSO_4^-][HO^\circ] - k_{45}[HSO_4^-] + k_{46}[SO_4^{\cdot-}][H^+]$
$ODE_{15}$	$SO_4^{\cdot-}$	$\frac{d[SO_4^{\cdot-}]}{dt} = k_{23}[HSO_4^-][HO^\circ] - k_{24}[SO_4^{\cdot-}][H_2O_2] - k_{25}[SO_4^{\cdot-}][HO_2^\circ] - k_{36}[C][SO_4^{\cdot-}]h$
$ODE_{16}$	$SO_4^{2\cdot-}$	$\frac{d[SO_4^{2\cdot-}]}{dt} = k_{24}[SO_4^{\cdot-}][H_2O_2] + k_{25}[SO_4^{\cdot-}][HO_2^\circ] + k_{45}[HSO_4^-] - k_{46}[SO_4^{2\cdot-}][H^+]$
$ODE_{17}$	$Cl^-$	$\frac{d[Cl^-]}{dt} = -k_{26}[Cl^-][HO^\circ] - k_{29}[Cl^-][Cl^-] + k_{30}[Cl_2^{\cdot-}][^{\circ}OH] + 2k_{31}[Cl_2^{\cdot-}][H_2O_2] + k_{32}[Cl^{\cdot-}][H_2O_2] + 2k_{33}[Cl_2^{\cdot-}][HO_2^\circ] + 2k_{34}[Cl_2^{\cdot-}][O_2^{\cdot-}]$
$ODE_{18}$	$HClO^{\cdot-}$	$\frac{d[HClO^{\cdot-}]}{dt} = k_{26}[Cl^-][HO^\circ] - k_{27}[HClO^{\cdot-}][H^+]$
$ODE_{19}$	$H_2ClO^*$	$\frac{d[H_2ClO^*]}{dt} = k_{27}[HClO^{\cdot-}][H^+] - k_{28}[H_2ClO^*] - k_{37}[C][H_2ClO^*]h$
$ODE_{20}$	$HClO^\circ$	$\frac{d[HClO^\circ]}{dt} = k_{30}[Cl_2^{\cdot-}][HO^\circ] - k_{30}[C][HClO^\circ]h$
$ODE_{21}$	$Cl^\cdot$	$\frac{d[Cl^\cdot]}{dt} = k_{28}[H_2ClO^*] - k_{29}[Cl^\cdot][Cl^-] - k_{32}[Cl^\cdot][H_2O_2] - k_{39}[C][Cl^\cdot]h$
$ODE_{22}$	$Cl_2^{\cdot-}$	$\frac{d[Cl_2^{\cdot-}]}{dt} = k_{29}[Cl^\cdot][Cl^-] - k_{30}[Cl_2^{\cdot-}][HO^\circ] - k_{31}[Cl_2^{\cdot-}][H_2O_2] - k_{33}[Cl_2^{\cdot-}][HO_2^\circ] - k_{34}[Cl_2^{\cdot-}][O_2^{\cdot-}] - k_{40}[C][Cl_2^{\cdot-}]h$

$k_1 = 3.7 \times 10^{-2} \text{ s}^{-1}$ ,  $k_2 = 2.6 \times 10^{10} \text{ M}^{-1} \text{ s}^{-1}$ ,  $\epsilon_{H_2O_2}(254 \text{ nm}) = 1800 \text{ M}^{-1} \text{ m}^{-1}$ ,  
 $\epsilon_{HO_2^\cdot}(254 \text{ nm}) = 22800 \text{ M}^{-1} \text{ m}^{-1}$ ,  $\Phi_{H_2O_2}(254 \text{ nm}) = 0.5 \text{ molEin}^{-1}$ ,  $\Phi_{HO_2^\cdot}(254 \text{ nm}) = 0.5 \text{ molEin}^{-1}$ ,  $\text{pH} > 11.6 \Rightarrow \delta_{R_3} = 0$ ,  $\delta_{R_4} = 1$ ,  $\text{pH} < 11.6 \Rightarrow \delta_{R_3} = 1$ ,  $\delta_{R_4} = 0$ ,  $k_3 = 1.58 \times 10^5 \text{ s}^{-1}$ ,  $k_4 = 1.0 \times 10^{10} \text{ M}^{-1} \text{ s}^{-1}$ ,  $k_5 = 2.7 \times 10^7 \text{ M}^{-1} \text{ s}^{-1}$ ,  $\text{pH} > 4.8 \Rightarrow \delta_{R_7} = 1$ ,  $\delta_{R_8} = 0$ ,  $\text{pH} < 4.8 \Rightarrow \delta_{R_7} = 0$ ,  $\delta_{R_8} = 1$ ,  $k_6 = 7.5 \times 10^9 \text{ M}^{-1} \text{ s}^{-1}$ ,  $k_7 = 5.5 \times 10^9 \text{ M}^{-1} \text{ s}^{-1}$ ,  $k_8 = 6.6 \times 10^9 \text{ M}^{-1} \text{ s}^{-1}$ ,  $k_9 = 7.0 \times 10^9 \text{ M}^{-1} \text{ s}^{-1}$ ,  $k_{10} = 8.3 \times 10^5 \text{ M}^{-1} \text{ s}^{-1}$ ,  $k_{11} = 3 \text{ M}^{-1} \text{ s}^{-1}$ ,  $k_{12} = 0.13 \text{ M}^{-1} \text{ s}^{-1}$ ,  $k_{13} = 9.7 \times 10^7 \text{ M}^{-1} \text{ s}^{-1}$ ,  $k_{C,HO^\cdot} = k_{14}$ ,  $k_{C,HO_2^\cdot} = k_{15}$ ,  $k_{C,CO_2^\cdot} = k_{16}$ ,  $k_{DOC,HO^\cdot} = k_{17} = 2.0 \times 10^8 \text{ M}^{-1} \text{ s}^{-1}$ ,  $k_{18} = 3.9 \times 10^8 \text{ M}^{-1} \text{ s}^{-1}$ ,  $k_{19} = 8.5 \times 10^6 \text{ M}^{-1} \text{ s}^{-1}$ ,  $k_{20} = 4.3 \times 10^5 \text{ M}^{-1} \text{ s}^{-1}$ ,  $k_{21} = 3.0 \times 10^7 \text{ M}^{-1} \text{ s}^{-1}$ ,  $k_{22} = 6.5 \times 10^8 \text{ M}^{-1} \text{ s}^{-1}$ ,  $k_{23} = 3.5 \times 10^5 \text{ M}^{-1} \text{ s}^{-1}$ ,  $k_{24} = 1.2 \times 10^7 \text{ M}^{-1} \text{ s}^{-1}$ ,  $k_{25} = 3.5 \times 10^9 \text{ M}^{-1} \text{ s}^{-1}$ ,  $k_{26} = 4.3 \times 10^9 \text{ M}^{-1} \text{ s}^{-1}$ ,  $k_{27} = 3.0 \times 10^{10} \text{ M}^{-1} \text{ s}^{-1}$ ,  $k_{28} = 5.0 \times 10^4 \text{ s}^{-1}$ ,  $k_{29} = 8.5 \times 10^9 \text{ M}^{-1} \text{ s}^{-1}$ ,  $k_{30} = 1.0 \times 10^9 \text{ M}^{-1} \text{ s}^{-1}$ ,  $k_{31} = 4.1 \times 10^4 \text{ M}^{-1} \text{ s}^{-1}$ ,  $k_{32} = 1.1 \times 10^9 \text{ M}^{-1} \text{ s}^{-1}$ ,  $k_{33} = 3.0 \times 10^9 \text{ M}^{-1} \text{ s}^{-1}$ ,  $k_{34} = 2.0 \times 10^9 \text{ M}^{-1} \text{ s}^{-1}$ ,  $k_{35} = ?$ ,  $k_{36} = ?$ ,  $k_{37} = ?$ ,  $k_{38} = ?$ ,  $k_{39} = ?$ ,  $k_{40} = ?$ ,  $k_{41} = 1 \times 10^{10} \text{ s}^{-1}$ ,  $k_{42} = 4.5 \times 10^3 \text{ M}^{-1} \text{ s}^{-1}$ ,  $k_{43} = 1 \times 10^{10} \text{ s}^{-1}$ ,  $k_{44} = 4.5 \times 10^{-1} \text{ M}^{-1} \text{ s}^{-1}$ ,  $k_{45} = 1 \times 10^{10} \text{ s}^{-1}$ ,  $k_{46} = 4.5 \times 10^{11} \text{ M}^{-1} \text{ s}^{-1}$

Table 1. Set of the ODE used in the kinetic model [9, 18, 27, 30–39].



## 2.2. Proposed kinetic model

In the developed kinetic model, three different ways of calculating the evolution of HO° concentration during time were presumed: (a) a non-pseudo-steady or transient state (i.e., the net formation rate of HO° is different from zero); (b) a pseudo-steady state; and (c) a simplified pseudo-steady state; correspondingly denoted as kinetic model A, B, and C.

In the prediction model A the concentration of HO° can be calculated with Eq. (23). From Eq. (23), the HO° concentration can be written as Eq. (24) (prediction model B).

$$\begin{aligned} \frac{d[\text{HO}^\circ]}{dt} = & 2\phi_{\text{H}_2\text{O}_2} I_{a, \text{H}_2\text{O}_2} \delta_{R_3} + 2\phi_{\text{HO}_2^-} I_{a, \text{HO}_2^-} \delta_{R_4} - k_5[\text{H}_2\text{O}_2][\text{HO}^\circ] \delta_{R_7} - \\ & k_5[\text{H}_2\text{O}_2][\text{HO}^\circ] \delta_{R_8} - k_6[\text{HO}^\circ][\text{HO}_2^-] - k_7[\text{HO}^\circ][\text{HO}^\circ] - k_8[\text{HO}^\circ][\text{HO}_2^\circ] - \\ & k_9[\text{HO}^\circ][\text{O}_2^{\circ-}] + k_{11}[\text{H}_2\text{O}_2][\text{HO}_2^\circ] + k_{12}[\text{H}_2\text{O}_2][\text{O}_2^{\circ-}] - k_{14}[\text{C}][\text{HO}^\circ] d - \\ & k_{17}[\text{DOC}][\text{HO}^\circ] - k_{18}[\text{CO}_3^{2-}][\text{HO}^\circ] - k_{19}[\text{HCO}_3^-][\text{HO}^\circ] - k_{23}[\text{HSO}_4^-][\text{HO}^\circ] - \\ & k_{26}[\text{Cl}^-][\text{HO}^\circ] - k_{30}[\text{Cl}_2^{\circ-}][\text{HO}^\circ] \end{aligned} \quad (23)$$

$$\begin{aligned} [\text{HO}^\circ] = & (2\phi_{\text{H}_2\text{O}_2} I_{a, \text{H}_2\text{O}_2} \delta_{R_3} + 2\phi_{\text{HO}_2^-} I_{a, \text{HO}_2^-} \delta_{R_4} + k_{11}[\text{H}_2\text{O}_2][\text{HO}_2^\circ] + k_{12}[\text{H}_2\text{O}_2][\text{O}_2^{\circ-}]) / \\ & (k_5[\text{H}_2\text{O}_2] \delta_{R_7} + k_5[\text{H}_2\text{O}_2] \delta_{R_8} + k_6[\text{HO}_2^-] + k_8[\text{HO}_2^\circ] + k_9[\text{O}_2^{\circ-}] + k_{14}[\text{C}] d + \\ & k_{17}[\text{DOC}] + k_{18}[\text{CO}_3^{2-}] + k_{19}[\text{HCO}_3^-] + k_{23}[\text{HSO}_4^-] + k_{26}[\text{Cl}^-] + k_{30}[\text{Cl}_2^{\circ-}]) \end{aligned} \quad (24)$$

Considering that the oxidant is in a high level (i.e.,  $k_5[\text{H}_2\text{O}_2] \delta_{R_7} + k_5[\text{H}_2\text{O}_2] \delta_{R_8} \gg \sum k_i[X_i]$ , where  $\sum k_i[X_i] = k_6[\text{HO}_2^-] + k_8[\text{HO}_2^\circ] k_9[\text{O}_2^{\circ-}] + k_{14}[\text{C}] d + k_{17}[\text{DOC}] + k_{18}[\text{CO}_3^{2-}] + k_{19}[\text{HCO}_3^-] + k_{23}[\text{HSO}_4^-] + k_{26}[\text{Cl}^-] + k_{30}[\text{Cl}_2^{\circ-}]$ ) and  $2\phi_{\text{H}_2\text{O}_2} I_{a, \text{H}_2\text{O}_2} \delta_{R_3} + 2\phi_{\text{HO}_2^-} I_{a, \text{HO}_2^-} \delta_{R_4} \gg \sum (k_{11}[\text{H}_2\text{O}_2][\text{HO}_2^\circ] + k_{12}[\text{H}_2\text{O}_2][\text{O}_2^{\circ-}])$ , Eq. (24) can be simplified to Eq. (25) (prediction model C).  $k_i$  and  $[X_i]$  are the reaction rate constants between HO° and species  $i$ , and the concentration of species  $i$ , respectively.

$$[\text{HO}^\circ] = \frac{2\phi_{\text{H}_2\text{O}_2} I_{a, \text{H}_2\text{O}_2} \delta_{R_3} + 2\phi_{\text{HO}_2^-} I_{a, \text{HO}_2^-} \delta_{R_4}}{k_5[\text{H}_2\text{O}_2] \delta_{R_7} + k_5[\text{H}_2\text{O}_2] \delta_{R_8}} \quad (25)$$

The initial values of DOC and inorganic anionic species ( $\text{CO}_3^{2-}$ ,  $\text{HCO}_3^-$ ,  $\text{SO}_4^{2-}$ ,  $\text{Cl}^-$ , etc.) are set according to the conditions of the water to be treated.

### 2.3. Numerical solution of the proposed kinetic models

The ODE system compiled in **Table 1** was solved applying MATLAB software and ODE15S function. For simultaneously solving the ODE set of the proposed kinetic models, it was necessary to define several photochemical parameters such as  $\phi_{\text{H}_2\text{O}_2}$ ,  $\phi_{\text{pollutant}}$ ,  $\phi_{\text{DOC}}$ ,  $\varepsilon_{\text{H}_2\text{O}_2}$ ,  $\varepsilon_{\text{HO}_2^\cdot}$ ,  $\varepsilon_{\text{pollutant}}$ ,  $\varepsilon_{\text{DOC}}$ ,  $I_0$  and  $l$ . Additionally, the initial concentrations of all the species involved in the system and the rate constants of the chemical reactions between those species were required (**Table 1**). During setting up the model, differential rate equations describing the time dependence of the concentration of the variety of the considered species were defined and plotted.

## 3. Results and discussion

In order to validate the proposed kinetic models, experimental data for PHE degradation by the UV/ $\text{H}_2\text{O}_2$  process were used from Alnaizy and Akgerman [19] study. These authors conducted a set of experiments in a completely mixed batch cylindrical photoreactor made on Pyrex glass. The used photochemical parameters and the kinetic reaction rate constants of PHE with  $\text{HO}^\cdot$ ,  $\text{O}_2^{\cdot-}$ , and  $\text{CO}_3^{\cdot-}$  are presented in **Table 2**.

Parameters	Notation	Numerical values	References
Quantum yield	$\phi_{\text{phenol}} = \phi_{\text{C}}$	0.07 mol Ein <sup>-1</sup>	[23]
Molar extinction coefficient	$\varepsilon_{\text{phenol}} = \varepsilon_{\text{C}}$	51 600 M <sup>-1</sup> m <sup>-1</sup>	[19]
Path length	$l$	63.5 mm	
Incident UV-light intensity (radiation of 254 nm > 90% and power = 15 W)	$I_0$	$1.516 \times 10^{-6}$ Ein L <sup>-1</sup> s <sup>-1</sup>	
Kinetic rate constant phenol- $\text{HO}^\cdot$	$k_{\text{phenol}, \text{HO}^\cdot} = k_{14}$	$6.6 \times 10^9$ M <sup>-1</sup> s <sup>-1</sup>	[40]
Kinetic rate constant phenol- $\text{O}_2^{\cdot-}$	$k_{\text{phenol}, \text{O}_2^{\cdot-}} = k_{16}$	$5.8 \times 10^3$ M <sup>-1</sup> s <sup>-1</sup>	[41]
Kinetic rate constant phenol- $\text{CO}_3^{\cdot-}$	$k_{\text{phenol}, \text{CO}_3^{\cdot-}} = k_{35}$	$2.2 \times 10^7$ M <sup>-1</sup> s <sup>-1</sup>	[42]

**Table 2.** Values of the parameters used in the kinetic model validation for phenol degradation.

### 3.1. Assumptions taken into consideration

As stated previously, the developed kinetic models A, B, and C employed the non-pseudo-steady, the pseudo-steady, and the simplified pseudo-steady state assumption, respectively, to estimate  $\text{HO}^\cdot$  concentration. In the proposed models, the impact of UV radiation individually

and/or the combined action of H<sub>2</sub>O<sub>2</sub> and UV light (including the effect of HO<sup>•</sup>, HO<sub>2</sub><sup>•</sup>, O<sub>2</sub><sup>•-</sup>, and CO<sub>3</sub><sup>•-</sup>) on PHE degradation was studied.

A PHE concentration of  $2.23 \times 10^{-3}$  M and a H<sub>2</sub>O<sub>2</sub>/PHE ratio of 495 were selected for validating the model. The used PHE solution was prepared by adding the appropriate amount of pollutant solution to deionized water [19]. Therefore, the effect of inorganic anions, excluding HCO<sub>3</sub><sup>-</sup> and CO<sub>3</sub><sup>2-</sup> was not taken into account. In this sense, in the PHE degradation rate expression (ODE<sub>1</sub>) the contribution of inorganic anion radicals, such as SO<sub>4</sub><sup>•-</sup>, H<sub>2</sub>ClO<sup>•</sup>, HClO<sup>•</sup>, Cl<sup>•</sup>, and Cl<sub>2</sub><sup>•-</sup> was not studied. It was assumed that the other terms included in ODE<sub>1</sub> contributed to pollutant degradation.

As the treated water was deionized, the presence of OM different from the parent compound in the initial solution was neglected ([DOC]<sub>0</sub> = 0 M). Hence, the DOC in the solution came from PHE photolysis and free radical (HO<sup>•</sup>, HO<sub>2</sub><sup>•</sup>, O<sub>2</sub><sup>•-</sup>, and CO<sub>3</sub><sup>•-</sup>) oxidation.

On the other hand, several authors agree that OM reduction by direct photolysis in a UV/H<sub>2</sub>O<sub>2</sub> oxidation process can be neglected [7–9]. That is the reason why this was not included in the proposed kinetic model. However, it is highlighted that the OM is able to absorb UV-light, preventing UV-penetration into the bulk and avoiding H<sub>2</sub>O<sub>2</sub>/HO<sub>2</sub><sup>-</sup> and pollutant direct photolysis. Therefore, the detrimental effect of UV-shielding in PHE degradation was taken into consideration. For including this effect in the kinetic model, OM molar extinction coefficient, referred as DOC molar extinction coefficient ( $\epsilon_{\text{DOC}}$ ), must be previously known. Although this parameter has already been measured [7, 8], its value is not a universal one, since DOM is a complex group of aromatic and aliphatic hydrocarbon structures with attached functional groups [20, 21]. As Alnaizy and Akgerman [19] did not measure this variable, a mean value from Peuravuori and Pihlaja [22] study was presumed. This value corresponded to  $\epsilon_{\text{DOC}(280\text{ nm})} = 35\,967\text{ M}^{-1}\text{ m}^{-1}$ , which was in the same order of magnitude than  $\epsilon_{\text{PHE}}$ . This number could be acceptable due to the formed aromatic intermediates during PHE conversion [19] conserve structural similarities with the parent compound, like the aromatic ring, responsible for the molecule excitation.

Additionally, it is widely known that the quantum yield of a compound is dependent on the excitation wavelength and the pH of the solution. For 254 nm, PHE quantum yield in an aqueous solution was found to be in the range of 0.02–0.12 mol Ein<sup>-1</sup> at pH 1.6–3.2 [23]. Therefore, an average value (0.07 mol Ein<sup>-1</sup>) was taken as PHE quantum yield.

Moreover, it is widely recognized that the solution pH decreases as the process proceeds. This variation in the pH can cause difficulties in modeling studies, since the presence of radical species such as HO<sub>2</sub><sup>•</sup>, and O<sub>2</sub><sup>•-</sup>, among other chemical species involved in the oxidation system, is significantly dependent on the pH of the medium. Therefore, to give a more realistic view of what happens inside the reaction medium, H<sub>2</sub>O<sub>2</sub> and HO<sub>2</sub><sup>-</sup> photolysis reactions (Eqs. (1) and (2), correspondingly), as well as reactions expressed in Eqs. (26) and (27) were discriminated in the model according to the solution pH time evolution, as it is simplified in **Figure 3**. For selecting the suitable reactions with regard to the pH changes over time, previous information about the evolution of the pH during the performance of the process is required. However, in some occasions this is not provided. In this case, the initial pH of the solution was 6.8 [19]. At

this pH, one of the predominant species into the bulk was  $\text{H}_2\text{O}_2$ , since the pKa of the  $\text{H}_2\text{O}_2/\text{HO}_2^-$  equilibrium is 11.6. Therefore, the photolysis of  $\text{HO}_2^-$  was neglected in the model performance (i.e.,  $\delta_{R_s}$  and  $\delta_{R_t}$ ). Additionally, the initial concentrations of  $\text{HO}^\circ$  and other considered species were assumed to be zero, with the exception of the pollutant and  $\text{H}_2\text{O}_2$ . On the other hand, it was found that the pH of the medium rapidly dropped from 6.8 to 4.7–4.2 (4.5 as a mean value) within the first 30 min of radiation [19]. Therefore, and according to **Figure 3**, Eq. (26) was considered during the first 30 min of the reaction while Eq. (27), after that time (i.e.,  $\delta_{R_t} = 1$ ,  $\delta_{R_s} = 0$  and  $\delta_{R_t} = 0$ ,  $\delta_{R_s} = 1$ , before and after the first 30 min of the process, respectively).

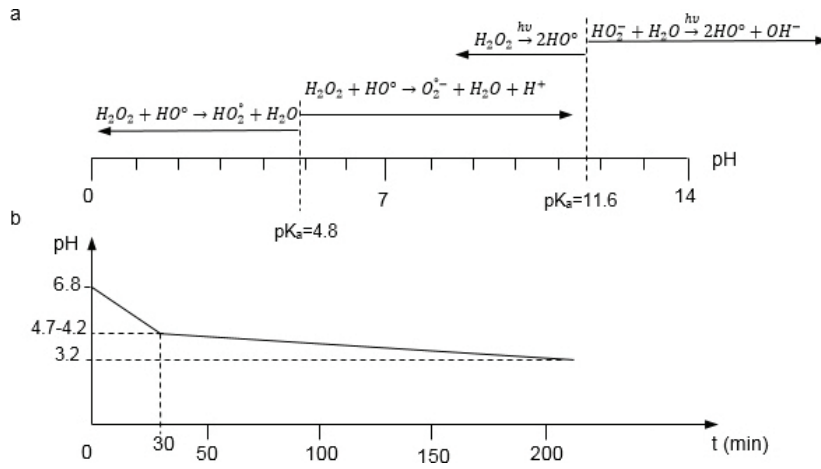


**Figure 3.** (a) Reaction discrimination diagram as a function of the solution pH and (b) pH evolution of the medium during the UV/ $\text{H}_2\text{O}_2$  process in a completely mixed batch photoreactor. Operating conditions:  $\text{H}_2\text{O}_2/\text{PHE} = 495$ ;  $[\text{C}]_0 = 2.23 \times 10^{-3} \text{ M}$ ;  $t = 220 \text{ min}$ .



### 3.2. Kinetic model validation

Initially, the associated ODE sets with model A, B, and C were solved. Parameters  $f = g = 0$  and  $d = h = 1$  were considered in order to solely investigate the influence of the direct photolysis,  $\text{HO}^\circ$ , and  $\text{CO}_3^{\circ-}$  on PHE degradation.

**Figure 4** compares the simulation results of the proposed kinetic models A, B, and C with the experimental data for  $2.23 \times 10^{-3}$  M PHE with a H<sub>2</sub>O<sub>2</sub>/PHE ratio of 495 and a reaction time of 220 min. The measured and simulated results for PHE direct photolysis alone are also presented. It is observed that more than 90% of the initial PHE concentration was removed after 220 min due to both direct photolysis and indirect degradation (primarily due to HO<sup>•</sup> attack). The effect of CO<sub>3</sub><sup>•-</sup> could be seen as marginal because of the reduced number of those radicals, in the range of 10<sup>-15</sup> M, and the low reaction rate constant with PHE compared to HO<sup>•</sup>. In addition, it is shown that PHE was not completely removed by direct UV photolysis under the tested photochemical conditions (**Table 2**), since approximately 50% of the total PHE degradation was attributed to UV photolysis, as it was experimentally determined by Alnaizy and Akgerman [19]. On the other hand, the figure demonstrates that the prediction kinetic model C was in good agreement with the available experimental data with a relative high correlation factor ( $R^2=99.34\%$ ). For prediction models A and B,  $R^2$  were 97.41 and 97.37%, respectively. As a result of the subtle differences between kinetic models A and B, the depicted line describing model A overlaps model B line. An acceptable agreement between model predictions considering only the UV radiation and experimental data was also verified ( $R^2 = 98.25\%$ ).

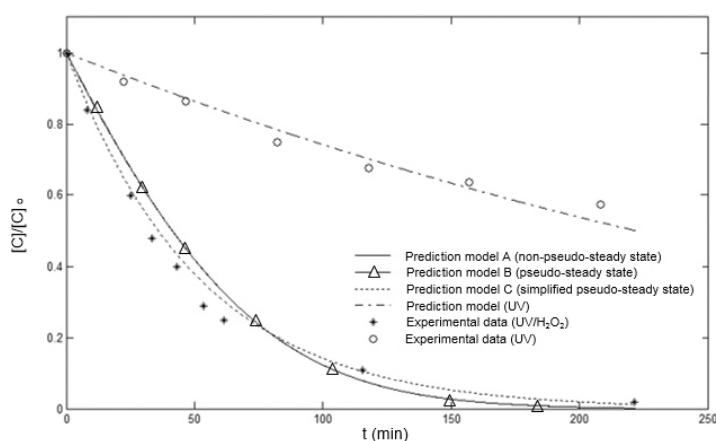


**Figure 4.** Comparison of the kinetic model predictions (lines) versus experimental data (o) and (+). Operating conditions: H<sub>2</sub>O<sub>2</sub>/PHE = 495; [C]<sub>0</sub> =  $2.23 \times 10^{-3}$  M; t = 220 min.

Furthermore, **Figure 4** clearly presents that the removal rate of the target pollutant was not significantly dependent on the hypothesis assumed to estimate the HO<sup>•</sup> level (non-pseudo-steady, pseudo-steady and simplified pseudo-steady state assumptions). This could be explained from the relatively low concentration of those reactive species in the solution (with a magnitude order of 10<sup>-14</sup> M) when compared to the level of other species involved in the system, such as HO<sub>2</sub><sup>•</sup> and O<sub>2</sub><sup>•-</sup>, whose concentrations were in the range of 10<sup>-7</sup> M. The number of HO<sup>•</sup> remaining in the solution is in concordance with the low final HO<sup>•</sup> levels found in the literature [24, 25] and even higher than those reported by Ray and Tarr [26].

In **Figure 5**, the evolution of the  $\text{HO}^\circ$ ,  $\text{HO}_2^\circ$ ,  $\text{O}_2^{\circ-}$ , DOC and  $\text{H}_2\text{CO}_3^*$  normalized estimated concentrations using the prediction model A is depicted. It is observed that  $\text{HO}_2^\circ$  number increased as the oxidation system proceeded, while  $\text{O}_2^{\circ-}$  level decreased. Typically, the effect of  $\text{HO}_2^\circ$  and  $\text{O}_2^{\circ-}$  radicals are neglected in the UV/ $\text{H}_2\text{O}_2$  system [6–8, 15, 17, 27, 28] since they are found to be less reactive than  $\text{HO}^\circ$ , as stated previously. However, when they are produced in a high level, they could also participate in the contaminant oxidation. That is the current case of  $\text{HO}_2^\circ$ , as  $[\text{HO}_2^\circ] \gggg [\text{HO}^\circ]$ . Therefore, the contribution of  $\text{HO}_2^\circ$  to PHE degradation should be studied. On the other hand, in this work the action of  $\text{O}_2^{\circ-}$  in PHE conversion can be omitted since  $\text{O}_2^{\circ-}$  level decreased with the reaction time, as expected, because of the drop in the pH solution.

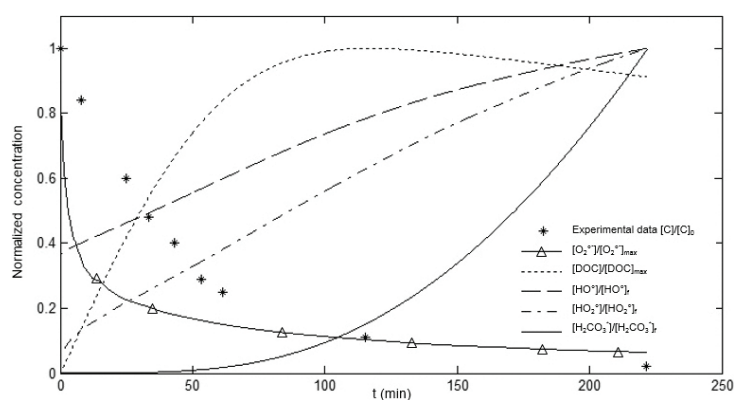


**Figure 5.** Concentration-time profiles of  $\text{HO}^\circ$  (---),  $\text{HO}_2^\circ$  (-.-.-),  $\text{O}_2^{\circ-}$  (-Δ-), DOC (···) and  $\text{H}_2\text{CO}_3^*$  (—) using the prediction kinetic model A. (\*) represents PHE experimental evolution. Operating conditions:  $\text{H}_2\text{O}_2/\text{PHE} = 495$ ;  $[\text{C}]_0 = 2.23 \times 10^{-3} \text{ M}$ ;  $t = 220 \text{ min}$ .

Furthermore, generally, there is a drop in the pH of the medium as the system progresses. This is probably due to acidic compound formation, such as carboxylic acids and  $\text{H}_2\text{CO}_3^*$  resulting from pollutant degradation and mineralization. In this study the decrease of the pH in the solution was predicted via DOC conversion and the sole generation of  $\text{H}_2\text{CO}_3^*$  by model A. As presented in **Figure 5**, DOC generation was progressively increasing as PHE was being degraded up to a certain point (117 min, corresponding to  $[\text{DOC}]_{\text{max}} = 2.061 \times 10^{-3} \text{ M}$ , and equivalent to ca. 93% of PHE degradation). From this point, DOC started to decrease until  $[\text{DOC}]_f = 1.879 \times 10^{-3} \text{ M}$ . That breakpoint represented the moment at which PHE was almost completely transformed into by-products. In addition, at this point, PHE mineralization began to be more evident, since  $\text{H}_2\text{CO}_3^*$  level rose approximately in a linear way, up to a final level of  $6.493 \times 10^{-14} \text{ M}$ , with the subsequent pH decrease. Similarities between the pattern of this DOC profile and that of the formed intermediate curves reported in Alnaizy and Akgerman [19] research are highlighted.

On the other hand, it is worth noting that  $\text{HO}^\circ$  level evolution with the reaction time was different when comparing the kinetic prediction model A or B with C. Obviating  $\text{HO}_2^\circ$  contribution to PHE degradation, **Figure 6** shows that the highest final  $\text{HO}^\circ$  level was achieved

in the prediction model A, with a maximum HO° concentration equal to  $9.435 \times 10^{-14}$  M. This value was similar to HO° final level in the prediction model B ( $9.400 \times 10^{-14}$  M) and different to that of the prediction model C, where HO° final concentration was  $4.486 \times 10^{-14}$  M (ca. 48% lower than the obtained in the kinetic model A or B).

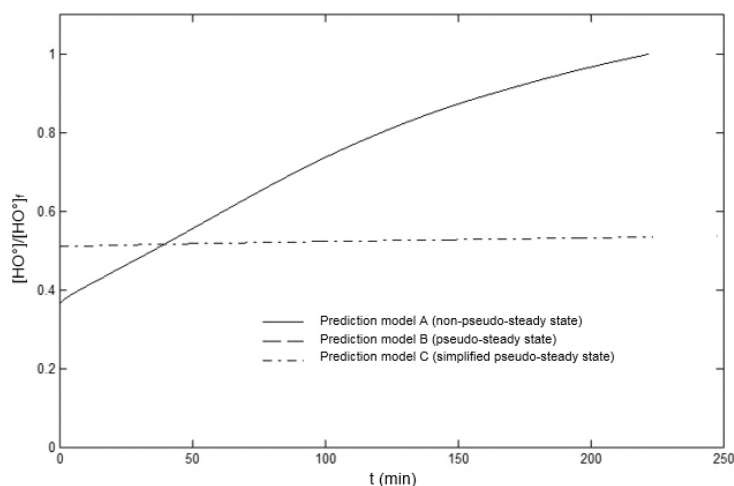


**Figure 6.** Estimated HO° concentration using the prediction models A (—), B (---), and C (-.-). Operating conditions: H<sub>2</sub>O<sub>2</sub>/PHE = 495; [C]<sub>0</sub> =  $2.23 \times 10^{-3}$  M; t = 220 min.

Approximately, in the first 40 min of the process a larger number of HO° in the aqueous medium with the developed kinetic model C was evidenced. Apparently, this amount of HO° was sufficient to degrade about 60% of PHE initial level under the studied experimental conditions. In contrast, models A and B, whose lines are overlapped, produced a lower number of HO° and the theoretical conversion of PHE remained above the experimental data. One possible reason for this discrepancy can be ascribed to DOM and dissolved oxygen positive effects in producing reactive oxygen species (ROS), as HO° [26], which were not considered. After 40 min of reaction, the HO° level was higher in the kinetic models A and B than in model C. This larger amount of HO° might lead to a faster conversion of the pollutant in comparison with the predicted model C, since the hypothetical depletion curve of PHE was below the measured data. Nevertheless, this rapid pollutant degradation did not occur actually. Therefore, there was an amount of HO° produced in excess that was not reacting with the contaminant. This surplus of HO° could be involved in free radical scavenging reactions. As model A and B consider the detrimental effect of HO° consuming reactions, it is suggested that their kinetic rate constants are higher than those ones used in this paper for these reactions to have a larger weight in the system. Additionally, the contradictory outcome between the actual situation and the theoretical one in the first and second stage of the process can also be attributed to the fact that just a fraction of the concentration of the species involved in the whole kinetic equations of the predicted models was actually reacting. Consequently, the real level of the species implicated in each kinetic reaction

should be considered. However, it is rather difficult to determine which amount of the chemical species is exactly involving in each reaction for each time step, especially due to the high reactivity of radicals as the oxidation system progresses. In this context, further studies are required to overcome this limitation.

From these findings, it is suggested that there was an effective level of the formed  $\text{HO}^\circ$ . Below that level, there was a lack of  $\text{HO}^\circ$  for an efficient pollutant conversion; and above it, an excessive number of  $\text{HO}^\circ$  was generated. That  $\text{HO}^\circ$  effective level could be of relevance for industrial applications in order to be maintained throughout the reaction time, allowing an efficient pollutant degradation.

### 3.3. Estimation of PHE- $\text{HO}_2^\circ$ reaction rate constant

In order to study the action of  $\text{HO}_2^\circ$  for pollutant degradation in the UV/ $\text{H}_2\text{O}_2$  system, PHE- $\text{HO}_2^\circ$  rate constant was calculated. For this purpose, the kinetic model A was used and it was estimated through a non-linear least-square objective function. The objective function for minimizing the error between the predicted and the measured data was defined as Eq. (28) [17].

$$\text{Minimize : } f = \sum \left( [C]_{\text{predicted}} - [C]_{\text{measured}} \right)^2 \quad (28)$$

where  $[C]_{\text{measured}}$  and  $[C]_{\text{predicted}}$  correspond to the evolution of experimental and calculated pollutant concentration, respectively. This expression is a function of PHE- $\text{HO}_2^\circ$  rate constant. The optimum value for PHE- $\text{HO}_2^\circ$  second-order rate constant was found to be  $1.6 \times 10^3 \text{ M}^{-1} \text{ s}^{-1}$ , which is consistent with the range of the reported values by Kozmér et al.  $((2.7 \pm 1.2) \times 10^3 \text{ M}^{-1} \text{ s}^{-1})$  [29]. The results of running the new prediction kinetic model A (with and without the contribution of  $\text{HO}_2^\circ$  to pollutant conversion) and the experimental data are presented in **Figure 7**. The figure shows that the prediction model A with the estimation

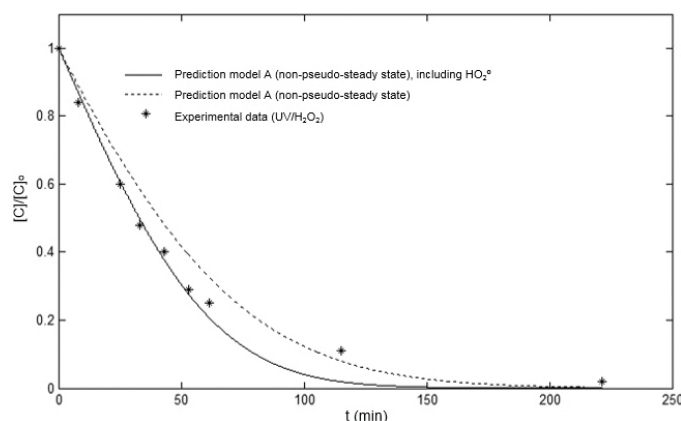


**Figure 7.** Comparison of experimental (symbols) vs predicted data (lines) using the kinetic model A with (—) and without (---) the action of  $\text{HO}_2^\circ$ . Operating conditions:  $\text{H}_2\text{O}_2/\text{PHE} = 495$ ;  $[C]_0 = 2.23 \times 10^{-3} \text{ M}$ ;  $t = 220 \text{ min}$ .



of PHE-HO<sub>2</sub><sup>°</sup> rate constant was in a stronger agreement with the experimental data ( $R^2 = 99.0\%$ ) than the previous predicted kinetic model A studied in section 3.2 ( $R^2 = 97.41\%$ ). The same conclusion can be drawn for kinetic model B and C, with a  $R^2$  of 98.78 and 99.57% using the calculated PHE-HO<sub>2</sub><sup>°</sup> rate constant, in comparison with 97.37 and 99.34%, respectively. Therefore, in order to achieve a better fit between experimental and predicted data, HO<sub>2</sub><sup>°</sup> action in pollutant degradation should be considered. Nonetheless, HO<sub>2</sub><sup>°</sup> contribution to PHE degradation is non-significant in comparison with the role developed by HO<sup>°</sup> attack.

#### 4. Conclusions

A kinetic model for studying pollutant degradation by the UV/H<sub>2</sub>O<sub>2</sub> system was developed, including the background matrix effect in scavenging free radicals and shielding UV-light and the reaction intermediate action, as well as the change of the pH as the UV/H<sub>2</sub>O<sub>2</sub> process proceeds. Three different ways for calculating HO<sup>°</sup> level time evolution were assumed (non-pseudo-steady, pseudo-steady and simplified pseudo-steady state; denoted as kinetic models A, B, and C, respectively). It was found that the assumption of pseudo-steady (simplified or not) or transient state for determining the HO<sup>°</sup> level evolution with time was not significant in PHE degradation rate due to the relatively low HO<sup>°</sup> level present into the bulk ( $\sim 10^{-14}$  M). On the other hand, taking into account the high levels of HO<sub>2</sub><sup>°</sup> formed in the reaction solution compared to HO<sup>°</sup> concentration ( $\sim 10^{-7}$  M  $\gg \gg \gg$   $\sim 10^{-14}$  M), HO<sub>2</sub><sup>°</sup> action in transforming PHE was considered. For this purpose, PHE-HO<sub>2</sub><sup>°</sup> reaction rate constant was calculated and estimated to be  $1.6 \times 10^3 \text{ M}^{-1} \text{ s}^{-1}$ , resulting in the range of data reported from literature. It was observed that, although including HO<sub>2</sub><sup>°</sup> action allowed slightly improving the kinetic model degree of fit, HO<sup>°</sup> developed the major role in PHE conversion, due to their high oxidation potential.

Additionally, it was found that there was an effective level of the HO<sup>°</sup> formed in solution. Below that level, there was a lack of HO<sup>°</sup> for an efficient pollutant conversion; and above it, an excessive number of HO<sup>°</sup> was generated. That HO<sup>°</sup> effective level calculated from kinetic model C could be of relevance for industrial applications in order to be maintained throughout the reaction time, allowing an efficient pollutant degradation.

In this study, there was an attempt to contemplate a wide range of the chemical reactions involved in the UV/H<sub>2</sub>O<sub>2</sub> process and although high correlation factors were obtained, it is suggested to include the positive effect of the OM and the dissolved oxygen in generating ROS, as well as the effect of other anions naturally present in water bodies, as phosphate and nitrate, for the model to be a more accurate approximation of reality.

#### Acknowledgements

This work was financially supported by the Colombian Administrative Department of Science, Technology and Innovation (COLCIENCIAS).

## Author details

Ainhoa Rubio-Clemente<sup>1,2\*</sup>, E. Chica<sup>3</sup> and Gustavo A. Peñuela<sup>1</sup>

\*Address all correspondence to: ainhoarubioclem@gmail.com

1 Grupo GDCON, Facultad de Ingeniería, Sede de Investigaciones Universitarias (SIU), Universidad de Antioquia UdeA, Colombia

2 Departamento de Ciencia y Tecnología de los Alimentos, Facultad de Ciencias de la Salud, Universidad Católica San Antonio de Murcia UCAM, Spain

3 Departamento de Ingeniería Mecánica, Facultad de Ingeniería, Universidad de Antioquia UdeA, Colombia

## References

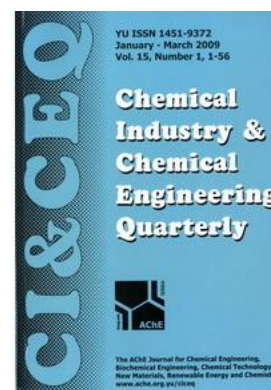
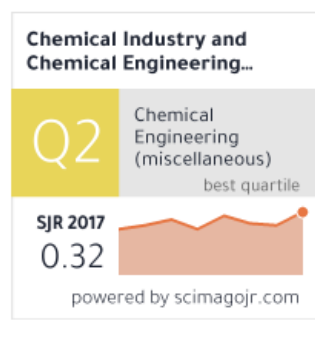
- [1] Rubio-Clemente, A., Torres-Palma, R.A., & Peñuela, G.A. Removal of polycyclic aromatic hydrocarbons in aqueous environment by chemical treatments: A review. *Sci. Total Environ.* 2014;408:201–225.
- [2] Rubio-Clemente, A., Chica, E., & Peñuela, G.A. Application of Fenton process for treating petrochemical wastewater. *Ingeniería y Competitividad.* 2014;16(2): 211–223.
- [3] Rubio-Clemente, A., Chica, E., & Peñuela, G.A. Petrochemical wastewater treatment by photo-Fenton process. *Water, Air, Soil Pollut.* 2015;226(3):61–78.
- [4] Dopar, M., Kušić, H., & Koprivanac, N. Treatment of simulated industrial wastewater by photo-Fenton process: Part I: The optimization of process parameters using design of experiments (DOE). *Chem. Eng. J.* 2011;173:267–279.
- [5] Litter, M., & Quici, N. Photochemical advanced oxidation processes for water and wastewater treatment. *Recent Pat. Eng.* 2010;4:217–241.
- [6] Wols, B.A., & Hofman-Caris, C.H.M. Review of photochemical reaction constants of organic micropollutants required for UV advanced oxidation processes in water. *Water Res.* 2012;46:2815–2827.
- [7] Song, W., Ravindran, V., & Pirbazari, M. Process optimization using a kinetic model for the ultraviolet radiation-hydrogen peroxide decomposition of natural and synthetic organic compounds in groundwater. *Chem. Eng. Sci.* 2008;63:3249–3270.
- [8] Audenaert, W.T.M., Vermeersch, Y., Van Hulle, S.W.H., Dejans, P., Dumoulin, A., & Nopens, I. Application of a mechanistic UV/hydrogen peroxide model at full-scale:

- Sensitivity analysis, calibration and performance evaluation. *Chem. Eng. J.* 2011;171:113–126.
- [9] Crittenden, J.C., Hu, S., Hand, D.W., & Green, S.A. A kinetic model for H<sub>2</sub>O<sub>2</sub>/UV process in a completely mixed batch reactor. *Water Res.* 1999;33(10):2315–2328.
- [10] Hong, A., Zappi, M.E., & Hill, D. Modeling kinetics of illuminated and dark advanced oxidation processes. *J. Environ. Eng.* 1996;122(1):58–62.
- [11] Huang, C.R., & Shu, H.Y. The reaction kinetics, decomposition pathways and intermediate formation of phenol in ozonation, UV/O<sub>3</sub> and UV/H<sub>2</sub>O<sub>2</sub> processes. *J. Hazard. Mater.* 1995;41:47–64.
- [12] Liao, C.H., & Gurol, M.D. Chemical oxidation by photolytic decomposition of hydrogen peroxide. *Environ. Sci. Technol.* 1995;29(12):3007–3014.
- [13] Primo, O., Rivero, M.J., Ortiz, I., & Irabien, A. Mathematical modelling of phenol photooxidation: Kinetics of the process toxicity. *Chem. Eng. J.* 2007;134(1–3):23–28.
- [14] Rosenfeldt, E.J., & Linden, K.G. The ROH,UV concept to characterize and the model UV/H<sub>2</sub>O<sub>2</sub> process in natural waters. *Environ. Sci. Technol.* 2007;41(7):2548–2553.
- [15] Yao, H., Sun, P., Minakata, D., Crittenden, J.C., & Huang, C.H. Kinetics and modeling of degradation of ionophore antibiotics by UV and UV/H<sub>2</sub>O<sub>2</sub>. *Environ. Sci. Technol.* 2013;47(9):4581–4589.
- [16] Zeng, Y., Hong, P.K.A., & Wavrek, D.A. Integrated chemical-biological treatment of benzo(a)pyrene. *Environ. Sci. Technol.* 2000;34(5):854–862.
- [17] Edalatmanesh, M., Dhib, R., & Mehrvar, M. Kinetic modeling of aqueous phenol degradation by UV/H<sub>2</sub>O<sub>2</sub> process. *Int. J. Chem. Kinet.* 2007;40(1):34–43.
- [18] De Laat, J., Le, G.T., & Legube, B. A comparative study of the effects of chloride, sulfate and nitrate ions on the rates of decomposition of H<sub>2</sub>O<sub>2</sub> and organic compounds by Fe(II)/H<sub>2</sub>O<sub>2</sub> and Fe(III)/H<sub>2</sub>O<sub>2</sub>. *Chemosphere.* 2004;55(5):715–723.
- [19] Alnaizy, R., & Akgerman, A. Advanced oxidation of phenolic compounds. *Adv. Environ. Res.* 2000;4(3):233–244.
- [20] Leenheer, J.A., & Croué, J.P. Characterizing aquatic organic matter: Understanding the unknown structures is key to better treatment of drinking water. *Environ. Sci. Technol.* 2003;37(1):18A–26A.
- [21] Wang, Z., Wu, Z., & Tang, S. Characterization of dissolved organic matter in a submerged membrane bioreactor by using three-dimensional excitation and emission matrix fluorescence spectroscopy. *Water Res.* 2009;43(6):1533–1540.

- [22] Peuravuori, J., & Pihlaja, K. Molecular size distribution and spectroscopic properties of aquatic humic substances. *Anal. Chim. Acta.* 1997;337(2):133–149.
- [23] Alapi, T., & Dombi, A. Comparative study of the UV and UV/VUV-induced photolysis of phenol in aqueous solution. *J. Photochem. Photobiol. A.* 2007;188((2–3)):409–418.
- [24] Gallard, H., & De Laat, J. Kinetic modelling of Fe(III)/H<sub>2</sub>O<sub>2</sub> oxidation reactions in dilute aqueous solution using atrazine as a model organic compound. *Water Res.* 2000;34(12):3107–3116.
- [25] Rosenfeldt, E.J., Linden, K.G., Canonica, S., & von Gunten, U. Comparison of the efficiency of °OH radical formation during ozonation and the advanced oxidation processes O<sub>3</sub>/H<sub>2</sub>O<sub>2</sub> and UV/H<sub>2</sub>O<sub>2</sub>. *Water Res.* 2006;40(20):3695–3704.
- [26] Ray, P.Z., & Tarr, M.A. Petroleum films exposed to sunlight produce hydroxyl radical. *Chemosphere.* 2014;103:220–227.
- [27] Kralik, P., Kušić, H., Koprivanac, N., & Božić, A.L. Degradation of chlorinated hydrocarbons by UV/H<sub>2</sub>O<sub>2</sub>: The application of experimental design and kinetic modeling approach. *Chem. Eng. J.* 2010;158(2):154–166.
- [28] Kušić, H., Koprivanac, N., Božić, A.L., Papić, S., Peternel, I., & Vujević, D. Reactive dye degradation by AOPs: Development of a kinetic model for UV/H<sub>2</sub>O<sub>2</sub> process. *Chem. Biochem. Eng. Q.* 2006;20(3):293–300.
- [29] Kozmér, Z., Arany, E., Alapi, T., Takács, E., Wojnárovits, L., & Dombi, A. Determination of the rate constant of hydroperoxyl radical reaction with phenol. *Radiat. Phys. Chem.* 2014;102:135–138.
- [30] Bielski, B.H.J., Cabelli, D.E., Arudi, L.R., & Ross, A.B. Reactivity of HO<sub>2</sub>/O<sub>2</sub><sup>-</sup> radicals in aqueous solution. *J. Phys. Chem. Ref. Data.* 1985;14(4):1041–1100.
- [31] Buxton, G.V., Greenstock, C.L., Helman, W.P., & Ross, A.B. Critical review of data constants for reactions of hydrated electrons, hydrogen atoms and hydroxyl radicals in aqueous solutions. *J. Phys. Chem. Ref. Data.* 1988;17(2):513–886.
- [32] Christensen, H.S., Sehested, K., & Corftizan, H. Reaction of hydroxyl radicals with hydrogen peroxide at ambient temperatures. *J. Phys. Chem.* 1982;86:15–88.
- [33] Schested, K., Rasmussen, O.L., & Fricke, H. Rate constants of OH with HO<sub>2</sub>, O<sub>2</sub><sup>-</sup> and H<sub>2</sub>O<sub>2</sub>+ from hydrogen peroxide formation in pulse-irradiated oxygenated water. *J. Phys. Chem.* 1968;72:626–631.
- [34] Weinstein, J., Benon, H.J., & Bielski, H.J. Kinetics of the interaction of HO<sub>2</sub> and O<sub>2</sub><sup>-</sup> radicals with hydrogen peroxide. The Haber-Weiss reaction. *J. Amer. Chem. Soc.* 1979;101:58–62.

- [35] Wols, B.A., Harmsen, D.J.H., Beerendonk, E.F., & Hofman-Caris, C.H.M. Predicting pharmaceutical degradation by UV (LP)/H<sub>2</sub>O<sub>2</sub> processes: A kinetic model. *Chem. Eng. J.* 2014;255:334–343.
- [36] Draganic, Z.D., Negrón-Mendoza, A., Sehested, K., Vujosevic, S.I., Navarro-Gonzales, R., Albarran-Sanchez, M.G. Radiolysis of aqueous solutions of ammonium bicarbonate over a large dose range. *Radiat. Phys. Chem.* 1991;38(3):317–321.
- [37] Neta, P., Huie, R.E., & Ross, A.B. Rate constants for reactions of inorganic radicals in aqueous solution. *J. Phys. Chem. Ref. Data.* 1988;17(3):1027–1284.
- [38] Fang, G.D., Dionysiou, D.D., Wang, Y., Al-Abed, S.R., & Zhou, D.M. Sulfate radical-based degradation of polychlorinated biphenyls: Effects of chloride ion and reaction kinetics. *J. Hazard. Mater.* 2012;227–228:394–401.
- [39] Mazellier, P., Leroy, É., De Laat, J., & Legube, B. Transformation of carbendazim induced by the H<sub>2</sub>O<sub>2</sub>/UV system in the presence of hydrogenocarbonate ions: Involvement of the carbonate radical. *New J. Chem.* 2002;26(12):1784–1790.
- [40] Dorfman, L.M., & Adams, G.E. Reactivity of the hydroxyl radical in aqueous solutions. Standard Reference Data System. National Bureau of Standards and Technology. 1973;46.
- [41] Yasuhisa, T., Hideki, H., & Muneyoshi, Y. Superoxide radical scavenging activity of phenolic compounds. *Int. J. Biochem.* 1993;25(4):491–494.
- [42] Chen, S.N., & Hoffman M.Z. Rate constants for the reaction of the carbonate radical with compounds of biochemical interest in neutral aqueous solution. *Radiat. Res.* 1973;56(1):40–47.



**Paper****Kinetic model describing the UV/H<sub>2</sub>O<sub>2</sub> photodegradation of phenol from water****Journal**

Scope: Papers having a primary focus on pure chemical sciences such as analytical, biochemical, food, environmental, inorganic, medicinal, microbiological, organic, pharmaceutical, physical or polymer chemistry as well as natural sciences (biology, microbiology, etc.) are strongly discouraged.

**Highlights**

- A kinetic model for organic pollutant degradation through the UV/H<sub>2</sub>O<sub>2</sub> system is developed.
- The model is validated using independent experimental data from literature for phenol abatement.
- A high extent of agreement was found between the calculated and the experimental data.
- The kinetic model allows determining the optimal conditions for an efficient pollutant removal.





AINHOA RUBIO-CLEMENTE<sup>1</sup>  
EDWIN CHICA<sup>2</sup>  
GUSTAVO A. PEÑUELA<sup>3</sup>

<sup>1</sup>Departamento de Ciencia y Tecnología de los Alimentos. Facultad de Ciencias de la Salud. Universidad Católica San Antonio de Murcia UCAM, s/n. Guadalupe-Murcia, España

<sup>2</sup>Departamento de Ingeniería Mecánica, Facultad de Ingeniería, Universidad de Antioquia UdeA, Medellín, Colombia

<sup>3</sup>Grupo GDCON, Facultad de Ingeniería, Sede de Investigaciones Universitarias (SIU), Universidad de Antioquia UdeA, Medellín, Colombia

SCIENTIFIC PAPER

UDC 547.56:66:544.526.5:54

## KINETIC MODEL DESCRIBING THE UV/H<sub>2</sub>O<sub>2</sub> PHOTODEGRADATION OF PHENOL FROM WATER

### Article Highlights

- A kinetic model for organic pollutant degradation through the UV/H<sub>2</sub>O<sub>2</sub> system is developed
- The model is validated using independent experimental data from literature for phenol abatement
- A high extent of agreement was found between the calculated and the experimental data
- The kinetic model allows determining the optimal conditions for an efficient pollutant removal

### Abstract

*A kinetic model for phenol transformation through the UV/H<sub>2</sub>O<sub>2</sub> system was developed and validated. The model includes the pollutant decomposition by direct photolysis and HO<sup>•</sup>, HO<sub>2</sub><sup>•</sup> and O<sub>2</sub><sup>•-</sup> oxidation. HO<sup>•</sup> scavenging effects of CO<sub>3</sub><sup>2-</sup>, HCO<sub>3</sub><sup>-</sup>, SO<sub>4</sub><sup>2-</sup> and Cl<sup>-</sup> were also considered, as well as the pH changes as the process proceeds. Additionally, the detrimental action of the organic matter and reaction intermediates in shielding UV and quenching HO<sup>•</sup> was incorporated. It was observed that the model can accurately predict phenol abatement using different H<sub>2</sub>O<sub>2</sub>/phenol mass ratios (495, 228 and 125), obtaining an optimal H<sub>2</sub>O<sub>2</sub>/phenol ratio of 125, leading to a phenol removal higher than 95% after 40 min of treatment, where the main oxidation species was HO<sup>•</sup>. The developed model could be relevant for calculating the optimal level of H<sub>2</sub>O<sub>2</sub> efficiently degrading the pollutant of interest, allowing saving in costs and time.*

*Keywords:* H<sub>2</sub>O<sub>2</sub> level, kinetic model, matrix background, phenol pollution, UV/H<sub>2</sub>O<sub>2</sub>.

The rapid economic growth of the last decade has led to an increase in the number of pollutants in the aquatic environment, positioning advanced oxidation processes (AOPs) as alternatives to the conventional techniques water treatment plants are operating with [1-6], which are unable to completely transform inhibitory organics such as phenol.

Phenol is a colorless to pink-colored solid or dense liquid substance with a particular sweet odor. It is highly soluble in water but also in organic solvents. It is a ubiquitous pollutant commonly found as a component of oil refinery wastes. It is also produced in pharmaceuticals and phenol manufacturing plants. Phenol can also be generated from the production of metallurgical coke from coal, and it is used in the manufacture of fertilizers, textiles and paints. Additionally, phenol can be formed from natural sources, such as the decomposition of organic matter [7]. Nevertheless, anthropogenic processes contribute in a larger extension in comparison with natural ones.

Once phenol is in the environment, it can enter aquatic environments due to its solubility in aqueous media, posing a risk for living beings. Furthermore, it can react with other components, such as chlorine,

Correspondence: A. Rubio-Clemente, Departamento de Ciencia y Tecnología de los Alimentos. Facultad de Ciencias de la Salud. Universidad Católica San Antonio de Murcia UCAM, Avenida de los Jerónimos, s/n. Guadalupe-Murcia. España.  
E-mail: ainhoa.rubioc@udea.edu.co  
Paper received: 19 November, 2016  
Paper revised: 24 January, 2017  
Paper accepted: 24 February, 2017

<https://doi.org/10.2298/CICEQ161119008R>

increasing its hydrophobicity and, subsequently, its tendency to be bioaccumulated through the food chain.

Phenol is a toxic compound. The toxicity of phenol is related to the reactivity of the compound with biomolecules, being responsible for the death of organisms when exposed to high amounts of this substance. It is also involved in reproductive problems, reducing fertility and producing changes in appearance and behavior, since living being hormonal system function can be affected [7]. Furthermore, it exhibits mutagenic and carcinogenic potential [7,8]. As a matter of fact, researchers evidenced mutagenic activity of phenol from hamster fibroblasts [7]. In addition, it induces immunotoxic, hematological and physiological effects [8]. In fact, it is included by the US Environmental Protection Agency in the List of Priority Pollutants [7]. Therefore, it must be removed from water.

In recent decades, different AOPs have been used for destroying organic compounds. Among the AOPs applied for water decontamination, the UV/H<sub>2</sub>O<sub>2</sub> system implementation has risen drastically in recent years for water treatment purposes [6]. This process involves the photolysis of hydrogen peroxide (H<sub>2</sub>O<sub>2</sub>) using ultraviolet radiation (UV), resulting in the production of hydroxyl radicals (HO<sup>•</sup>) [9-11]. The HO<sup>•</sup> is very reactive and attack non-selectively a variety of organic and inorganic substances because their oxidation potential ( $E = 2.8$  V) [12] is higher than other oxidizing agents such as ozone ( $E = 2.07$  V) and chlorine ( $E = 1.36$  V), transforming those substances into CO<sub>2</sub>, H<sub>2</sub>O and inorganic salts [10,13].

The efficiency of the UV/H<sub>2</sub>O<sub>2</sub> system depends on various parameters, such as the oxidant dosage, pollutant concentration and structure, UV-light intensity and predominant wavelength, irradiation time, solution initial pH, temperature and matrix constituents (including natural organic matter and inorganic ions, which may quench HO<sup>•</sup> and/or shield UV radiation penetration into the bulk), among other parameters [3,10].

This homogeneous chemical oxidation process has several advantages in comparison to other water treatment methods, such as no mass transfer limitations occur and no sludge requiring a subsequent treatment and disposal is produced. Additionally, it can be produced at room temperature and pressure [6,10]. Nevertheless, this process has associated high electrical and oxidizing agent costs [10,14,15], and kinetic models seem to be a good option to optimize operating conditions without incurring in high operating costs.

This work is aimed at proposing a kinetic model for the prediction of phenol decontamination by the

UV/H<sub>2</sub>O<sub>2</sub> system including the action of HO<sup>•</sup>, O<sub>2</sub><sup>•-</sup> and HO<sub>2</sub><sup>•</sup>. The HO<sup>•</sup> scavenging effects of carbonate (CO<sub>3</sub><sup>2-</sup>), bicarbonate (HCO<sub>3</sub><sup>-</sup>), sulfate (SO<sub>4</sub><sup>2-</sup>) and chloride (Cl<sup>-</sup>) ions were considered on the performance of the system as well as the pH changes in the bulk as the oxidation process proceeds. Additionally, the detrimental action of the organic matter and reaction intermediates in shielding UV and quenching HO<sup>•</sup> was incorporated. The model is based on the extensively accepted chemical and photochemical reactions, and the rate constants involved in the studied AOP. On the other hand, MATLAB software was used to find the numerical solution to the set of ordinary differential equations (ODE) characterizing the current model. In addition, the proposed kinetic model was validated by comparing the experimental data from Alnaizy and Akgerman study [16] and the model predictions obtained at different operating conditions in terms of phenol abatement.

## EXPERIMENTAL

A kinetic model describing the UV/H<sub>2</sub>O<sub>2</sub> process was developed taking into account the impact of radical species such as HO<sup>•</sup>, HO<sub>2</sub><sup>•</sup>, O<sub>2</sub><sup>•-</sup>, CO<sub>3</sub><sup>•-</sup>, SO<sub>4</sub><sup>•-</sup>, H<sub>2</sub>CIO<sup>•</sup>, Cl<sup>•</sup> and Cl<sub>2</sub><sup>•-</sup> on the pollutant conversion. In addition, the role of the dissolved organic matter (DOM), in terms of dissolved organic carbon (DOC), and the degradation by-products in absorbing UV radiation and scavenging radicals were included. In the development of the proposed kinetic model, the contribution of UV radiation in phenol transformation was also taken into account. Furthermore, the model incorporates the change of pH in the solution as the advanced oxidation process proceeds due to the formation of short chain organic acids.

### Mechanistic kinetic model

The chemical and photochemical reaction scheme, reaction rate constants and values of the parameters involved in the UV/H<sub>2</sub>O<sub>2</sub> system are compiled in Tables 1 and 2.

As it can be observed from the tables, 22 different chemical species (including radicals, radical ions, inorganic ions and molecules) and 51 reactions (differentiated in photolysis reactions - first-order reactions, equilibrium reactions - acid-base reactions, and second-order reactions, corresponding to the elementary reactions and those ones related to the matrix background) were considered.

In addition, correlation factors ( $\delta_{Ri}$ ) were included in order to study the generation and consumption of some chemical species as the pH in the bulk is increased or reduced. In this sense, when  $\delta_{Ri} = 1$ , the

Table 1. Elementary reactions and kinetic equations for species disappearance and formation in the UV/H<sub>2</sub>O<sub>2</sub> system

No.	Reaction	Parameters and rate constants	Ref.	Kinetic equations
R <sub>1</sub>	H <sub>2</sub> O <sub>2</sub> $\xrightarrow{k_1}$ HO <sub>2</sub> <sup>-</sup> + H <sup>+</sup>	$k_1 = 3.7 \times 10^{-2} \text{ s}^{-1}$ $k_2 = 2.6 \times 10^{10} \text{ M}^{-1} \text{ s}^{-1}$ $pK_a = 11.6$	[17]	$\frac{d[\text{H}_2\text{O}_2]}{dt} = -k_1[\text{H}_2\text{O}_2]$ $\frac{d[\text{HO}_2^-]}{dt} = k_1[\text{H}_2\text{O}_2]$ $\frac{d[\text{H}^+]}{dt} = k_1[\text{H}_2\text{O}_2]$
R <sub>2</sub>	HO <sub>2</sub> <sup>-</sup> + H <sup>+</sup> $\xrightarrow{k_2}$ H <sub>2</sub> O <sub>2</sub>			$\frac{d[\text{HO}_2^-]}{dt} = -k_2[\text{HO}_2^-][\text{H}^+]$ $\frac{d[\text{H}^+]}{dt} = -k_2[\text{HO}_2^-][\text{H}^+]$ $\frac{d[\text{H}_2\text{O}_2]}{dt} = k_2[\text{HO}_2^-][\text{H}^+]$
R <sub>3</sub>	H <sub>2</sub> O <sub>2</sub> $\xrightarrow{h\nu}$ 2HO <sup>*</sup>	$\epsilon_{\text{H}_2\text{O}_2} (254 \text{ nm}) = 1800 \text{ M}^{-1} \text{ s}^{-1}$ [9] $\epsilon_{\text{HO}_2^-} (254 \text{ nm}) = 22800 \text{ M}^{-1} \text{ s}^{-1}$ $\varphi_{\text{H}_2\text{O}_2} (254 \text{ nm}) = 0.5 \text{ mol Ein}^{-1}$ $\varphi_{\text{HO}_2^-} (254 \text{ nm}) = 0.5 \text{ mol Ein}^{-1}$ $\text{pH} > 11.6 \Rightarrow \delta_{R_2} = 0, \delta_{R_4} = 1$ $\text{pH} < 11.6 \Rightarrow \delta_{R_3} = 1, \delta_{R_4} = 0$		$\frac{d[\text{H}_2\text{O}_2]}{dt} = -\varphi_{\text{H}_2\text{O}_2} I_{\text{a,H}_2\text{O}_2} \delta_{R_3}$ $\frac{d[\text{HO}^*]}{dt} = 2\varphi_{\text{H}_2\text{O}_2} I_{\text{a,H}_2\text{O}_2} \delta_{R_3}$ $I_{\text{a,H}_2\text{O}_2} = I_0 f_{\text{H}_2\text{O}_2} \{1 - \exp[-2.3/(\epsilon_{\text{H}_2\text{O}_2} [\text{H}_2\text{O}_2] + \epsilon_{\text{HO}_2^-} [\text{HO}_2^-] + \epsilon_{\text{C}} [\text{C}] + \epsilon_{\text{DOC}} [\text{DOC}])]\}$ $f_{\text{H}_2\text{O}_2} = \frac{\epsilon_{\text{H}_2\text{O}_2} [\text{H}_2\text{O}_2]}{\epsilon_{\text{H}_2\text{O}_2} [\text{H}_2\text{O}_2] + \epsilon_{\text{HO}_2^-} [\text{HO}_2^-] + \epsilon_{\text{C}} [\text{C}] + \epsilon_{\text{DOC}} [\text{DOC}]}$
R <sub>4</sub>	HO <sub>2</sub> <sup>-</sup> + H <sub>2</sub> O $\xrightarrow{h\nu}$ 2HO <sup>*</sup> + OH <sup>-</sup>			$\frac{d[\text{HO}_2^-]}{dt} = -\varphi_{\text{HO}_2^-} I_{\text{a,HO}_2^-} \delta_{R_4}$ $\frac{d[\text{HO}^*]}{dt} = 2\varphi_{\text{HO}_2^-} I_{\text{a,HO}_2^-} \delta_{R_4}$ $\frac{d[\text{OH}^-]}{dt} = \varphi_{\text{HO}_2^-} I_{\text{a,HO}_2^-} \delta_{R_4}$ $I_{\text{a,HO}_2^-} = I_0 f_{\text{HO}_2^-} \{1 - \exp[-2.3/(\epsilon_{\text{H}_2\text{O}_2} [\text{H}_2\text{O}_2] + \epsilon_{\text{HO}_2^-} [\text{HO}_2^-] + \epsilon_{\text{C}} [\text{C}] + \epsilon_{\text{DOC}} [\text{DOC}])]\}$ $f_{\text{HO}_2^-} = \frac{\epsilon_{\text{HO}_2^-} [\text{HO}_2^-]}{\epsilon_{\text{H}_2\text{O}_2} [\text{H}_2\text{O}_2] + \epsilon_{\text{HO}_2^-} [\text{HO}_2^-] + \epsilon_{\text{C}} [\text{C}] + \epsilon_{\text{DOC}} [\text{DOC}]}$
R <sub>5</sub>	HO <sub>2</sub> <sup>*</sup> $\xrightarrow{k_3}$ O <sub>2</sub> <sup>-</sup> + H <sup>+</sup>	$k_3 = 1.58 \times 10^5 \text{ s}^{-1}$ [18] $k_4 = 1.0 \times 10^{10} \text{ M}^{-1} \text{ s}^{-1}$ $pK_a = 4.8$		$\frac{d[\text{HO}_2^*]}{dt} = -k_3[\text{HO}_2^*]$ $\frac{d[\text{O}_2^{\cdot-}]}{dt} = k_3[\text{HO}_2^*]$ $\frac{d[\text{H}^+]}{dt} = k_3[\text{HO}_2^*]$
R <sub>6</sub>	O <sub>2</sub> <sup>-</sup> + H <sup>+</sup> $\xrightarrow{k_4}$ HO <sub>2</sub> <sup>*</sup>			$\frac{d[\text{O}_2^{\cdot-}]}{dt} = -k_4[\text{O}_2^{\cdot-}][\text{H}^+]$ $\frac{d[\text{H}^+]}{dt} = -k_4[\text{O}_2^{\cdot-}][\text{H}^+]$ $\frac{d[\text{HO}_2^*]}{dt} = k_4[\text{O}_2^{\cdot-}][\text{H}^+]$

Table 1. Continued

No.	Reaction	Parameters and rate constants	Ref.	Kinetic equations
$R_7$	$\text{H}_2\text{O}_2 + \text{HO}^* \xrightarrow{k_5} \text{O}_2^- + \text{H}^+ + \text{H}_2\text{O}$	$k_5 = 2.7 \times 10^7 \text{ M}^{-1} \text{ s}^{-1}$ pH > 4.8 $\Rightarrow \delta_{R_7} = 1, \delta_{R_8} = 0$ pH < 4.8 $\Rightarrow \delta_{R_7} = 0, \delta_{R_8} = 1$	[19]	$\frac{d[\text{H}_2\text{O}_2]}{dt} = -k_5 [\text{H}_2\text{O}_2] [\text{HO}^*] \delta_{R_7}$ $\frac{d[\text{HO}^*]}{dt} = -k_5 [\text{H}_2\text{O}_2] [\text{HO}^*] \delta_{R_7}$ $\frac{d[\text{O}_2^-]}{dt} = k_5 [\text{H}_2\text{O}_2] [\text{HO}^*] \delta_{R_7}$ $\frac{d[\text{H}^+]}{dt} = k_5 [\text{H}_2\text{O}_2] [\text{HO}^*] \delta_{R_7}$
$R_8$	$\text{H}_2\text{O}_2 + \text{HO}^* \xrightarrow{k_5} \text{HO}_2^* + \text{H}_2\text{O}$			$\frac{d[\text{H}_2\text{O}_2]}{dt} = -k_5 [\text{H}_2\text{O}_2] [\text{HO}^*] \delta_{R_8}$ $\frac{d[\text{HO}^*]}{dt} = -k_5 [\text{H}_2\text{O}_2] [\text{HO}^*] \delta_{R_8}$ $\frac{d[\text{HO}_2^*]}{dt} = k_5 [\text{H}_2\text{O}_2] [\text{HO}^*] \delta_{R_8}$
$R_9$	$\text{HO}^* + \text{HO}_2^- \xrightarrow{k_6} \text{HO}_2^* + \text{OH}^-$	$k_6 = 7.5 \times 10^9 \text{ M}^{-1} \text{ s}^{-1}$	[20]	$\frac{d[\text{HO}^*]}{dt} = -k_6 [\text{HO}^*] [\text{HO}_2^-]$ $\frac{d[\text{HO}_2^-]}{dt} = -k_6 [\text{HO}^*] [\text{HO}_2^-]$ $\frac{d[\text{HO}_2^*]}{dt} = k_6 [\text{HO}^*] [\text{HO}_2^-]$ $\frac{d[\text{OH}^-]}{dt} = k_6 [\text{HO}^*] [\text{HO}_2^-]$
$R_{10}$	$\text{HO}^* + \text{HO}^* \xrightarrow{k_7} \text{H}_2\text{O}_2$	$k_7 = 5.5 \times 10^9 \text{ M}^{-1} \text{ s}^{-1}$	[19]	$\frac{d[\text{HO}^*]}{dt} = -k_7 [\text{HO}^*] [\text{HO}^*]$ $\frac{d[\text{H}_2\text{O}_2]}{dt} = k_7 [\text{HO}^*] [\text{HO}^*]$
$R_{11}$	$\text{HO}^* + \text{HO}_2^- \xrightarrow{k_8} \text{H}_2\text{O} + \text{O}_2$	$k_8 = 6.6 \times 10^9 \text{ M}^{-1} \text{ s}^{-1}$	[21]	$\frac{d[\text{HO}^*]}{dt} = -k_8 [\text{HO}^*] [\text{HO}_2^-]$ $\frac{d[\text{HO}_2^-]}{dt} = -k_8 [\text{HO}^*] [\text{HO}_2^-]$
$R_{12}$	$\text{HO}^* + \text{O}_2^- \xrightarrow{k_9} \text{O}_2 + \text{OH}^-$	$k_9 = 7.0 \times 10^9 \text{ M}^{-1} \text{ s}^{-1}$	[9]	$\frac{d[\text{O}_2^-]}{dt} = -k_9 [\text{HO}^*] [\text{O}_2^-]$ $\frac{d[\text{HO}^*]}{dt} = -k_9 [\text{HO}^*] [\text{O}_2^-]$ $\frac{d[\text{OH}^-]}{dt} = k_9 [\text{HO}^*] [\text{O}_2^-]$
$R_{13}$	$\text{HO}_2^* + \text{HO}_2^- \xrightarrow{k_{10}} \text{H}_2\text{O}_2 + \text{O}_2$	$k_{10} = 8.3 \times 10^5 \text{ M}^{-1} \text{ s}^{-1}$	[18]	$\frac{d[\text{HO}_2^*]}{dt} = -k_{10} [\text{HO}_2^*] [\text{HO}_2^-]$ $\frac{d[\text{H}_2\text{O}_2]}{dt} = k_{10} [\text{HO}_2^*] [\text{HO}_2^-]$

Table 1. Continued

No.	Reaction	Parameters and rate constants	Ref.	Kinetic equations
R <sub>14</sub>	$\text{H}_2\text{O}_2 + \text{HO}_2^* \xrightarrow{k_{11}} \text{HO}^* + \text{H}_2\text{O} + \text{O}_2$	$k_{11} = 3 \text{ M}^{-1} \text{ s}^{-1}$	[22]	$\frac{d[\text{H}_2\text{O}_2]}{dt} = -k_{11}[\text{H}_2\text{O}_2][\text{HO}_2^*]$ $\frac{d[\text{HO}_2^*]}{dt} = -k_{11}[\text{H}_2\text{O}_2][\text{HO}_2^*]$ $\frac{d[\text{HO}^*]}{dt} = k_{11}[\text{H}_2\text{O}_2][\text{HO}_2^*]$
R <sub>15</sub>	$\text{H}_2\text{O}_2 + \text{O}_2^{\bullet-} \xrightarrow{k_{12}} \text{HO}^* + \text{O}_2 + \text{OH}^-$	$k_{12} = 0.13 \text{ M}^{-1} \text{ s}^{-1}$	[22]	$\frac{d[\text{H}_2\text{O}_2]}{dt} = -k_{12}[\text{H}_2\text{O}_2][\text{O}_2^{\bullet-}]$ $\frac{d[\text{O}_2^{\bullet-}]}{dt} = -k_{12}[\text{H}_2\text{O}_2][\text{O}_2^{\bullet-}]$ $\frac{d[\text{HO}^*]}{dt} = k_{12}[\text{H}_2\text{O}_2][\text{O}_2^{\bullet-}]$ $\frac{d[\text{OH}^-]}{dt} = k_{12}[\text{H}_2\text{O}_2][\text{O}_2^{\bullet-}]$
R <sub>16</sub>	$\text{HO}_2^* + \text{O}_2^{\bullet-} \xrightarrow{k_{13}} \text{HO}_2^- + \text{O}_2$	$k_{13} = 9.7 \times 10^7 \text{ M}^{-1} \text{ s}^{-1}$	[18]	$\frac{d[\text{HO}_2^*]}{dt} = -k_{13}[\text{HO}_2^*][\text{O}_2^{\bullet-}]$ $\frac{d[\text{O}_2^{\bullet-}]}{dt} = -k_{13}[\text{HO}_2^*][\text{O}_2^{\bullet-}]$ $\frac{d[\text{HO}_2^-]}{dt} = k_{13}[\text{HO}_2^*][\text{O}_2^{\bullet-}]$
R <sub>17</sub>	$\text{C} \xrightarrow{h\nu} \text{DOC} + ?$	$\epsilon_{\text{C}}, \varphi_{\text{C}}$	-	$\frac{d[\text{C}]}{dt} = -\varphi_{\text{C}} I_{\text{a,C}}$ $\frac{d[\text{DOC}]}{dt} = \varphi_{\text{C}} I_{\text{a,C}}$ $I_{\text{a,C}} = I_0 f_{\text{C}} \{1 - \exp[-2.3 I (\epsilon_{\text{H}_2\text{O}_2} [\text{H}_2\text{O}_2] + \epsilon_{\text{HO}_2^*} [\text{HO}_2^*] + \epsilon_{\text{C}} [\text{C}] + \epsilon_{\text{DOC}} [\text{DOC}])]\}$
R <sub>18</sub>	$\text{C} + \text{HO}^* \xrightarrow{k_{14}} \text{DOC} + ?$	$k_{\text{C,HO}^*} = k_{14}$	-	$\frac{d[\text{C}]}{dt} = -k_{14}[\text{C}][\text{HO}^*]$ $\frac{d[\text{HO}^*]}{dt} = -k_{14}[\text{C}][\text{HO}^*]$ $\frac{d[\text{DOC}]}{dt} = k_{14}[\text{C}][\text{HO}^*]$
R <sub>19</sub>	$\text{C} + \text{HO}_2^* \xrightarrow{k_{15}} \text{DOC} + ?$	$k_{\text{C,HO}_2^*} = k_{15}$	-	$\frac{d[\text{C}]}{dt} = -k_{15}[\text{C}][\text{HO}_2^*]$ $\frac{d[\text{HO}_2^*]}{dt} = -k_{15}[\text{C}][\text{HO}_2^*]$ $\frac{d[\text{DOC}]}{dt} = k_{15}[\text{C}][\text{HO}_2^*]$
R <sub>20</sub>	$\text{C} + \text{O}_2^{\bullet-} \xrightarrow{k_{16}} \text{DOC} + ?$	$k_{\text{C,O}_2^{\bullet-}} = k_{16}$	-	$\frac{d[\text{C}]}{dt} = -k_{16}[\text{C}][\text{O}_2^{\bullet-}]$ $\frac{d[\text{O}_2^{\bullet-}]}{dt} = -k_{16}[\text{C}][\text{O}_2^{\bullet-}]$ $\frac{d[\text{DOC}]}{dt} = k_{16}[\text{C}][\text{O}_2^{\bullet-}]$

Table 2. Effect of the matrix background in the UV/H<sub>2</sub>O<sub>2</sub> system

No.	Reaction	Parameters and rate constants	Ref.	Kinetic equations
R <sub>21</sub>	DOC + HO• $\xrightarrow{k_{17}}$ H <sub>2</sub> CO <sub>3</sub> <sup>*</sup> + H <sub>2</sub> O	$k_{\text{DOC, HO}^\bullet} = k_{17} = 2.0 \times 10^8 \text{ M}^{-1} \text{ s}^{-1}$	[23]	$\frac{d[\text{DOC}]}{dt} = -k_{17}[\text{DOC}][\text{HO}^\bullet]$ $\frac{d[\text{HO}^\bullet]}{dt} = -k_{17}[\text{DOC}][\text{HO}^\bullet]$ $\frac{d[\text{H}_2\text{CO}_3^*]}{dt} = k_{17}[\text{DOC}][\text{HO}^\bullet]$
R <sub>22</sub>	DOC $\xrightarrow{h\nu}$ ?	$\epsilon_{\text{DOC}}, \varphi_{\text{DOC}}$	-	$\frac{d[\text{DOC}]}{dt} = -\varphi_{\text{DOC}} I_{\text{a,DOC}}$ $I_{\text{a,DOC}} = I_0 f_{\text{DOC}} \{1 - \exp[-2.3(\epsilon_{\text{H}_2\text{O}_2}[\text{H}_2\text{O}_2] + \epsilon_{\text{HO}_2}[\text{HO}_2] + \epsilon_{\text{C}}[\text{C}] + \epsilon_{\text{DOC}}[\text{DOC}])]\}$ $f_{\text{DOC}} = \frac{\epsilon_{\text{DOC}}[\text{DOC}]}{\epsilon_{\text{H}_2\text{O}_2}[\text{H}_2\text{O}_2] + \epsilon_{\text{HO}_2}[\text{HO}_2] + \epsilon_{\text{C}}[\text{C}] + \epsilon_{\text{DOC}}[\text{DOC}]}$
R <sub>23</sub>	CO <sub>3</sub> <sup>2-</sup> + HO• $\xrightarrow{k_{18}}$ CO <sub>3</sub> <sup>-</sup> + OH <sup>-</sup>	$k_{18} = 3.9 \times 10^8 \text{ M}^{-1} \text{ s}^{-1}$	[19]	$\frac{d[\text{CO}_3^{2-}]}{dt} = -k_{18}[\text{CO}_3^{2-}][\text{HO}^\bullet]$ $\frac{d[\text{HO}^\bullet]}{dt} = -k_{18}[\text{CO}_3^{2-}][\text{HO}^\bullet]$ $\frac{d[\text{OH}^-]}{dt} = k_{18}[\text{CO}_3^{2-}][\text{HO}^\bullet]$ $\frac{d[\text{CO}_3^-]}{dt} = k_{18}[\text{CO}_3^{2-}][\text{HO}^\bullet]$
R <sub>24</sub>	HCO <sub>3</sub> <sup>-</sup> + HO• $\xrightarrow{k_{19}}$ CO <sub>3</sub> <sup>-</sup> + H <sub>2</sub> O	$k_{19} = 8.5 \times 10^6 \text{ M}^{-1} \text{ s}^{-1}$	[19]	$\frac{d[\text{HCO}_3^-]}{dt} = -k_{19}[\text{HCO}_3^-][\text{HO}^\bullet]$ $\frac{d[\text{HO}^\bullet]}{dt} = -k_{19}[\text{HCO}_3^-][\text{HO}^\bullet]$ $\frac{d[\text{CO}_3^-]}{dt} = k_{19}[\text{HCO}_3^-][\text{HO}^\bullet]$
R <sub>25</sub>	H <sub>2</sub> O <sub>2</sub> + CO <sub>3</sub> <sup>-</sup> $\xrightarrow{k_{20}}$ HCO <sub>3</sub> <sup>-</sup> + HO <sub>2</sub> <sup>*</sup>	$k_{20} = 4.3 \times 10^5 \text{ M}^{-1} \text{ s}^{-1}$	[24]	$\frac{d[\text{H}_2\text{O}_2]}{dt} = -k_{20}[\text{H}_2\text{O}_2][\text{CO}_3^-]$ $\frac{d[\text{CO}_3^-]}{dt} = -k_{20}[\text{H}_2\text{O}_2][\text{CO}_3^-]$ $\frac{d[\text{HCO}_3^-]}{dt} = k_{20}[\text{H}_2\text{O}_2][\text{CO}_3^-]$ $\frac{d[\text{HO}_2^*]}{dt} = k_{20}[\text{H}_2\text{O}_2][\text{CO}_3^-]$
R <sub>26</sub>	HO <sub>2</sub> <sup>-</sup> + CO <sub>3</sub> <sup>-</sup> $\xrightarrow{k_{21}}$ CO <sub>3</sub> <sup>-</sup> + HO <sub>2</sub> <sup>*</sup>	$k_{21} = 3.0 \times 10^7 \text{ M}^{-1} \text{ s}^{-1}$	[24]	$\frac{d[\text{HO}_2^-]}{dt} = -k_{21}[\text{HO}_2^-][\text{CO}_3^-]$ $\frac{d[\text{CO}_3^-]}{dt} = -k_{21}[\text{HO}_2^-][\text{CO}_3^-]$ $\frac{d[\text{CO}_3^{2-}]}{dt} = k_{21}[\text{HO}_2^-][\text{CO}_3^-]$ $\frac{d[\text{HO}_2^*]}{dt} = k_{21}[\text{HO}_2^-][\text{CO}_3^-]$

Table 2. Continued

No.	Reaction	Parameters and rate constants	Ref.	Kinetic equations
$R_{27}$	$O_2^* + CO_3^{*-} \xrightarrow{k_{22}} CO_3^{2-} + O_2$	$k_{22} = 6.5 \times 10^8 \text{ M}^{-1} \text{ s}^{-1}$	[25]	$\frac{d[O_2^*]}{dt} = -k_{22}[O_2^*][CO_3^{*-}]$ $\frac{d[CO_3^{*-}]}{dt} = -k_{22}[O_2^*][CO_3^{*-}]$ $\frac{d[CO_3^{2-}]}{dt} = k_{22}[O_2^*][CO_3^{*-}]$
$R_{28}$	$HSO_4^- + HO^* \xrightarrow{k_{23}} SO_4^{*-} + H_2O$	$k_{23} = 3.5 \times 10^5 \text{ M}^{-1} \text{ s}^{-1}$	[26]	$\frac{d[HSO_4^-]}{dt} = -k_{23}[HSO_4^-][HO^*]$ $\frac{d[HO^*]}{dt} = -k_{23}[HSO_4^-][HO^*]$ $\frac{d[SO_4^{*-}]}{dt} = k_{23}[HSO_4^-][HO^*]$
$R_{29}$	$SO_4^{*-} + H_2O_2 \xrightarrow{k_{24}} SO_4^{2-} + H^+ + HO_2^*$	$k_{24} = 1.2 \times 10^7 \text{ M}^{-1} \text{ s}^{-1}$	[26]	$\frac{d[SO_4^{*-}]}{dt} = -k_{24}[SO_4^{*-}][H_2O_2]$ $\frac{d[H_2O_2]}{dt} = -k_{24}[SO_4^{*-}][H_2O_2]$ $\frac{d[SO_4^{2-}]}{dt} = k_{24}[SO_4^{*-}][H_2O_2]$ $\frac{d[H^+]}{dt} = k_{24}[SO_4^{*-}][H_2O_2]$ $\frac{d[HO_2^*]}{dt} = k_{24}[SO_4^{*-}][H_2O_2]$
$R_{30}$	$SO_4^{*-} + HO_2^* \xrightarrow{k_{25}} SO_4^{2-} + H^+ + O_2$	$k_{25} = 3.5 \times 10^9 \text{ M}^{-1} \text{ s}^{-1}$	[26]	$\frac{d[SO_4^{*-}]}{dt} = -k_{25}[SO_4^{*-}][HO_2^*]$ $\frac{d[HO_2^*]}{dt} = -k_{25}[SO_4^{*-}][HO_2^*]$ $\frac{d[SO_4^{2-}]}{dt} = k_{25}[SO_4^{*-}][HO_2^*]$ $\frac{d[H^+]}{dt} = k_{25}[SO_4^{*-}][HO_2^*]$
$R_{31}$	$Cl^- + HO^* \xrightarrow{k_{26}} HClO^*$	$k_{26} = 4.3 \times 10^9 \text{ M}^{-1} \text{ s}^{-1}$	[26]	$\frac{d[Cl^-]}{dt} = -k_{26}[Cl^-][HO^*]$ $\frac{d[HO^*]}{dt} = -k_{26}[Cl^-][HO^*]$ $\frac{d[HClO^*]}{dt} = k_{26}[Cl^-][HO^*]$
$R_{32}$	$HClO^* + H^+ \xrightarrow{k_{27}} H_2ClO^*$	$k_{27} = 3.0 \times 10^{10} \text{ M}^{-1} \text{ s}^{-1}$	[26]	$\frac{d[HClO^*]}{dt} = -k_{27}[HClO^*][H^+]$ $\frac{d[H^+]}{dt} = -k_{27}[HClO^*][H^+]$ $\frac{d[H_2ClO^*]}{dt} = k_{27}[HClO^*][H^+]$

Table 2. Continued

No.	Reaction	Parameters and rate constants	Ref.	Kinetic equations
$R_{33}$	$\text{H}_2\text{ClO}^* \xrightarrow{k_{28}} \text{H}_2\text{O} + \text{Cl}^*$	$k_{28} = 5.0 \times 10^4 \text{ s}^{-1}$	[26]	$\frac{d[\text{H}_2\text{ClO}^*]}{dt} = -k_{28} [\text{H}_2\text{ClO}^*]$ $\frac{d[\text{Cl}^*]}{dt} = k_{28} [\text{H}_2\text{ClO}^*]$
$R_{34}$	$\text{Cl}^* + \text{Cl}^- \xrightarrow{k_{29}} \text{Cl}_2^{*-}$	$k_{29} = 8.5 \times 10^9 \text{ M}^{-1} \text{ s}^{-1}$	[26]	$\frac{d[\text{Cl}^*]}{dt} = -k_{29} [\text{Cl}^*][\text{Cl}^-]$ $\frac{d[\text{Cl}^-]}{dt} = -k_{29} [\text{Cl}^*][\text{Cl}^-]$ $\frac{d[\text{Cl}_2^{*-}]}{dt} = k_{29} [\text{Cl}^*][\text{Cl}^-]$
$R_{35}$	$\text{Cl}_2^{*-} + \text{HO}^* \xrightarrow{k_{30}} \text{HClO}^* + \text{Cl}^-$	$k_{30} = 1.0 \times 10^9 \text{ M}^{-1} \text{ s}^{-1}$	[27]	$\frac{d[\text{Cl}_2^{*-}]}{dt} = -k_{30} [\text{Cl}_2^{*-}][\text{HO}^*]$ $\frac{d[\text{HO}^*]}{dt} = -k_{30} [\text{Cl}_2^{*-}][\text{HO}^*]$ $\frac{d[\text{HClO}^*]}{dt} = k_{30} [\text{Cl}_2^{*-}][\text{HO}^*]$ $\frac{d[\text{Cl}^-]}{dt} = k_{30} [\text{Cl}_2^{*-}][\text{HO}^*]$
$R_{36}$	$\text{Cl}_2^{*-} + \text{H}_2\text{O}_2 \xrightarrow{k_{31}} \text{HO}_2^* + 2\text{Cl}^- + \text{H}^+$	$k_{31} = 4.1 \times 10^4 \text{ M}^{-1} \text{ s}^{-1}$	[26]	$\frac{d[\text{Cl}_2^{*-}]}{dt} = -k_{31} [\text{Cl}_2^{*-}][\text{H}_2\text{O}_2]$ $\frac{d[\text{H}_2\text{O}_2]}{dt} = -k_{31} [\text{Cl}_2^{*-}][\text{H}_2\text{O}_2]$ $\frac{d[\text{HO}_2^*]}{dt} = k_{31} [\text{Cl}_2^{*-}][\text{H}_2\text{O}_2]$ $\frac{d[\text{Cl}^-]}{dt} = 2k_{31} [\text{Cl}_2^{*-}][\text{H}_2\text{O}_2]$ $\frac{d[\text{H}^+]}{dt} = k_{31} [\text{Cl}_2^{*-}][\text{H}_2\text{O}_2]$
$R_{37}$	$\text{Cl}^* + \text{H}_2\text{O}_2 \xrightarrow{k_{32}} \text{HO}_2^* + \text{Cl}^- + \text{H}^+$	$k_{32} = 1.1 \times 10^9 \text{ M}^{-1} \text{ s}^{-1}$	[26]	$\frac{d[\text{Cl}^*]}{dt} = -k_{32} [\text{Cl}^*][\text{H}_2\text{O}_2]$ $\frac{d[\text{H}_2\text{O}_2]}{dt} = -k_{32} [\text{Cl}^*][\text{H}_2\text{O}_2]$ $\frac{d[\text{HO}_2^*]}{dt} = k_{32} [\text{Cl}^*][\text{H}_2\text{O}_2]$ $\frac{d[\text{Cl}^-]}{dt} = k_{32} [\text{Cl}^*][\text{H}_2\text{O}_2]$ $\frac{d[\text{H}^+]}{dt} = k_{32} [\text{Cl}^*][\text{H}_2\text{O}_2]$
$R_{38}$	$\text{Cl}_2^{*-} + \text{HO}_2^* \xrightarrow{k_{33}} \text{O}_2 + 2\text{Cl}^- + \text{H}^+$	$k_{33} = 3.0 \times 10^9 \text{ M}^{-1} \text{ s}^{-1}$	[26]	$\frac{d[\text{Cl}_2^{*-}]}{dt} = -k_{33} [\text{Cl}_2^{*-}][\text{HO}_2^*]$ $\frac{d[\text{HO}_2^*]}{dt} = -k_{33} [\text{Cl}_2^{*-}][\text{HO}_2^*]$ $\frac{d[\text{Cl}^-]}{dt} = 2k_{33} [\text{Cl}_2^{*-}][\text{HO}_2^*]$



Table 2. Continued

No.	Reaction	Parameters and rate constants	Ref.	Kinetic equations
$R_{38}$	$\text{Cl}_2^{*+} + \text{HO}_2^* \xrightarrow{k_{33}} \text{O}_2 + 2\text{Cl}^- + \text{H}^+$	$k_{33} = 3.0 \times 10^9 \text{ M}^{-1} \text{ s}^{-1}$	[26]	$\frac{d[\text{H}^+]}{dt} = k_{33} [\text{Cl}_2^{*+}] [\text{HO}_2^*]$
$R_{39}$	$\text{Cl}_2^{*+} + \text{O}_2^* \xrightarrow{k_{34}} \text{O}_2 + 2\text{Cl}^-$	$k_{34} = 2.0 \times 10^9 \text{ M}^{-1} \text{ s}^{-1}$	[26]	$\frac{d[\text{Cl}_2^{*+}]}{dt} = -k_{34} [\text{Cl}_2^{*+}] [\text{O}_2^*]$ $\frac{d[\text{O}_2^*]}{dt} = -k_{34} [\text{Cl}_2^{*+}] [\text{O}_2^*]$ $\frac{d[\text{Cl}^-]}{dt} = 2k_{34} [\text{Cl}_2^{*+}] [\text{O}_2^*]$
$R_{40}$	$\text{C} + \text{CO}_3^{*-} \xrightarrow{k_{35}} \text{DOC} + ?$	$k_{35}$	-	$\frac{d[\text{C}]}{dt} = -k_{35} [\text{C}] [\text{CO}_3^{*-}]$ $\frac{d[\text{CO}_3^{*-}]}{dt} = -k_{35} [\text{C}] [\text{CO}_3^{*-}]$ $\frac{d[\text{DOC}]}{dt} = k_{35} [\text{C}] [\text{CO}_3^{*-}]$
$R_{41}$	$\text{C} + \text{SO}_4^{*-} \xrightarrow{k_{36}} \text{DOC} + ?$	$k_{36}$	-	$\frac{d[\text{C}]}{dt} = -k_{36} [\text{C}] [\text{SO}_4^{*-}]$ $\frac{d[\text{SO}_4^{*-}]}{dt} = -k_{36} [\text{C}] [\text{SO}_4^{*-}]$ $\frac{d[\text{DOC}]}{dt} = k_{36} [\text{C}] [\text{SO}_4^{*-}]$
$R_{42}$	$\text{C} + \text{H}_2\text{ClO}^* \xrightarrow{k_{37}} \text{DOC} + ?$	$k_{37}$	-	$\frac{d[\text{C}]}{dt} = -k_{37} [\text{C}] [\text{H}_2\text{ClO}^*]$ $\frac{d[\text{H}_2\text{ClO}^*]}{dt} = -k_{37} [\text{C}] [\text{H}_2\text{ClO}^*]$ $\frac{d[\text{DOC}]}{dt} = k_{37} [\text{C}] [\text{H}_2\text{ClO}^*]$
$R_{43}$	$\text{C} + \text{HClO}^* \xrightarrow{k_{38}} \text{DOC} + ?$	$k_{38}$	-	$\frac{d[\text{C}]}{dt} = -k_{38} [\text{C}] [\text{HClO}^*]$ $\frac{d[\text{HClO}^*]}{dt} = -k_{38} [\text{C}] [\text{HClO}^*]$ $\frac{d[\text{DOC}]}{dt} = k_{38} [\text{C}] [\text{HClO}^*]$
$R_{44}$	$\text{C} + \text{Cl}^* \xrightarrow{k_{39}} \text{DOC} + ?$	$k_{39}$	-	$\frac{d[\text{C}]}{dt} = -k_{39} [\text{C}] [\text{Cl}^*]$ $\frac{d[\text{Cl}^*]}{dt} = -k_{39} [\text{C}] [\text{Cl}^*]$ $\frac{d[\text{DOC}]}{dt} = k_{39} [\text{C}] [\text{Cl}^*]$
$R_{45}$	$\text{C} + \text{Cl}_2^{*-} \xrightarrow{k_{40}} \text{DOC} + ?$	$k_{40}$	-	$\frac{d[\text{C}]}{dt} = -k_{40} [\text{C}] [\text{Cl}_2^{*-}]$ $\frac{d[\text{Cl}_2^{*-}]}{dt} = -k_{40} [\text{C}] [\text{Cl}_2^{*-}]$ $\frac{d[\text{DOC}]}{dt} = k_{40} [\text{C}] [\text{Cl}_2^{*-}]$

Table 2. Continued

No.	Reaction	Parameters and rate constants	Ref.	Kinetic equations
$R_{46}$	$\text{H}_2\text{CO}_3^* \xrightarrow{k_{41}} \text{HCO}_3^- + \text{H}^+$	$k_{41} = 1.0 \times 10^{10} \text{ s}^{-1}$ $k_{42} = 4.5 \times 10^3 \text{ M}^{-1} \text{ s}^{-1}$ $\text{p}K_a = 6.3$	[28]	$\frac{d[\text{H}_2\text{CO}_3^*]}{dt} = -k_{41}[\text{H}_2\text{CO}_3^*]$ $\frac{d[\text{HCO}_3^-]}{dt} = k_{41}[\text{H}_2\text{CO}_3^*]$ $\frac{d[\text{H}^+]}{dt} = k_{41}[\text{H}_2\text{CO}_3^*]$
$R_{47}$	$\text{HCO}_3^- + \text{H}^+ \xrightarrow{k_{42}} \text{H}_2\text{CO}_3^*$			$\frac{d[\text{HCO}_3^-]}{dt} = -k_{42}[\text{HCO}_3^-][\text{H}^+]$ $\frac{d[\text{H}^+]}{dt} = -k_{42}[\text{HCO}_3^-][\text{H}^+]$ $\frac{d[\text{H}_2\text{CO}_3^*]}{dt} = k_{42}[\text{HCO}_3^-][\text{H}^+]$
$R_{48}$	$\text{HCO}_3^- \xrightarrow{k_{43}} \text{CO}_3^{2-} + \text{H}^+$	$k_{43} = 1.0 \times 10^{10} \text{ s}^{-1}$ $k_{44} = 4.5 \times 10^{-1} \text{ M}^{-1} \text{ s}^{-1}$ $\text{p}K_a = 10.3$	[28]	$\frac{d[\text{HCO}_3^-]}{dt} = -k_{43}[\text{HCO}_3^-]$ $\frac{d[\text{CO}_3^{2-}]}{dt} = k_{43}[\text{HCO}_3^-]$ $\frac{d[\text{H}^+]}{dt} = k_{43}[\text{HCO}_3^-]$
$R_{49}$	$\text{CO}_3^{2-} + \text{H}^+ \xrightarrow{k_{44}} \text{HCO}_3^-$			$\frac{d[\text{CO}_3^{2-}]}{dt} = -k_{44}[\text{CO}_3^{2-}][\text{H}^+]$ $\frac{d[\text{H}^+]}{dt} = -k_{44}[\text{CO}_3^{2-}][\text{H}^+]$ $\frac{d[\text{HCO}_3^-]}{dt} = k_{44}[\text{CO}_3^{2-}][\text{H}^+]$
$R_{50}$	$\text{HSO}_4^- \xrightarrow{k_{45}} \text{SO}_4^{2-} + \text{H}^+$	$k_{45} = 1.0 \times 10^{10} \text{ s}^{-1}$ $k_{46} = 4.5 \times 10^{11} \text{ M}^{-1} \text{ s}^{-1}$ $\text{p}K_a = 1.9$	[26]	$\frac{d[\text{HSO}_4^-]}{dt} = -k_{45}[\text{HSO}_4^-]$ $\frac{d[\text{SO}_4^{2-}]}{dt} = k_{45}[\text{HSO}_4^-]$ $\frac{d[\text{H}^+]}{dt} = k_{45}[\text{HSO}_4^-]$
$R_{51}$	$\text{SO}_4^{2-} + \text{H}^+ \xrightarrow{k_{46}} \text{HSO}_4^-$			$\frac{d[\text{SO}_4^{2-}]}{dt} = -k_{46}[\text{SO}_4^{2-}][\text{H}^+]$ $\frac{d[\text{H}^+]}{dt} = -k_{46}[\text{SO}_4^{2-}][\text{H}^+]$ $\frac{d[\text{HSO}_4^-]}{dt} = k_{46}[\text{SO}_4^{2-}][\text{H}^+]$

species considered in the particular reaction  $R_i$  were considered; while such as species were obviated if  $\delta_{R_i} = 0$ . A more detailed explanation about how the pH changes in the solution were addressed has been reported in Rubio-Clemente *et al.* [29]. Moreover, the ODE set of the chemical species involved in the system can also be consulted in Rubio-Clemente *et al.* [29].

Considering the reactions, constants and parameters summarized in Tables 1 and 2, the degradation of the pollutant can be estimated as indicated in Eq. (1):

$$-\frac{dC}{dt} = \varphi_{C^*} I_{a,C} + k_{14}[\text{HO}^*][C] + k_{15}[\text{HO}_2^*][C] + k_{16}[\text{O}_2^*][C] + \sum_{i=35}^{40} k_i[C][AR_i] \quad (1)$$

where:

$$\varphi_{C/a,C}, k_{14} [\text{HO}^*][\text{C}], k_{15} [\text{HO}_2^*][\text{C}],$$

$$k_{16} [\text{O}_2^*][\text{C}] \text{ and } \sum_{i=35}^{40} k_i [\text{C}][\text{AR}_i]$$

correspondingly refer to the specific contributions of UV radiation, and the oxidation of HO<sup>\*</sup>, HO<sub>2</sub><sup>\*</sup>, O<sub>2</sub><sup>\*</sup> and the formed anions radicals (AR) (CO<sub>3</sub><sup>\*</sup>, SO<sub>4</sub><sup>\*</sup>, H<sub>2</sub>ClO<sup>\*</sup>, HClO<sup>\*</sup>, Cl<sup>\*</sup> and Cl<sub>2</sub><sup>\*</sup>) to the overall pollutant degradation.

For examining the role of the terms mentioned above, four parameters (*d*, *f*, *g* and *h*) were included in Eq. (1), resulting in Eq. (2):

$$-\frac{dC}{dt} = \varphi_{C/a,C} + k_{14} [\text{HO}^*][\text{C}]d + k_{15} [\text{HO}_2^*][\text{C}]f +$$

$$+ k_{16} [\text{O}_2^*][\text{C}]g + \sum_{i=35}^{40} k_i [\text{C}][\text{AR}_i]h \quad (2)$$

Consequently, for evaluating the pollutant removal by the exclusive action of UV radiation, *d* = *f* = *g* = *h* = 0 (*i.e.*, the initial level of oxidant radical species is equal to zero). In turn, HO<sup>\*</sup> action was considered when *d* = 1 and *f* = *g* = *h* = 0. For studying the contribution of HO<sub>2</sub><sup>\*</sup>, O<sub>2</sub><sup>\*</sup> and other anion radicals included in Table 2, *f*, *g* and *h* were equaled to 1, respectively.

Since the mathematical model considers the contribution of different anions, such as CO<sub>3</sub><sup>2-</sup>, HCO<sub>3</sub><sup>-</sup>, SO<sub>4</sub><sup>2-</sup> and Cl<sup>-</sup>, in the pollutant conversion, it might be used for the treatment of water with salt content. This enables the applicability of the developed kinetic model to be expanded depending on the characteristics of the water of interest to be treated.

### Numerical analysis

In order to obtain the numerical solution of the proposed kinetic model for the degradation of organic pollutants using the UV/H<sub>2</sub>O<sub>2</sub> system, MATLAB software and ODE15S function were used. Additionally, the differential rate equations representing the concentration evolution of the pollutant throughout the reaction time were plotted.

## RESULTS AND DISCUSSION

Taking into account the reactions compiled in Table 1 and 2, as well as the parameters and the rate constants involved in each chemical and photochemical reaction, a kinetic model was developed. The kinetic model was validated using the experimental values from Alnaizy and Akgerman [16], where phenol was used as the probe compound and the UV/H<sub>2</sub>O<sub>2</sub> process was carried out in a completely mixed

batch cylindrical photoreactor made on Pyrex glass. The considered UV-light intensity (*I<sub>0</sub>*) and illuminated path length (*l*) were 1.516 × 10<sup>-6</sup> Ein L<sup>-1</sup> s<sup>-1</sup> (radiation of 254 nm > 90% and power = 15 W) and 63.5 mm, respectively [16]. The adopted quantum yield and molar extinction coefficient of phenol (*φ<sub>phenol</sub>* and *ε<sub>phenol</sub>*) were 0.07 mol Ein<sup>-1</sup> [30] and 51600 M<sup>-1</sup> m<sup>-1</sup> [16], respectively. In turn, the assumed values of the kinetic rate constants of phenol with HO<sup>\*</sup> (*k<sub>14</sub>*), O<sub>2</sub><sup>\*</sup> (*k<sub>16</sub>*) and CO<sub>3</sub><sup>\*</sup> (*k<sub>35</sub>*) were respectively 6.6 × 10<sup>9</sup>, 5.8 × 10<sup>3</sup> and 2.2 × 10<sup>7</sup> M<sup>-1</sup> s<sup>-1</sup> [31-33]. Additionally, a phenol working solution of 2.23 × 10<sup>-3</sup> M prepared in deionized water was selected and the effect of different H<sub>2</sub>O<sub>2</sub>/phenol ratios (495, 228 and 125), obtained by varying the initial level of H<sub>2</sub>O<sub>2</sub> and keeping the concentration of phenol constant [16], were studied.

### Model hypotheses

Since the reaction water used in the UV/H<sub>2</sub>O<sub>2</sub> experiments was deionized water [16], the contribution of SO<sub>4</sub><sup>\*</sup>, H<sub>2</sub>ClO<sup>\*</sup>, HClO<sup>\*</sup>, Cl<sup>\*</sup> and Cl<sub>2</sub><sup>\*</sup> were not included in the study of phenol conversion. Therefore, among the anions considered in the model, only HCO<sub>3</sub><sup>-</sup> and CO<sub>3</sub><sup>2-</sup> were studied. In this sense, to examine the contribution of CO<sub>3</sub><sup>\*</sup> (due to the reaction between HO<sup>\*</sup> and HCO<sub>3</sub><sup>-</sup> or CO<sub>3</sub><sup>2-</sup>), along with the photolysis and the oxidation of the pollutant through HO<sup>\*</sup>, *d* = *h* = 1 and *f* = *g* = 0. On the other hand, to analyze the role of HO<sub>2</sub><sup>\*</sup> in the pollutant degradation, as well as HO<sup>\*</sup> and CO<sub>3</sub><sup>\*</sup>, *d* = *f* = *h* = 1 and *g* = 0. In turn, when *d* = *f* = *g* = *h* = 1, and no inorganic anions different from HCO<sub>3</sub><sup>-</sup> and CO<sub>3</sub><sup>2-</sup> are present in the studied water, in addition to the species mentioned above, the kinetic model considers the action of O<sub>2</sub><sup>\*</sup>.

On the other hand, and taking into account the high oxidation potential and kinetic reaction rate constant, HO<sup>\*</sup> is generally the radical developing the main action in pollutant conversion [6,14,17,23,34-37]. Therefore, a special attention to the evolution of its concentration with time must be paid. In this vein, the evolution of HO<sup>\*</sup> level during the reaction time can be expressed as indicated in Eq. (3):

$$\frac{d[\text{HO}^*]}{dt} = 2\varphi_{\text{H}_2\text{O}_2} I_{a,\text{H}_2\text{O}_2} \delta_{R3} + 2\varphi_{\text{HO}_2} I_{a,\text{HO}_2} \delta_{R4} -$$

$$-k_5 [\text{H}_2\text{O}_2][\text{HO}^*] \delta_{R7} - k_5 [\text{H}_2\text{O}_2][\text{HO}^*] \delta_{R8} -$$

$$-k_6 [\text{HO}^*][\text{HO}_2^-] - k_7 [\text{HO}^*][\text{HO}^*] -$$

$$-k_8 [\text{HO}^*][\text{HO}_2^*] - k_9 [\text{HO}^*][\text{O}_2^*] +$$

$$+k_{11} [\text{H}_2\text{O}_2][\text{HO}_2^*] + k_{12} [\text{H}_2\text{O}_2][\text{O}_2^*] -$$

$$-k_{14} [\text{C}][\text{HO}^*] - k_{17} [\text{DOC}][\text{HO}^*] - \quad (3)$$

$$\begin{aligned}
 & -k_{18}[\text{CO}_3^{2-}][\text{HO}^\bullet] - k_{19}[\text{HCO}_3^-][\text{HO}^\bullet] - \\
 & -k_{23}[\text{HSO}_4^-][\text{HO}^\bullet] - k_{26}[\text{Cl}^-][\text{HO}^\bullet] - \\
 & -k_{30}[\text{Cl}_2^{2-}][\text{HO}^\bullet]
 \end{aligned}$$

Nevertheless, since HO<sup>•</sup> is a highly reactive species, it can be assumed that HO<sup>•</sup> level change during time is negligible. Therefore, HO<sup>•</sup> concentration can be expressed as Eq. (4):

$$\begin{aligned}
 [\text{HO}^\bullet] = & (2\varphi_{\text{H}_2\text{O}_2}/\varphi_{\text{a,H}_2\text{O}_2}\delta_{R3} + 2\varphi_{\text{HO}_2^-}/\varphi_{\text{a,HO}_2^-}\delta_{R4} + \\
 & + k_{11}[\text{H}_2\text{O}_2][\text{HO}_2^\bullet] + k_{12}[\text{H}_2\text{O}_2][\text{O}_2^{\bullet-}]) / \\
 & / (k_5[\text{H}_2\text{O}_2]\delta_{R7} + k_5[\text{H}_2\text{O}_2]\delta_{R8} + k_6[\text{HO}_2^-] + \\
 & + k_8[\text{HO}_2^\bullet] + k_9[\text{O}_2^{\bullet-}] + k_{14}[\text{C}] + k_{17}[\text{DOC}] + \\
 & + k_{18}[\text{CO}_3^{2-}] + k_{19}[\text{HCO}_3^-] + k_{23}[\text{HSO}_4^-] + \\
 & + k_{26}[\text{Cl}^-] + k_{30}[\text{Cl}_2^{2-}])
 \end{aligned} \quad (4)$$

Considering that the oxidant is in a high level, due to the high H<sub>2</sub>O<sub>2</sub>/phenol ratios studied (*i.e.*,  $k_5[\text{H}_2\text{O}_2]\delta_{R7} + k_5[\text{H}_2\text{O}_2]\delta_{R8} \gg \sum k_i[X_i]$ ), where:

$$\begin{aligned}
 \sum k_i[X_i] = & k_6[\text{HO}_2^-] + k_8[\text{HO}_2^\bullet] + k_9[\text{O}_2^{\bullet-}] + \\
 & + k_{14}[\text{C}] + k_{17}[\text{DOC}] + k_{18}[\text{CO}_3^{2-}] + k_{19}[\text{HCO}_3^-] + \\
 & + k_{23}[\text{HSO}_4^-] + k_{26}[\text{Cl}^-] + k_{30}[\text{Cl}_2^{2-}]
 \end{aligned}$$

and

$$\begin{aligned}
 & 2\varphi_{\text{H}_2\text{O}_2}/\varphi_{\text{a,H}_2\text{O}_2}\delta_{R3} + 2\varphi_{\text{HO}_2^-}/\varphi_{\text{a,HO}_2^-}\delta_{R4} \gg \\
 & \gg \sum (k_{11}[\text{H}_2\text{O}_2][\text{HO}_2^\bullet] + k_{12}[\text{H}_2\text{O}_2][\text{O}_2^{\bullet-}])
 \end{aligned}$$

Eq. (4) can be simplified to Eq. (5).  $k_i$  and  $[X_i]$  are the rate constants between HO<sup>•</sup> and species  $i$ , and the concentration of species  $i$ , respectively:

$$[\text{HO}^\bullet] = \frac{2\varphi_{\text{H}_2\text{O}_2}/\varphi_{\text{a,H}_2\text{O}_2}\delta_{R3} + 2\varphi_{\text{HO}_2^-}/\varphi_{\text{a,HO}_2^-}\delta_{R4}}{k_5[\text{H}_2\text{O}_2]\delta_{R7} + k_5[\text{H}_2\text{O}_2]\delta_{R8}} \quad (5)$$

Additionally, the initial concentration of DOC different from the DOC provided by phenol was assumed to be equal to 0.

In agreement with several authors [9,14,37], the decrease in DOC by means of direct photolysis ( $R_{22}$  from Table 2) was obviated.

As the process proceeds, DOC from the photo-oxidation of phenol and the intermediates can impair phenol transformation since it can absorb UV-light and react with reactive oxygen species (ROS), such as HO<sup>•</sup>.

With regard to the amount of light quenched by DOC, it was assumed a DOC molar extinction coef-

ficient ( $\epsilon_{\text{DOC}(280 \text{ nm})}$ ) of 35967 M<sup>-1</sup> m<sup>-1</sup> [38] since this parameter was not considered in Alnaizy and Akgerman study [16].

Finally, the pH variation during the reaction time was included in the proposed kinetic model; as according to Alnaizy and Akgerman [16] the pH decreases as the oxidation process proceeds. In this vein, those kinetic reactions significantly dependent on the pH of the bulk, such as  $R_3$ ,  $R_4$ ,  $R_7$  and  $R_8$ , were promoted and discriminated as explained in Rubio-Clemente *et al.* [29].

#### Degradation of phenol by direct photolysis and UV/H<sub>2</sub>O<sub>2</sub>

Considering the previously mentioned hypotheses and in order to study the effect of UV light in phenol conversion, parameters  $d$ ,  $f$ ,  $g$  and  $h$  from Eq. (2) were equaled to 0. Thus, Eq. (2) is reduced to Eq. (6):

$$-\frac{dC}{dt} = \varphi_C/\varphi_{\text{a,C}} \quad (6)$$

Additionally, for examining the effect of HO<sup>•</sup> and CO<sub>3</sub><sup>•-</sup>,  $d$  and  $h$  were equaled to 1, and  $f$  and  $g$ , to 0. Therefore, Eq. (2) is simplified as Eq. (7):

$$-\frac{dC}{dt} = \varphi_C/\varphi_{\text{a,C}} + k_{14}[\text{HO}^\bullet][\text{C}] + \sum_{i=35}^{40} k_i[\text{C}][\text{AR}_i] \quad (7)$$

In Figure 1, the experimental data and those ones calculated by the proposed kinetic model concerning the transformation of phenol by direct photolysis and the contribution of HO<sup>•</sup> and CO<sub>3</sub><sup>•-</sup> for 2.23×10<sup>-3</sup> M phenol and a H<sub>2</sub>O<sub>2</sub>/phenol ratio of 495 for a reaction time of 220 min are illustrated.

From the figure, it can be observed that model predictions are in a good agreement with experimental data both related to phenol direct photolysis alone and indirect oxidation with a correlation factor of 98.25 and 99.34%, respectively.

Additionally, it can be found that phenol initial level was reduced about 40% after 220 min of treatment considering the exclusive effect of UV radiation. This can be explained by the photolytic activity of phenol under the irradiation wavelength used in the studied AOP. However, higher removal of phenol is obtained when H<sub>2</sub>O<sub>2</sub> is added to the system, resulting in more than 90% of removal, primarily due to the action of HO<sup>•</sup>. Between HO<sup>•</sup> and CO<sub>3</sub><sup>•-</sup>, the main role in removing phenol was developed by HO<sup>•</sup>, due to the rate constant between phenol and CO<sub>3</sub><sup>•-</sup> is comparatively lower than the rate constant between phenol and HO<sup>•</sup>; and because the CO<sub>3</sub><sup>•-</sup> level was found to be in a concentration in the range of 10<sup>-15</sup> M. This fact

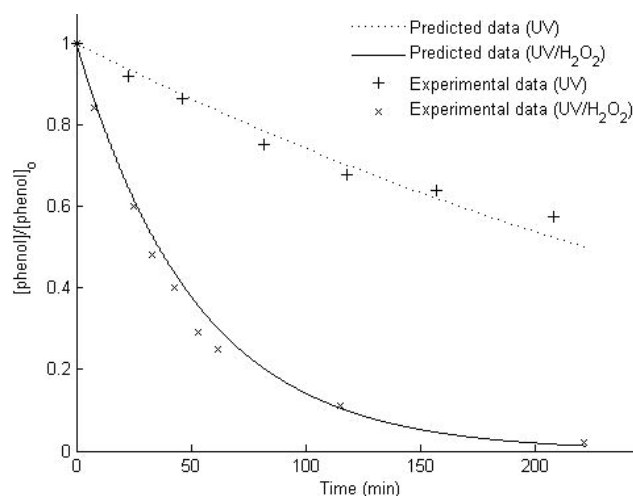


Figure 1. Phenol degradation predicted data (lines) versus experimental data (symbols). Operating conditions:  $[\text{phenol}]_0 = 2.23 \times 10^{-3} \text{ M}$ ;  $\text{H}_2\text{O}_2/\text{phenol} = 495$ ;  $t = 220 \text{ min}$ .

was determinant in obviating the action of  $\text{CO}_3^{\bullet-}$  in transforming phenol for the studied working conditions.

On the other hand, the effect of  $\text{HO}_2^{\bullet}$  and  $\text{O}_2^{\bullet-}$  was investigated. It was observed that both species were in the system in the range of  $10^{-7} \text{ M}$ ; a very larger concentration in comparison with  $\text{HO}^{\bullet}$  ( $\sim 10^{-14} \text{ M}$ ). Nevertheless, as the pH of the reaction medium decreases, the amount of  $\text{O}_2^{\bullet-}$  is reduced. Additionally, the reaction rate constant between phenol and this radical is  $5.8 \times 10^3 \text{ M}^{-1} \text{ s}^{-1}$  [32]. Therefore, the contribution of  $\text{O}_2^{\bullet-}$  in phenol degradation can be neglected.

With regard to the action of  $\text{HO}_2^{\bullet}$  in converting phenol, phenol- $\text{HO}_2^{\bullet}$  kinetic reaction rate constant must be known. For this purpose, the kinetic reaction rate constant calculated in Rubio-Clemente *et al.* [29] was used, which was equal to  $1.6 \times 10^3 \text{ M}^{-1} \text{ s}^{-1}$ , consistent with literature data ( $(2.7 \pm 1.2) \times 10^3 \text{ M}^{-1} \text{ s}^{-1}$ ) [39]. Including this value in the ODE set of the proposed kinetic model, the degree of agreement between the experimental and the proposed data was calculated to be 99.57%. In this vein, it was found that the correlation factor of the model slightly increases in 0.23%. Therefore, although the amount of  $\text{HO}_2^{\bullet}$  is far greater than the amount of  $\text{HO}^{\bullet}$ , in this case its action in the UV/H<sub>2</sub>O<sub>2</sub> system for transforming phenol can be obviated; probably due to the low reactivity of this radical with the pollutant. Therefore, the main role in phenol conversion for the considered experimental conditions was developed by  $\text{HO}^{\bullet}$ .

During phenol oxidation, different reaction intermediates are formed; among them 1,2-benzenediol,

1,3-benzenediol and 1,4-benzenediol, corresponding to catechol, resorcinol and hydroquinone, respectively, were reported [16]. Additionally, *p*-benzoquinone was found among phenol degradation by-products [16]. Once these intermediates are generated, the oxidation action of the oxidant species is continued, especially that of  $\text{HO}^{\bullet}$ , as explained above. Consequently, organic acids, like maleic, formic and oxalic acid, among others, are yielded, resulting in a decrease of the pH in the bulk, as indicated previously.

#### Influence of initial concentration of H<sub>2</sub>O<sub>2</sub>

Keeping constant the initial level of phenol ( $2.23 \times 10^{-3} \text{ M}$ ), the effect of H<sub>2</sub>O<sub>2</sub> initial concentration, considering H<sub>2</sub>O<sub>2</sub>/phenol mass ratios of 125, 228 and 495, is represented in Figure 2, where the experimental data and the predictions from the proposed kinetic model are compared. It can be observed that the optimal H<sub>2</sub>O<sub>2</sub>/phenol ratio causing a transformation of phenol higher than 95% after 40 min of treatment is 125, which corresponds to Alnaizy and Akgerman findings [16]. A further increase of H<sub>2</sub>O<sub>2</sub>/phenol ratio from 125 to 228 results in a reduction of phenol degradation, which is magnified when H<sub>2</sub>O<sub>2</sub>/phenol ratio is equal to 495.

It is important to note that in the UV/H<sub>2</sub>O<sub>2</sub> system, when H<sub>2</sub>O<sub>2</sub> is irradiated with a wavelength of 254 nm,  $\text{HO}^{\bullet}$  is produced according to  $R_3$  from Table 1, which exhibits a high oxidation potential [12] and attacks the pollutant, leading to a higher phenol removal in a shorter reaction time. Therefore, it could be thought that an increase in H<sub>2</sub>O<sub>2</sub> level would lead to a rise in phenol conversion. However, two opposing

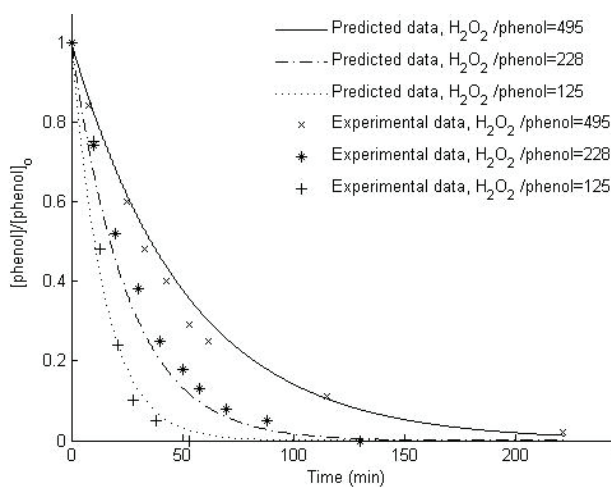


Figure 2. Phenol degradation predicted data (lines) versus experimental data (symbols). Operating conditions:  $[\text{phenol}]_0 = 2.23 \times 10^{-3} \text{ M}$ ;  $\text{H}_2\text{O}_2/\text{phenol} = 495$  (—), 228 (- · -), 125 (····);  $t = 220 \text{ min}$ .

effects occur. A rise in the initial level of  $\text{H}_2\text{O}_2$  results in a higher production of  $\text{HO}^\bullet$ , which is available to attack the organic pollutant. Nevertheless, when  $\text{H}_2\text{O}_2$  is in excess, it acts scavenging  $\text{HO}^\bullet$ , as indicated in reaction  $R_7$  from Table 1. Furthermore, even though a high  $\text{H}_2\text{O}_2$  concentration can generate a great number of  $\text{HO}_2^\bullet$ , they have a lower oxidation potential in comparison with  $\text{HO}^\bullet$ . Moreover,  $\text{HO}_2^\bullet$  can react with  $\text{HO}^\bullet$  ( $R_{11}$  from Table 1). In addition, when  $\text{HO}^\bullet$  is in excess, it can suffer recombination ( $R_{10}$  from Table 1), reducing the number of  $\text{HO}^\bullet$  available in the bulk. Hence, the overall efficiency of the applied AOP in removing phenol, and eventually leading to its mineralization is decreased.

The detrimental effect of an excess of  $\text{H}_2\text{O}_2$  is supported by Figure 3, representing the time-evolution profiles of the  $\text{HO}^\bullet$  level for the  $\text{H}_2\text{O}_2/\text{phenol}$  ratios studied. From the figure, it can be observed that the ratio providing the lowest and the highest concentration of  $\text{HO}^\bullet$  throughout the reaction time is 495 and 125, respectively. These results are coincident with those findings illustrated in Figure 2, where the  $\text{H}_2\text{O}_2/\text{phenol}$  ratio providing the lowest and the highest phenol conversion extent was, correspondingly, 495 and 125.

Consequently, and in order to save in operating costs,  $\text{H}_2\text{O}_2$  optimal level achieving an efficient pollutant removal must be found. Nonetheless, this can

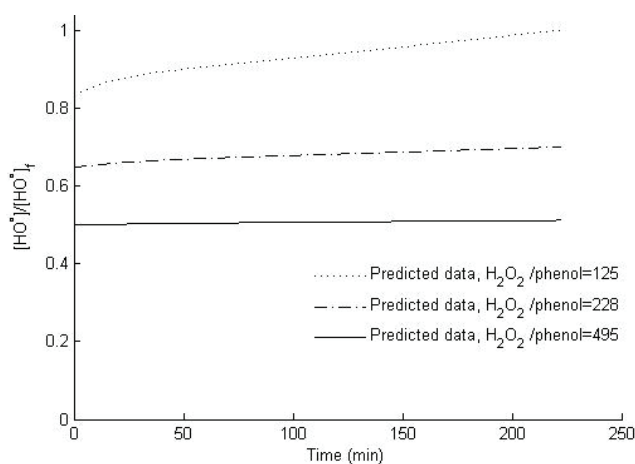


Figure 3. Estimated  $\text{HO}^\bullet$  time-profile. Operating conditions:  $[\text{phenol}]_0 = 2.23 \times 10^{-3} \text{ M}$ ;  $\text{H}_2\text{O}_2/\text{phenol} = 495$  (—), 228 (- · -), 125 (····);  $t = 220 \text{ min}$ .

be an arduous and expensive task. In this sense, the proposed kinetic model allows calculating the optimal concentration of the oxidizing agent to be used when implementing the UV/H<sub>2</sub>O<sub>2</sub> system for an efficient phenol removal without incurring high costs related to the use of an unnecessary amount of oxidant.

## CONCLUSION

A kinetic model for pollutant degradation by the UV/H<sub>2</sub>O<sub>2</sub> process was developed. The model predictions were checked with experimental results from Alnaizy and Akgerman work [16] for phenol direct photolysis alone and in combination with indirect oxidation at different H<sub>2</sub>O<sub>2</sub>/phenol ratios. It was found that the proposed kinetic model fits well with the experimental data, which is a probe of the accuracy of the model.

Additionally, the model provides an understanding of the impact of the initial level of H<sub>2</sub>O<sub>2</sub> being able to optimize this parameter. In fact, it was observed that the optimal H<sub>2</sub>O<sub>2</sub> concentration enabling a removal of the pollutant higher than 95% after 40 min of treatment corresponded to a H<sub>2</sub>O<sub>2</sub>/phenol ratio of 125. The action of HO<sub>2</sub><sup>\*</sup> in transforming phenol was also studied due to the high concentration of these species formed during the process compared to HO<sup>\*</sup> (~10<sup>-7</sup> M >> ~10<sup>-14</sup> M). It was found that, although the degree of agreement of the correlation factor was increased from 99.34 to 99.57%, the radical developing the main action in phenol abatement under the operating conditions was HO<sup>\*</sup>.

The developed kinetic model could be of relevance in the optimization of the operating conditions when implementing the UV/H<sub>2</sub>O<sub>2</sub> process, allowing saving in costs and time.

## Nomenclature

AOP	advanced oxidation process
AR	anion radicals
C	target compound
<i>E</i>	oxidation potential (V)
$\epsilon_X$	molar extinction coefficient of a species X (M <sup>-1</sup> m <sup>-1</sup> )
DOC	dissolved organic carbon
DOM	dissolved organic matter
$\delta_{Ri}$	correction factor
$f_x$	fraction of the UV radiation absorbed by a species
$I_{a,x}$	intensity of the UV radiation absorbed by a species (Ein L <sup>-1</sup> s <sup>-1</sup> )
$I_0$	incident UV radiation intensity (Ein L <sup>-1</sup> s <sup>-1</sup> )
$k_i$	second order (M <sup>-1</sup> s <sup>-1</sup> ) or first order (s <sup>-1</sup> ) reaction rate constant

<i>l</i>	optical path length of the photoreactor (mm)
ODE	ordinary differential equations
$\phi_x$	quantum yield of the photolysis of a species (mol Ein <sup>-1</sup> )
$R_i$	(photo)chemical reaction
ROS	reactive oxygen species
<i>t</i>	irradiation time (min)
UV	ultraviolet
[X]	concentration of a species X

## Acknowledgements

The authors thank the Colombian Administrative Department of Science, Technology and Innovation (COLCIENCIAS) for its financial support.

## REFERENCES

- [1] R. Zhang, Y. Yang, C.H. Huang, L. Zhao, P. Sun, *Water Res.* **103** (2016) 283-292
- [2] M.D. Murcia, N.O. Vershinin, N. Briantceva, M. Gomez, E. Gomez, E. Cascales, A.M. Hidalgo, *Chem. Eng. J.* **266** (2015) 356-367
- [3] A. Rubio-Clemente, R.A. Torres-Palma, G.A. Peñuela, *Sci. Total Environ.* **408** (2014) 201-225.
- [4] A. Rubio-Clemente, E. Chica, G.A. Peñuela, *Ambiente Agua* **8** (2013) 93-103
- [5] M. Dopar, H. Kušić, N. Koprivanac, *Chem. Eng. J.* **173** (2011) 267-279
- [6] N. Daneshvar, M.A. Behnajady, M. Mohammadi, M.S. Seyed, *Desalination* **230** (2008) 16-26
- [7] J. Michalowicz, W. Duda, *Pol. J. Environ. Stud.* **16** (2007) 347-362
- [8] N.S. Gad, M.S. Saad, *Glob. Veter.* **2** (2008) 312-319
- [9] J.C. Crittenden, S. Hu, D.W. Hand, S.A. Green, *Water Res.* **33** (1999) 2315-2328
- [10] M. Litter, N. Quici, *Recent Pat. Eng.* **4** (2010) 217-241
- [11] B.A. Wols, C.H.M. Hofman-Caris, *Water Res.* **46** (2012) 2815-2827
- [12] J. Saien, H. Nejati, *J. Hazard. Mater.* **148** (2007) 491-495
- [13] D.B. Hasan, A.R.A. Aziz, W.M.A.W. Daud, *Chem. Eng. Res. Design* **90** (2012) 298-307
- [14] W. Song, V. Ravindran, M. Pirbazari, *Chem. Eng. Sci.* **63** (2008) 3249-3270
- [15] C. Comninellis, A. Kapalka, S. Malato, S.A. Parsons, I. Poullos, D. Mantzavinos, *J. Chem. Technol. Biotechnol.* **83** (2008) 769-776
- [16] R. Alnaizy, A. Akgerman, *Adv. Environ. Res.* **4** (2000) 233-244
- [17] P. Kralik, H. Kušić, N. Koprivanac, A.L. Božić, *Chem. Eng. J.* **158** (2010) 154-166
- [18] H.J. Bielski, H.J. Benon, D.E. Cabelli, L.A. Ravindra, A.B. Alberta, *J. Phys. Chem. Ref. Data* **14** (1985) 1041-1100
- [19] G.V. Buxton, C.L. Greenstock, W.P. Helman, A.B. Ross, *J. Phys. Chem. Ref. Data* **17** (1988) 513-886

- [20] H.S. Christensen, K. Sehested, H. Corftizan, J. Phys. Chem. **86** (1982) 15-88
- [21] K. Sehested, O.L. Rasmussen, H. Fricke, J. Phys. Chem. **72** (1968) 626-631
- [22] J. Weinstein, H.J. Benon, H.J. Bielski, J. Am. Chem. Soc. **101** (1979) 58-62
- [23] B.A. Wols, D.J.H. Harmsen, E.F. Beerendonk, C.H.M. Hofman-Caris, Chem. Eng. J. **255** (2014) 334-343
- [24] Z.D. Draganic, A. Negron-Mendoza, K. Sehested, S.I. Vujosevic, R. Navarro-Gonzales, M.G. Albarran-Sanchez, I.G. Draganic, Radiat. Phys. Chem. **38** (1991) 317-321
- [25] P. Neta, R.E. Huie, A.B. Ross, J. Phys. Chem. Ref. Data **17** (1988) 1027-1284
- [26] J. De Laat, G.T. Le, B. Legube, Chemosphere **55** (2004) 715-723
- [27] G.D. Fang, D.D. Dionysiou, Y. Wang, S.R. Al-Abed, D.M. Zhou, J. Hazard. Mater. **227-228** (2012) 394-401
- [28] P. Mazellier, É. Leroy, J. De Laat, B. Legube, New J. Chem. **26** (2002) 1784-1790
- [29] A. Rubio-Clemente, E. Chica, G.A. Peñuela, in Waste-water Treatment and Resource Recovery, R. Farooq, Ed., InTech Open, Rijeka, In press
- [30] T. Alapi, A. Dombi, J. Photochem. Photobiol., A **188** (2007) 409-418
- [31] L.M. Dorfman, G.E. Adams, Nati. Bur. Stand. Technol. **46** (1973)
- [32] T. Yasuhisa, H. Hideki, Y. Muneyoshi, Int. J. Biochem. **25** (1993) 491-494
- [33] S.N. Chen, M.Z. Hoffman, Radiat. Res. **56** (1973) 40-47
- [34] H. Yao, P. Sun, D. Minakata, J.C. Crittenden, C.H. Huang, Environ. Sci. Technol. **47** (2013) 4581-4589
- [35] H. Kušić, N. Koprivanac, A.L. Božić, S. Papić, I. Peternel, D. Vujević, Chem. Biochem. Eng. Q. **20** (2006) 293-300
- [36] M. Edalatmanesh, R. Dhib, M. Mehrvar, Int. J. Chem. Kinet. **40** (2007) 34-43
- [37] W.T.M. Audenaert, Y. Vermeersch, S.W.H. Van Hulle, P. Dejans, A. Dumoulin, I. Nopens, Chem. Eng. J. **171** (2011) 113-126
- [38] J. Peuravuori, K. Pihlaja, Anal. Chim. Acta **337** (1997) 133-149
- [39] Z. Kozmér, E. Arany, T. Alapi, E. Takács, L. Wojnárovits, A. Dombi, Radiat. Phys. Chem. **102** (2014) 135-138.

AINHOA RUBIO-CLEMENTE<sup>1</sup>  
EDWIN CHICA<sup>2</sup>  
GUSTAVO A. PEÑUELA<sup>3</sup>

<sup>1</sup>Departamento de Ciencia y Tecnología de los Alimentos. Facultad de Ciencias de la Salud. Universidad Católica San Antonio de Murcia UCAM, s/n. Guadalupe-Murcia, España

<sup>2</sup>Departamento de Ingeniería Mecánica, Facultad de Ingeniería, Universidad de Antioquia UdeA, Medellín, Colombia

<sup>3</sup>Grupo GDCON, Facultad de Ingeniería, Sede de Investigaciones Universitarias (SIU), Universidad de Antioquia UdeA, Medellín, Colombia

NAUČNI RAD

## KINETIČKI MODEL UV/H<sub>2</sub>O<sub>2</sub> FOTODEGRADACIJE FENOLA IZ VODE

*Razvijen je i provenen kinetički model za konverziju fenola u UV/H<sub>2</sub>O<sub>2</sub> sistemu. Model uključuje razgradnju zagađujućih materija direktnom fotolizom i oksidacijom sa HO<sup>•</sup>, HO<sub>2</sub><sup>•</sup> i O<sub>2</sub><sup>•</sup>, hvatanje HO<sup>•</sup> pomoću, CO<sub>3</sub><sup>2-</sup>, HCO<sub>3</sub><sup>-</sup>, SO<sub>4</sub><sup>2-</sup> i Cl<sup>-</sup>, kao i promenu pH za vreme procesa. Takođe, razmotreno je štetno delovanje organskih materija i intermedijera reakcije u UV zaštiti i smanjenju HO<sup>•</sup> fluorescencije. Uočeno je da model može precizno predvideti smanjenje fenola korišćenjem različitih masenih odnosa H<sub>2</sub>O<sub>2</sub>/fenol (495, 228 i 125). Model definiše optimalni odnos H<sub>2</sub>O<sub>2</sub>/fenola od 125 sa uklanjanjem fenola više od 95% nakon 40 min tretmana, ukoliko HO<sup>•</sup> je glavna oksidaciona vrsta. Razvijeni model može biti relevantan za izračunavanje optimalnog nivoa H<sub>2</sub>O<sub>2</sub> za efikasnu degradaciju zagađivača od interesa, čime se znatno štedi na vremenu i troškovima.*

*Ključne reči:* nivo H<sub>2</sub>O<sub>2</sub>, kinetički model, zagađenje fenolom, UV/H<sub>2</sub>O<sub>2</sub>.



## **CONCLUDING REMARKS**



## 5. CONCLUDING REMARKS

PAHs are often distinguished by the number of fused benzene rings they possess (Wick et al., 2011). In general, PAHs may be divided into two groups, depending upon their physical and chemical properties: a) low-molecular-weight PAHs, containing three or fewer aromatic rings, and b) high-molecular-weight PAHs, containing more than three aromatic rings. Sources related to energy production are the most important ones releasing PAHs into the environment. PAHs can be classified as either pyrogenic (mainly formed from the incomplete combustion of organic materials, such as coal, oil, wood or fossil fuels) or petrogenic inputs (Vela et al., 2012). In areas under the influence of urban and industrial activities, the major contributors to anthropogenic emissions are vehicular sources, mainly due to the combustion of petrol and diesel, and emissions related to industrial processes. In addition, PAHs are widely distributed in the environment, as reported by Sharma et al. (2018) and Vela et al. (2012).

If these pollutants were harmless compounds, there would be nothing to be worried about; however, PAHs have the potential to cause adverse environmental effects. In fact, they have been reported to exhibit carcinogenic, mutagenic and teratogenic potential (like BaP) and have an acute phototoxicity (such as AN), generating derivative compounds more dangerous than the original toxic compound (Zeng et al., 2018). Additionally, they can cause the deterioration of the immune system and are suspected to be endocrine disruptors (Vela et al., 2012). It is worth noting that these detrimental effects are synergistically increased when PAHs exist as mixtures.

Because of the detrimental effects linked to the presence of PAHs, especially AN and BaP, they take part of the list of priority substances to be monitored and controlled. However, due to the hydrophobicity of PAHs, the compounds of interest are found in water at trace and ultra-trace levels, in the order of  $\text{ng L}^{-1}$  or  $\mu\text{g L}^{-1}$ , as it has been found in several recent research works around the world, highlighting the works conducted by Sharma et al. (2018), Zeng et al. (2018), and

Santos et al. (2018), among others. This fact limits the identification and quantification of the target substances by the traditional analytical methods and procedures, especially when present in real aqueous samples, due to the background constituents that could mask the presence of the analytes to be analyzed. Therefore, new analytical methods for determining the behavior of a mixture of AN and BaP contained in real surface water at trace and/or ultra-trace concentration are required.

Along with the need to analyze very low levels of the target pollutants, a reduced analysis time, and costs, and a high compound resolution are demanded. In this regard, chromatographic techniques, such as HPLC, are required due to the benefits linked to their use for analyzing compounds in environmental matrices at extremely low concentrations.

For a sensitive identification and quantification of the compound of interest in a short period of time and with the lowest analysis costs, the optimization of the operating chromatographic conditions influencing the system is needed. Under this scenario, the flow rate, mobile phase strength, column temperature, injection volume, and the excitation and emission wavelengths were selected.

With regard to the column stationary phase, a Kinetex core shell technology C18 column (150 mm x 4.6 mm i.d., 5  $\mu$ m of particle size) from Phenomenex was chosen due to the high PAH separation efficiencies reported (Trably et al. 2004).

Concerning the type of mobile phase, a binary system composed of an organic solvent and deionized water was chosen. For the selection of the organic solvent, acetonitrile was considered to be the most appropriated in comparison with methanol since acetonitrile gives better peak shapes and shorter analysis times, as also found Zhou et al., (2009), and it is less viscous; therefore, the increase of the pressure of the column is avoided. No additional modifier was selected for the mobile phase since reproducibility is enhanced when simple mobile phases are used (Ji et al. 2005). Regarding the mobile phase strength, a range from 70 to 90% of acetonitrile content was studied. It is important to mention that as the acetonitrile content is increased, the retention time is reduced. This phenomenon occurs due to the analyte of interest elutes more rapidly. Since BaP is highly hydrophobic and the last eluting compound in the considered

chromatographic system, high levels of acetonitrile must be used in the mobile phase. Finally, due to only two compounds were required to be resolved, isocratic conditions were chosen. Additionally, it is highlighted that the baseline deformation is reduced when operating under isocratic conditions.

Regarding the column temperature, it influences the retention time and the system pressure, as well as the stability and selectivity of the column (Ji et al. 2005). As the temperature is raised, reductions in the retention times and system pressures are evidenced. However, analysis costs are augmented when operating under high column temperatures. Therefore, the selected range for this parameter was from 25 to 35 °C. The flow rate is another factor affecting the chromatographic system. A range comprised between 1 and 1.5 mL min<sup>-1</sup> was selected; not so high flow rates since high column pressures and low retention times would be obtained. Finally, the injection volume of the sample is of great interest, especially when analyzing compounds at extremely low concentrations. Hence, the injection volume range was selected from 50 to 100 µL.

Furthermore, taking profit on the characteristics of the analytes of interest and the advantages ascribed to the use of the fluorescence property of the compounds (Marcé & Borrull 2000), a FLD was selected. The excitation and emission wavelength ranges were obtained from the literature, experimental tests and our own knowledge, and resulted to be from 230 to 280 nm and from 408 to 424 nm, respectively.

In turn, the evaluated responses factors were the resolution between the compounds of interest and the areas and heights of AN and BaP for identification and quantification purposes, respectively. The retention time of BaP was also selected as response to be assessed in order to save organic solvent and valuable analytical time.

Considering the relationships between the selected responses, they were grouped into three indexes, explaining the chromatographic behavior of AN and BaP under the tested operating conditions. The referred indexes describe the elution of AN and BaP, the peak shape of AN and that of BaP, respectively. The first index represents the identification of the compounds of interest, where the

strength and the flow rate of the mobile phase used developed a main role. Concerning the second index, in turn, it refers to the quantification of AN, and the excitation wavelength was observed to be crucial. Finally, the third index, represents the quantification of BaP and, as expected, was also influenced by the excitation wavelength; however, the injection volume and the flow rate of the mobile phase were also observed to exert a main function.

For this purpose, principal component analysis (PCA) was used. PCA is a chemometric tool aiming at building a number of lineal combinations of the response factors considered containing the major variability (Machala et al., 2001; Golobočanin et al. 2004).

Once the indexes were found, the operating factors describing them were optimized using design of experiments (DOE). The particular DOE used was a fractional factorial design with 5 central points.

Statistical data were analyzed and treated using Statgraphics Centurion XVII and a confidence interval of 95%, respectively.

Finally, the optimal operating conditions found were 1 mL min<sup>-1</sup>, 90%, 35 °C, 100 µL, and 416 nm for the flow rate, acetonitrile content of the mobile phase, column temperature, injection volume and the emission wavelength, respectively. The optimal excitation wavelengths were 254 nm and 267 nm for AN and BaP.

Additionally, the developed analytical method was validated. A sensitive analytical method was obtained with limits of detection of 5.54 and 4.26 ng L<sup>-1</sup> for AN and BaP, respectively. Low limits of quantification were also achieved for AN (75 ng L<sup>-1</sup>) and BaP (30 ng L<sup>-1</sup>). Intra- and inter-day precisions lower than 2 and 11%, respectively, were found. Accuracy was also verified and relative standard deviations (RSD) lower than 10% were evidenced. Furthermore, satisfactory recoveries (RSD < 13%) were found in different matrices of real natural water.

Therefore, the developed and validated method showed to be suitable for the identification and quantification of a mixture of the target analytes at ultra-trace levels in relatively clean real natural water by direct injection of the sample in only 5 min of analysis time.

On the other hand, it is noteworthy that PAHs are organic pollutants resistant to degradation (Vela et al., 2012); i.e., they can remain in the environment for a long period of time without being altered from physical, chemical nor biological processes. Therefore, PAHs are persistent compounds. In addition, conventional processes water treatment facilities are operating with seems to be not designed for tackling the problem of the presence of these contaminants in water, since conventional physico-chemical and biological methods have been found unsuccessful at the degradation of PAHs. Consequently, the development and implementation of more efficient alternative treatments were needed and, among them, advanced oxidations processes (AOPs) are considered as interesting options.

From the state-of-the-art research, several AOPs were found to be effective for PAH degradation, especially UV-C-based oxidation system, such as the UV-C/H<sub>2</sub>O<sub>2</sub> process. In this regard, this photochemical AOP was selected to be studied as a good alternative to traditional processes for destroying AN and BaP, generating harmless by-products, mineralizing the organic matter naturally contained in water and inactivating the wild microbial load of water.

The selected photochemical AOP was conducted in a borosilicate glass 3.3 cylindrical jacketed reactor, previously designed and manufactured. The photoreactor dimensions are 11 cm internal diameter x 35 cm length and 0.3 cm wall thickness, and has an effective operating volume of 2 L. It has a lid manufactured of stainless steel 304 type containing four circumferentially uniformly spaced tubes made of quartz, whose dimensions are 1'' diameter and 33 cm length. Inside the tubes, the ultraviolet lamps that can be interchangeable depending on the irradiation type needed for the AOP to be performed, are placed. Such as lamps are connected to an external control system allowing turning on and off each of the lamps independently. As radiation sources, low pressure Hg-vapor germicidal lamps with a main wavelength emission at 254 nm, especially used for the UV-C/H<sub>2</sub>O<sub>2</sub>, was used. The lamps used were 15 mm (T5) diameter, 29 cm length and 8 W power. The system, including the quartz tubes, was adjusted for these dimensions.

The photoreactor enables the solution within the reaction chamber to be maintained at a specific and constant temperature due to it is equipped with a refrigeration system consisting of a cooling jacket also made of borosilicate glass 3.3, a pump, a radiator and a fan. A control system allows operating the cooling circuit automatically. The temperature within the bulk is measured by a type-K thermocouple. When the temperature is above a user-defined value, the recirculation system of the cooling fluid is activated, maintaining the temperature of the reaction medium at a constant value. Additionally, the solution within the reactor is magnetically stirred using a magnetic stirrer bar to ensure homogenization. Finally, the photoreactor can operate in continuous, semi-batch and batch modes; however, during the current experimentation, batch operating mode was selected.

The natural water used was surface water sampled from a Colombian reservoir called "El Peñol" dam, located in Guatapé, Antioquia (N 6° 17' 41.1583" O 75° 9' 31.0821"). The water was characterized by its relatively low natural organic matter content (2.03 mg C L<sup>-1</sup>, in terms of total organic carbon (TOC)) and inorganic anions. In addition, the turbidity, pH, temperature and conductivity were 1.09 NTU, 7.35, 23.58 °C and 0.39 mS cm<sup>-1</sup>, respectively. The bacterial load concentration, in terms of total coliforms, was 10<sup>3</sup>–10<sup>4</sup> CFU 100 mL<sup>-1</sup>. Due to in the water of study AN and BaP were absent, they were spiked at ultra-trace concentrations. All the parameters were analyzed in triplicate using standardized analytical methods and protocols (WEF & AWWA, 2012).

During the implementation of the UV-C/H<sub>2</sub>O<sub>2</sub> process, several factors influencing the system were studied, mainly the irradiance and the level of H<sub>2</sub>O<sub>2</sub>, due to they have been proved to exert a main role in the performance of the selected system (Rubio-Clemente et al., 2014). It was evidenced that the integrated system was able to achieve an efficient removal of the pollutants of interest (higher than 99% using only 1 UV-C low pressure lamp in an irradiation period of 15 min), being the HO• the chemical species developing the main action. The mineralization of the organic matter naturally present in the water of study was also efficiently obtained (~ 45% under the action of 3 UV-C lamps of 8 W each combined with 10 mg L<sup>-1</sup> H<sub>2</sub>O<sub>2</sub> after 90 min of treatment). Additionally, the production of compounds more dangerous than the original toxics was not found.



For the analysis of AN and BaP evolution profiles the analytical method developed was used. In turn, TOC determination was carried out using the 5310 B high-temperature combustion method (WEF & AWWA, 2012). The reaction intermediates were identified and relatively quantified using a GC-MS analytical method coupled to a micro liquid-liquid extraction phase, derived from Pena et al. (2009), whose further details can be found in Rubio-Clemente et al. (2018c).

The UV-C/H<sub>2</sub>O<sub>2</sub> system allowed for very positive results in terms of the degradation of the pollutants of interest and organic matter mineralization, avoiding the production of harmful degradation by-products. Furthermore, throughout this process, a residual H<sub>2</sub>O<sub>2</sub> level equivalent to a rate  $[H_2O_2]/[H_2O_2]_0$  higher than 0.6 was observed in water after the treatment application. This residual H<sub>2</sub>O<sub>2</sub> could guarantee microbial inactivation before its decomposition. For the determination of the residual H<sub>2</sub>O<sub>2</sub>, a spectrophotometric analytical method was developed using once again multivariate statistical tools, particularly a 2<sup>3</sup> full factorial DOE. The analytical method was based on the colored complexes formed between ammonium monovanadate (NH<sub>4</sub>VO<sub>3</sub>) and H<sub>2</sub>O<sub>2</sub> in acidic media, as reported previously by Pupo et al. (2005). The factors affecting the analytical system and the ranges evaluated were the final concentration of the NH<sub>4</sub>VO<sub>3</sub> ( $6 \times 10^{-3}$ – $1.2 \times 10^{-2}$  M), the quartz cell path length (1–5 cm) and the absorption wavelength (450–454 nm).

Under optimal operating conditions, the analytical method developed allows quantifying levels of H<sub>2</sub>O<sub>2</sub> in real aqueous matrices up to 0.1 mg L<sup>-1</sup>. Additionally, the interfering substances commonly found in water matrices, such as Fe<sup>3+</sup>, Fe<sup>2+</sup>, Cl<sup>-</sup>, NO<sub>3</sub><sup>-</sup>, PO<sub>4</sub><sup>3-</sup>, NH<sub>4</sub><sup>+</sup>, Mg<sup>2+</sup>, Na<sup>+</sup>, Mn<sup>2+</sup>, F<sup>-</sup>, K<sup>+</sup>, CO<sub>3</sub><sup>2-</sup> and Ca<sup>2+</sup>, were evaluated. Finally, the method was validated, obtaining a selective and sensitive method.

The UV-C/H<sub>2</sub>O<sub>2</sub> oxidation system was also assessed in order to overcome the problem of microbial pollution in natural water, and results were compared with the UV-C/US and UV-C/US/H<sub>2</sub>O<sub>2</sub> oxidation processes, whose main parameters, including the irradiance, frequency, input power and H<sub>2</sub>O<sub>2</sub> content, were previously optimized. For the US experimental study, a sonoreactor was used. The sonochemical reactor consisted of a power electronic system able to

transform the electrical oscillation into ultrasonic vibrations, generating ultrasonic waves; a sonoreactor with 1 L of effective operating volume; and a set of four interchangeable piezoelectric transducers to be used when sonochemistry-based experiments were required to be generated into a specific operating frequency, including 50, 80, 120, and 135 kHz. The input power of the sonoreactor is adjustable between 0 and 60 W. The sonoreactor was provided with two interchangeable lids made of borosilicate glass 3.3; one of them with a quartz tube coupled at the bottom to allow performing the experiments where the action of a 6 W UV-C light is coupled to the US waves, among others.

During these experimentations, the sonoreactor was operated in batch mode.

By irradiating the water samples using 6 W and 8 W UV-C lamps, with a UV-C dose accumulation of 186.75, 99 and 33 mJ cm<sup>-2</sup> during the UV-C/H<sub>2</sub>O<sub>2</sub>, UV-C/US and the UV-C/H<sub>2</sub>O<sub>2</sub>/US oxidation systems, respectively, a total removal of the wild bacterial load contained naturally in water was obtained and no subsequent regrowth was observed after 24 h and 48 h of having implemented the referred treatments and keeping in the dark. It must be highlighted that for the bacterial load evolution profiles, the 9222 membrane filtration method (WEF & AWWA, 2012) was used.

The obtained results enable us to infer in a more accurately manner the consequences of implementing the UV-C/H<sub>2</sub>O<sub>2</sub> system for disinfection purposes in comparison with the findings that are achieved when synthetic water matrixes and laboratory microorganism cultures are used.

During the evaluation of the disinfection capacity of the mentioned oxidation system, a cost analysis was also carried out. It was found that the UV-C/H<sub>2</sub>O<sub>2</sub> system was the most economical process, with EE/O associated of 6.95 kWh m<sup>-3</sup>. In this way, the microbial disinfection was demonstrated to be plausible and without incurring high energy costs by the UV-C/H<sub>2</sub>O<sub>2</sub> advanced oxidation technology.

Nonetheless, it is also important to note that operating costs are decisive when a system is implemented, especially when it is scaled up. Due to the

electrical costs associated to the operation of the reactor used, in spite of the UV-C/H<sub>2</sub>O<sub>2</sub> system resulted to be the most economical one among the oxidation processes tested, other alternative measurements that makes the oxidation system even more economical are needed. In this regard, and considering the maximal efficiency of the UV-C/H<sub>2</sub>O<sub>2</sub> process occurs under UV-C and the short amount in solar light corresponding to the UV-C electromagnetic radiation range, the implementation of PV cells are positioned as an optimal option for those areas where sun, as natural resource, is not restrictive. Therefore, a PV array was sized and installed for supplying the energy requirements of the treated water. The PV system was initially sized for any type of advanced oxidation processes due to the high costs associated, especially to the UV-C-based technologies. Afterwards, the sized PV array was applied for providing the electrical requirements needed by the UV-C/H<sub>2</sub>O<sub>2</sub> system.

For assuring a high efficiency and operation of the PV systems, the selection and design of the batteries, inverter, controller, power electronic devices and wiring, as the required equipment, are of great importance. Therefore, during the sizing of a PV array, selecting the proper technology to reduce losses and improve the power conversion efficiency of the PV system is needed (Meral et al., 2011). Furthermore, in order to determine in a proper way the amount of electricity produced, a reliable knowledge of the equipment efficiency used for the PV array operation is essential. Consequently, for the calculation of the current PV system sizing, the efficiency of the equipment used was taken into account. Moreover, several environmental factors contributing to the system output losses, including sub-optimal orientation with respect to the sun, soiling, shading and, in some countries, seasonal snow cover, must be also taken into account for an efficient PV array design (Meral et al., 2011).

For a PV system to be efficient, its size must be determined correctly (Omar and Shaari, 2009; Rauschenbach, 2012; Sulaiman et al., 2010, 2011). For the PV system sizing, the most important design factor is the power consumed by the equipment used during the AOP operation. Thus, the first step in designing a solar PV system is to find out the total power of the energy consumed by the devices involved in the water treatment process. Sizing the PV modules, inverter, batteries and the solar charge controller constitute the second step. For this

purpose, the electricity demand must be considered so that the system is not over or undersized. PV module sizing procedure must be based on the nominal power of the modules so that the required power rating can be met by different combinations of the modules in series or parallel (Boxwell, 2015; Foster et al., 2010; Han et al., 2013; McEvoy et al., 2003; Omar and Saari, 2009; Solanki, 2013; Sulaiman et al., 2010). Moreover, in the system where AC power output is needed an inverter is used. Furthermore, the battery plays an important role in matching the load requirements in stand-alone PV systems. The battery type recommended to be used in a solar PV system is deep cycle battery, with capacity to store sufficient energy so that it can operate at cloudy days and during nights. Finally, the solar charge controller must be selected for matching the voltage of the PV array and batteries, taking into account that the solar charge controller must have enough capacity to handle the current from the PV array. Specifically for the UV-C/H<sub>2</sub>O<sub>2</sub> treatment, electrical energy is consumed during the effluent mechanical stirring, UV-C radiation generation, recirculation pumping and the systems of refrigeration and ventilation.

Considered the aspects mentioned above, a PV system without batteries was used for supplying the required power in the AOP implementation. The PV array consisted of 9 PV modules of 250 W<sub>p</sub> that were installed with an optimum tilt angle of 15.64°. The PV system was used to directly power a UV-C/H<sub>2</sub>O<sub>2</sub> system for degrading natural water containing AN and BaP at a concentration of 12 and 3 µg L<sup>-1</sup>, respectively. The results obtained were comparable to those ones obtained under traditional electrical grid for the same operating conditions.

From this research, it was concluded that AOPs can be powered using PV energy in a reliable and autonomous way, especially in NIZs.

Moreover, the investment costs of the UV-C/H<sub>2</sub>O<sub>2</sub>-PV system for small applications were estimated. It was found that the high costs associated with PV modules and equipment, compared to conventional energy sources, constitute the primary limiting factor for the technology. However, the PV array can be also connected directly to the equipment used in the water treatment systems without batteries, as demonstrated, obtaining good efficiencies in water treatment. Thus the environmental threat of improper battery disposal is eliminated and,

subsequently, the sustainability of the process is increased. Furthermore, the investment costs decrease compared to the costs associated with a PV system with batteries. Thus PV systems can be designed for a variety of applications and operational requirements, and can be used for either centralized or distributed power generation.

The PV system sized allowed for the use of renewable energy both in developing and non-developing countries. In this regard, the treatment of water to be drinkable was observed to be plausible in countries with lack of economical resources and in communities far from interconnected zones, which account for a vast area of the territory in African and Latin American countries, such as Colombia.

Additionally, the obtained results might be of great interest for other studies related to direct connection of PV systems to other AOPs powered by PV energy both in developed and developing countries, allowing an environmentally-friendly and sustainable development of such as countries.

Finally, in this Thesis in order to find out the optimal operating conditions without a large and costly experimental stage, a kinetic model for the implementation of the UV-C/H<sub>2</sub>O<sub>2</sub> system was constructed and validated.

The kinetic model includes the effect of the background matrix and the degradation by-products in shielding light and quenching free radicals, as well as the change of the solution pH as the action of UV-C light and the oxidizing agent is combined.

In order to discern the evolution of the concentration of HO• formed within the bulk and whether the type of hypothesis assumed is determinative in this phenomenon, three different assumptions were considered to calculate the level of such as reactive chemical species: non pseudo-steady, pseudo-steady and simplified pseudo-steady state hypothesis. It was found non-significant differences between the three assumptions considered previously, probably due to the relatively low concentration of HO• present in the bulk ( $\sim 10^{-14}$  M).

For the development of the kinetic model, the chemical reactions involved were compiled and a system of ODE for each of the chemical species included was established. The solution of the ODE set was found using MATLAB software and ODE15S function.

Furthermore, the model was validated. It was achieved that the proposed kinetic model fits well with experimental data (Alnaizy & Akgerman, 2000) which is a probe of the accuracy of the model. For this purpose, nonlinear objective function of least squares was used to calculate the reaction kinetic rate constant of the pollutant considered and that of HO<sub>2</sub><sup>•</sup>. The kinetic rate constant of the estimated reaction was  $1.6 \times 10^3 \text{ M}^{-1} \text{ s}^{-1}$ , which resulted to be in the range of data reported from literature.

It was also found that HO<sup>•</sup> played a fundamental role in the degradation of the pollutant considered, leaving the action of HO<sub>2</sub><sup>•</sup> relegated to the background. It was observed that, although including HO<sub>2</sub><sup>•</sup> action allowed slightly improving the kinetic model degree of fit, the chemical species developing the main function in the elimination of the pollutant is HO<sup>•</sup> due to its high oxidation potential.

Furthermore, the generation of an effective level of HO<sup>•</sup> within the bulk was observed. Below that level, there was a lack of HO<sup>•</sup> for an efficient pollutant conversion; and above it, an excessive number of HO<sup>•</sup> was generated. That HO<sup>•</sup> effective level could be of relevance for industrial applications in order to be maintained throughout the reaction time, contributing to an efficient pollutant degradation.

The kinetic model could be relevant for calculating the optimal level of H<sub>2</sub>O<sub>2</sub> efficiently degrading the pollutant of interest, as well as the effective level of HO<sup>•</sup> to be maintained throughout the UV-C/H<sub>2</sub>O<sub>2</sub> system reaction time for achieving an efficient pollutant degradation. allowing saving in costs and time.

Additionally, the kinetic modeling development of processes that are just taking off on a large scale, as it is the case of the UV-C/H<sub>2</sub>O<sub>2</sub> system, is of great interest not only for the industry but also for the government, since it allows to optimize the operating conditions of a relevant and efficient process, such as the UV-C/H<sub>2</sub>O<sub>2</sub> system, without incurring high economical and timing costs.

In this regard, this work contributes to the implementation of the UV-C/H<sub>2</sub>O<sub>2</sub> system for water treatment both using the conventional electrical grid and installing an integrated PV system, allowing the degradation of refractory pollutants to traditional systems and the mineralization of the organic matter contained in real water matrices without the production of compounds more dangerous than the parent pollutants.

Furthermore, the disinfection potential of the oxidation system has been proved, which makes the process a possible candidate for treating water with the purpose of being distributed to humans, providing the accomplishment of the rest of parameters set in the regulations related to drinking water production.

Therefore, the UV-C/H<sub>2</sub>O<sub>2</sub> system might be applied as alternative treatment to conventional water treatment processes for natural water purification purposes as long as other regulated water quality criteria are accomplished.

However, it is highlighted that, due to the great variety of aqueous matrix constituents present in natural water, further studies are needed to clarify the degradation mechanism of AN and BaP, and the influence of particular water matrix components on the selected PAHs, as well as the TOC mineralization and microbial load inactivation. For this objective, synthetic water matrices spiked with different levels of each constituent would be required to understand the influence of each individual component and mixtures of them, since interactive effects among water matrix components can occur, as demonstrated by Ge et al. (2016) for the correlated action of Cl<sup>-</sup> and dissolved Fe(III) in 9-hydroxyfluorene photodegradation, as Cl<sup>-</sup> might transform into Cl<sup>•</sup> when interacting with Fe(III), with the subsequent facilitation of the pollutant photodegradation. In addition, to examine the role of the triplet state dissolved organic matter (<sup>3</sup>DOM\*) and the ROS formed in the reaction solution, different inhibiting substances can be used, such as 2,4,6-trimethylphenol for quenching the effect of the excited triplet state of irradiated humic substances (Porrás et al., 2016). In an effort to examine the action of singlet oxygen (<sup>1</sup>O<sub>2</sub>) in ciprofloxacin oxidation after irradiation, these authors also used furfuryl alcohol due to its capacity to scavenge <sup>1</sup>O<sub>2</sub>. This substance was also employed by Grossman et al. (2016) to investigate the role of singlet oxygen on photolysis kinetics of AN and pyrene in water. Ge et al. (2016) and Sheng et al. (2015) used sodium azide (NaN<sub>3</sub>) to trap HO<sup>•</sup> and <sup>1</sup>O<sub>2</sub>, and isopropanol and

dimethyl sulfoxide, respectively, to quench HO<sup>•</sup>. Isopropanol was also used by Shemer & Linden (2007) to quench the HO<sup>•</sup> yielded in the medium solution.

Furthermore, in order to discern whether an alternative process can be used at large scale in drinking water facilities, other parameters besides the pollutant of interest destruction, organic matter degradation and total coliform removal must be analyzed, and among them, the disinfection by-products are of special interest because of the harmful effects associated with, especially in this research, since a residual H<sub>2</sub>O<sub>2</sub> was found after applying the UV-C/H<sub>2</sub>O<sub>2</sub> system. The residual H<sub>2</sub>O<sub>2</sub> could react with the organic matter not converted through the oxidation system and produce disinfection by-products.

Moreover, when deciding the most efficient process, a complete cost study, including operating costs (reagents used, lamp replacement, etc.) and capital costs, should be conducted.



## **REFERENCES**



---

**REFERENCES**

- Abdel-Shafy, H. I., & Mansour, M. S. (2016). A review on polycyclic aromatic hydrocarbons: source, environmental impact, effect on human health and remediation. *Egyptian Journal of Petroleum*, 25(1), 107-123.
- Alnaizy, R., & Akgerman, A. (2000). Advanced oxidation of phenolic compounds. *Adv. Environ. Res.*, 4(3):233–244.
- Audenaert, W.T.M., Vermeersch, Y., Van Hulle, S.W.H., Dejans, P., Dumoulin, A., & Nopens, I. (2011). Application of a mechanistic UV/hydrogen peroxide model at full-scale: Sensitivity analysis, calibration and performance evaluation. *Chemical Engineering Journal*, 171, 113–126.
- Boix, C., Ibáñez, M., Sancho, J.V., Rambla, J., Aranda, J.L., Ballester, S., & Hernández, F. (2015). Fast determination of 40 drugs in water using large volume direct injection liquid chromatography tandem mass spectrometry. *Talanta*, 131, 719–27.
- Bounty, S., Rodriguez, R.A., Linden, K.G. (2012). Inactivation of adenovirus using low-dose UV/H<sub>2</sub>O<sub>2</sub> advanced oxidation. *Water Research*, 46(19), 6273–6278.
- Boxwell, M. (2015). *Solar Electricity Handbook. A simple practical guide to solar energy designing and installing photovoltaic solar electric systems*, fifteenth ed. Code Green Publishing, United Kingdom.
- Bridier, A., Briandet, R., Thomas, V., & Dubois-Brissonnet, F. (2011). Resistance of bacterial biofilms to disinfectants: a review. *Biofouling*, 27(9), 1017–1032.
- Chizhova, T., Hayakawa, K., Tishchenko, P., Nakase, H., & Koudryashova, Y. (2013). Distribution of 555 PAHs in the northwestern part of the Japan Sea. *Deep-Sea Research Part II*, 86, 19–24.
- Crittenden, J.C., Hu, S., Hand, D.W., & Green, S.A. (1999). A kinetic model for H<sub>2</sub>O<sub>2</sub>/ UV process in a completely mixed batch reactor. *Water Research*, 33(10), 2315– 2328.

De la Fuente-Núñez, C., Reffuveille, F., Fernández, L., & Hancock, R.E. (2013). Bacterial biofilm development as a multicellular adaptation: antibiotic resistance and new therapeutic strategies. *Current Opinion in Microbiology*, 16(5), 580–589.

Directive (2013). Directive 2013/39/EU of the European Parliament and of the Council of 12 August 2013 amending Directives 2000/60/EC and 2008/105/EC as regards priority substances in the field of water policy. *Official Journal of the European Union L*, 226, 1-17.

Ebrahimi-Najafabadi, H., Leardi, R. & Jalali-Heravi, M. (2014). Experimental design in analytical chemistry-part I: theory. *Journal of AOAC International*, 97, 3-11.

Engelhardt, H. (2012). *High performance liquid chromatography*. Editorial Springer-Verlag, Berlin Heidelberg New York.

ECLAC. (2004). *Renewable energy sources in Latin America and The Caribbean. Situation and policy proposals*. United Nations, Bonn, Germany, retrieved in 17.09.18 from <http://www.cepal.org/publicaciones/xml/9/14839/lcl2132i.pdf>.

ESMAP (2010). *Review of policy framework for increased reliance on wind energy in Colombia*. In Energy Unit. Sustainable Development Department. Latin America and Caribbean Region, The World Bank, 2010, retrieved in 17.09.18 from [https://www.esmap.org/sites/esmap.org/files/P108945\\_Colombia\\_Review%20of%20Policy%0Framework%20for%20Increased%20Reliance%20on%20Wind%20Energy\\_Vergara.pdf](https://www.esmap.org/sites/esmap.org/files/P108945_Colombia_Review%20of%20Policy%0Framework%20for%20Increased%20Reliance%20on%20Wind%20Energy_Vergara.pdf).

Fernández-González, V., Concha-Graña, E., Muniategui-Lorenzo, S., López-Mahía, P. & Prada-Rodríguez, D. (2007). Solid-phase microextraction-gas chromatographic-tandem mass spectrometric 570 analysis of polycyclic aromatic hydrocarbons. Towards the European Union water directive 2006/0129 EC. *Journal of Chromatography, A* 1176, 48–56.

Ferreira S.L.C., Bruns R.E., da Silva E.G.P., dos Santos W.N.L., Quintella C.M., David J.M., de Andrade J.B., Breikreitz M.C., Jardim I.C.S.F., & Neto B.B. (2007). Statistical designs and response surface techniques for the optimization of chromatographic systems. *Journal of Chromatography A*, 1158, 2-14.

- Foster, R., Ghassemi, M., Cota, A. (2010). *Solar energy: Renewable energy and the environment*. CRC Press, United States.
- García, S. & Pérez, R.M. (2012). *Aplicaciones de la cromatografía líquida con detector de diodos y fluorescencia al análisis de contaminantes medioambientales*. Informes Técnicos Ciemat. Editorial Ciemat, Madrid.
- Gassie, L.W., & Englehardt, J.D. (2017). Advanced oxidation and disinfection processes for onsite net-zero greywater reuse: A review. *Water Research*, 125, 384-399.
- Ge L., Na G., Chen C.E., Li J., Ju M., Wang Y., Li K., & Zhang, P. (2016). Aqueous photochemical degradation of hydroxylated PAHs: Kinetics, pathways, and multivariate effects of main water constituents. *Science of the Total Environment*, 547, 166-172.
- Giannakis, S., Androulaki, B., Comninellis, C., & Pulgarin, C. (2018a). Wastewater and urine treatment by UVC-based advanced oxidation processes: Implications from the interactions of bacteria, viruses, and chemical contaminants. *Chemical Engineering Journal*, 343, 270–282.
- Golobočanin, D. D., Škrbić, B. D. & Miljević, N. R. (2004). Principal component analysis for soil contamination with PAHs. *Chemometrics and Intelligent Laboratory Systems*, 72, 219-223.
- Han, C., Liu, J., Liang, H., Guo, X., Li, L. (2013). An innovative integrated system utilizing solar energy as power for the treatment of decentralized wastewater. *J. Environ. Sci.* 25, 274–279.
- Hebert, A., Feliars, C., Lecarpentier, C., Neale, P. A., Schlichting, R., Thibert, S., & Escher, B. I. (2018). Bioanalytical assessment of adaptive stress responses in drinking water: A predictive tool to differentiate between micropollutants and disinfection by-products. *Water Research*, 132, 340-349.
- Hernandez, L. & González, C. (2002). *Introducción al análisis instrumental*. Editorial Ariel, Barcelona.

- Hong, A., Zappi, M.E., & Hill, D. (1996). Modeling kinetics of illuminated and dark advanced oxidation processes. *Journal of Environmental Engineering*, 122(1), 58–62.
- Huang, C.R., & Shu, H.Y. (1995). The reaction kinetics, decomposition pathways and intermediate formation of phenol in ozonation, UV/O<sub>3</sub> and UV/H<sub>2</sub>O<sub>2</sub> processes. *Journal of Hazardous Materials*, 19(41), 47–64.
- Hulsmans, A., Joris, K., Lambert, N., Rediers, H., Declerck, P., Delaedt, Y., Ollevier, F., & Liers, S. (2010). Evaluation of process parameters of ultrasonic treatment of bacterial suspensions in a pilot scale water disinfection system. *Ultrasonics Sonochemistry*, 17(6), 1004–1009.
- Ji Y.B., Xu Q.S., Hu Y.Z., & Vander Y. (2005). Development, optimization and validation of a fingerprint of Ginkgo biloba extracts by high-performance liquid chromatography. *Journal of Chromatography A*, 1066: 97-104.
- Khodae, N., Mehdinia, A., Esfandiarnejad, R., & Jabbari, A. (2016). Ultra-trace analysis of PAHs by designing simple injection of large amounts of analytes through the sample reconcentration on SPME fiber after magnetic solid phase extraction. *Talanta*, 147,59–62.
- Lee, R.F. (2003). Photo-oxidation and photo-toxicity of crude and refined oils: Review article. *Spill Science & Technology Bulletin*, 8(2),157–162.
- Liao, C.H., & Gurol, M.D. (1995). Chemical oxidation by photolytic decomposition of hydrogen peroxide. *Environmental Science Technology*, 29(12), 3007–3014.
- Linley E., Denyer S.P., McDonnell G., Simons C., & Maillard J.Y. (2012). Use of hydrogen peroxide as a biocide: new consideration of its mechanisms of biocidal action. *Journal of Antimicrobial Chemotherapy*, 67 (7), 1589–1596.
- Litter, M.I., & Quici, N. (2010). Photochemical advanced oxidation processes for water and wastewater treatment. *Recent Patents on Engineering* 4, 217–241.
- Liu, J. J., Wang, X.C. & Fan, B. (2011). Characteristics of PAHs adsorption on inorganic particles and activated sludge in domestic wastewater treatment. *Bioresource Technology*, 102, 5305–5311.

- Lopez-Alvarez, B., Villegas-Guzman, P., Peñuela, G.A., Torres-Palma, R.A. (2016) Degradation of a toxic mixture of the pesticides carbofuran and iprodione by UV/H<sub>2</sub>O<sub>2</sub>: evaluation of parameters and implications of the degradation pathways on the synergistic effects. *Water, Air & Soil Pollution*, 227(6), 214–226.
- Lyons, N.A., & Kolter, R. (2015). On the evolution of bacterial multicellularity. *Current Opinion in Microbiology* 24, 21-28.
- Ma, X. Y., Li, Q., Wang, X. C., Wang, Y., Wang, D., & Ngo, H. H. (2018). Micropollutants removal and health risk reduction in a water reclamation and ecological reuse system. *Water Research*, 138, 272-281.
- Machala, M., Dusek, L., Hilscherova, K., Kubinova, R., Jurajda, P., Neca, J., Ulrich, R., Gelnar, M., Studnicková, Z., & Holoubek, I. (2001). Determination and multivariate statistical analysis of biochemical responses to environmental contaminants in feral freshwater fish *Leuciscus cephalus* L. *Environmental Toxicology and Chemistry*, 20, 1141-1148.
- Mahamuni, N.N., & Adewuyi, Y.G. (2010). Advanced oxidation processes (AOPs) involving ultrasound for waste water treatment: a review with emphasis on cost estimation. *Ultrasonics Sonochemistry*, 17(6), 990–1003.
- Malvestiti, J.A., Dantas, R.F. (2018). Disinfection of secondary effluents by O<sub>3</sub>, O<sub>3</sub>/H<sub>2</sub>O<sub>2</sub> and UV/H<sub>2</sub>O<sub>2</sub>: Influence of carbonate, nitrate, industrial contaminants and regrowth. *Journal of Environmental Chemical Engineering*, 6(1), 560–567.
- Marcé R.M., & Borrull F. (2000). Solid-phase extraction of polycyclic aromatic compounds. *Journal of Chromatography A*, 885, 273-290.
- Matilainen, A., & Sillanpää, M. (2010). Removal of natural organic matter from drinking water by advanced oxidation processes. *Chemosphere*, 80(4), 351–365.
- Miklos, D.B., Remy, C., Jekel, M., Linden, K.G., Drewes, J.E., & Hübner, U. (2018). Evaluation of advanced oxidation processes for water and wastewater treatment—A critical review. *Water Research*, 139, 118-131.
- McEvoy, A., Markvart, T., Castañer, L., Markvart, T., Castaner, L. (2003). *Practical handbook of photovoltaics: Fundamentals and applications*, Elsevier Science, Amsterdam.

- Meral M.E., F. Dinçer. (2011). A review of the factors affecting operation and efficiency of photovoltaic based electricity generation systems, *Renew. Sustain. Energy Rev.* 15, 2176–2184.
- Oliferova, L., Statkus, M., Tsysin, G., Shpigun, O., & Zolotov, Y. (2005). On-line solid-phase extraction 630 and HPLC determination of polycyclic aromatic hydrocarbons in water using fluorocarbon polymer sorbents. *Analytica Chimica Acta*, 538, 35–40.
- Omar, A.M., Shaari, S. (2009). Sizing verification of photovoltaic array and grid-connected inverter ratio for the Malaysian building integrated photovoltaic project. *Int. J. Low-Carbon Technol.* 4, 254–257.
- Palková, Z. (2004). Multicellular microorganisms: laboratory versus nature. *EMBO Reports*, 5(5), 470–476.
- Penru, Y., Guastalli, A.R., Esplugas, S., & Baig, S. (2012). Application of UV and UV/H<sub>2</sub>O<sub>2</sub> to seawater: Disinfection and natural organic matter removal. *Journal of Photochemical & Photobiology A*, 233, 40–45.
- Petridis, N.P., Sakkas, V.A., & Albanis, T.A. (2014). Chemometric optimization of dispersive suspended microextraction followed by gas chromatography-mass spectrometry for the determination of polycyclic aromatic hydrocarbons in natural water. *Journal of Chromatography A*, 1355:46–52.
- Pogorzelec, M., & Piekarska, K. (2018). Application of semipermeable membrane devices for long-term monitoring of polycyclic aromatic hydrocarbons at various stages of drinking water treatment. *Science of the Total Environment*, 631, 1431–1439.
- Porrás J., Bedoya C., Silva-Agredo J., Santamaría A., Fernández J.J., & Torres-Palma R.A. (2016). Role of humic substances in the degradation pathways and residual antibacterial activity during the photodecomposition of the antibiotic ciprofloxacin in water. *Water Research*, 94, 1-9.
- Primo, O., Rivero, M.J., Ortiz, I., & Irbien, A. (2007). Mathematical modelling of phenol photooxidation: Kinetics of the process toxicity. *Chemical Engineering Journal*, 134(1–3), 23–28.



- Pupo Nogueira, R.F., Oliveira, M.C., Paterlini, W.C. (2005). Simple and fast spectrophotometric determination of  $H_2O_2$  in photo-Fenton reactions using metavanadate. *Talanta*, 66, 86-91
- Rahmanov, N.R., Ahmadova, S.T., & Bilbao, J. (2013). Distributed generation system with renewable energy sources: Grid modeling and simulation. *Eurocon, Zagreb*, 984-991.
- Rauschenbach, H. S. (2012). *Solar cell array design handbook: the principles and technology of photovoltaic energy conversion*, Springer Netherlands, The Netherlands.
- Resolution (2007). Resolution 2115 of 2007 of the Ministry of Social Protection, Ministry of Environment, Housing and Territorial Development of 7 June 2007, by means of which the characteristics, basic tools and frequencies of the control and monitoring system related to the water quality for human consumption. Government of Colombia, 1-23.
- Ribeiro, A.R., Nunes, O.C., Pereira, M.F., & Silva, A.M. (2015). An overview on the advanced oxidation processes applied for the treatment of water pollutants defined in the recently launched Directive 2013/39/EU. *Environment International*, 75, 33–51.
- Rodríguez-Chueca, J., García-Cañibano, C., Lepistö, R.J., Encinas, Á., Pellinen, J., & Marugán, J. (2018). Intensification of UV-C tertiary treatment: Disinfection and removal of micropollutants by sulfate radical based Advanced Oxidation Processes. *J Hazard Mat.* In press.
- Rosenfeldt, E.J., & Linden, K.G. (2007). The ROH,UV concept to characterize and the model UV/ $H_2O_2$  process in natural waters. *Environmental Science Technology*, 41(7), 2548–2553.
- Rozas, O., Vidal, C., Baeza, C., Jardim, W.F., Rossner, A., & Mansilla, H. (2016). Organic micropollutants (OMPs) in natural waters: oxidation by UV/ $H_2O_2$  treatment and toxicity assessment. *Water Research*, 98, 109–118.
- Rubio-Clemente, A., Chica, E., & Peñuela, G.A. (2018a). Direct large-volume injection analysis of polycyclic aromatic hydrocarbons in water. *Universitas Scientiarum*, 23(2), 171-189.

Rubio-Clemente A, Chica E, & Peñuela, G. (2018b). Total coliforms inactivation in natural water by UV/H<sub>2</sub>O<sub>2</sub>, UV/US and UV/US/H<sub>2</sub>O<sub>2</sub> systems". *Environmental Science and Pollution Research*, In press.

Rubio-Clemente A, Chica E, & Peñuela, G. (2018c). Photovoltaic array for powering advanced oxidation processes: Sizing, application and investment costs for the degradation of a mixture of anthracene and benzo[a]pyrene in natural water by the UV/H<sub>2</sub>O<sub>2</sub> system. *Journal of Environmental Chemical Engineering*, 6(2), 2751-2761.

Rubio-Clemente, A., Torres-Palma, R. A., & Peñuela, G. A. (2014). Removal of polycyclic aromatic hydrocarbons in aqueous environment by chemical treatments: a review. *Science of the Total Environment*, 478, 201-225.

Rubio-Clemente, A., Chica, E., & Peñuela, G. A. (2017a). Rapid determination of anthracene and benzo(a)pyrene by high-performance liquid chromatography with fluorescence detection. *Analytical Letters*, 50(8), 1229-1247.

Rubio-Clemente A, Chica E, Cardona A, & Peñuela, G. (2017b). Sensitive spectrophotometric determination of hydrogen peroxide in aqueous samples from advanced oxidation processes: Evaluation of possible interferences". *Afinidad*, 75, 579, 159-166.

Rubio-Clemente A., Chica E., & Peñuela G. (2017c). Kinetic modeling of the UV/H<sub>2</sub>O<sub>2</sub> process: Determining the effective hydroxyl radical concentration, *Physico-Chemical Wastewater Treatment and Resource Recovery*, Prof. Robina Farooq (Ed.), InTech, 19-41.

Rubio-Clemente A, Chica E, & Peñuela G. (2017d). Kinetic model describing the UV/H<sub>2</sub>O<sub>2</sub> photodegradation of phenol from water. *Chemical Industry and Chemical Engineering Quarterly*, 2017 23 (4) 547-562.

Santos, E., Souza, M. R., Junior, A. R. V., Soares, L. S., Frena, M., & Alexandre, M. R. (2018). Polycyclic aromatic hydrocarbons (PAH) in superficial water from a tropical estuarine system: Distribution, seasonal variations, sources and ecological risk assessment. *Marine pollution bulletin*, 127, 352-358.

Sharma, B. M., Melymuk, L., Bharat, G. K., Pribylová, P., Sánka, O., Klánová, J., & Nizzetto, L. (2018). Spatial gradients of polycyclic aromatic hydrocarbons (PAHs)

in air, atmospheric deposition, and surface water of the Ganges River basin. *Science of the Total Environment*, 627, 1495-1504.

Shemer H., & Linden K.G. (2007). Photolysis, oxidation and subsequent toxicity of a mixture of polycyclic aromatic hydrocarbons in natural waters. *Journal of Photochemistry and Photobiology A: Chemistry*, 187 (2), 186-195.

Solanki, C.S. (2013). *Solar Photovoltaic Technology and Systems: A Manual for Technicians, Trainers and Engineers*, PHI Learning Private Limited, Delhi.

Song, W., Ravindran, V., & Pirbazari, M. (2008). Process optimization using a kinetic model for the ultraviolet radiation-hydrogen peroxide decomposition of natural and synthetic organic compounds in groundwater. *Chemical Engineering Science*, 63, 3249–3270.

Souza BS, Dantas RF, Cruz A, Sans C, Esplugas S, & Dezotti M (2014) Photochemical oxidation of municipal secondary effluents at low H<sub>2</sub>O<sub>2</sub> dosage: study of hydroxyl radical scavenging and process performance. *Chemical Engineering Journal*, 237, 268–276.

Sulaiman, S.I., Rahman, T.K.A., Musirin, I. (2010). Novel intelligent sizing algorithm for grid-connected photovoltaic system design. *Int. Rev. Model. Sim.* 3, 639–652.

Sulaiman, S.I., Rahman, T.K.A., Musirin, I., Shaari, S. (2011). Sizing grid-connected photovoltaic system using genetic algorithm, in: *Industrial Electronics and Applications (ISIEA), 2011 IEEE Symposium*, IEEE, Langkawi, pp. 505–509.

Trably E., Delgènes N., Patureau D., & Delgènes J.P. (2004). Statistical tools for the optimization of a highly reproducible method for the analysis of polycyclic aromatic hydrocarbons in sludge samples. *International Journal of Environmental Analytical Chemistry*, 84 (13), 995-1008.

Tröger, R., Klöckner, P., Ahrens, L., & Wiberg, K. (2018). Micropollutants in drinking water from source to tap-Method development and application of a multiresidue screening method. *Science of the Total Environment*, 627, 1404-1432.

Urbano, V.R., Peres, M.S., Maniero, M.G., & Guimarães, J.R. (2017). Abatement and toxicity reduction of antimicrobials by UV/H<sub>2</sub>O<sub>2</sub> process. *Journal of Environmental Management*, 193, 439–447.

Vela, N., Martínez-Menchón, M., Navarro, G., Pérez-Lucas, G., & Navarro, S. (2012). Removal of polycyclic aromatic hydrocarbons (PAHs) from groundwater by heterogeneous photocatalysis 670 under natural sunlight. *Journal of Photochemistry and Photobiology A*, 232, 32–40.

Wang, D., Wang, Y., Singh, V. P., Zhu, J., Jiang, L., Zeng, D., Liu, D., Zeng, X., Wu, J., Wang L., & Zeng, C. (2018). Ecological and health risk assessment of PAHs, OCPs, and PCBs in Taihu Lake basin. *Ecological Indicators*, 92, 171-180.

WEF & AWWA, 2012. *Standard Methods for the Examination of Water and Wastewater*, 22nd ed., American Public Health Association, Washington, DC., 2012.

Wick A, Haus N, Sukkariyah B, Haering K, Daniels W. (2011). Remediation of PAH-contaminated soils and sediments: a literature review. CSES Department, internal research document.

Wols, B.A., & Hofman-Caris, C.H.M. (2012). Review of photochemical reaction constants of organic micropollutants required for UV advanced oxidation processes in water. *Water Research*, 46, 2815–2827.

Yao, H., Sun, P., Minakata, D., Crittenden, J.C., & Huang, C.H. (2013). Kinetics and modeling of degradation of ionophore antibiotics by UV and UV/H<sub>2</sub>O<sub>2</sub>. *Environmental Science Technology*, 47(9), 4581–4589.

Zeng, Q., Jeppesen, E., Gu, X., Mao, Z., & Chen, H. (2018). Distribution, fate and risk assessment of PAHs in water and sediments from an aquaculture-and shipping-impacted subtropical lake, China. *Chemosphere*, 201, 612-620.

Zhou Y., Song J.Z., Choi F.F.K., Wu H.F., Qiao C.F., Ding L.S., Gesang S.L., & Xu H.X. (2009). An experimental design approach using response surface techniques to obtain optimal liquid chromatography and mass spectrometry conditions to determine the alkaloids in *Meconopsi* species. *Journal of Chromatography A* 1216, 7013-7023.

---

Zuorro, A., Fidaleo, M., Lavecchia, R. (2014). Degradation and antibiotic activity reduction of chloramphenicol in aqueous solution by UV/H<sub>2</sub>O<sub>2</sub> process. *Journal of Environmental Management*, 133, 302–308.



# **APPENDIX**

## **WORK QUALITY**








Scimago Journal & Country Rank Enter Journal Title, ISSN or Publisher Name

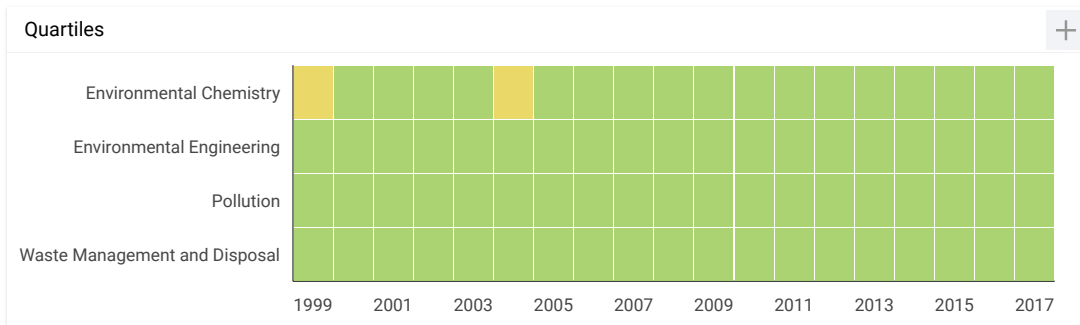
Home Journal Rankings Country Rankings Viz Tools Help About Us

# Science of the Total Environment

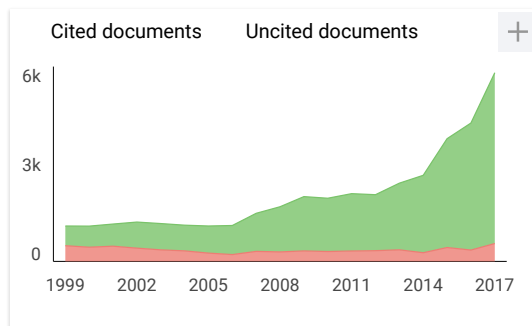
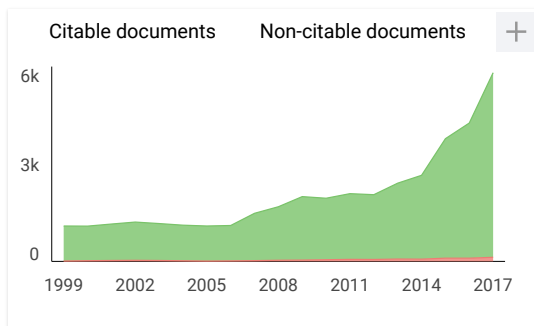
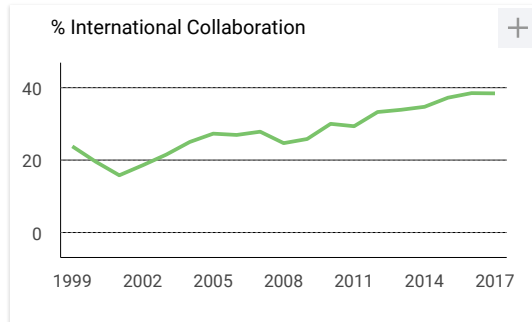
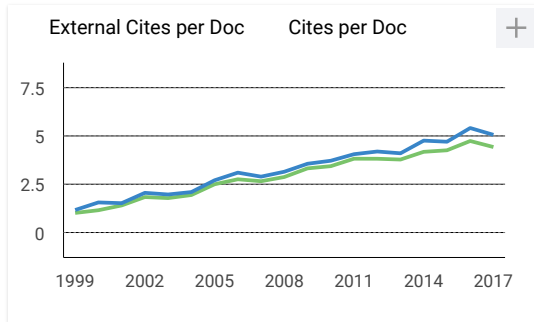
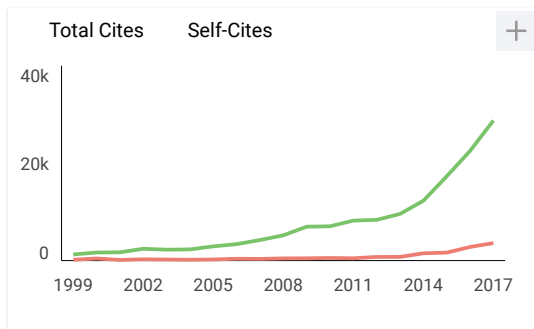
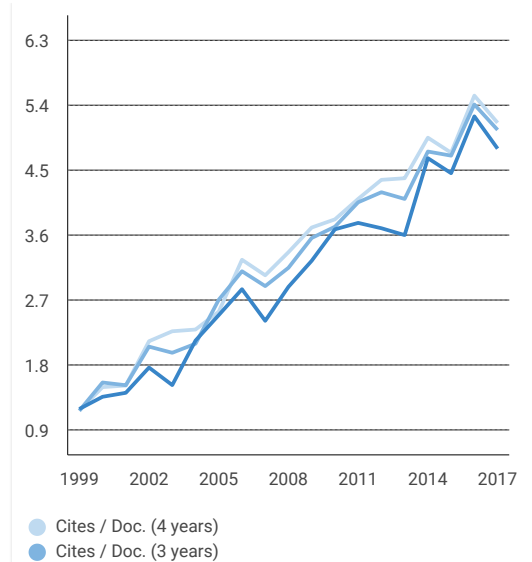
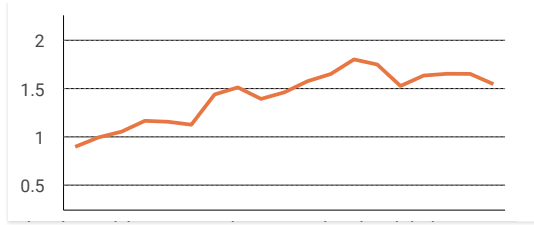
# 190

H Index

<b>Country</b>	Netherlands -  <a href="#">SJR Ranking of Netherlands</a>
<b>Subject Area and Category</b>	<a href="#">Environmental Science</a> <a href="#">Environmental Chemistry</a> <a href="#">Environmental Engineering</a> <a href="#">Pollution</a> <a href="#">Waste Management and Disposal</a>
<b>Publisher</b>	<a href="#">Elsevier BV</a>
<b>Publication type</b>	Journals
<b>ISSN</b>	00489697
<b>Coverage</b>	1972-ongoing
<b>Scope</b>	The journal is an international medium for publication of original research on the environment with emphasis on changes caused by human activities. It is concerned with changes in the natural levels and distribution of chemical elements and their compounds that may affect the well-being of the living world, or represent a threat to human health.
	<a href="#">Homepage</a>
	<a href="#">Join the conversation about this journal</a>



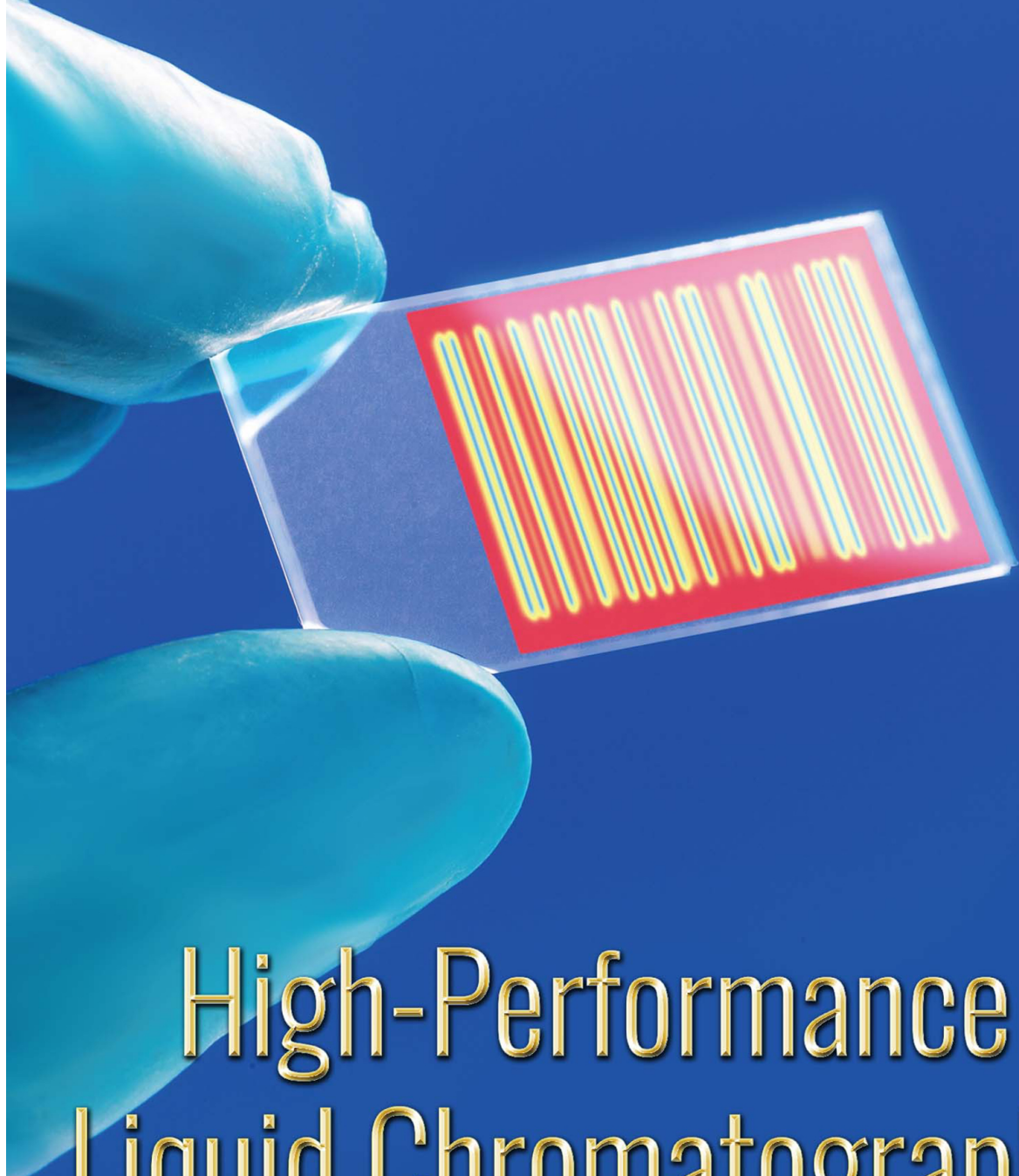
<b>SJR</b> <span style="float: right;">+</span>	<b>Citations per document</b> <span style="float: right;">+</span>



Show this widget in your own website

Just copy the code below and paste within your html code:

```
<a href="https://www.scimaç
```



# High-Performance Liquid Chromatography

Types, Parameters and Applications

---

Ivan Lucero  
Editor

Analytical Chemistry and Microchemistry

NOVA



Complimentary Contributor Copy



Scimago Journal & Country Rank Enter Journal Title, ISSN or Publisher Name

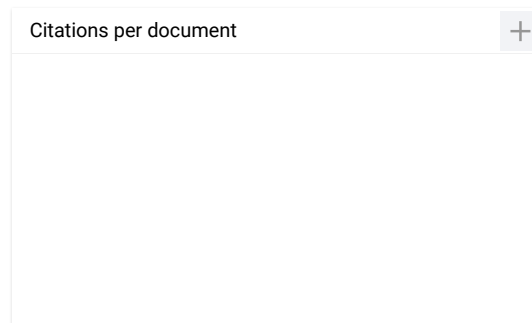
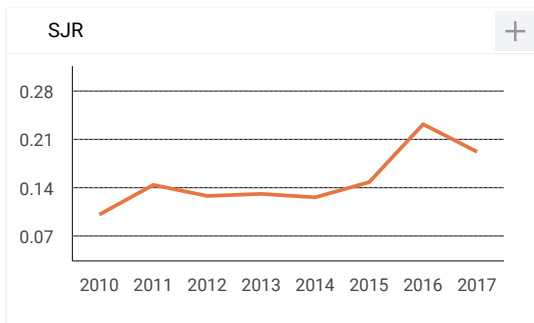
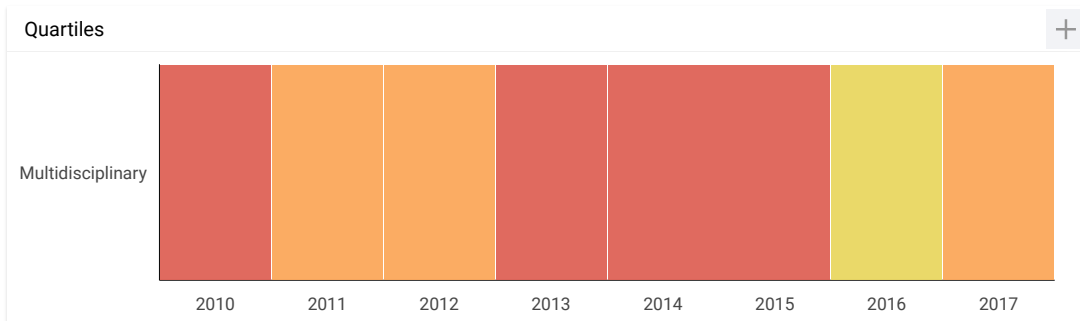
- Home
- Journal Rankings
- Country Rankings
- Viz Tools
- Help
- About Us

# Universitas Scientiarum

Country	Colombia -  <a href="#">SJR Ranking of Colombia</a>
Subject Area and Category	Multidisciplinary Multidisciplinary
Publisher	<a href="#">Pontificia Universidad Javeriana</a>
Publication type	Journals
ISSN	01227483
Coverage	2009-ongoing
	 <a href="#">Join the conversation about this journal</a>

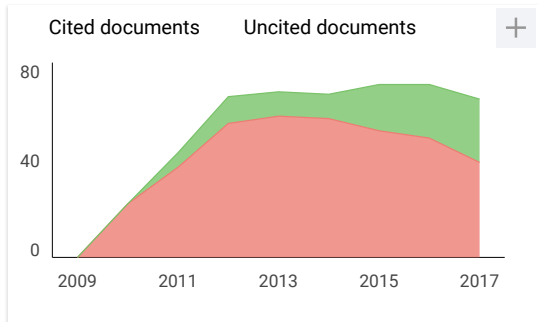
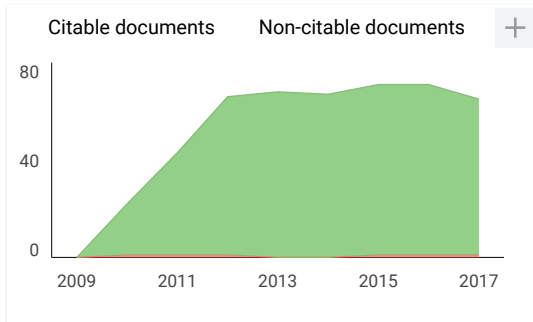
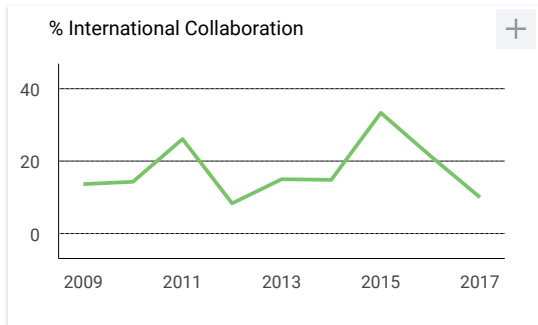
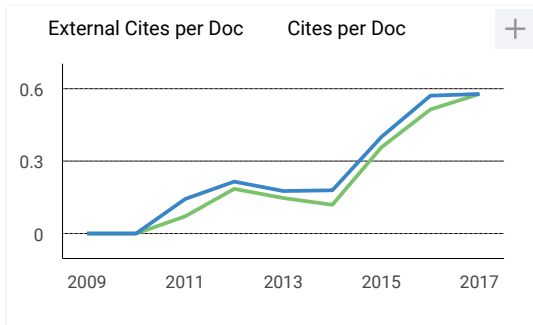
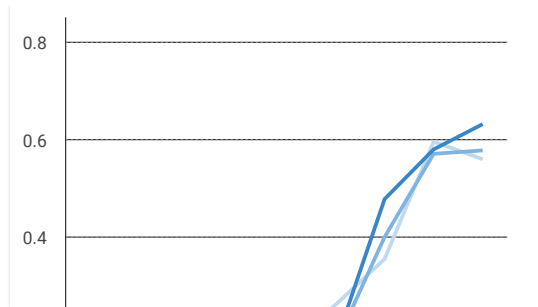
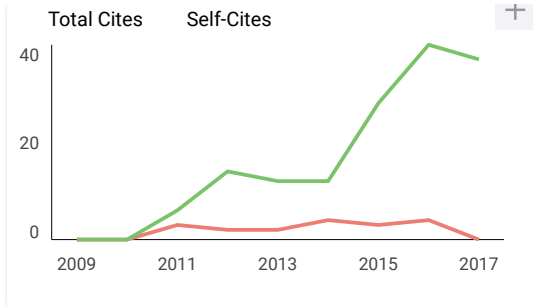
# 7

H Index



22/9/2018

Universitas Scientiarum



Universitas Scientiarum ← Show this widget in your own website

**Q3** Multidisciplinary  
best quartile

**SJR 2017**  
0.19

powered by scimagojr.com

Just copy the code below and paste within your html code:

```
<a href="https://www.scimaç"
```

Irwan Abdullah 2 months ago

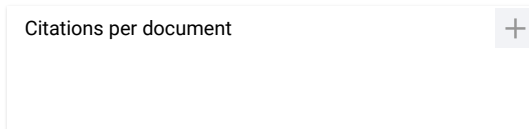
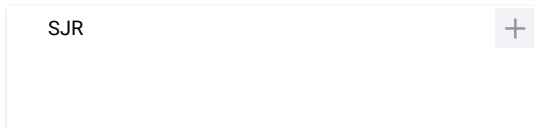
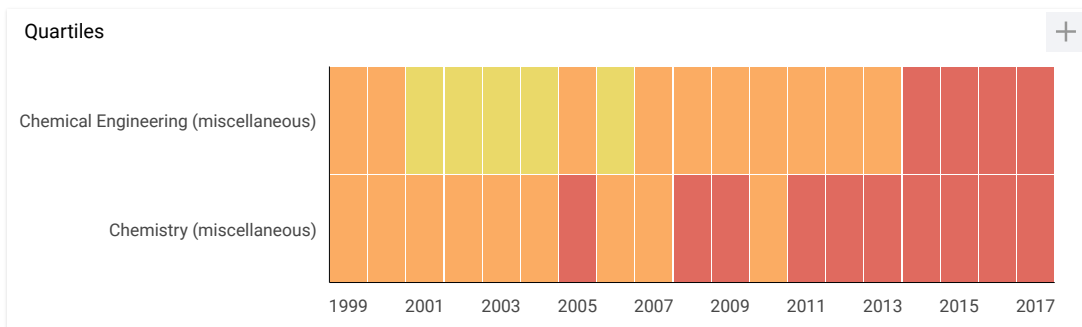


# Afinidad

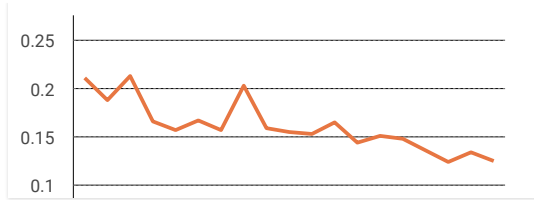
# 14

H Index

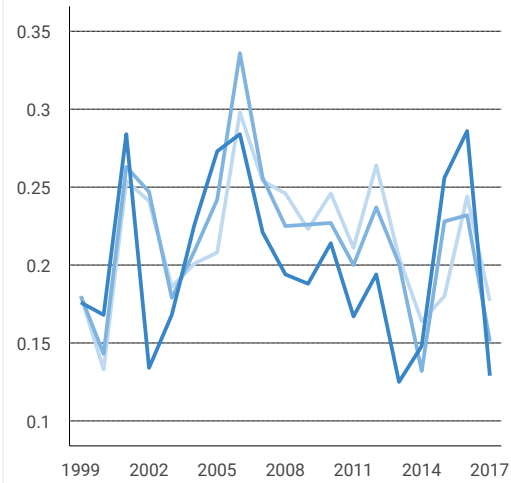
<b>Country</b>	Spain - <a href="#">SJR Ranking of Spain</a>
<b>Subject Area and Category</b>	<a href="#">Chemical Engineering</a> <a href="#">Chemical Engineering (miscellaneous)</a>  <a href="#">Chemistry</a> <a href="#">Chemistry (miscellaneous)</a>
<b>Publisher</b>	<a href="#">Asociacion de Quimicos e Lngerieros</a>
<b>Publication type</b>	Journals
<b>ISSN</b>	00019704
<b>Coverage</b>	1996-ongoing
<b>Scope</b>	AFINIDAD accepts review articles, original papers (experimental reports as well as theoretical studies) and short communications on all aspects of chemical engineering, process engineering, chemistry and biotechnology.
	<a href="#">Homepage</a>
	<a href="#">Join the conversation about this journal</a>



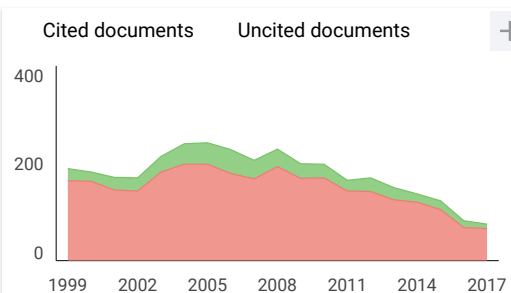
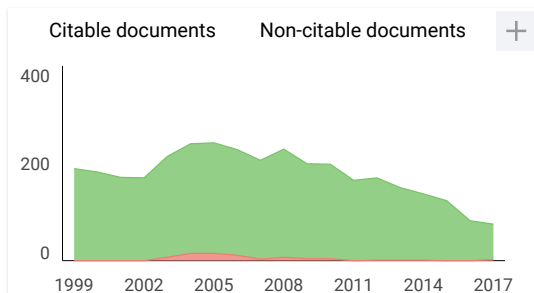
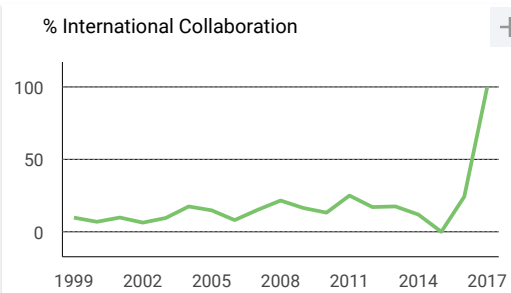
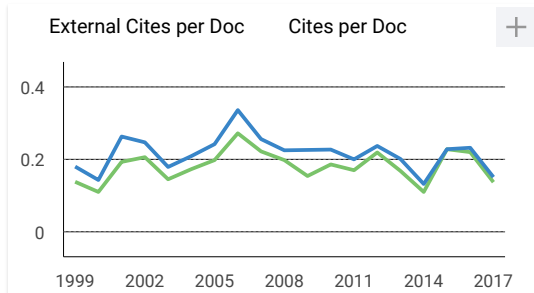
25/9/2018



Afinidad



● Cites / Doc. (4 years)



Show this widget in your own website

Just copy the code below and paste within your html code:

```
<a href="https://www.scimaç
```



Scimago Journal & Country Rank

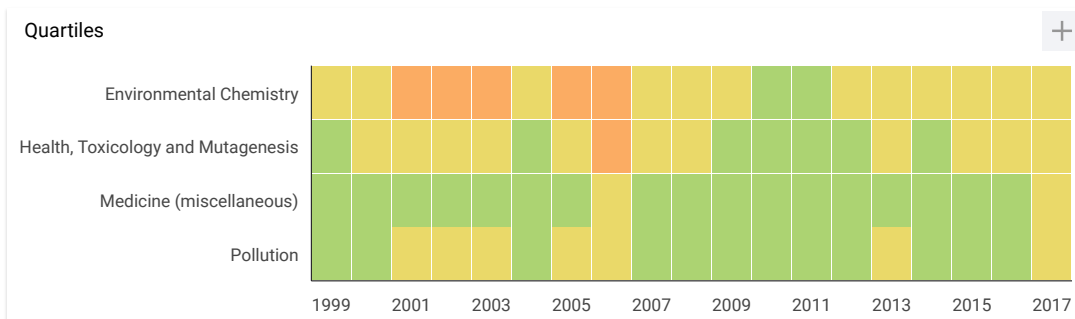
- Home
- Journal Rankings
- Country Rankings
- Viz Tools
- Help
- About Us

# Environmental Science and Pollution Research

# 74

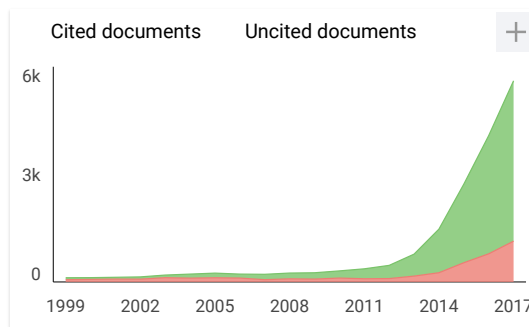
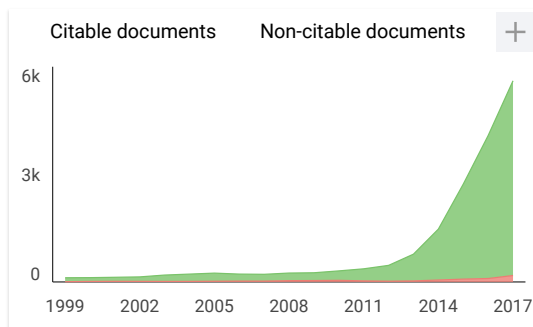
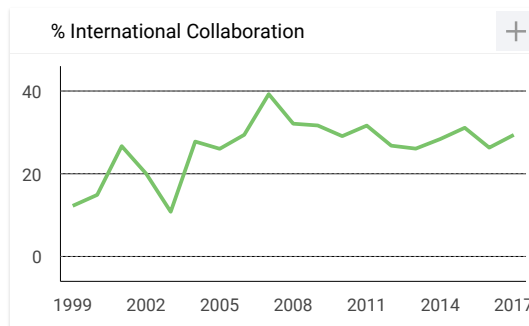
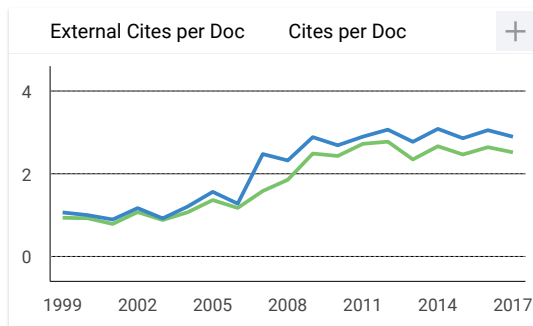
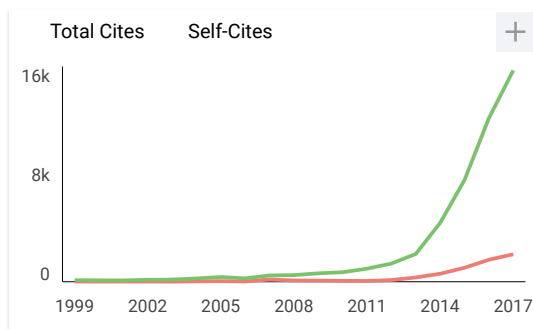
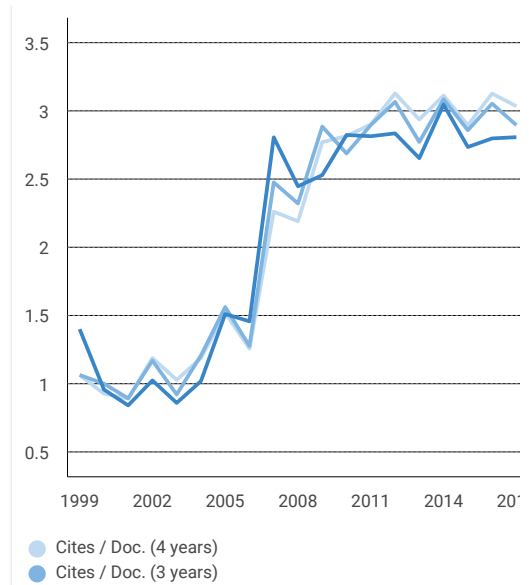
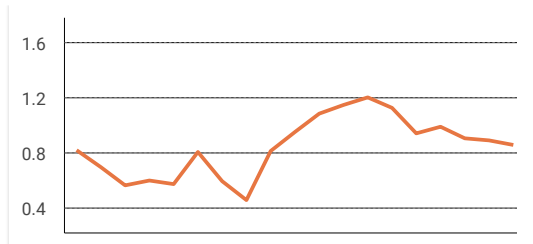
H Index

<b>Country</b>	Germany - <a href="#">SIR Ranking of Germany</a>
<b>Subject Area and Category</b>	<a href="#">Environmental Science</a> <a href="#">Environmental Chemistry</a> <a href="#">Health, Toxicology and Mutagenesis</a> <a href="#">Pollution</a>  <a href="#">Medicine</a> <a href="#">Medicine (miscellaneous)</a>
<b>Publisher</b>	<a href="#">Springer Verlag</a>
<b>Publication type</b>	Journals
<b>ISSN</b>	09441344
<b>Coverage</b>	1994-ongoing
<b>Scope</b>	Environmental Science and Pollution Research (ESPR) serves the international community in all areas of Environmental Science and related subjects with emphasis on chemical compounds. It reports from a broad interdisciplinary outlook. Apart from the strictly scientific contributions as research articles (short and full papers) and reviews, ESPR publishes: news & views from research and technology, legislation and regulation, hardware and software, education, literature, institutions, organizations, conferences.
<a href="#">?</a>	<a href="#">Homepage</a>
<a href="#">?</a>	<a href="#">Join the conversation about this journal</a>



SJR <span style="float: right;">+</span>	Citations per document <span style="float: right;">+</span>
--	---





**Environmental Science and Pollution Research** ← Show this widget in your own website

Environmental Chemistry  
Q2 best quartile

SJR 2017  
0.86

powered by scimagojr.com

Just copy the code below and paste within your html code:



```
<a href="https://www.scimagojr.com" style="display: inline-block; border: 1px solid black; padding: 2px 5px;">https://www.scimagojr.com
```

**SJR**

Scimago Journal &amp; Country Rank Enter Journal Title, ISSN or Publisher Name

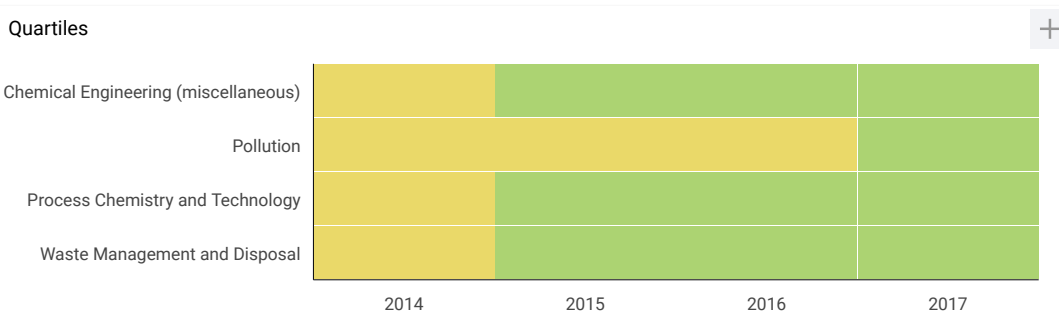

[Home](#) [Journal Rankings](#) [Country Rankings](#) [Viz Tools](#) [Help](#) [About Us](#)

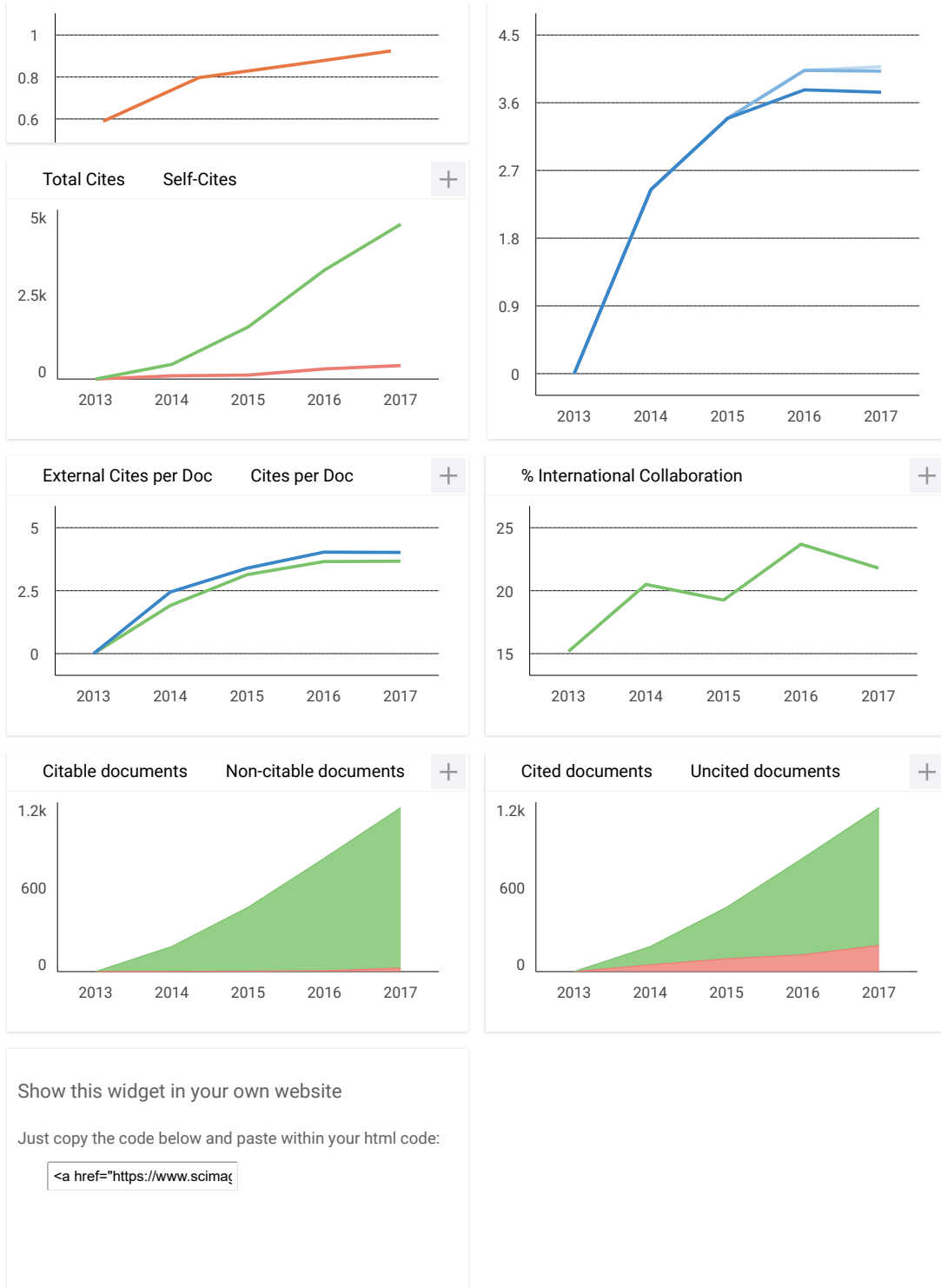
# Journal of Environmental Chemical Engineering

<b>Country</b>	<a href="#">United Kingdom</a> -  <a href="#">SJR Ranking of United Kingdom</a>
<b>Subject Area and Category</b>	<a href="#">Chemical Engineering</a> <a href="#">Chemical Engineering (miscellaneous)</a> <a href="#">Process Chemistry and Technology</a>  <a href="#">Environmental Science</a> <a href="#">Pollution</a> <a href="#">Waste Management and Disposal</a>
<b>Publisher</b>	<a href="#">Elsevier BV</a>
<b>Publication type</b>	Journals
<b>ISSN</b>	22133437
<b>Coverage</b>	2013-ongoing
	 <a href="#">Join the conversation about this journal</a>

# 37

H Index

SJR Citations per document 



---

# PHYSICO-CHEMICAL WASTEWATER TREATMENT AND RESOURCE RECOVERY

---

Edited by Robina Farooq and Zaki Ahmad

---

**INTECH**



Scimago Journal & Country Rank

Enter Journal Title, ISSN or Publisher Name

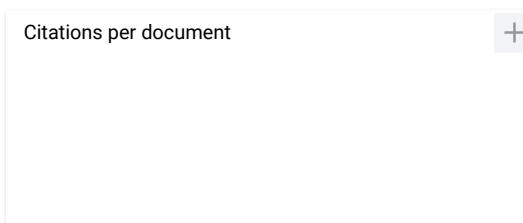
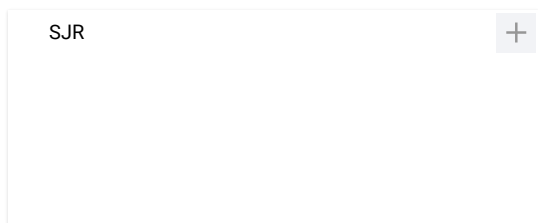
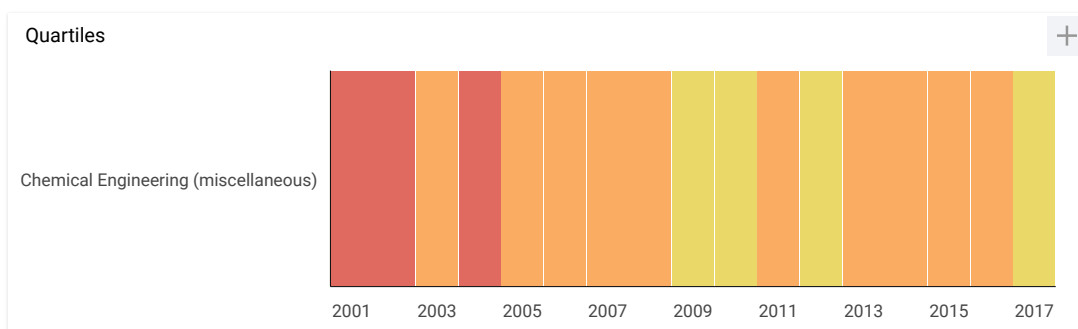
- Home
- Journal Rankings
- Country Rankings
- Viz Tools
- Help
- About Us

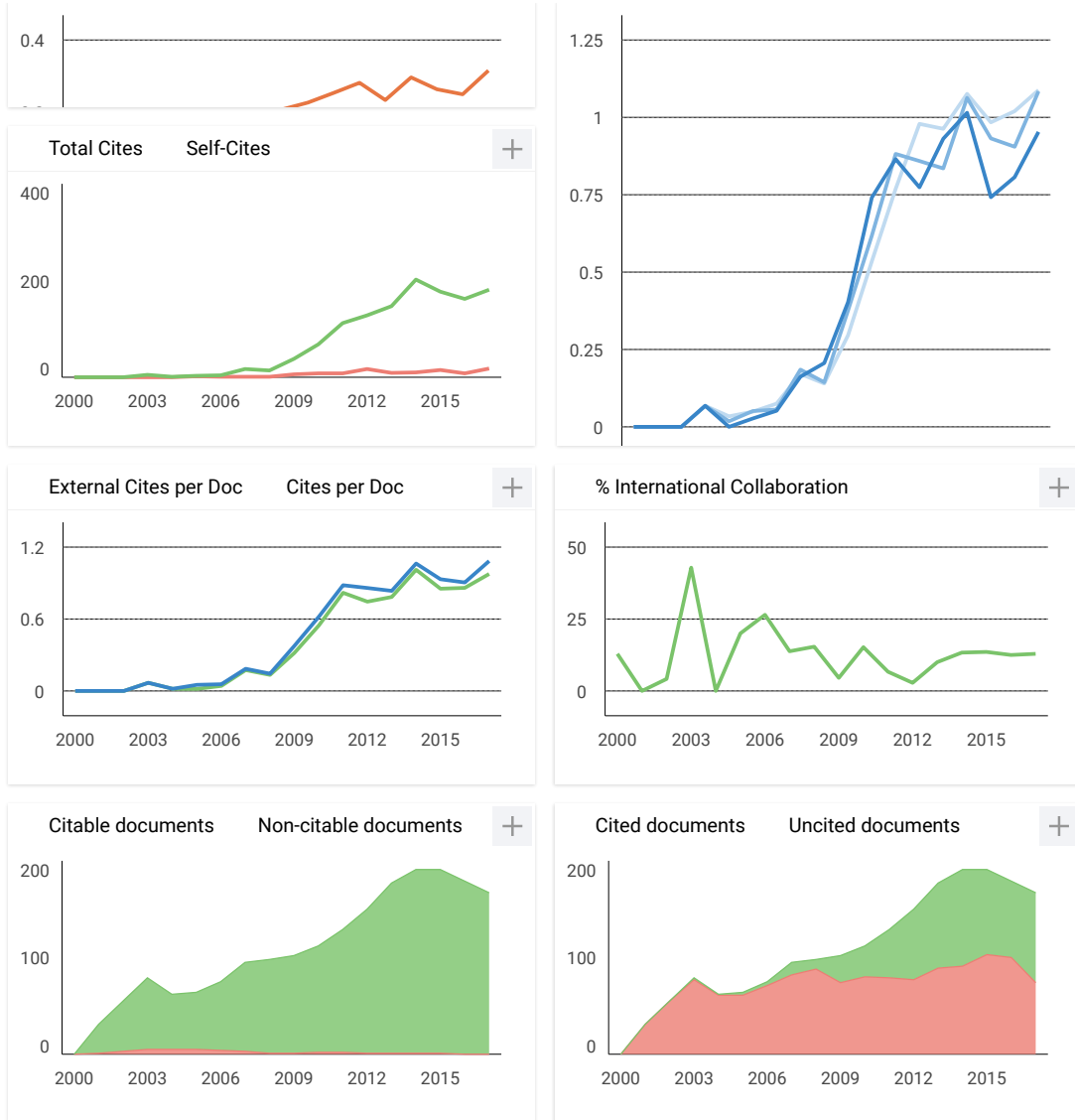
# Chemical Industry and Chemical Engineering Quarterly

<b>Country</b>	Serbia -  SIR Ranking of Serbia
<b>Subject Area and Category</b>	Chemical Engineering Chemical Engineering (miscellaneous)
<b>Publisher</b>	Association of Chemical Engineers of Serbia'
<b>Publication type</b>	Journals
<b>ISSN</b>	14519372
<b>Coverage</b>	2008-ongoing
	<a href="#">Homepage</a>
	<a href="#">Join the conversation about this journal</a>

# 18

H Index





**Chemical Industry and Chemical Engineering...**

← Show this widget in your own website

**Q2**

Chemical Engineering (miscellaneous)

best quartile

**SJR 2017**

**0.32**

powered by scimagojr.com

Just copy the code below and paste within your html code:

```
<a href="https://www.scimagojr.com/journalsearch.php?q=12100154910&tip=sid&clean=0" style="border: 1px solid #ccc; padding: 2px 5px; display: inline-block;">https://www.scimagojr.com/journalsearch.php?q=12100154910&tip=sid&clean=0
```